Surfactant coated aerosol powders and their properties.

by

Anthony James Hickey

Submitted for the degree of

Doctor of Philosophy

The University of Aston in Birmingham

November 1984

The University of Aston in Birmingham

Surfactant Coated Aerosol Powders And Their Properties

By A.J. Hickey

For the degree of Doctor of Philosophy

Year 1984

The hygroscopic growth of aerosols is an important factor effecting particle size. The consequence of the hygroscopic growth of pharma - ceutical aerosols is a change in their deposition characteristics, such that there is an increase in the total amount deposited in the lung.

In this study the hygroscopic growth of disodium fluorescein (DF) aerosol powders was investigated by coating the powders with lauric and capric acids. The coating procedure was carried out in dichloromethane and chloroform, which acted as cosolvents for the fatty acids.

An assessment of the extent and the nature of the coating was carried out. The qualitative assessment of the coating was achieved by infra - red spectroscopy, electronscanning chemical analysis and scanning electron microscopy. The quantitative analysis was carried out by differential refractometry, ultra - violet spectroscopy and gas liquid chromatography. These powders were generated under conditior approaching those in the lung, of 97 % relative humidity and 37°C.

Coated and uncoated DF aerosol powders were introduced into a controlled temperature and relative humidity apparatus, designed and constructed for the investigation of hygroscopic growth in these studies. A vertical spinning disc device was used to generate the powders.

Under conditions of controlled temperature and relative humidity mentioned, the growth ratio of disodium fluorescein alone was 1.45 compared with 1.68, for a nominal coating of DF with lauric acid of 0.12 gg^{-1}, 1.0 for a nominal lauric acid coating of 0.2 gg^{-1}, and 1.02 for a nominal capric acid coating of 0.18 gg^{-1}.

The range of control of hygroscopic growth of these aerosols has implications for the deposition of these preparations in the respiratory tract. These implications are discussed in the light of the current knowledge of the effects of hygroscopic growth on the deposition of pharmaceutical and environmental aerosols.

A series of experiments in which pulmonary ventilation using a simple radioaerosol generator and delivery system are reported showing that particle size determination may be used to aid the design of diagnostic aerosol generators.

Keywords :

Hygroscopic growth Surface active agents

Aerosol generation Aerosol characterisation

A C K N O W L E D G E M E N T S

I wish to express my gratitude to Drs., F.J.T. Fildes, W.J. Irwin, P.R. Byron and I. Gonda for their advice and support during this project.

I would also like to thank Drs., G.V. Jackson, A.F.A. El Khalik, A.R. Rees and N.S.R. Roberts for their assistance during this period.

This project was supported by I.C.I. plc and particular recognition should be given to the contribution made by the members of staff in the Formulation Research and Pharmacokinetics sections of the Pharmaceuticals Division, and the New Science Group of Mond Division. The work carried out in conjunction with the Nuclear Physics Department of Dudley Road Hospital, Birmingham, was instructive and a valuable experience for which I am grateful to the staff involved.

Finally I must thank my Parents and Lesley for the years of support and encouragement that they have given me.

LIST OF CONTENTS

LIST OF TABLES

LIST OF FIGURES

C H A P T E R O N E

I n t r o d u c t i o n

1. Introduction

An aerosol may be defined as a system consisting of solid or liquid particles dispersed in a gaseous medium (1).

Particulate substances may be classified according to the origin or manner of formation. Thus virus, bacterium and pollen are clearly understood. Smoke is commonly used to mean the mixture of fine liquid droplets and solid particles produced by the combustion of fuel and tobacco, for example. Mist and fog refers to liquid droplets, usually formed from the condensation of vapours around suitable nuclei, such as in natural atmospheric fog. Dust, in the popular sense, means the fine solid particles that have settled out in household environments. In industry the term dust refers to the fine particles of solid materials formed by the mechanical disintegration of matter and dispersed in the air. These definitions have been put forward by Hatch and Gross (2).

Aerosols are used in the treatment of respiratory disorders and diseases of the lung (3). The delivery of drugs via the gastro - intestinal or parenteral routes require large doses in order to achieve pharmacologically active levels in the respiratory tract. Aerosol inhalation therapy presents the drug directly to the sites which govern respiratory disorders or diseases of the lung.

The most significant use of inhalation aerosols is in the treatment of asthma and bronchitis (4). The range of drugs used in such treatment reflects the complexity of the innervation and pharmacology of the respiratory tract.

1.1 The Innervation And The Pharmacology Of The Lung.

The central and peripheral nervous systems may be subdivided into their component parts. The central nervous system consists of the brain,

spinal cord, sensory (afferent) and motor (efferent) branches. The peripheral, autonomic nervous system consists of the parasympathetic and sympathetic branches (5). Recently a third, nonadrenergic, noncholinergic system has been observed (6). The autonomic nervous system controls many aspects of pulmonary function. (7).

Attention has focused on airway smooth muscle because of the speed and ease with which airway calibre changes occur (8,9). Airway obstruction in asthma and chronic bronchitis may, however, arise from increased microvascular leakage, resulting in bronchial mucosal oedema, and from plugging of the airways by mucus secretions (10 - 12). These events may be brought about by the release of inflammatory mediators such as histamine (13,14), leukotrienes (13 - 16) and prostaglandins (17) derived from mast cells and other inflammatory cells in the asthmatic airway (18 - 20).

1.1.1 The Sympathetic Branch.

The sympathetic branch of the autonomic nervous system is characterised by the neurotransmitter at the postganglionic synapse which is noradrenaline, from which it derives the descriptive name, the adrenergic system (5).

Histochemical and electron microscope studies show adrenergic innervation to be scanty in the respiratory tract (21 - 23). Functional sympathetic innervation has not been demonstrated in studies involving electrical field stimulation (8,21) or by the inhibition (9) or stimulation (24) of noradrenaline release. Sympathetic nerves supply parasympathetic ganglia in human airways (22) and therefore may modulate neurotransmission at this level (25).

Circulating catecholamines may be important in the physiological regulation of airway tone, since human airway muscle is potently

relaxed by adrenergic agonists in vivo and in vitro, whilst not appearing to be functionally innervated by adrenergic axons (26). Noradrenaline is unlikely to be responsible as it is not active in the physiological range and has little effect during infusion (27). Adrenaline is a circulating hormone and has potent effects on metabolism and airway function (28,29). Catecholamines may play a protective role in asthma. Adrenergic receptors may be divided into two types in terms of their activity. Alpha - receptors generally excite, with the exception of the intestine, where relaxation occurs (5). Beta - receptors generally relax, with the exception of the heart, where stimulation occurs (5). Normal human subjects are unaffected, in terms of airway tone (30) or bronchial reactivity (31), by beta - agonists. They may, however, cause bronchoconstriction in the asthmatic subject (32,33).

Most emphasis has been placed on adrenergic receptor regulation of airway smooth muscle. It is increasingly apparent that adrenergic agents may also effect airway tone by influencing mast cells and other inflammatory cells, bronchial blood vessels and microvascular permeability, mucus secretion, and neurotransmission (19).

1.1.1.1 Beta - agonists.

Beta - agonists are widely distributed within the lung (34) which is consistent with their involvement in many aspects of pulmonary function. Autoradiographic evidence suggests that beta - receptors progressively increase in density from the trachea to the terminal bronchioles (34,35). In human airway smooth muscle the absence of $beta_1$ - receptors is suggested by the absence of bronchodilator effect in asthmatic subjects with a $beta_1$ selective agonist (36). This observation has been confirmed by in vitro studies (9). Functional beta receptors on pulmonary mast cells (37,38), of the

$beta_2$ - subtype (39), have been observed in isolated human lung mast cells (40). Beta - agonists increase airway mucus secretion (11,12), reduce histamine induced microvascular leakage (10) and modulate the cholinergic neurotransmission at ganglia (25) or postganglionic nerves (41).

1.1.1.2 Alpha - agonists.

Alpha adrenergic receptors that mediate contraction of airway smooth muscle have been demonstrated in many species, including humans (42,43). Alpha adrenergic receptors may be classified into two subtypes depending on the selectivity of the specific antagonists (44), both subtypes may be present in airway smooth muscle (45). Alpha - agonists have produced contraction in human lung strips (46) and canine tracheal muscle (47). Alpha - agonists also stimulate fluid and mucin secretion from submucosal glands in several species (11,12)and facilitate allergen induced release of mediators from human lung fragments (48).

1.1.2 The Parasympathetic Branch.

The parasympathetic branch of the autonomic nervous system is characterised by the neurotransmitter at the postganglionic synapse which is acetylcholine, from which it derives the descriptive name, the cholinergic system (5).

The parasympathetic nervous system plays an important role in the regulation of airway calibre in many species, including humans, and is the dominant constriction mechanism in the airways (49).

Efferent fibres travel in the vagus nerve and synapse in small ganglia situated in the airway wall, from which short postsynaptic fibres directly supply the airway smooth muscle and submucosal glands. Electrical stimulation of vagal motor nerves causes bronchoconstriction which is inhibited by the muscarinic antagonist atropine and is

potentiated by acetylcholinesterase inhibitors (50).

Muscarinic receptors are found in high density in tracheal (51,52) and large airway (53,54) smooth muscle. The density of these receptors decreases as the airways become smaller, so that terminal bronchioles are almost devoid of muscarinic receptors (35,53).

1.1.3 The Third Nervous System Of The Lung.

A third, nonadrenergic, noncholinergic nervous system is well described in the intestinal tract (55) and has been described in the lung (56,57). This nervous system is inhibitory for airway smooth muscle and, therefore, defective function of this system could contribute to bronchial hypereactivity in asthma.

Electrical field stimulation in the presence of muscarinic and adrenergic antagonists stimulates in vitro relaxation of smooth muscle in several species. This response is abolished by the nerve blocker tetrodotoxin, which indicates that it is mediated by nerves (56).

Electron microscope studies have demonstrated features in these airway nerves which differentiate them from cholinergic and adrenergic nerves (58). In the absence of a functional sympathetic innervation of airway smooth muscle, this nonadrenergic inhibitory system is the only nerve mediated means of relaxation in human airway smooth muscle (8,21 - 23).

A likely candidate for neurotransmitter in this system is vasoactive intestinal peptide (VIP) (59). VIP - immunoreactive nerves have been identified in the lungs of many species (59). In the human lung VIP nerves are closely associated with airway smooth muscle, submucosal glands, and pulmonary vessels and are present in airway ganglia (59). In animal and human airways VIP relaxes airway smooth muscle in vitro (8,60) and in animals it protects against histamine

Figure 1.1 : Schematic diagram of the balance in the lung between the various components of the autonomic nervous system to achieve normal airway smooth muscle tone.

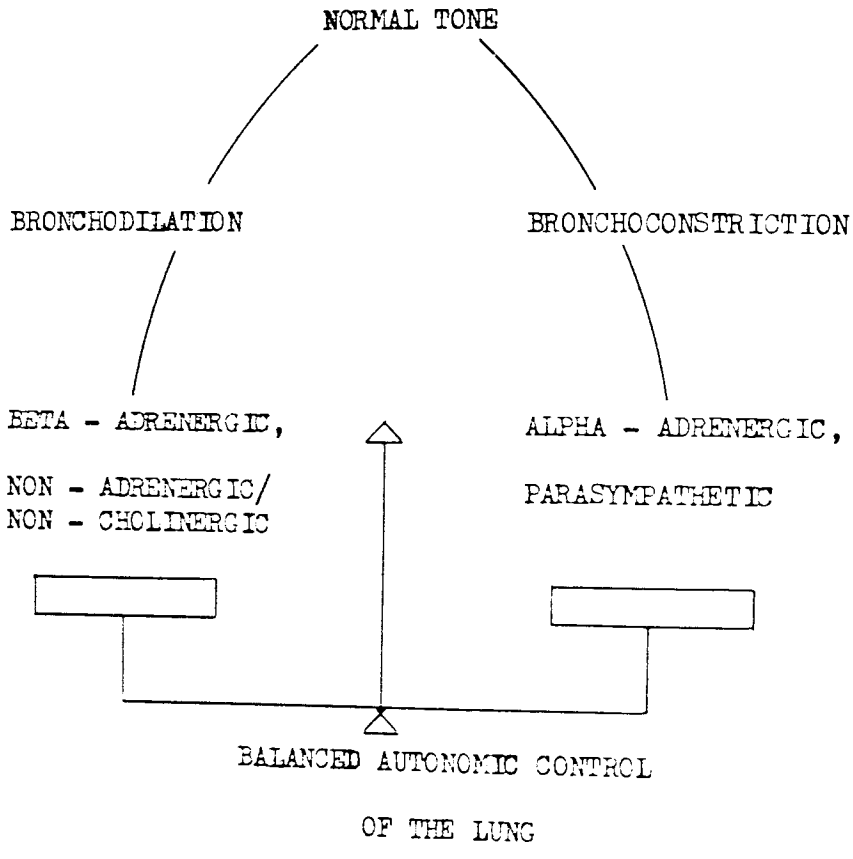

and prostaglandin induced bronchoconstriction in vivo (61).

Figure 1.1 summarises the balance in the lung between the various components of the autonomic nervous system to achieve normal airway smooth muscle tone.

1.1.4 The Pharmacology Of Bronchodilation.

It has been stated that many of the receptor sites in the lung are not only responsible for bronchodilation but also for mucus secretion (11,12), inhibition of microvascular leakage (10) and vasoconstriction (28,29). In order to generalise the presentation of drugs available for the treatment of asthma and bronchitis airway muscle tone and histamine will be considered,as parameters by which the effectiveness of the drug may be measured.

Figure 1.2 shows the activity of the sympathetic and parasympathe branches of the autonomic nervous system at the cellular level.

The component of the sympathetic system responsible for bronchodilation is the beta - adrenergic constituent. Beta - adrenergi agonists bind to adenylate cyclase and facilitate the conversion of adenosine triphosphate (ATP) to cyclic (3'5') adenosine monophosphate (AMP) which in turn results in bronchodilation and inhibition of histamine release. Many $beta_2$ - ago nists are used in clinical therapy, one of which is isoprenaline and its analogues (62).

Phosphodiesterase converts cyclic AMP to its inactive form, 5' AMP. The overall increase in cyclic AMP would produce the same effects as those of beta - agonists. Xanthine derivatives inactivate phosphodiesterase and consequently are useful in inhalation therapy. An example of such a compound is theophylline (63).

The parasympathetic branch of the autonomic nervous system is

Figure 1,2 : Schematic diagram of the sympathetic and parasympathetic branches of the autonomic nervous system at the cellular level.

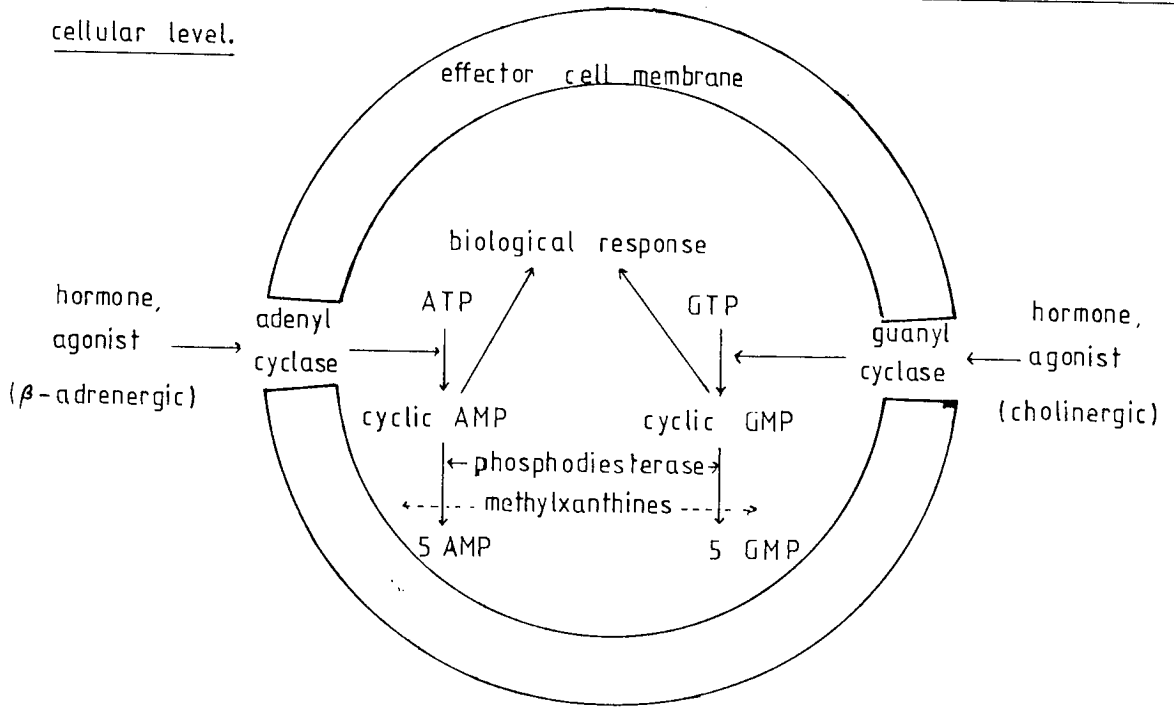

cyclic AMP - biological response = bronchodilation

cyclic GMP - biological response = bronchoconstriction

Figure 1.3 : Schematic diagram of the effect of an allergen at the cellular level on the release of inflammatory mediators.

a) Basic mechanism leading to the release of inflammatory mediators.

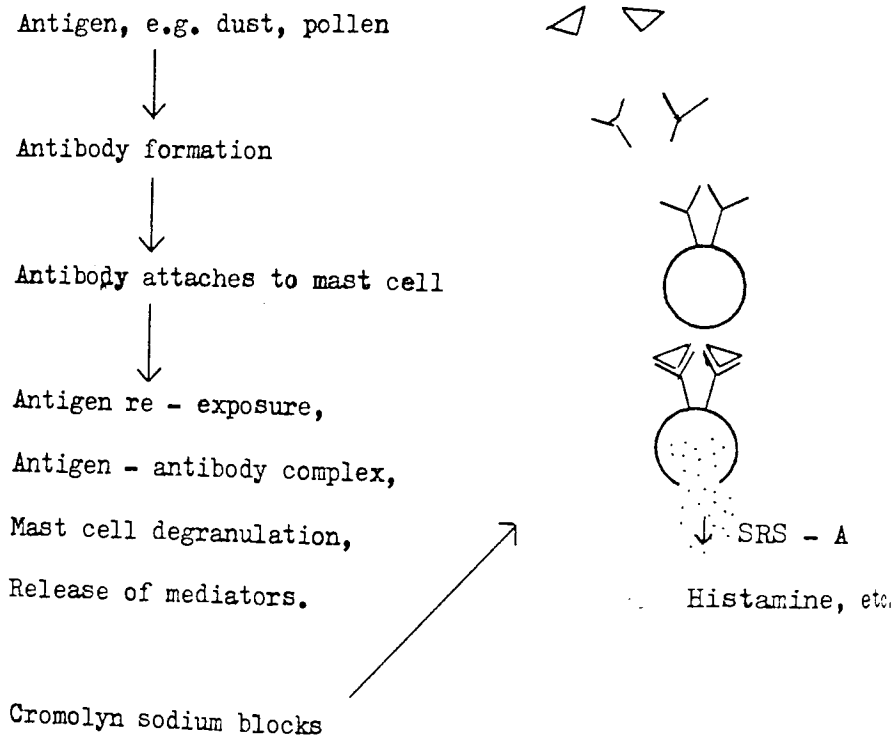

b) The oxidative metabolism of arachidonic acid by human lung mast cells.

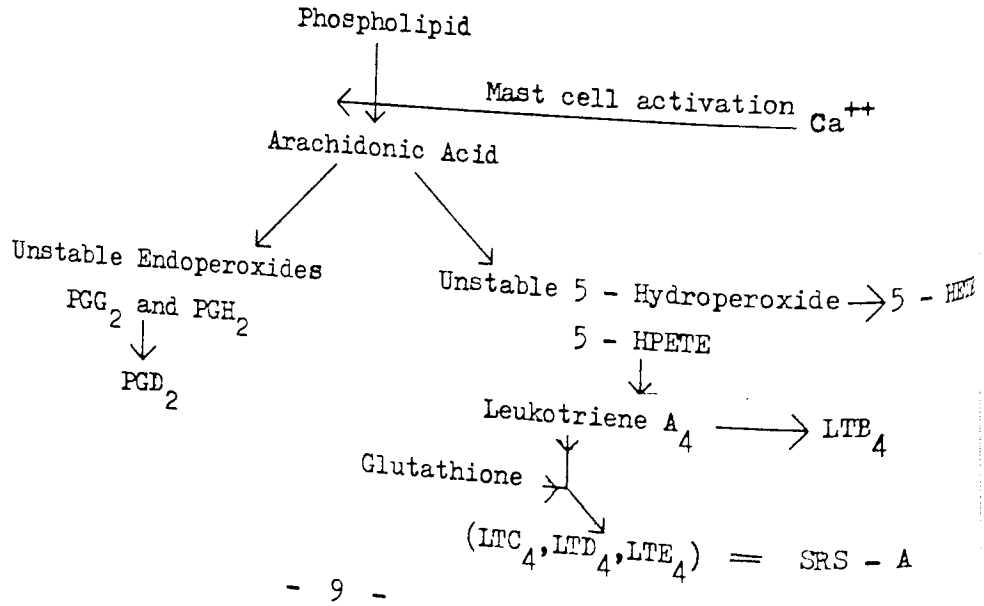

responsible for the bronchoconstriction of airway smooth muscle. Cholinergic agonists bind to guanyl cyclase and facilitate the conversion of guanosine triphosphate (GTP) to cyclic (3'5') guanosine monophosphate (GMP) which in turn results in bronchoconstriction and histamine release. Muscarinic receptor (postganglionic synapse cholinergic receptor) antagonists such as atropine (50) and ipratropium (64) inhibit this chain of events.

The neuronal control of bronchodilation via the nonadrenergic, noncholinergic system is as yet not used to any advantage clinically as the neurotransmitter involved remains unknown (59,65,66)

Figure 1.3 shows the effect of an allergen at the cellular level on the release of inflammatory mediators. These have been implicated in mucosal oedema and vagally stimulated bronchoconstriction (10,61). Sodium cromoglycate is used prophylactically to reduce mast cell degranulation and thus to reduce the release of inflammatory mediators (67,68).

1.2 Therapeutic And Diagnostic Aerosols.

The drugs which have been described above for the treatment of certain respiratory disorders must be considered the most frequently administered components of inhalation aerosols in clinical therapy. Other therapeutic and diagnostic aerosols are in use.

Local anaesthesia of bronchial airways with lidocaine aerosols has shown promising results (69 - 73). There is less evidence for the efficacy of antimicrobial, antifungal and mucolytic aerosols (74 - 79). It might be thought that humidification of airways and reduction of the viscosity of sputum would improve the mucociliary clearance in chronic bronchitis or cystic fibrosis. 'Bland' aerosols, such as water or saline , have not been shown to exhibit beneficial effects

clinically (80 - 85). Aerosol vaccination against certain diseases of the respiratory tract has been investigated but further studies are required before any meaningful conclusions can be drawn (86,87).

There is a growing interest in the diagnostic application of inhalation aerosols. Aerosolised solutions of bronchospastic agents are administered in provocation tests for the diagnosis and assessment of bronchial asthma (88,89). Radio - labelled aerosols may be used to image the lungs using certain detector devices (90,91).

Aerosol generating devices are frequently developed (92 - 94, Chapter 5) with a view to improving the deposition characteristics of the aerosol particles in the respiratory tract. Standard procedures for the use of certain types of generator are also being investigated (95), in order to optimise the respiratory variables involved with deposition. The passage of aerosol particles or droplets from the aerosol generator to the patient is fraught with problems. Pressurised pack inhalers generate the drug in solvent droplets. These droplets require time to evaporate in order that the fraction of the dose, of a particle size in the respirable range, is large enough to have the desired therapeutic effect. The degree of variation due to the practices of patients during self administration of therapeutic aerosols from pressurised packs has been noted (96 - 104). Spacer devices have been developed for these pressurised packs (105,106) to ensure adequate time for solvent evaporation and to standardise the delivery of the aerosol from the generator to the patients mouth.

In order to optimise the therapeutic effect of a drug delivered as an aerosol it is desireable to deposit drug particles at their site of action. Beta adrenergic receptors progressively increase in density from the trachea to the terminal bronchioles (Section 1.1.1.1, 34,35). The pulmonary region, consisting of terminal bronchioles

and alveoli, is highly vascularised. The effect of inhibition of microvascular leakage (10) and vasoconstriction (28,29) would be of great significance in this region. The therapeutic effect of depositing $beta_2$ - adrenergic agonists in the lower regions of the respiratory tract has been demonstrated (107). It has been shown that for a variety of pharmaceutical aerosols much of the dose is lost by deposition in the throat or in the upper respiratory tract where it is subsequently cleared by the action of cilia mucus and swallowing (2,77). As a consequence of this very little reaches the lower respiratory airways (108,109). The mechanisms of deposition within the lung would seem, therefore, to have a fundamental bearing on the therapeutic effect of a drug delivered as an aerosol.

1.3 Mechanisms Of Aerosol Deposition Within The Lung.

Before considering the factors effecting deposition of aerosols within the lung a brief resume of the parameters used to describe an aerosol particle size distribution is required.

1.3.1 Particle Size Distribution.

The most commonly used measurement for the particle size is the mass median aerodynamic diameter. The mass median is the point above and below which 50% of the aerosol resides, by mass. The aerodynamic diameter accounts for shape and density (110)

$$D_{ae} = \left[\rho_p \, C(D_e) \, D_e^2 / \rho_0 K \, C(D_{ae}) \right]^{1/2} \qquad 1.1$$

Where ρ_p is the density of the particle, K is the shape factor, D_{ae} and D_e are the aerodynamic equivalent and equivalent volume diameters,

and $C(D_{ae})$ and $C(D_e)$ are the Cunningham slip factors for the respective diameters. The equivalent volume diameter may be defined as the diameter of a sphere of the same volume as the particle. The aerodynamic equivalent diameter may be defined as the diameter of a sphere of unit density having the same falling velocity as the particle. Cunningham's slip factor is a semi - empirical factor which corrects Stokes' law of viscous resistance for the effect of slip. When particles are moving through the air they interact with air molecules, thus the sedimentation velocity is a function of the force in the direction of movement, the resistance forces of viscosity of the air and the radius of the particle. When a particle is small, a discontinuity of momentum transfer occurs at the surface of the particle, which is related to the mean free path of the air molecules. This discontinuity reduces the effective air viscosity and the particles are said to slip. In general this correction factor concerns particles below 1 μm. The shape factor becomes significant when the particle deviates radically from a sphere. Equation 1.1 may be simplified to,

$$D_{ae} = \sqrt{\rho_p} \cdot D_e \qquad 1.2$$

when near spherical particles greater than 1 μm are examined.

The distribution of most aerosols may be described as logarithmically normal. That is a slightly skewed distribution which becomes normal if the logarithms of the particle size are plotted against frequency, or fraction deposited. The distribution is described by the geometric standard deviation which may be calculated (111) as follows,

$$\ln \sigma_g = \left[\sum_i^N \ln(r_i/\bar{r}_g)^2 / N \right]^{1/2} \qquad 1.3$$

Figure 1,4 : Schematic diagram of the anatomy of the lung and graph of the fraction deposited in different parts based on the particle size and distribution of an aerosol.

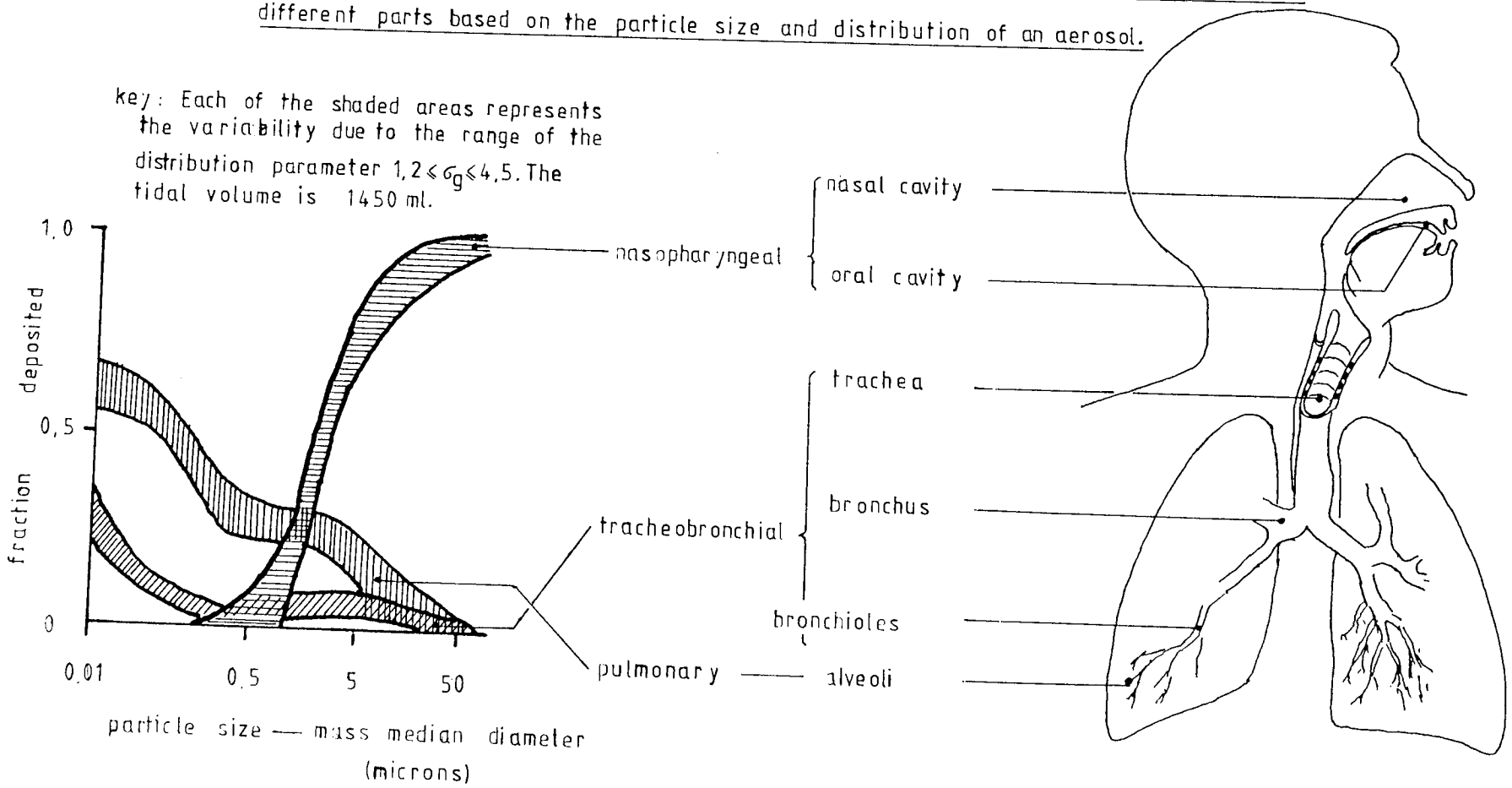

Where σ_g is the geometric standard deviation, N is the number of particles, r_i the individual particle radius and $\bar{r}_g$ is the geometric mean radius,

$$\bar{r}_g = \left[\prod_i^N r_i \right]^{1/N} \qquad 1.4$$

1.3.2 The Anatomy And Physiology Of The Respiratory Tract.

In considering the mechanisms of aerosol deposition within the lung and factors which may influence them it is of some importance to first consider the anatomy and air velocities within the respiratory tract. The temporal aspects of the passage of air through various anatomical regions and the point during the breathing cycle are also relevant factors.

The respiratory system is usefully broken down into three main parts which are illustrated in Figure 1.4 (2,112). These regions are the nasopharyngeal structure, the system of branching ducts beginning with the trachea and ending with the terminal bronchioles which serve to distribute the inhaled air throughout the lungs, and the pulmonary structure within which oxygen and carbon dioxide are exchanged between respired air and the blood.

The figure also illustrates the deposition of respired particles in these various regions in terms of the fraction deposited for a certain particle size. The hatched regions indicate a wide range of particle size distributions ($1.2 < \sigma_g < 4.5$) and these estimates are based on a single flow rate, 1.45 L min^{-1}. In general it may be observed that smaller particles deposit in the lower airways and large ones in the upper airways.

The angles of branching and diameter and lengths of different

Table 1.1 : Schematic representation of the respiratory tract.

Region	Diameter cm	Length cm	Velocity cm s^{-1}	Passage time s
Mouth	2	7	100	0,07
Pharynx	3	3	45	0,07
Trachea	1,4	11	150	0,07
Prim bronchi	1,0	6,5	190	0,03
Sec bronchii	0,4	3	200	0,0 15
Ter bronchi	0,2	1,5	100	?,0 15
Quart bronchi	0,15	0,5	22	0,02
Terminal				
bronchioles	0,06	0,3	2	0,15
Resp bronchi	0,05	0,15	1,4	0,1
Alveolar ducts	0,02	0,02	-	-
Alveolar sacs	0,03	0,03	-	-

After Landahl (113, 138)

elements of the airways and of the pulmonary air spaces have to be visualised in an arbitrary and oversimplified form to make practical use of anatomical data. Table 1.1 (2) shows some of the details of the divisions of the respiratory system which have been assumed by Landahl (113) and the anatomical, flow rate and transit features in these areas.

For a given volume of ventilation per minute, the actual rate of airflow throughout the respiratory cycle varies from zero to maximum and back to zero. Thus, as air velocity and time of air transit within the system determine the effectiveness of particle deposition, it is evident that this must vary over a considerable range within the cycle.

At least two regions which are ventilated at different rates have been identified. Of the total inspired air 40% ventilates one sixth of the lung and the remaining 60% the other five sixths. In consequence of such unequal distribution of ventilation, air velocities and times of air passage will vary producing different probabilities of deposition of inhaled particles from one site to another at the same structural depth.

The volume of the nasopharyngeal chamber and airways is 150 ml. Thus with a resting (tidal) volume of 600 ml only 75% of the air reaches the pulmonary air spaces. There is evidence to suggest that sequential breathing patterns occur resulting in poorly ventilated regions.

The complexity of the anatomical and dynamic factors involved in deposition can readily be appreciated from the brief outline of the factors involved.

The physiological factors which influence aerosol deposition in the lung have been investigated experimentally (114 - 119) and theoretically (120 - 127). Flow rates within the lung effect deposition

Table 1.1 : Schematic representation of the respiratory tract.

and airway obstruction (128), breathing rate (129,130) and breath holding (131 - 133) determine these rates. Since species variations (134, 135) and the state of the lung, whether healthy or diseased (135,136), influence the physiological factors, they are being investigated with a view to establishing predictable patterns in deposition.

The nature of particle deposition forces and their relationship to aerodynamic particle size have been the subject of many studies and reports. A variety of models for aerosol deposition in the respiratory tract have been proposed. The most notable are those of Findeisen (137), Landahl (113,138) and Weibel (139).

Rohrer (140) measured the diameter and length of the elements of the bronchial tree and constructed a dimensional model om which he based his reasoning on flow resistance in the human airways.

Findeisen was the first to examine the problem of respiratory deposition of aerosols in physical - mathematical terms. After dividing the airways into nine successive sections, starting with the trachea, he assumed a constant rate of respiration ($f = 15\ min^{-1}$, $V = 200$ ml) from which he calculated the air velocities and times of air passage through successive zones. Using these parameters average angles of branching from one order to the next could be postulated.

Landahl modified the assumed anatomical arrangement in some respects. In this model the airways were divided into 12 sections by including the mouth and pharynx and two orders of alveolar ducts. The parameters adopted in this model were a tidal volume of 450 ml, a breathing frequency of 15 min^{-1}, pauses of half seconds at the beginning and middle of each cycle and a constant respiration rate of 300 ml s^{-1}. The local velocities and times of air passage through the successive sections were obtained using this flow rate and a

variety of breathing frequencies and tidal volumes in Landahl's calculation of respiratory deposition. In all cases the inspiratory and expiratory phases are assumed to consist of a constant air flow rate. Work based on this model has been carried out by Beeckmans (141).

Weibel (139) has criticised the Findeisen/Landahl model as being based on insufficient actual data and thus, he suggests, the dimension of even the proximal airways are not correct. The zones consisting of different branching factors are also criticised as inadequately representing the pulmonary architecture.

Weibel proposed two alternative models, the first emphasised the regular features of the airways and the second accounted for some of the irregularities. The fundamental geometry of dichotomy was the basis for these models which refer to the average adult lung and comprise the airways of the conductive, transitory, and respiratory zone, as well as the blood vessels (alveolar capillaries) of the respiratory zone.

Experimental data on the deposition of aerosols in vivo have been described by Lippmann (118,142 - 144). Lippmann has noted that among normal subjects and non - bronchitic smokers each individual has a characteristic and reproducible relationship of particle size to deposition. This contrasts with the great variation from subject to subject among both non - smokers, cigarette smokers and patients with lung disease. Other studies pertaining to alveolar penetration, deposition and mixing have been performed (141,145). Deposition studies directed at particles with minimal settling and diffusional deposition tendencies, i.e. 0.1 to 1.0 µm, have been described by Davies (146,147). Particulate deposition studies of the nasal airways have been reported (148 - 150) as well as deposition by mouth inhalation (109). Other studies have been carried out emphasising deposition

Of highly diffusive aerosols (133).

In 1966 the Task Group on lung dynamics examined the models and experimental data available in the literature and described the deposition of aerosols in three areas of the lung, the nasopharyngeal, tracheobronchial and pulmonary regions (112). The authors' major concern was the deposition of hazardous aerosols.

The Task Group's predictive model uses Findeisen's simplified anatomy and his impaction and sedimentation equations (137). For diffusional deposition the equations of Gormley and Kennedy (151) were used and entry through the nose assumed.

For a tidal volume of 1450 ml there were relatively small differences in estimated deposition over a wide range of geometric standard deviations ($1.2 \leq \sigma_g \leq 4.5$). The comparison of this model with earlier predictive models indicates that Landahl's model is closest but overestimates alveolar deposition for particles with aerodynamic diameters larger than 3.5 μm. The major conclusion of the group was that regional deposition within the respiratory tract may be estimated using a single aerosol measurement, the mass median diameter. Subsequently authors (152,153) have reaffirmed the importance of the geometric standard deviation, taken in conjunction with the mass median diameter, in mouth breathing, for describing the character of an aerosol. This may be of particular relevance due to the heterodisperse nature of therapeutic aerosols (154). The degree of dispersity of an aerosol, which may be described by the geometric standard deviation, has been shown to significantly influence aerosol deposition in the respiratory tract. Models have also been developed for mouth inhalation where the complex nasal filtration and deposition does not occur (154,155).

From the Task Group model it was suggested that particles

must be below 10 μm before they deposit in regions below the nasopharynx Between 1 and 5 μm the aerosol deposits predominantly in the tracheobronchial and pulmonary regions and below 1 μm pulmonary deposition alone predominates. This guide to the deposition of aerosol particles may be explained in terms of the various methods of deposition which may occur.

1.3.3 Methods Of Deposition.

Reviews of particulate deposition have been published by various authors (112,156 - 161). The physical factors of deposition are governed by parameters associated with the particle, of particle size (146, 162 - 165), shape (120,164,166 - 169) and density (164,110). These parameters are of interest therapeutically because of the possibility of modifying the aerosol particles in order to achieve a desired deposition pattern.

The methods by which particles may be deposited in the respiratory tract may be listed as : impaction ; interception ; sedimentation ; diffusion ; electrical and thermal precipitation.

1.3.3.1 Inertial Impaction.

Inertial impaction arises from the tendency of a particle moving in a stream of air to follow its previous trajectory and impact upon some tissue. This occurs, for example, at bronchial branch points.

Inertial precipitation is limited by the balance between the inertial and resistance forces. This balance is proportional to the stopping distance of the particle as it moves through air. For a particle travelling on an air stream which undergoes a sudden bend. the effective stopping distance for sideways movement of the particle at right angles to the direction of travel will be, S_d, where

$$S_d = \nu_{TS} U_0 \sin \theta / g \qquad 1.5$$

U_0 is the velocity of the air stream, and thus of the particle, approaching the bend of angle θ and $U_0 \sin \theta$ is therefore the component of the initial particle velocity at right angles to the direction of flow, ν_{TS} is the settling velocity.

The probability that inertial impaction will occur is proportional to the ratio of the stopping distance to the radius or diameter of the airway. This dimensionless ratio is called the Stokes' number.

$$Stk = S_d / d' \qquad 1.6$$

The Stokes' number is the ratio of the particle's persistence to the size of the obstacle. As the Stokes' number approaches zero, particles track the streamlines perfectly. As the Stokes' number increases, the particles resist changing their direction with the gas streamlines.

1.3.3.2 Interception.

Particles may be intercepted as they pass from one tube into a smaller one because the streamlines along which they move enter the second tube at a distance from its walls that is less than the radius of the particle.

1.3.3.3 Sedimentation.

The sedimentation velocity may be represented as a function of particle diameter which may be computed from Stokes' law for viscous drag of a moving sphere.

$$F = 6\pi\eta r \nu \qquad 1.7$$

Where F is force Nm^{-1}, η is viscosity at 20 °C and atmospheric pressure in air, r is the radius of the sphere and ν is the constant velocity of movement when the force g is balanced by viscous drag, f. Thus

$$6\pi\eta r\nu = 4(\rho_p - \rho_g)\pi r^3 g / 3 \qquad 1.8$$

and

$$\nu_{TS} = 2\rho_p r^2 g / 9\eta \qquad 1.9$$

Where ν_{TS} is the terminal settling velocity or sedimentation velocity, g is the acceleration due to gravity, ρ_p is the density of the particle, ρ_g is the density of the gas. The latter is included to account for the buoyancy effect, but this can usually be neglected because ρ_p is much greater than ρ_g.

1.3.3.4 Diffusion.

The Brownian motion of microscopic particles arises as a consequence of random bombardment by the gas molecules which surround them. The root mean square displacement along any axis during a time t is,

$$\bar{x} = \left[2tKTC / 3\pi\eta d\right]^{1/2} \qquad 1.10$$

Where K is Boltzmann's constant, T is absolute temperature, t is time and C is Cunningham's slip factor, d is the diameter of the particle.

The accepted value for the mean free path of air molecules at a temperature of 23 °C and barometric pressure of 76 cm Hg is 0.0653 µm. Since the mean free path of gas molecules is inversely proportional to their concentration , from the ideal gas equation of state, the mean free path, λ, of air molecules in micrometer units at temperature, T (°K) and pressure, P (cm Hg) can be calculated as :

Table 1.2 : Comparison of slip correction calculations at 21°C and 76 cm Hg.

D (μm)	Cunningham Approx^{n} A = 1.26	Fuchs	Reif	Hinds
0.001	(165)	217	222	216
0.005	(33.7)	43.9	44.9	43.6
0.01	(17.3)	22.3	22.7	22.1
0.05	(4.27)	5.01	5.04	4.94
0.1	(2.6)	2.895	2.888	2.854
0.5	1.327	1.327	1.329	1.328
1.0	1.163	1.162	1.164	1.163

$$\lambda = 0.0653\ (76/P)(T/296.2) \qquad 1.11$$

Based upon the mean free path, λ, an approximation for the slip correction, C(D), for spherical particles of geometric diameter, D, is given by :

$$C(D) = 1 + 2A(\lambda/D) \qquad 1.12$$

lations at 21°C

with,
$$A = \alpha + \beta\, e^{-(\gamma D/2\lambda)} \qquad 1.13$$

Hinds

The terms α, β and γ are constants which are determined experimentally. Values for these experimentally determined constants have been given by various authors (164,170 - 172). The Cunningham equation assumes that A is constant, with a value of 1.26 (172). At 21°C and 76 cm Hg the constant value for A is not significantly different from the values values obtained using the experimentally determined constants, for particles above 0.5 µm in diameter (110). Table 1.2 shows values for the slip correction at the aforementioned temperature and pressure. It can be seen that the slip correction factor begins to become significant at 1 µm and smaller diameters, that is to say the value deviates significantly from 1.0.

216
43.6
22.1
4.94
2.854
1.328
1.163

Diffusion (173) only becomes important in the deposition of an aerosol in the smaller airways where the distances are short and the residence times comparitively long. This method of deposition is significant for small particles.

1.3.3.5 Electrostatic, Thermal And Other Methods Of Deposition.

Electrostatic precipitation is a method of deposition important where the particles are charged. The particles interact with the walls

of the respiratory tract by image forces (173,174) at the site of deposition. Some minor forces are thermal, diffusiophoretic and sonic forces (173).

1.3.4 Condensation Growth.

Any factor which brings about a change in the particle size distribution of an aerosol will alter its deposition characteristics. Condensation growth may bring about a change in the deposition of aerosol particles or droplets. Some consideration must, therefore, be given to the methods of condensation growth.

1.3.4.1 Methods Of Condensation Growth.

The formation and growth of aerosol particles by condensation is the principle method of aerosol production in nature (175,176) and the most important mass transfer process between the gas phase and the particle phase (176). The rate of condensation growth depends on the saturation ratio, particle size and particle size relative to the mean free path of the medium, air. Generally the role of the gas is central to the description of transport processes involving aerosol particles. To quantify this role, the particle Knudsen number is conventionally defined as, $Kn = 2\lambda/d$, where λ is the gas molecular mean free path and d is the particle diameter. In these terms, the kinetic condition $Kn \leqslant 0.25$ is termed the collision dominated or continuum regime, since the gas can be treated as a fluid or continuum The condition $Kn \geqslant 10$ is termed the free molecular regime since particle - gas collisions are isolated showing the particles to follow primarily collisionless trajectories as in the case for individual molecules in a dilute gas. The transition regime, $0.25 \leqslant Kn \leqslant 10$, fall between the collision dominated and free molecular regimes.

The method of condensation growth may be placed in one of two categories depending on the initiation process for particle formation. These categories are known as homogeneous and heterogeneous nucleation processes.

Homogeneous nucleation is the formation of particles from a supersaturated vapour without the assistance of condensation nuclei or ions. The process is also called self nucleation. This type of particle formation seldom arises in nature but can be studied artificially (177,178). It is a useful starting point for the consideration of the more common conditions encountered.

In the absence of foreign particles, aggregates of the condensed phase can arise only as the result of chance collisions of molecules in the supersaturated vapour. These small aggregates or embryos are continually formed and disrupted because of microscopic thermal and density fluctuations in the vapour. Only if they surpass a certain critical size determined by the prevailing supersaturation and temperature, can they survive and continue to grow, otherwise they evaporate and disappear. The supersaturated vapour is a metastable phase, and the embryos can grow to become nuclei for the development of the liquid phase only if they attain a size at which they are more stable than the vapour phase. The probability of forming an aggregate of critical size increases as the supersaturation is increased. The critical diameter d^*, which the aggregate, assumed spherical, must attain in order to be in, unstable, equilibrium with the vapour was first derived from thermodynamic arguments (179) and is known as the Kelvin equation.

$$d^* = 4M\sigma_{LV} / \rho_{LV} RT \ln \frac{p}{p_\infty} \qquad 1.14$$

where p_∞ is the supersaturation pressure, p is the equilibrium vapour pressure, T is temperature over the plane surface of the liquid, σ_{LV} is the specific surface energy of the liquid - vapour interface, ρ_{LV} is the density of the liquid (strictly liquid - vapour density), R is the universal gas constant and, M is the molecular weight of liquid.

The atmosphere is never sufficiently clean for condensation to occur homogeneously or upon ions. Particles of dust (180), smoke (181, 182), hygroscopic crystals (183 - 185) and small droplets (186) of solution may also serve as condensation centres.

Heterogeneous nucleation is a process of particle formation and growth that is promoted by the presence of condensation nuclei or ions. For a given saturation ratio a particle must initially reach a diameter, d^*, to grow and become a stable droplet. A theoretical (187) saturation ratio of 220 is required for growth to commence on an individual water molecule (d = 0.0004 μm). Experimental measurements of pure materials have shown that particle formation and growth occurs at saturation ratios far less than this, less than 10 for pure materials and less than 1.02 for nucleated condensation (187). In the case of soluble nuclei, condensation can occur in unsaturated conditions and size stable droplets can be formed. Nucleated condensation is the primary mechanism for cloud formation in the atmosphere (187,188).

Insoluble nuclei provide a passive site for condensation in supersaturated vapour. At a given supersaturation, an insoluble nucleus larger than d^* with an adsorbed layer of vapour behaves like a droplet of that size and grows by condensation. Under favourable conditions the size of the nuclei required for growth at a given supersaturation is given by d^* in the Kelvin equation, 1.14.

The normal atmosphere contains about 1,000 ions cm^{-3} (179). These ions are continuously created by the action of cosmic radiation

and radioactive gases that emanate from the ground. Ions are singly charged clusters of about 30 air molecules (179). These molecular clusters differ from those described previously in that they are stable.

The presence of a charged molecular cluster slightly distorts the saturation ratio versus d^* curve, facilitating the formation and growth of droplets at supersaturations greater than about 2.0. Since the atmosphere contains numerous condensation nuclei that can cause particle formation and growth at much lower supersaturations, air ions have little effect on the formation of particles larger than 0.01 μm in the atmosphere (189).

The ability of air ions to promote particle formation and growth at high saturation ratios has been used in Wilson cloud chamber experiments to observe the tracks associated with radioactive decay (190,191). Radioactive disintegration produces an alpha particle, it travels centimeters through the air leaving behind a wake of thousands of air ions. The growth of these particles enables the path to be traced with suitable lighting.

Sodium chloride nuclei (192,193) are formed in great numbers by the action of waves and bubbles in the oceans (194) and exist throughout the global atmosphere (187, 188).

The primary mechanism of water droplet formation in the atmosphere is the growth of soluble droplets (183 - 185, 195 - 197). Supersaturation rarely exceeds a few percent since water vapour associates with the growing soluble nuclei. The salt concentration will increase with decreasing particle size thus reducing the vapour pressure at the droplet surface. The Kelvin effect causes an increase in the vapour pressure as the particle size decreases. The relationship between satuturation ratio and particle size for droplets containing dissolved materials is given by,

$$p/p_s = (1 + (6imM_w/M_s\rho\pi d_p^3))^{-1} \exp(4\gamma M_w/\rho RTd_p) \quad 1.15$$

Where m is the mass of the dissolved salt having a molecular weight M_s, M_w is the molecular weight of the solvent, usually water, ρ is the density of the solvent, and i is the number of ions each molecule of salt forms when it dissolves.

1.3.4.2 The Effect Of Condensation Growth On Inhalation Aerosols.

The presence of aerosols in the atmosphere in the form of particles or droplets of salt (183 - 185, 195 - 197) or radioactive (149,162) materials has given rise to some concern over their potentially hazardous nature if inhaled (148,149,198,199). Theoretical (183 - 185, 195,196)and experimental investigations have been carried out. The experimental work has been undertaken in both man (200,201) and experimental animals (202 - 204). The importance of condensation growth in the deposition of environmental aerosols has been responsible for much of the research carried out in this area of aerosol science. Understanding the factors which contribute to deposition in the respiratory tract might lead to a reduction in the hazard posed by environmental aerosols. The same concepts are, however, equally well applied to the formulation of pharmaceutical aerosols, where modified deposition characteristics may improve the therapeutic effect of a particular inhalation aerosol.

It was noted in the previous section, from equation 1.14, that temperature and relative humidity are important considerations in condensation growth. Shortly after entry into the respiratory tract, an aerosol experiences a humidity corresponding to the vapour above isotonic tissue fluids at 37°C, that is approximately 99.5% (205,206).

An equation has been derived from which it is possible to predict

the growth of hygroscopic aerosols, assuming ideal solution behaviour (205). The dynamic growth ratio is,

$$R_a = D_{ae,l}/D_{ae,s} = (1/g_s)^{1/3} \rho_l/\rho_p \qquad 1.16$$

Where $D_{ae,l}$ is the equilibrium aerodynamic equivalent diameter of a particle in the lung, $D_{ae,s}$ is the aerodynamic equivalent diameter of the dry particle, ρ_l is the density of the particle in the lung and ρ_p is the density of a dry particle,

and,
$$g_s = m_p/(m_{w,l} + m_p) \qquad 1.17$$

Where m_p is the mass of the dry particle and $m_{w,l}$ is the mass of water in the aerosol particle in the lung.

Experimental and theoretical investigations of hygroscopic growth of a variety of aerosols have been carried out. Pure acids and salts (178, 207, 208), pharmaceutical compounds (200,209 - 214) and household products (215,216) have all been examined.

Using equations 1.16 and 1.17 the increase in aerodynamic equivalent diameter has been calculated (205) for some salts, assuming a 1 μm initial diameter, under conditions such as those in the lung. The growth in the aerodynamic diameter was shown to vary between 1.9 for lead nitrate and 4.7 for sodium hydroxide.

Sodium chloride has been used as a standard aerosol for contrasting the growth rates of pharmaceutical aerosols (207,208). Assuming ideal solution behaviour the growth ratio for sodium chloride at 99.5% relative humidity has been estimated as 4.1 (205). Experimentally a growth ratio of 3.7, at 98% relative humidity and 37 °C, has been observed (21). This difference may be explained by the assumption of

ideal solution behaviour for the estimated values (214).

A number of both predictive (205, 208, 214) and experimental (209 - 213) investigations of the hygroscopic growth of pharmaceutical aerosols have placed the growth ratios for these compounds in the range 2.0 to 3.0. For example one author (214) quotes a growth ratio of 2.6 for disodium cromoglycate and isoprenaline sulphate dihydrate. Martonen (210) has indicated that isoprenaline hydrochloride particles reach a maximum growth ratio, of between 1.2 and 2.0 for particles ranging from 5 to 2 μm respectively, by the first airway generation. This corresponds to the observation that (217) the temperature and relative humidity reach a maximum at this point. An upper limit for the time taken for this to occur is 0.2 seconds. High Reynolds numbers indicative of turbulent flow will contribute to the speed of growth in the upper airways (210). The Reynolds number is proportional to the ratio of inertial forces to frictional forces acting on each element of the fluid (171). The Reynolds number may be expressed as

$$Re = \rho Vd/\eta \qquad 1.18$$

Where ρ is the density of the fluid, in this case air, V is the relative velocity between the fluid and an object such as a particle, d is the characteristic linear dimension such as the diameter of a pipe and η is the viscosity. Using constants for air at 20°C a simpler form for the Reynolds number is obtained

$$Re = 6.6\ Vd \qquad 1.19$$

The implications of hygroscopic growth in the respiratory tract is of importance in the deposition of pharmaceutical aerosols. The

probability of hygroscopic growth affecting particle deposition in the respiratory tract has been recognised for some years (192,218). The relative humidity in the nasopharynx is high enough for significant hygroscopic growth to begin almost immediately upon entering the respiratory tract (205,206). Some caution in the expectation of hygroscopic growth has been suggested (208) since experimental observation of deposition in the respiratory tract implies that overestimates of growth may occur. This may be explained by the assumption of ideal mixing in the trachea which ignores the laryngeal jet (115). A lower relative humidity on the wall of the upper airways may be caused by a higher ion concentration in the mucus (217). Since hygroscopic growth rates increase with the degree of relative humidity (210),growth will prog ressively increase as the particles pass into the respiratory tract. Hygroscopic growth has been observed to augment total deposition of sodium chloride aerosols by 60% (208). The overall efficiencies of the major deposition mechanisms in the respiratory tract are greatly influenced by hygroscopic growth. Sedimentation diffusion have been observed to reverse in significance as the mechanisms of deposition of submicron hygroscopic compared with non - hygroscopic aerosols,and significant increases in impaction in the upper airways also occur. Correctly formulating and accounting for these effects may permit pharmaceutical aerosols to be selectively deposited at target sites within the lung and thus improve clinical aerosol therapy (208).

Surfactants are included in aerosol formulations as emulsifiers and as valve lubricators (219,220). Both increases (215) and reductions (221,222) in the association of water with hygroscopic particles have been attributed to the presence of surfactants. It seems possible that some control of hygroscopicity might be achieved by known,

quantitative and qualitative, association between selected surfactants and hygroscopic aerosol powders.

1.4 The Aim Of The Present Work.

Coating the surface of hygroscopic aerosol particles, with a compound of a different hydrophobic or hydrophilic nature, might modify the tendency of the surface to interact with water molecules in the atmosphere. The hygroscopic growth of therapeutic aerosols is influenced by the degree of relative humidity which may lead to inappropriate deposition characteristics in the lung. Controlling the effects of hygroscopic growth by formulation would seem, therefore, to be a useful tool in clinical aerosol therapy. Surfactants would appear to be suitable coating materials because of their hydrophobic and hydrophilic composition. This hypothesis, of the suitability of the surfactants as coating materials, may be examined by : Generating characterised coated aerosols and ; testing the hygroscopic growth of coated versus uncoated powders.

The first section describes work carried out to investigate the most suitable coating materials and assay techniques. The procedures adopted were then used to produce and characterise the coated powders.

The second section describes the generation and particle size analysis of these powders in an environment of temperature and relative humidity approaching that in the lung.

C H A P T E R T W O

Coating of disodium fluorescein using various surfactants.

2. Coating Of Disodium Fluorescein Using Various Surfactants.

2.1 Introduction.

The use of surfactants as coating materials in these studies requires consideration of the nature of these compounds, their interactions with each other and their interaction with other substances.

2.1.1 Suface Activity.

Surface activity is a dynamic phenomenon, since the final state of a surface or interface represents a balance between the tendency towards adsorption and the tendency towards complete mixing due to the thermal motion of the molecules.

A surface active agent (surfactant) may be described as a substance which alters the conditions prevailing at the interface. All surfactants are characterised by consisting of two regions, a hydrocarbon chain, which is hydrophobic, and a hydrophilic group. The nature of the hydrophilic, polar, region of the surfactant enables the classification of surfactants to be subdivided into anionic, cationic and non - ionic. Examples of these are sodium dodecyl sulphate, dodecyl trimethyl ammonium bromide and n - dodecyl hexaoxyethylene glycol monoether respectively. Two further groups of surfactants exist, ampholytic surfactants which are zwitterionic and can behave as any of the aforementioned example depending on the pH at which they are maintained, such as alkyl betaine, and natural surfactants which usually contain a glycerol moiety, such as phosphatidylcholine. Surfactants may, therefore, be described as amphiphilic.(From the Greek 'amphi -' and '- philos')

The formation of aggregates (223) and micelles (224,225) in solutions of surfactants is well documented.

The term 'micelle' should designate any soluble aggregate spontaneously and reversibly formed from amphiphilic molecules or ions (226). The micellisation processes according to the commonly used equilibrium thermodynamical descriptions, namely the multiple equilibrium model and the pseudo phase model, are, like the micelle definition, equally well applicable to aqueous and non - polar surfactant solutions (227). The second model best conforms to the definition of a micelle described above.

The interactions governing the formation of surfactant aggregates in apolar media are different from those in aqueous solutions, in spite of the apparently similar building principle of lipophilic and hydrophilic micelles. The differences between interactions encountered in aqueous and non - polar surfactant solutions have been considered at a molecular level with reference to the stability or existence of micelles in apolar media (224). It has been concluded that once equilibrium between monomers and micelles, equivalent to the pseudo phase model, ceases to be operative and is replaced by a stepwise aggregation equilibrium, the concept of a critical micelle concentration, CMC, is inapplicable. The two models for the process of interaction between surfactant molecules, described above, are therfore considered to be mutually exclusive (223).

2.1.2 Inverted Or Reversed Micelles.

The formation of surfactant aggregates has been referred to briefly in the previous section, 2.1.1 . The driving force for aggregation in aqueous media is the extrusion of hydrocarbon chains from solution upon micelle formation, resulting in an overall decrease in the free energy of the system. In non - aqueous solution, aggregation of surfactant molecules depends upon both the solvent and surfactant structure.

Interactions between solvent and surfactant hydrocarbon chain groups tend to minimise the size of the aggregate, while interactions between the polar groups of the surfactants promote aggregation, in apolar solvent.

Kinetic treatments in both aqueous and non - aqueous micellar systems have been based on the Hartley model (228,229) of opposing hydrophobic interactions and electrostatic repulsions which are responsible for micellisation in water.

Surfactant association in apolar solvents is predominantly the consequence of dipole - dipole and ion pair interactions between the amphiphiles. This differs from the Hartley model and concepts derived for surfactant association in water may not necessarily be applicable to those in apolar solvents (230).

In a non - aqueous solution of concentration, C, existing as simple molecules, m, and micelles composed of n molecules in equivalent concentration, M_n , the mass law is as follows.

$$KM_n = m^n = (C - nM_n)^n \qquad 2.1$$

Where K is the dissociation constant of the micelles.

A phase separation model was advocated for use by Shinoda and Hutchinson (231), and successfully applied by Singleterry (232) and Fowkes (233) to describe the aggregation of dinonylnaphthalene sulphonates in benzene. The phase separation model postulates that micellisation is a phase transition. In its simplest form it does not contain a size - limitimg step and therefore it is of little value in accounting for the formation of the small aggregates seen in apolar media.

The application of the mass action law to the overall aggregation process $nm \overset{K_n}{\rightleftharpoons} M_n$, where K_n is the association constant of the process

affords a model. Thus with the conservation of mass :

$$[m] / [D] + n ([m] / [D])^{n} [D]^{n-1} K_{n} = 1 \qquad 2.2$$

Where [D] is the total molal concentration of detergent. From this equation assuming that K_n is the product of n - 1 individual and equal mass action constants, the following equation is obtained,

$$[m] / [D] + n [M_n] / [D] = 1 \qquad 2.3$$

and the CMC is then obtained,

$$CMC = 1/K = [D] \qquad 2.4$$

Where $[D] K = 1$.

This system allows for two aggregational states, monomers and micelles. This does not account for the distribution in molecular weights. Smooth transitions from monomer dimer trimer etc. with concentration dependent growth of aggregates have been observed. These gradual physical changes have been described (234) in terms of a sequential type self - association model. Assuming all values of equilibrium concentration are the same, K_{12} , K_{23} --- K_{ij} are assumed to be equal,

$$\text{monomer} + \text{monomer} \overset{K_{12}}{\rightleftharpoons} \text{dimer}$$

$$\text{dimer} + \text{monomer} \overset{K_{23}}{\rightleftharpoons} \text{trimer}$$

$$(n-1) - \text{mer} + \text{monomer} \overset{K_{ij}}{\rightleftharpoons} n - \text{mer}$$

then the weight fraction of the monomer, f , is related to the stoichiometric concentration of detergent [D] by the following equation

$$(1 - f^{1/2})/f = K_{ij} [D] \qquad 2.5$$

It has been indicated that it would be possible to modify the multiple equilibrium model to account for a critical concentration (235). Application of the mass action law to the aggregation, and conserving mass with respect to monomer yields,

$$[m] / [D] + \sum_{n-2}^{n} n ([m] / [D])^{n} [D]^{n-1} \prod_{n-2}^{n} K_{n-1} = 1 \qquad 2.6$$

A size limiting step may be introduced by requiring a functional relationship between the equilibrium constants and the association number , $K_n = f(n)$.(236)

The number of monomers involved in most surfactant aggregates in non - polar solvents is relatively small (typically less than 10 for alkylammonium carboxylates compared with up to 100 for aqueous micelles, 237.); consequently a spherical micelle structure would not provide effective shielding of the polar head groups from the solvent and its formation could be considered unlikely (238). The alternative model is that of a lamellar micelle in which the polar and hydrophobic groups are placed end to end and tail to tail, with water and organic solvents between them.(239,240)

The kinetics of formation and decomposition of micelles and of the association - dissociation of the monomer to and from the micelle have rarely been studied in reversed micellar solutions (241). This infrequency was attributed to two causes : 1. since the aggregation number of the micelle is very low, an abrupt and large change in the

physico - chemical properties of the solution cannot be expected at the CMC, and ; 2. micelle formation and monomer exchange reactions are too rapid to be observed by conventional techniques.

2.1.3 Adsorption From Solution.

The method by which surfactants interact with other substances is by adsorption at the interface. The interface may be a gas - liquid, liquid - liquid or solid - liquid juncture, the latter being significant in the present work.

Langmuir presented a general equation for the isotherm of localised adsorption that was suitable for describing the adsorption of solutes. Langmuir's approach (242) was concerned with monolayer coverage. The assumptions made for this model were : that molecules are adsorbed at active centres on the adsorbent surface which they occupy for a finiteperiod of time; owing to the small radius of action of adsorption forces and to their saturability, every active centre while adsorbing molecules becomes incapable of further adsorption. Langmuir's adsorption equation concerns the simplifying assumptions that the heat of adsorption is independent of surface coverage, thus ignoring adsorbate interaction and the weakening effect on the intermolecular forces by distance between the adsorbent and adsorbate. Fowler and Guggenheim (243) have adopted an approach which provides a modification for lateral interaction in the Langmuir model. Attempts have been made to generalise monolayer and multilayer concepts in order to describe the isotherms of different shapes by a single equation. Brunauer, Emmett and Teller (BET)(244) developed such a generalised theory in respect to adsorption of vapours which has since become known as the BET theory. The assumptions of the BET theory are : the adsorbent surface hasa definite number of active sites which are equivalent energetically and are capable of retaining

the adsorbate molecules ; the interaction of the neighbouring adsorbed molecules is neglected ; the molecules in each layer act as an adsorption site for subsequently adsorbed molecules ; it is assumed that all the adsorbed molecules in the second and subsequent layers have the same partition function as in the liquid state, which differs from the partition function of the first layer. Brunauer (245) has classified adsorption isotherms into five types.

The BET theory has been very useful in the interpretation of solute adsorption. This theory assumes that every molecule of a liquid has only two close neighbours , from the top and bottom chain, while the molecules of a real liquid are surrounded by many more adjacent molecules. Moreover Giles (246,247) has found both theoretically and experimentally the shape of some isotherms, of solute from solution, can be accounted for by postulating that adsorbate interaction does occur under particular conditions. The assumption that the adsorbent surface has a definite number or active sites which are equivalent energetically is an oversimplification (248,249).

The Langmuir model for adsorption assumes that while the adsorbed molecules occupy sites of energy Q they do not interact with each other. Fowler and Guggenheim (243) have adopted an approach which accounts for lateral interaction.

The probability of a given site of energy Q being occupied is N/S, and if each site has z neighbours the probability of a neighbour site being occupied is zN/S. So the fraction of adsorbed molecules is $z\theta/2$, the factor one half correcting for double counting and θ being total monolayer coverage. If the lateral interaction energy is ω, the added energy of adsorption is $z\omega\theta/2$, and the added differential energy of adsorption is just $z\omega\theta$.

The modified Langmuir equation then becomes,

$$b'C = \theta/(1 - \theta) \qquad 2.7$$

where C is the equilibrium concentration and,

$$b' = b_o \exp(Q - z\omega\theta)/RT = b \exp(z\omega\theta/RT) \qquad 2.8$$

rearranging these equations,

$$b\,C = \left(\theta/(1 - \theta)\right) \exp(-z\omega\theta/RT) \qquad 2.9$$

this is equivalent to the Frumkin or Volmer (250) expression

$$b\,C = \left(\theta/(1 - \theta)\right) \exp(-2\,a\,\theta) \qquad 2.10$$

therefore, $a = z\omega/2RT$, where a is the interaction energy between adsorbed molecules.

The adsorption of organic substances may yield sigmoid or logarithmic isotherms (246), depending on whether attractive or repulsive interaction predominates between the adsorbed particles.

The forces responsible for solute adsorption may be chemical or physicochemical and physical or mechanical (251). The chemical or physicochemical forces may be listed as : covalent bonding ; hydrogen bonds and other polar forces ; ion exchange attraction ; van der Waal's forces and; hydrophobic forces. The physical or mechanical forces are : restriction of movement of solute aggregates in micropores and; facilitation of entry of solute by the progressive breakdown of the substrate structure.

2.1.4 Techniques Employed And Choice Of Model Compound.

The techniques which may be used to investigate the phenomena in sections 2.1.1 - 2.1.3 have been outlined by Kertes and Gutmann (238) and include differential refractometry and surface tension measurement. These techniques have been used to investigate the interaction between surfactant molecules and between surfactant and powder molecules in non - aqueous solvents. Other techniques, such as gas liquid chromatography, infra - red spectroscopy and electron scanning chemical analysis, have been used to investigate the extent and nature of the interaction between the surfactant and the aerosol powder after removal from non - aqueous solvents. The purpose of these investigations was to coat model hygroscopic powders with a compound likely to effect their behaviour when generated as aerosols, under conditions of relative humidity and temperature approaching those of the lung.

Disodium fluorescein has been used as a model aerosol (252 - 254) powder. This compound has the properties of being hygroscopic and is readily assayed by spectrofluorimetry. A number of parallel experiments using this model aerosol powder in vivo were being carried out and consequently the use of this substance in these investigations would enable direct comparison with the work of other members of the research group. Since the powders to be used were hygroscopic the solvent, in which the adsorption at the surface of disodium fluorescein is to be attempted, must be non - aqueous and exhibit little or no solvent properties for this compound. Preliminary investigations established dichloromethane as such a solvent. The surfactants which may be used as coating materials for the model aerosol powders were investigated and are discussed in the following sections.

2.2 Materials And Methods.

2.2.1 Materials.

2.2.1.1 Apparatus.

i) Brice Phoenix Differential Refractometer, visual laboratory type, model BP - 2,000 - V. Phoenix Precision Instrument Company 3803 - 05, North - Fifth Street.

ii) Churchill Chiller Thermo - Circulator. Churchill Instrument Company Limited, Welmgate Road, Perivale, Greenford, Middlesex, England.

iii) Microbalance Type 2B, serial number 2B104. C.I. Electronics Limited, Brunel Road, Chuchfields, Salisbury, Wiltshire.

iv) Bryans XY Recorder 26000 A4. Bryans Southern Instruments Limited, Willow Lane, Mitcham, Surrey. CR4 4UL

v) Oertling Balance, model number R - 41, Oertling Limited, Cray Valley Works, St Mary Cray, Orpington. BR1 2HA

vi) Beckman Acta V. Ultra - Violet Spectrophotometer.

vii) Pye Unicam, series 204, Gas Liquid Chromatography apparatus, Pye Unicam Limited, York Street, Cambridge. CB1 2PX

viii) Infra - Red Spectrophotometer, Unicam SP200, Pye Unicam Limited, address as vii)

ix) Kratos ES 300 Spectrometer, A.E.I. Scientific Instruments, Barton Dock Road, Urmiston, Manchester. M31 2LD

x) Scanning Electron Microscope, Cambridge Model 2A, Cambridge Medical Instruments Limited, Rustat Road, Cambridge. CB1 3QH

xi) Strohlein Area Meter, Strohlein and Company, Hysol, Harlow. CM18 6QZ

2.2.1.2 Chemicals.

i) Acetone, chloroform, hexane and dichloromethane, AR grade. Fisons Scientific Apparatus, Loughborough, Leicestershire.

ii) AR Grade Disodium Fluorescein (BN 69305) - 6303h. (soluble fluorescein, resocinolphthalein sodium, uranin(e), uranine yellow) $C_{20}H_{10}Na_2O_5$, M. Weight 376.28. Micronised, 3.0 - 4.0 µm mass median diameter.

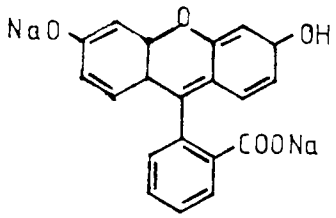

The water content of disodium fluorescein ranged from 11.9 to 27.5% by weight, as measured by Karl Fischer method, between various batches. The variation between bottles of the batch used in these studies was 12.1 ± 0.3 % , where three samples were assayed.

The carbon content for this batch was found to be 54.2 % as compared with a theoretical content of 56.0 % . The sodium content of this batch was 12.4 % as compared with a theoretical value of 10.7 % . Less than 5% difference was detected between expected and observed carbon contents of all fluorescein batches. The carbon content

determined by autoanalysis was invariably less than the theoretical content. In contrast, the proportion of sodium found experimentally was always greater than the theoretical value. This implies that any contamination was likely to be inorganic in nature.

The suppliers were Koch Light Laboratories, Colnbrook, Bucks.

iii) Oleyl alcohol (cis 9 - octadecen - 1 - ol), $C_{17}H_{33}CH_2OH$, M.Wt. 268.49 g, at 20°C ρ is 0.85 g cm^{-3}, n_D^{20} - 1.4606.

Stearyl alcohol (1 - octadecanol), $CH_3(CH_2)_{17}OH$, M.Wt. 270.5 g, at 20°C ρ is 0.8124 g cm^{-3}.

Boron trifluoride methanol.

The suppliers were BDH Chemicals Limited, Poole, Dorset.

iv) Lauric acid (dodecanoic acid) , $CH_3(CH_2)_{10}CO_2H$, M.Wt. 200.33 g , at 20°C ρ is 0.8679 g cm^{-3}.

Lauryl alcohol (1 - dodecanol) , $CH_3(CH_2)_{10}CH_2OH$, M.Wt. 186.32 g, at 20°C ρ is 0.8309 g cm^{-3}, n_D^{20} 0.8309 .

Capric acid (decanoic acid), $CH_3(CH_2)_8CO_2H$, M.Wt. 172.27 g , at 20°C ρ is 0.8858 g cm^{-3}.

1 - Undecanol (1 - hendecanol), $CH_3(CH_2)_9CH_2OH$, M.Wt. 172.31 g, at 20°C ρ is 0.8298 g cm^{-3}.

Suppliers Sigma Chemical Company Limited, Michigan. The purity of these samples was quoted as 99 % by the suppliers. In GLC examination of these compounds no analogues were detected. In the section concerning electron scanning chemical analysis the elemental analysis of the surface of these pure compounds indicates the presence of carbon and oxygen in the expected proportions.

v) Texofor 'A' range (polyoxyethylene glycol monoether of n - hexadecanol)

The molecular weights of the respective Texofor A_n 's are : n = 18, 1035.37 g ; n = 10, 682.95 g ; n = 6, 506.74 g and ; n = 2, 330.54 g.

The suppliers were ABM Chemicals, Pole Acre Lane, Woodley, Stockport, Cheshire, SK6 1PQ.

2.2.2 Methods.

A variety of techniques have been employed to investigate the association of surfactant with disodium fluorescein powder in non - aqueous solution.

2.2.2.1 Differential Refractometry.

Examination of the refractive index of surfactant solutions prior to, and following the addition of disodium fluorescein gives an estimate of the amount of surfactant removed from solution and hence of the extent of the association of the surfactant with the powder. The apparatus employed in this method of analysis of surfactant concentration in solution is shown in Figure 2.1 .

The green filter on the turret of the lamp housing was selected, having a wavelength of 546 nm . An estimate of the difference in refractive index which can be attributed to the cells must be carried out. This, solvent zero, can be found by taking a reading with the rotatable cell holder handle turned towards the lamp and a second reading taken with the handle facing the eyepiece. These readings are referred to as d_1 and d_2 respectively. Five readings were taken in each position and the average was then calculated.

The solution compartment of the differential cell was filled with one millilitre of the sample solution and allowed approximately 5 to 10 minutes for the temperature equilibration, of the solution and its solvent. The cell was maintained at 20°C. The reading was then taken as described. From this reading the Δd can be calculated,

$$\Delta d = (d_2 - d_1) - \text{solvent zero} \qquad 2.11$$

The refractive index is given by $\Delta n = K \Delta d$, where Δn is the refractive index difference between the solution and its solvent, K

Figure 2.1 Schematic diagram of a Brice - Phoenix Differential Refractometer.

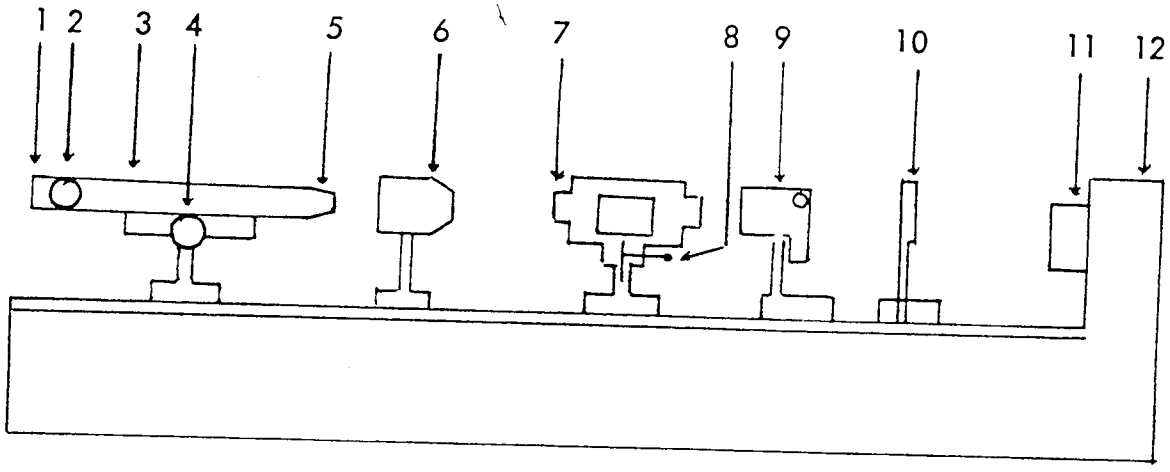

Key : -

1) Eyepiece focus

2) Filar micrometer drum and eyepiece

3) Microscope

4) Image focal adjust

5) Microscope objective

6) Projector lens

7) Jacketed cell housing

8) Rotatable cell holder handle

9) Adjustable slit

10) Semi - transparent mirror

11) Filter turret

12) Lamp housing

Table 2.1 : Preparation of various surfactants in dichloromethane solution for examination by differential refractometry.

Surfactant	Concentration (M)	Disodium Fluorescein (g)	Results Refer To Figure
Oleyl Alcohol			
	0.25 0.3 0.35 0.4 0.45 0.5 0.55 0.6	0.25	2.3 a)
	0.05 0.1 0.15 0.2 0.25 0.3 0.35 0.4 0.45 0.5	0.25	2.3 a)
Stearyl Alcohol			
	0.02 0.03 0.04 0.05 0.06 0.07 0.08 0.1	0.2	2.4 a)
Texofor			
A18	0.01 0.02 0.03 0.04 0.05 0.06 0.08 0.1	0.2	2.3 b)
A10	0.01 0.02 0.03 0.04 0.05 0.06 0.08 0.1	0.2	2.3 c)
A6	0.01 0.02 0.03 0.04 0.05 0.06 0.08 0.1	0.2	2.4 b)
A2	0.01 0.02 0.03 0.04 0.05 0.06 0.08 0.1	0.2	2.4 c)
Lauric Acid			
	0.05 0.1 0.15 0.2 0.25 0.3 0.35 0.4	0.2	2.5 a)
Lauryl Alcohol			
	0.05 0.075 0.1 0.125 0.15 0.175 0.2 0.275	0.15	2.5 b)
Undecanol			
	0.15 0.2 0.25 0.3 0.35 0.4 0.45 0.5	0.2	2.5 c)

is the calibration constant for a selected wavelength and Δd is the total slit image displacement, solvent zero corrected, in instrument units.

In these studies calibrations with known surfactant solutions were carried out and therefore the refractive index difference is not required. The slit image displacement is adequate for the interpretation of the surfactant concentration in solution. The use of this parameter has been advocated by Kertes and Gutmann (238).

i) Preparation Of Samples For Refractive Index Measurement.

All solutions were made up in 50 ml stoppered flasks. Duplicate 25 ml samples were prepared in order that control solutions, to which no disodium fluorescein was added, could be directly compared with those to which disodium fluorescein was added. Gravimetric techniques were used throughout.

The solutions were allowed to equilibrate for 72 hours and samples were kept at room temperature, 25 °C. At the end of this period aliquots of the solutions were removed and centrifuged at 3,500 r.p.m. for thirty minutes. The centrifuge tubes contain a volume of 10 ml and were covered with a sealing film to reduce evaporation over the period of centrifugation. Preliminary experiments established the various parameters of equilibrium time, temperature and centrifuge setting.

The surfactant solutions prepared and the amount of disodium fluorescein added to these solutions are shown in Table 2.1 .
The surfactant solutions were subjected to differential refractometric analysis as described.

Table 2.2 : List of solutions used for the surface tension calibration and their known surface tension at given temperatures (255).

Solutions	Temperature °C	mNm^{-1}
Acetone	20	23.7
Benzene	20	28.85
20% w/w Acetone/Water	25	41.1
10% w/w Acetone/Water	25	48.9
5% w/w Acetone/Water	25	55.5
Water	40	69.56
Water	30	71.18
Water	20	72.75

Table 2.3 : Preparation of various surfactants in dichloromethane and dichloromethane/chloroform solution for examination by surface tension measurement.

Surfactant	Solvent	Concentration (M)	Results Refer To Figure
Lauric Acid	Dichloromethane	0.05 to 0.4 Steps of 0.05	2.7a)
Texofor A6	"	0.01 to 0.06 Steps of 0.01,0.08,0.1.	2.7b)
Lauryl Alcohol	"	0.05 to 0.225 Steps of 0.025	2.7c)
Capric Acid	"	0.014 to 0.14 Steps of 0.014	2.7d)
Lauric Acid	Dichloromethane/ Chloroform	0.002 to 0.02 Steps of 0.002 0.05 to 0.2 Steps of	2.20a)
Capric Acid	"	0.014 to 0.14 Steps of 0.14	2.20b)

2.2.2.2 Surface Tension Measurement.

Measuring the surface tension of the solutions may indicate the extent of the association between surfactant molecules in solution which in turn has implications for their association with disodium fluorescein.

A water jacketed glass dish, 10 cm in diameter, was maintained at specific temperatures. Volumes of 10 ml of solution were placed in the jacketed dish and the surface tension of the liquids was measured as galvanometer deflections arising from a microbalance attached to which was a platinum plate, 5 mm x 10 mm x 0.2 mm, resting at the meniscus of the liquid. The arbitrary deflections of the galvanometer were recorded by a pen recorder and can be correlated with the known surface tension of the solutions taken from a reference source (255). The technique employed is known as the Wilhelmy plate technique (256 - 258).

A calibration curve was prepared from which subsequent data were interpretted. Details of the preparation of the calibration solutions for surface tension measurement are shown in Table 2.2.

Solutions of surfactants in dichloromethane and chloroform - dichloromethane are listed in Table 2.3, as they were prepared.

2.2.2.3 Ultra - Violet Spectroscopy.

A further method of examining the surfactant solutions for the interaction of surfactant molecules and disodium fluorescein is U. - V. spectroscopy.

A portion of dilute solution of the sample being investigated was transferred to a 1 cm cell. A matched cell containing pure solvent was also prepared, and each cell was placed in the appropriate place in the spectrophotometer. This was so arranged that two equal beams of Ultra - Violet or visible light could be passed, one through the solution and the other through the pure solvent.

i) Preparation Of Samples For Ultra - Violet Spectroscopy.

The extent of solubilisation of a dye and the concentration at which it occurs may be established by Ultra - Violet spectroscopy (259).

Eight concentrations of lauryl alcohol in dichloromethane were prepared, 0.05 to 0.225 M in 0.025M intervals and 0.275 and 0.375 M, to which 0.25 g of disodium fluorescein was added. The samples were allowed to equilibrate for the same period and treated in the same way as for the differential refractometry studies.

A scan was carried out to establish where the disodium fluorescein absorbance maximum occurred. Once the absorbance maximum was established readings for each of the samples at this wavelength were taken.

2.2.2.4 Surface Area Measurement.

In order to obtain an accurate assessment of the degree to which the disodium fluorescein powder is associated with the surfactant the surface area of the powder is required.

Two sealed vessels can be equilibrated with each other, in this apparatus, and independently connected to either side of a U - tube manometer. One vessel contains the sample and the second is the control vessel. Nitrogen gas was introduced into both vessels and they were allowed to equilibrate with each other. The vessels were then disconnected from each other and the temperature at which they were maintained was reduced by placing them in liquid nitrogen. By reconnecting the vessels to the manometer any difference in pressure between the vessels resulting from surface adsorption of nitrogen could be detected.

i)Procedure For Specific Surface Area Measurement.

A nomogram , supplied by the manufacturers, may be used to obtain

Table 2.4 : Calculated amounts of aliphatic acids and alcohol required to form a monolayer at the surface of disodium fluorescein powder based on the specific surface area measurement.

Surfactant	Molecular Weight (g)	Monolayer Equivalent $mg\ g^{-1}$
Lauryl Alcohol	186.3	0.73
Lauric Acid	200.3	0.78
Capric Acid	172.3	0.68

surface area from the manometer reading. The following equation is employed,

$$S_g = \frac{A\Delta h}{m} - \frac{B}{\rho} \qquad 2.12$$

Where S_g is the specific surface area (m^2g^{-1}), Δh is the pressure difference on the manometer (mm), m is the sample weight (g) A and B are coefficients and ρ is the density of the powder ($g\ cm^{-3}$).

At barometric pressure of 733.75 mm Hg and room temperature, 19.5 °C, the differential manometer reading for the sample of micronised disodium fluorescein was 55 mm . From the nomogram A and B were 0.1424 and 0.115 respectively. The sample weight was 19.8397g . Substituting these values in equation 2.12, with the powder density of 1.49 g cm^{-1}, gives a value for the specific surface area of 0.472 m^2g^{-1}.

The calculation of the amount of surfactant which would form a monolayer on this sample of disodium fluorescein may be carried out. Vertically orientated fatty acids occupy (259) a surface area of 20 Å per molecule. From this figure and the specific surface area measurement the amount of certain compounds required to form a monolayer on the surface of the disodium fluorescein can be calculated. The The following equation describes the calculation,

$$C_{ads} = S_g M_w / S_m N_A \qquad 2.13$$

where S_g is as above, S_m is the surface area occupied by one molecule (m^2molecule), N_A is Avogadro's constant, M_w is the molecular weight of surfactant and C_{ads} is the amount of surfactant associated with unit amount of disodium fluorescein (gg^{-1}).

Table 2.4 details the monolayer equivalents calculated by the

above procedure for lauryl alcohol, lauric acid and capric acid.

2.2.2.5 Gas Liquid Chromatography (GLC).

GLC is a recognised technique for the quantitative measurement of fatty acids (260,261). This technique may be useful in investigating the association of these particular compounds with disodium fluorescein powder. The method of estimating the extent of the association between the surfactant and the powder may involve observing the surfactan removal from solution or its appearance at the powder surface directly.

The apparatus consists of a heated injection port which encloses a rubber septum through which the sample is injected using a microsyringe. The injection port is connected to a glass column which is maintained at constant temperature. The glass column contains an inert solid phase which may be treated with an active ingredient in order to improve the resolution of the elution of the sample constituents. The carrier gas flow delivers the sample to the flame ionisation detector.

i) Column Conditions.

Lauryl alcohol : A 0.5 metre glass column was used with a 3% OV101 treated chromosorb W, or gas chrom Q, packing. The injection port temperature was 200 °C, that of the column was 180 °C and the detector temperature was 250 °C. The carrier gas, nitrogen, was kept at a constant flow rate of 35 ml min^{-1}(0.6 Kg cm^{-2}). The mixture of air and hydrogen used in the flame ionisation detector was maintained at flow rates of 30 and 300 ml min^{-1} (0.5 and 1.0 Kg cm^{-2}) respectively.

Lauric and capric acids : A 1.5 metre glass column was used with a 3% SE 30 treated column packing. The acids were derivitised before

application to the column. The injection port temperature was 200 °C, that of the column was 180 °C and the detector temperature was 250 °C. The carrier gas and F.I.D. gas flows were regulated as described for lauryl alcohol.

ii) Derivitisation of Fatty Acids.

The samples were prepared by weighing into a vessel 50 mg, using a balance accurate to five figures. An internal standard, Table 2.5, was added to these samples. A volume of 2 ml of BF_3 - methanol was added to each sample vessel, a screw capped tube, and heated to 80 °C for 5 minutes after which the sample was extracted into two 4 ml volumes of chloroform/hexane (1:4). Finally this was reduced to 1ml by bubbling with nitrogen at room temperature.

iii) Preparation Of Samples.

A calibration curve was prepared for lauric acid, lauryl alcohol and capric acid. The details of the preparation are shown in Table 2.5 .

The inclusion of an internal standard in the preparation enables a graph of the peak height ratio, of the test sample to the internal standard, against the concentration tobe plotted. The internal standard eliminates the possibility of error due to variation in experimental conditions, such as volume of sample injected, column conditions and derivitisation procedures.

The adsorption isotherms indicating the association of the surfactants, lauric acid, lauryl alcohol and capric acid with disodium fluorescein may be prepared from the GLC results.

An investigation of the effect of the addition of chloroform on the association between the surfactant and the disodium fluorescein was carried out.

Table 2.5 : Preparation of the samples for GLC, including details of the internal standard.

Sample	Range mg ml^{-1}	Interval mg ml^{-1}	Standard	Standard Conc.^{n} mg
Lauryl Alcohol	0 - 40	4	Capryl Alcohol	40
Lauric Acid	0 - 6.0	0.2 and 1.0	Capric Acid	1.0
Capric Acid	0 - 3.5	0.5	Lauric Acid	5.0

Table 2.6 : Preparation of various surfactant solutions in dichloro - methane/chloroform solution for examination by GLC.

Sample	Chloroform Volume ml	Concentrations of Surfactant (M)	Results Refer To Figure
Lauric Acid	None	0.004 to 0.02 Steps of 0.002	2.11 a)
"	1.0	"	2.11 b)
"	2.5	"	2.11 c)
"	5.0	"	2.11 d)
"	5.0	0.002 to 0.02 Steps of 0.002	2.12 a)
"	"	0.0 to 0.005 Steps of 0.0005	2.12 b)
"	"	0.004 to 0.009 Steps of 0.0005	2.12 b)
"	"	0.005 to 0.015 Steps of 0.001	2.12 b)
"	"	0.002 to 0.02 Steps of 0.002	2.12 b)
Capric Acid	"	0.002 to 0.02 Steps of 0.002	2.13 a)
Lauryl Alcohol	"	0.05 to 0.225 Steps of 0.025	2.13 b)
Lauric Acid	"	0.075 to 0.225 Steps of 0.05, 0.025,0.03125,0.375,0.045,0.05	2.18 a)

iv) Calculation of Surfactant Association With Disodium Fluorescein.

The initial concentrations of surfactant in solution, which were prepared in these studies, are shown in Table 2.6 . The GLC gives the amount of surfactant present in the sample at the conclusion of the experiment. When the surfactant present in the sample is compared with the original weight of the powder, the fraction of the weight attributable to disodium fluorescein can be estimated. This fraction may be used to calculate the amount of surfactant associated with unit amount (g) of disodium fluorescein. Finally the equilibrium concentration of the supernatant may be estimated.

$$C_{ads} = a_s/(a_m - a_s) \qquad 2.14$$

and,

$$C = (C_I M_w V - m_s C_{ads})(1/M_w V) \qquad 2.15$$

Where m_s is the original weight of disodium fluorescein powder used in the experiment (g), a_m is the amount of coated powder derivitised (g), a_s is the amount of surfactant detected by GLC (g), C_I is the initial concentration of surfactant (M), C_{ads} is the amount of surfactant associated with a unit amount of disodium fluorescein (gg^{-1}), M_w is the molecular weight of surfactant (g) and V is the volume of solvent (ml).

2.2.2.6 Infra - Red Spectroscopy.

Infra - red spectroscopy may be used to investigate the components of a molecule in terms of the bonds between atoms since the energy of most molecular vibrations correspond to the IR region of the electromagenetic spectrum. This technique may be used to examine the qualitative nature of the association between the surfactants and the powder, in terms of the point of attachment and the nature of the bond formed.

i) Preparation Of Samples.

The coated powders and various control samples were ground with 10 to 100 times the bulk of pure, dried, potassium bromide and the mixture pressed into a disc using a special mould and a hydraulic press, at 10 K Tonnes.

Pure disodium fluorescein was mixed with pure lauric acid at concentrations between 0 and 0.5 gg^{-1}. The mixture was then prepared and examined in the spectrum 4,000 cm^{-1} to 625 cm^{-1}. The peak height ratio between the peaks at 2,900 and 920 cm^{-1} were calculated and plotted against the amount of lauric acid.

Disodium fluorescein, lauric acid and capric acid, sodium laurate and lauric and capric acid coated powders were examined. Using the calibration curve described above an adsorption isotherm was prepared from 0.0075 to 0.0225 in 0.005 M intervals and 0.025, 0.0325, 0.0375, 0.045 and 0.05 M solutions of lauric acid in dichloromethane/chloroform (5:1).

ii) Solution Infra - Red.

Solutions of lauric acid in dichloromethane/chloroform were examined in a 1 cm solution cell. The concentrations employed were 0.025, 0.05 0.075, 0.1, 0.15 and 0.2 M.

2.2.2.7 X - Ray Photoelectron Spectroscopy.

This technique may also be known as Electron Scanning Chemical Analysis or ESCA. This method is a powerful technique of determining how the outermost atomic layers of solid surfaces change with depth. The manner in which solid surfaces interact with their environment is determined not by bulk composition but by surface composition and properties, where surface means the topmost atomic layers of the specimen.

Information about the composition, chemical state and molecular

Figure 2.2: Schematic diagram of the X - ray photoelectron process employed in X - ray photoelectron spectroscopy.

Key : e^- - electron
h - photon energy
E_k - kinetic energy
E_b - binding energy
θ - angle of scatter

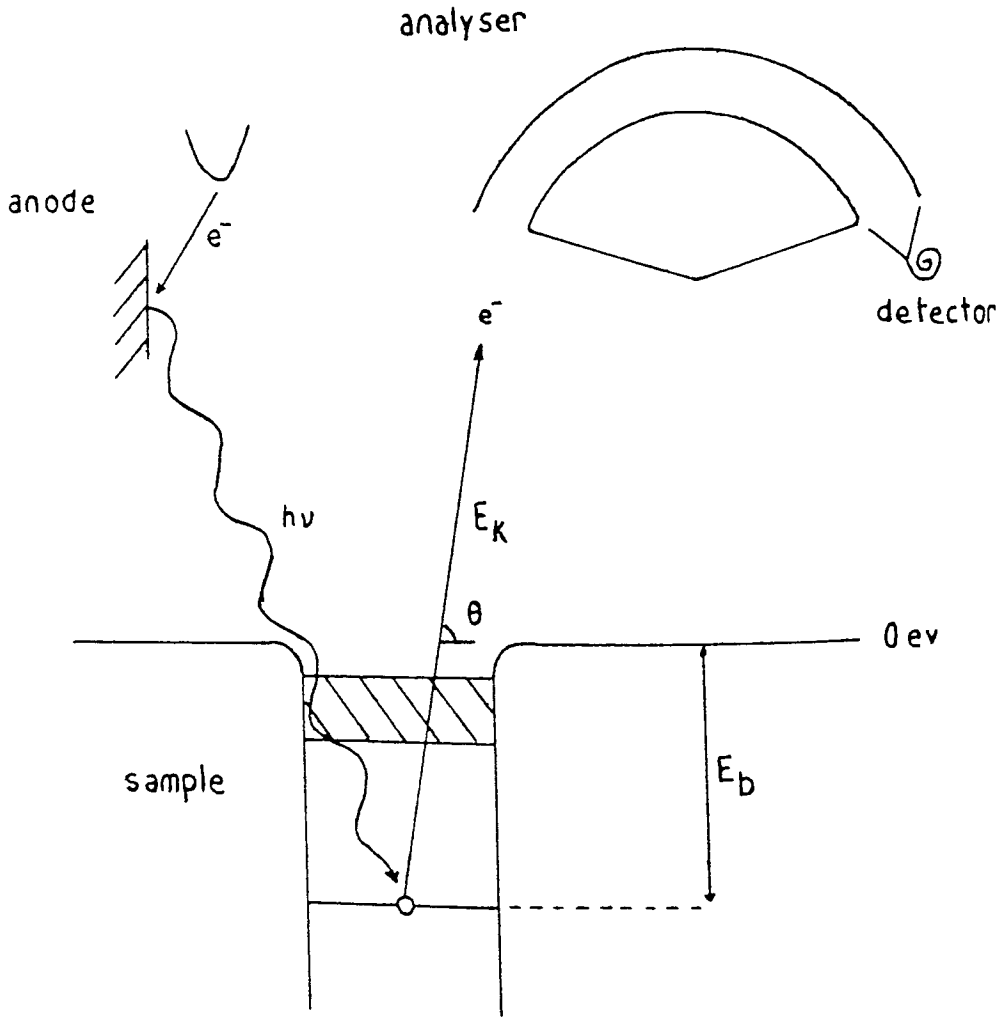

bonding in these topmost layers is crucial in order to gain knowledge and understanding of the manner in whichthose specimens will behave when placed in any particular environment.

i) Operating Procedure.

X - Rays were produced from a magnesium anode using an irradiation power of 240 W. The routine vacuum in the sample chamber was about 5×10^{-8} Torr.

Figure 2.2 shows the basic processes in ESCA. An X - Ray flux from a water cooled Magnesium anode irradiates the specimen surface, interaction with bound electrons (binding energy E_b) produces photoelectrons of kinetic energy E_k.

$$E_k = h\nu - E_b - \phi \qquad 2.16$$

Where $h\nu$ is the photon energy, and ϕ is the spectrometer work function. The emergent photoelectrons are collected at an angle θ to the specimen surface and energy analysed in a dispersive electrostatic analyser.(D.E.A.)

There are two methods of controlling the trajectory of the photoelectrons. Firstly the potential difference across the retardation lenses may be varied and that across the D.E.A. held constant. Secondly the role of these parts of the apparatus may be reversed. The method used in these experiments is the first of the two described, that is fixed analyser transmission (FAT) mode with sweeping retardation lenses.

For a homogeneous sample, the intensity of the photoelectron peak is given by

$$I = \int_{y_1}^{y_2} dI \qquad 2.17$$

and, $$dI = s \, X \, S' \, F_1 \, C(y) \, e^{-y/\lambda} \, dy \qquad 2.18$$

Where s is the analysed area, including surface roughness, X is the cross section of the photoelectron beam, S' is the factor of transmission of the analyser, F_1 is the X - Ray flux, C(y) is the concentration of the element at the depth of y, and λ is the mean free path of the electron (262).

The purpose of this method of examination of the surface is to elucidate the completeness and depth of surface layers of surfactant on the model aerosol powder. The relationship between the peak intensity for a specific photoelectron, that is a photoelectron from a particular atom, with (I) or without (I_0) an overlayer and the depth of the overlayer (d) may be described by,

$$I = I_0 \, e^{-d/\lambda} \qquad 2.19$$

In practice the intensity of a particular photoelectron may be expressed as a peak height or area. The peaks may need some interpretation. The carbon peak for example may be resolved into its components by fitting a series of curves of a Gaussian nature.

A variety of carbon, oxygen and sodium peaks representing photoelectrons displaced from different energy shells of the particular atom were examined in these experiments.

Samples of disodium fluorescein alone, lauric acid, sodium laurate, and lauric and capric acid coated disodium fluorescein were examined. The nominal coated powders were 0.63 gg^{-1} and 0.12 gg^{-1} lauric acid and 0.11 gg^{-1} capric acid samples, which were examined

2.2.2.8 Scanning Electron Microscopy.

The scanning electron microscoscope (SEM) utilises a finely focussed electron beam which is scanned over the surface and, in its basic form, an image is produced on a synchronously scanned cathode ray tube showing the variations in secondary electrons yield over the surface. The image contains mainly topographical information and is characterised by high resolution, 60 to 100 Å, and great depth of field which can be achieved.

i) Procedure.

The sample was coated with a thin film of gold by vacuum deposition on a stub mounting. The sample was placed in a vacuum chamber (minimum 10^{-8} Torr) and bombarded with electrons. The backscattered electrons are collected and focussed by retardation lenses and imaged as described above.

Three samples were examined, disodium fluorescein alone and one each of the lauric and capric acid coated powders.

2.3 Results And Discussion.

The major constraints on the selection of a solvent, other than the solubility of the model aerosol powder, were concerned with the boiling point and the density of the solvent. If the boiling point was too low the solutions would evaporate during handling procedures and consequently cause errors in the assay. Careful selection of the solvent with a density approaching that of the model aerosol powder may improve the the suspension of the powder by the solvent during the adsorption equilibrium period.

The best chlorofluorocarbon, Freon, from the point of view of density has a density of 1.456, that of disodium fluorescein being

1.46 - 1.49 g cm^{-3} (252,263), but its boiling point is - 94°C. It would therefore be impossible to use this solvent at room temperature. In contrast, both Freon 112 and 113 have boiling points which are suitable, these are 92.8°C and 47.57°C respectively, but their densities are 1.634 and 1.565 respectively (255). Disodium fluorescein would float in these solvents. The solvent selected, dichloromethane, has a boiling point of 40.2°C and a density of 1.325 g cm^{-3} (255).

2.3.1 Preliminary Investigations.

2.3.1.1 Differential Refractometry.

In the present studies the measurement of the refractive index may be used as an indication of the presence of surfactant in solution. The correlation of the refractive index measurement with the concentration of surfactant enables a calibration curve to be prepared. The subsequent addition of powders followed by the measurement of the refractive index gives some indication of the association between the surfactant and powder in terms of the reduced surfactant concentration in solution.

Figures 2.3 and 2.4 show the refractive index measurements plotted as Δd against the initial concentration (M) for oleyl alcohol, stearyl alcohol and the four Texofors A18, A10, A6 and A2. All of these plots consist of a calibration using the surfactant solutions alone and the equivalent solutions to which disodium fluorescein had been added.

The oleyl alcohol, Texofor A18 and A10 plots exhibit certain common features. Firstly there appears to be a concentration at which the Δd for the test samples and the calibration start to diverge. Prior to this point no distinct differences between the calibration and the

Figure 2.3: Differential refractometry : Δd plotted against concentration (M) in dichloromethane for a) Oleyl alcohol b) Texofor A18 and c) Texofor A10.

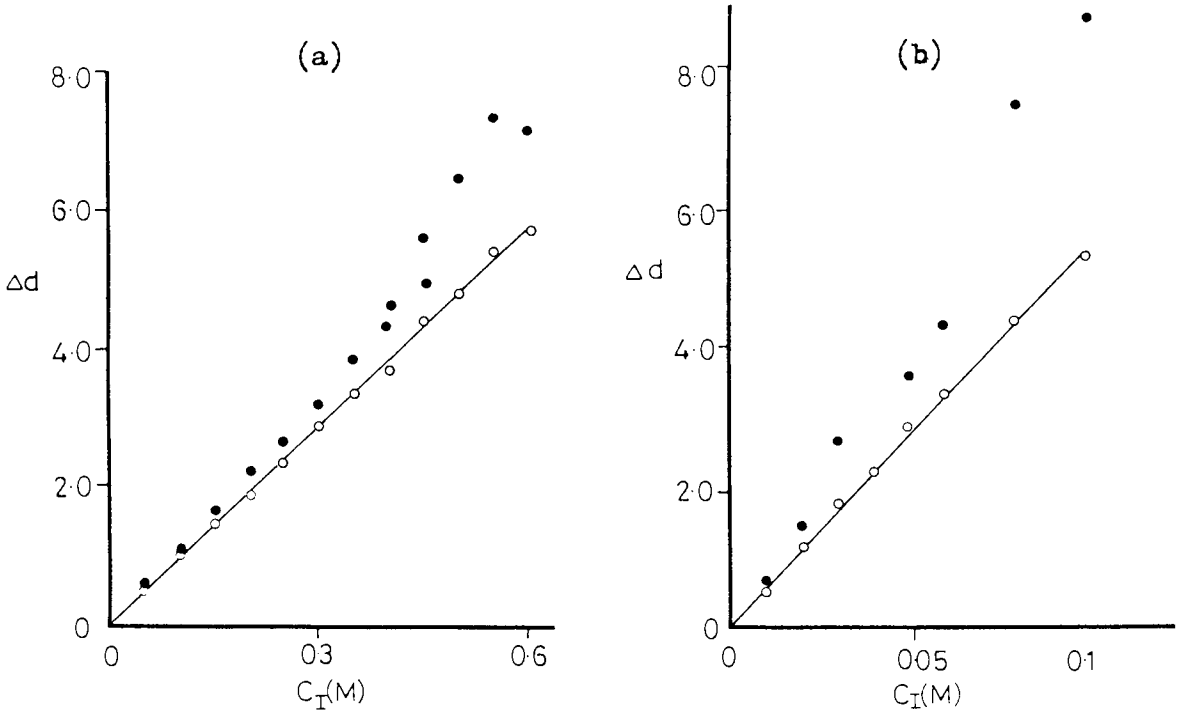

Key :-

- • Samples to which disodium fluorescein was added.
- ○ Samples to which no disodium fluorescein was added.

Δd Slit image displacement.

C_I Initial concentration (M)

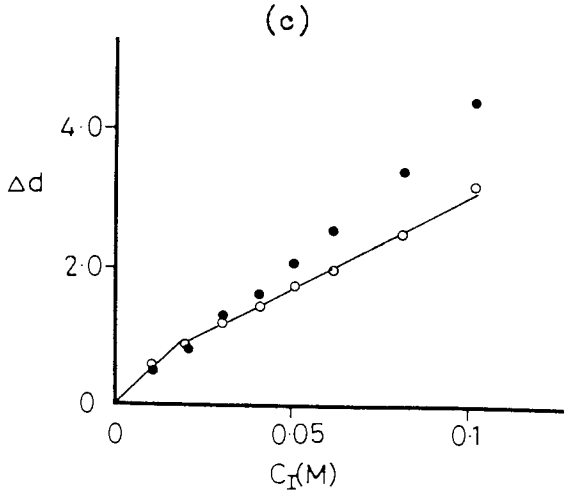

test samples can be distinguished.

Table 2.6 indicates the positions at which the divergence occurs and the values of Δd for the test and calibration plots at the point of greatest divergence.

The explanation for this increase in the refractive index of the solutions is most probably that solubilisation of the disodium fluorescein by the surfactant in solution is occurring. Dye solubilisation has been used as a means of measuring the critical micelle concentration (CMC) for fatty acids in carbon tetrachloride (264). This author recognises, however, that premicellar aggregation and even micelle formation occur prior to the accepted CMC. It was noted that since the aggregation number of the micelle in non - aqueous solution is very low, an abrupt and large change in the physico - chemical properties of the solution cannot be expected at the CMC (241). The divergence of the test and calibration samples must be interpretted as the first detectable changes resulting from the formation of micelles. The point of divergence may not indicate the CMC but does suggest that the CMC is at or below this concentration, if a recognisable CMC exists (223).

The formation of inverted micelles in non - aqueous solvent was outlined in the introduction. Texofor A18 and A10 appear to solubilise the dye, disodium fluorescein, at 0.02 and 0.04 M respectively. The difference in the length of the polyoxyethylene chain would account for the positions of the point of divergence (265). Oleyl alcohol also solubilises the dye but at a much higher concentration than Texofor A18 or A10. This may be explained in terms of the polar head groups, that of oleyl alcohol being much less polar than those of Texofor A18 or A10. This is hardly a surprising observation since it has been noted that the major interactions in apolar solvents are dipole - dipole

Figure 2.4 : Differential refractometry : Δd plotted against concentration (M) in dichloromethane for a) Stearyl alcohol, b) Texofor A6 and c) Texofor A2.

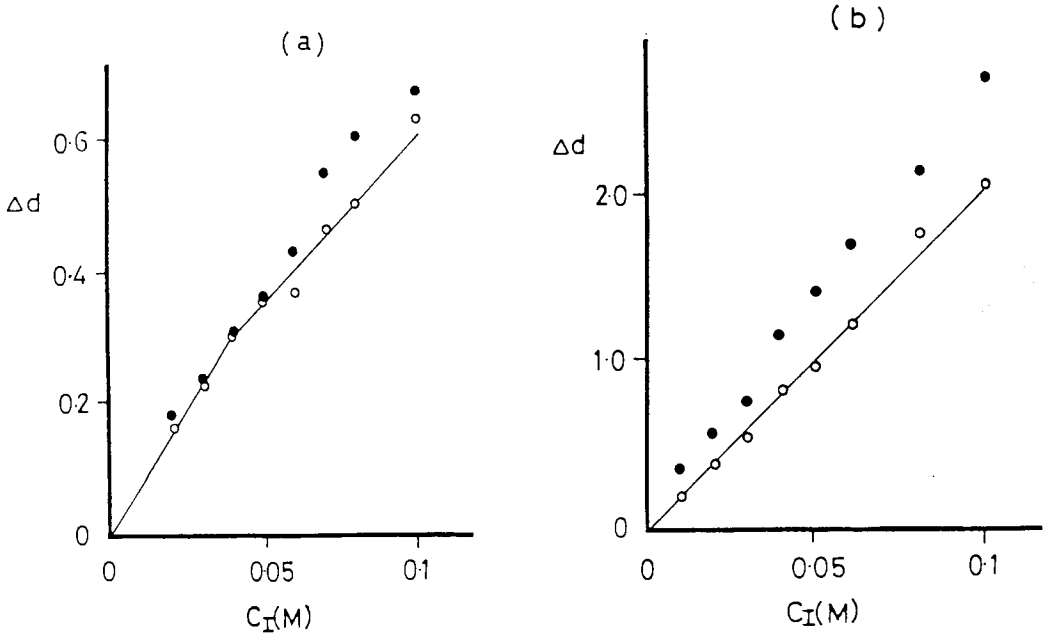

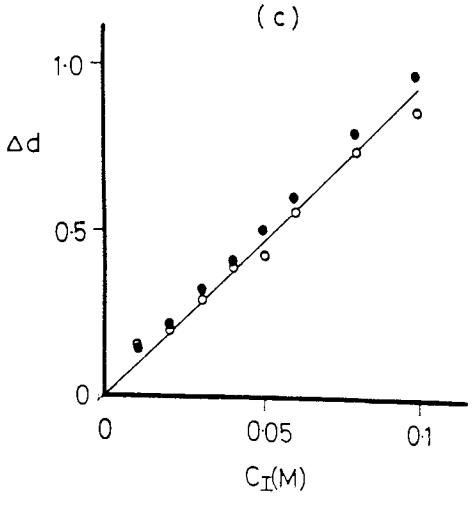

Key :-

- • Samples to which disodium fluorescein was added.
- ○ Samples to which no disodium fluorescein was added.

Δd Slit image displacement.

C_I Initial concentration (M).

and ion pair interactions (230,266,267).

The stearyl alcohol, Texofor A6 and A2 samples, shown in Figure 2.4, exhibit very little difference between the test and calibration solutions. The Δ d's for maximum divergence, of the test from the control samples, and the concentration at which this occurs are reproduced in Table 2.7.

If adsorption were to take place in these solutions it would be expected that the test solutions would contain reduced concentrations of surfactant in comparison with the calibration solutions.

The refractive indices for Texofor A6, A2 and stearyl alcohol at the point of greatest divergence suggest that there is little difference between the test and calibration samples. It can be concluded from this observation that reducing the polarity of the head groups results in reduced dye solubilisation, and by inference reduced surfactant - surfactant interaction (264). There is, however, no evidence of adsorption, in terms of reduced surfactant concentration in the test compared with the calibration solutions.

Following the previous observations it seemed likely that by choosing a compound with the appropriate combination of hydrocarbon chain length and polar head group that adsorption rather than solubilisation could be effected.

The lauric acid, lauryl alcohol and undecanol refractive index measurements, plotted as Δd against the initial concentration (M), are presented in Figure 2.5. The plots of lauric acid and lauryl alcohol data both show reduced Δd for the test samples in comparison with the calibration. The undecanol plot shows a reduction of the Δ d followed by an increase in this parameter.

Table 2.7 shows the maximum reduction in Δd for the test in comparison with the calibration, for these three samples, and the

Table 2.7 : Concentrations (M) at which the divergence between the test and calibration plots begin to occur and the concentration, d at which the maximum divergence of the test from the calibration occurs.

Sample	Point of Divergence (M)	Δd^{max}_{test}	Δd^{max}_{calib}	C^{max}(M)
Oleyl Alcohol	0.3	7.4	5.85	0.6
Texofor A18	0.02	9.071	5.544	0.1
Texofor A10	0.04	4.557	3.299	0.1
Stearyl Alcohol	-	0.435	0.336	0.06
Texofor A6	-	2.767	2.153	0.1
Texofor A2	-	1.011	0.937	0.1

Figure 2.5 : Differential refractometry : Δd plotted against concentration (M) in dichloromethane for a) Lauric acid, b) Lauryl alcohol and c) undecanol.

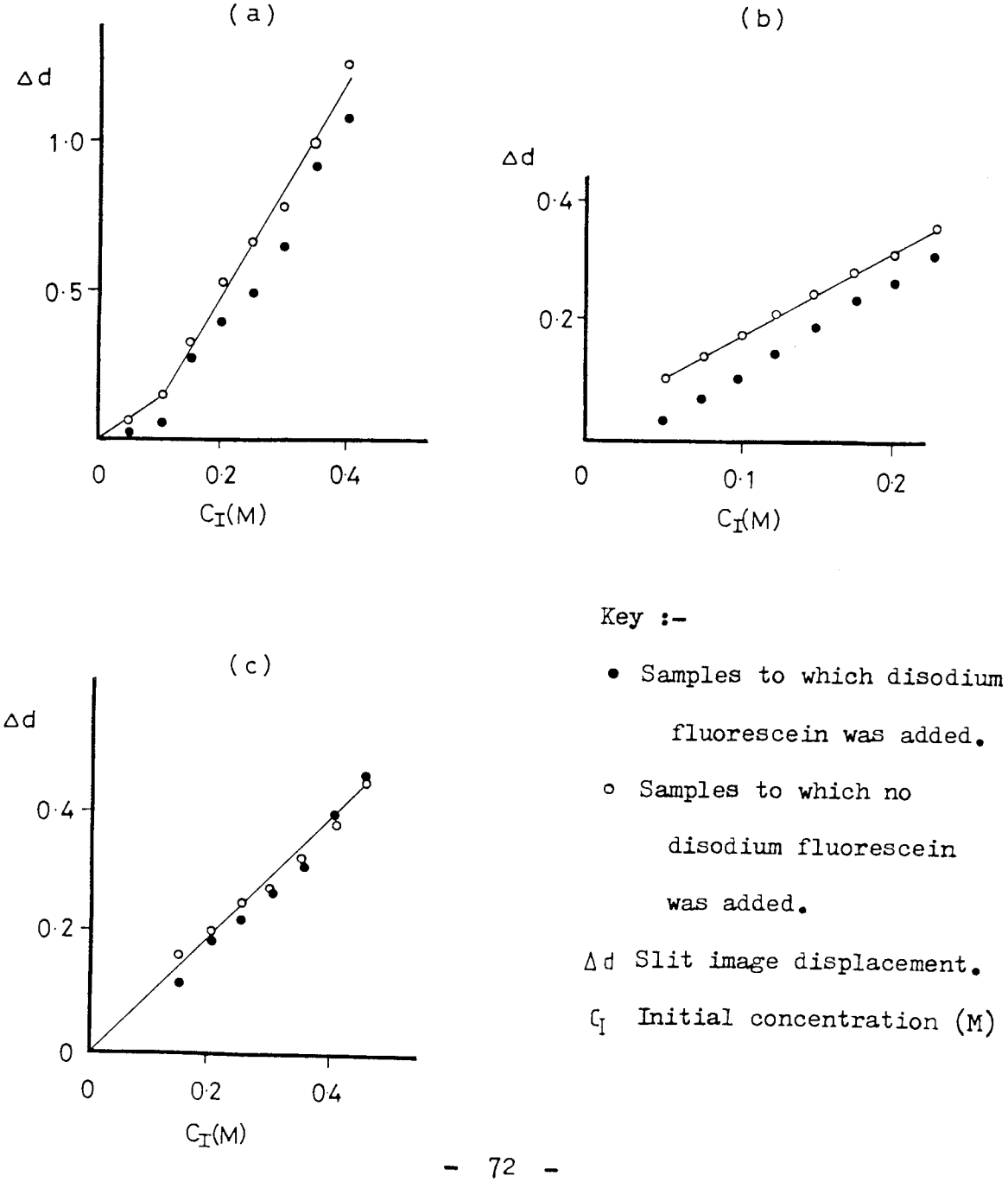

Key :-

- • Samples to which disodium fluorescein was added.
- ○ Samples to which no disodium fluorescein was added.

Δd Slit image displacement.

C_I Initial concentration (M)

concentration at which this occurs.

The results obtained by differential refractometry may be quantified by comparing the test Δ d with that of the calibration. The following equation may be applied, assuming linearity,

$$C = C_I \Delta d_{eq} / \Delta d_{In} \qquad 2.20$$

It follows that, $C'_{ads} = C_I - C$

This may be converted to the appropriate units by,

$$C_{ads} = (C_I - C)\ M_w\ V/1{,}000\ m \qquad 2.21$$

Where C is the equilibrium concentration (M), C_I is the initial concentration (M), Δd_{eq} and Δd_{In} are the refractive index differences for the equivalent concentrations, C'_{ads} is the adsorbed concentration (M), C_{ads} is the amount adsorbed (gg^{-1}), M_w is the molecular weight of the surfactant (g), V is the volume of solution (ml), m is the mass of disodium fluorescein (g).

In the examples of lauric acid, lauryl alcohol and undecanol some reduction in the surfactant concentration was noted with the addition of disodium fluorescein. By using the method of treatment of results outlined above a nominal maximum amount of compound associated with disodium fluorescein can be calculated. These data are presented in Table 2.8 .

The amount of surfactant associated with disodium fluorescein is very large, in the range 0.6 to 1.6 gg^{-1} for these samples. It must be emphasised that due to the proximity of the refractive index of the solvent, 1.4242,and the surfactant, 1.4606 for oleyl alcohol,

Table 2.8 : The maximum reduction in Δd for the test compared with the calibration samples of lauric acid, lauryl alcohol and undecanol, and the calculated equivalent amount associated with disodium fluorescein (gg^{-1})

Surfactant	Concentration (M)	Δd^{min}_{test}	Δd^{min}_{calib}	Associated Conc.^{n} (gg^{-1})
Lauric Acid	0.25	0.677	0.508	1.55
Lauryl Alcohol	0.1	0.173	0.106	1.242
Undecanol	0.25	0.259	0.23	0.603

Table 2.9 : Critical Micelle Concentrations as measured by surface tension, Wilhelmy plate technique at 25 ± 0.1°C, solutions in dichloromethane.

Sample	Critical Micelle Concentration (M)
Lauric Acid	0.1
Texofor A6	0.05
Lauryl Alcohol	0.12
Capric Acid	0.042

small changes in Δd would appear to accompany large changes in concentration in solution.

Lauric acid and lauryl alcohol seem to be involved in adsorption at the surface of disodium fluorescein, as indicated by the differential refractometry, and may, therefore be worthy of further investigation.

2.3.1.2 Surface Tension Measurement.

Surface tension measurement was carried out, in order to investigate the behaviour of the surfactant molecules in solution.

The calibration curve shown in Figure 2.6 is linear with a slope 1.1 and an intercept of 0.711.

The plots of surface tension, mNm^{-1} , against concentration of surfactant in solution, M, for lauric acid, lauryl alcohol , Texofor A6 and capric acid in dichloromethane are shown in Figure 2.9. These all exhibit minima which are shown in Table 2.9. The subsequent rise in the surface tension suggests that the energy of formation of micelles is lower than that for other aggregates or random distribution of monomers (264). Consequently it might be expected that the surface tension would rise as an indication that the solute is more concentrated in the bulk of the solution, as micelles, than at the interface (251). The reductions in surface tension from that of pure solvent are of an order consistent with the surface tension of pure aliphatic hydrocarbons, 19 to 23 mNm^{-1} (238).

The concentration at which micelles appear to form are indicated by the reduction in surface tension of surfactant solutions . The CMC's for lauric acid and Texofor A6 would appear to occur at 0.1M and 0.05M respectively, as indicated in Table 2.9 from Figure 2.7.

Figure 2,6: Calibration plot of the instrumental response of the microbalance to solutions of known surface tension (mNm^{-1}).

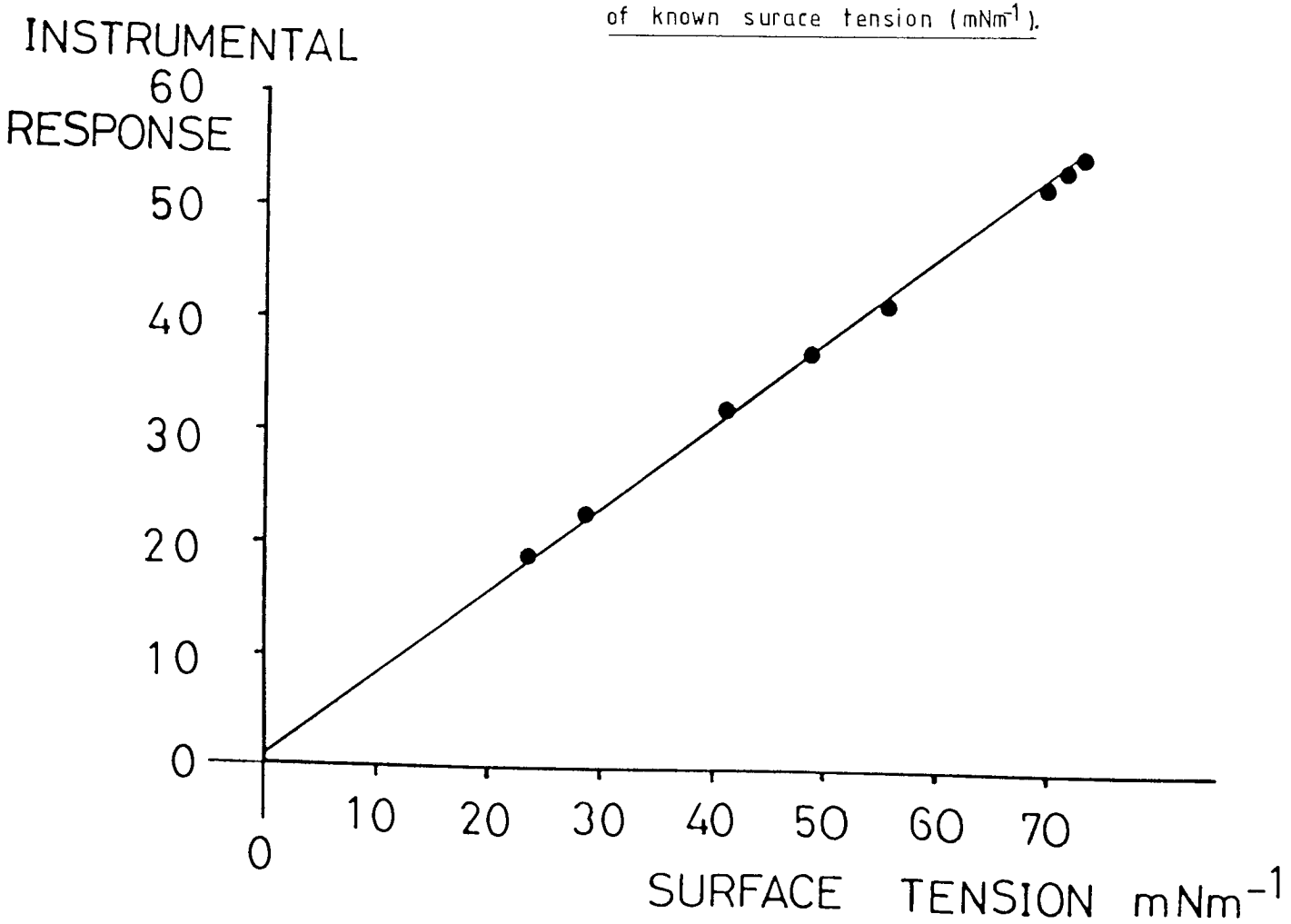

Figure 2.7 : Surface tension measurements : Surface tension (mNm^{-1}) plotted against concentration (M) for a) Lauric acid, b) Texofor A6, c) Lauryl alcohol and d) Capric acid in dichloromethane.

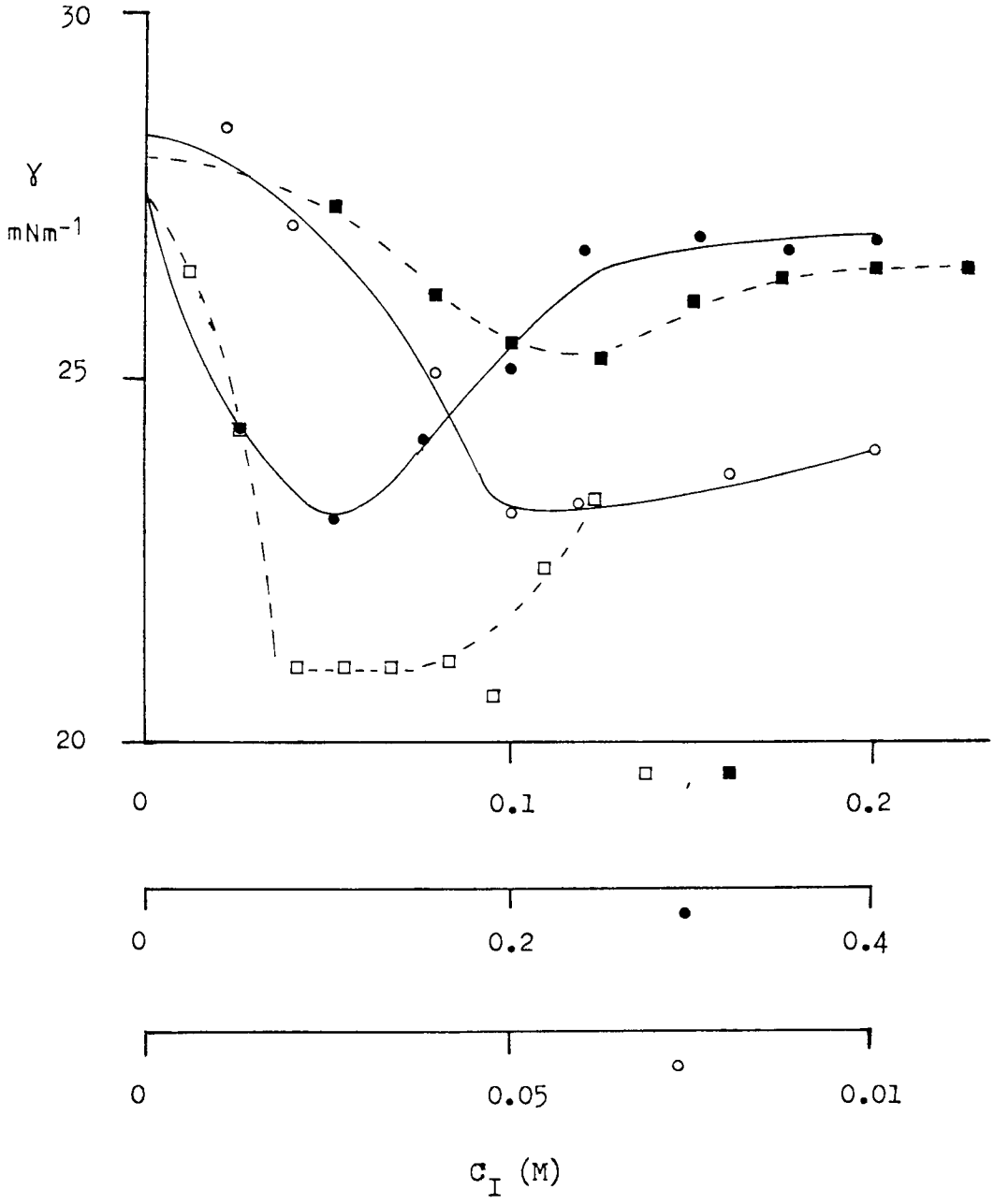

Key :- a) ●= Lauric acid c) ■= Lauryl alcohol γ= surface tension

b) ○= Texofor A6 d) □= Capric acid C_I = Initial Concentration

These values can be contrasted with the point of solubilisation of disodium fluorescein measured by differential refractometry, shown in Table 2.7 and 2.8 from Figures 2.4 b) and 2.5 a). The dye solubilisation method indicates that the CMC 's for lauric acid and Texofor A6 occur at or before 0.25 and 0.1 M respectively. The formation of micelles of lauric acid in carbon tetrachloride at 298°K has been investigated (264) using infra - red spectroscopy and dye solubilisation, of disodium fluorescein, techniques. The CMC as measured by these techniques was estimated as 0.0016M by infra - red spectroscopy, and 0.0025M by dye solubilisation. The difference in these, literature, values was accounted for by steric hindrance to the formation of micelles around the dye molecules. In these studies dichloromethane was used as the solvent rather than carbon tetrachloride. The difference in the values obtained in dichloromethane as compared with those observed in carbon tetrachloride may be explained in terms of the dielectric permeability of the solvent. Reduction in the CMC has been observed with the lowering of the dielectric constant of the solvent (267,268).

The lauryl alcohol CMC as measured by surface tension is approximately 0.12 M. This compares directly with that estimated from the solubilisation data of approximately 0.1 M. The dye solubilisation data for lauryl alcohol is difficult to interpret since there is only a minor point of inflection in the test curve, shown in Figure 2.5 . Literature infra - red data (269)may be compared with the data obtained by surface tension measurement. The CMC for lauryl alcohol in carbon tetrachloride is 0.077 M which is a concentration nearly 50 times greater than that for lauric acid in similar conditions (264). The CMC measured for capric acid in dichloromethane, shown in Figure 2.7 d) and Table 2.9, was 0.042 M. This is lower than that of lauric acid of 0.1 M. The effect of reducing the chain length of a molecule in

a low dielectric medium is to slightly decrease the CMC (264). In the experiments carried out in dichloromethane, a moderately non - polar solvent (ϵ = 9.08 at 20 °C) the opposite effect, to that mentioned, was observed, of a slight increase in the CMC. This result may be explained in terms of a dielectric effect. In dichloromethane tail group interactions may be responsible for the movement in the relative CMC's of capric and lauric acids as the influence of the polar head group attraction would be reduced with increased dielectric permeability (268). To what extent this effect would contribute to the shift in the lauryl alcohol CMC is not Known.

2.3.1.3 Ultra - Violet Spectroscopy.

The spectrum for disodium fluorescein in dichloromethane is shown in Figure 2.8 .

The plot of percentage absorbance against initial concentration for supernatants, taken from a solution of lauryl alcohol to which disodium fluorescein was added, is shown in Figure 2.9 . The initial region up to 0.125 M is an area of constant low absorbance equivalent to the solubility of disodium fluorescein in the solvent. The second region shows an increase in absorbance at which it can be assumed that micelles have been formed.

This result pinpoints the position of dye solubilisation more accurately than the differential refractometry data and confirms the validity of the surface tension measurement data.

2.3.2 Final Procedures.

In the examples discussed the predominant factor influencing the data has been the solubilisation if the dye by the surfactant solutions. The technique of differential refractometry has been criticised as being insensitive to large differences in solution concentrations of

Figure 2.8 : Ultra - violet spectroscopy : spectrum for disodium fluorescein in dichloromethane.

Figure 2.9 : Ultra - violet spectroscopy : absorbance at 516 nm plotted against lauryl alcohol concentration (M).

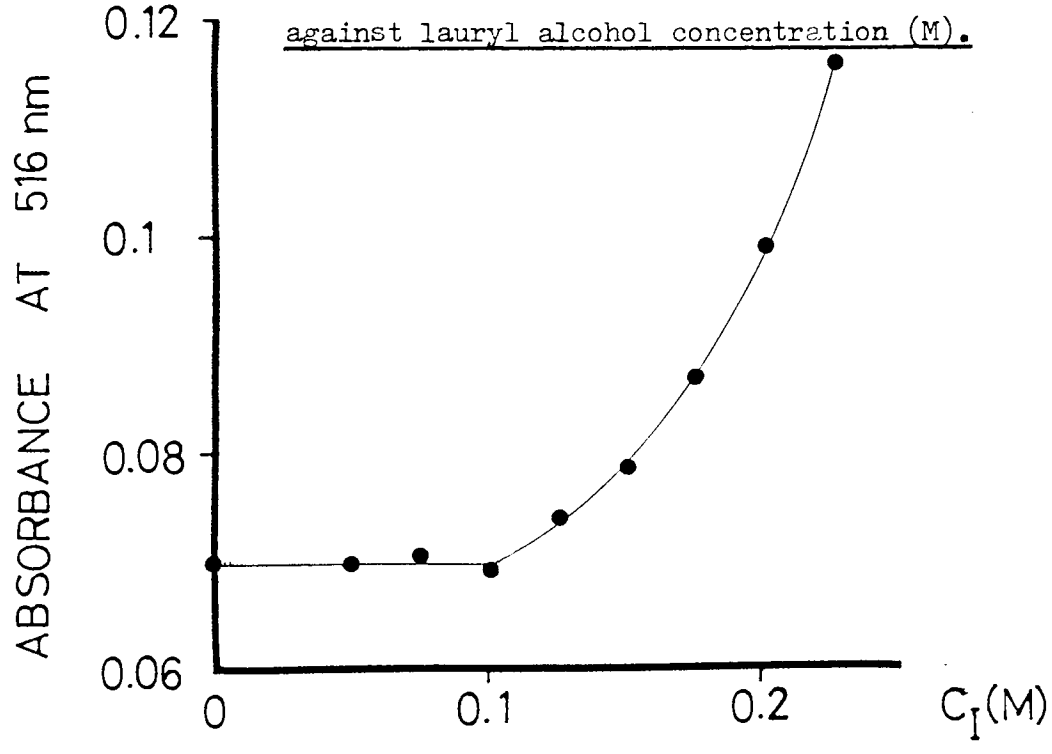

Figure 2.10 : Gas liquid chromatography : Calibration plots of peak height ratio against concentration (M) for a) lauric acid, b) capric acid and c) lauryl alcohol.

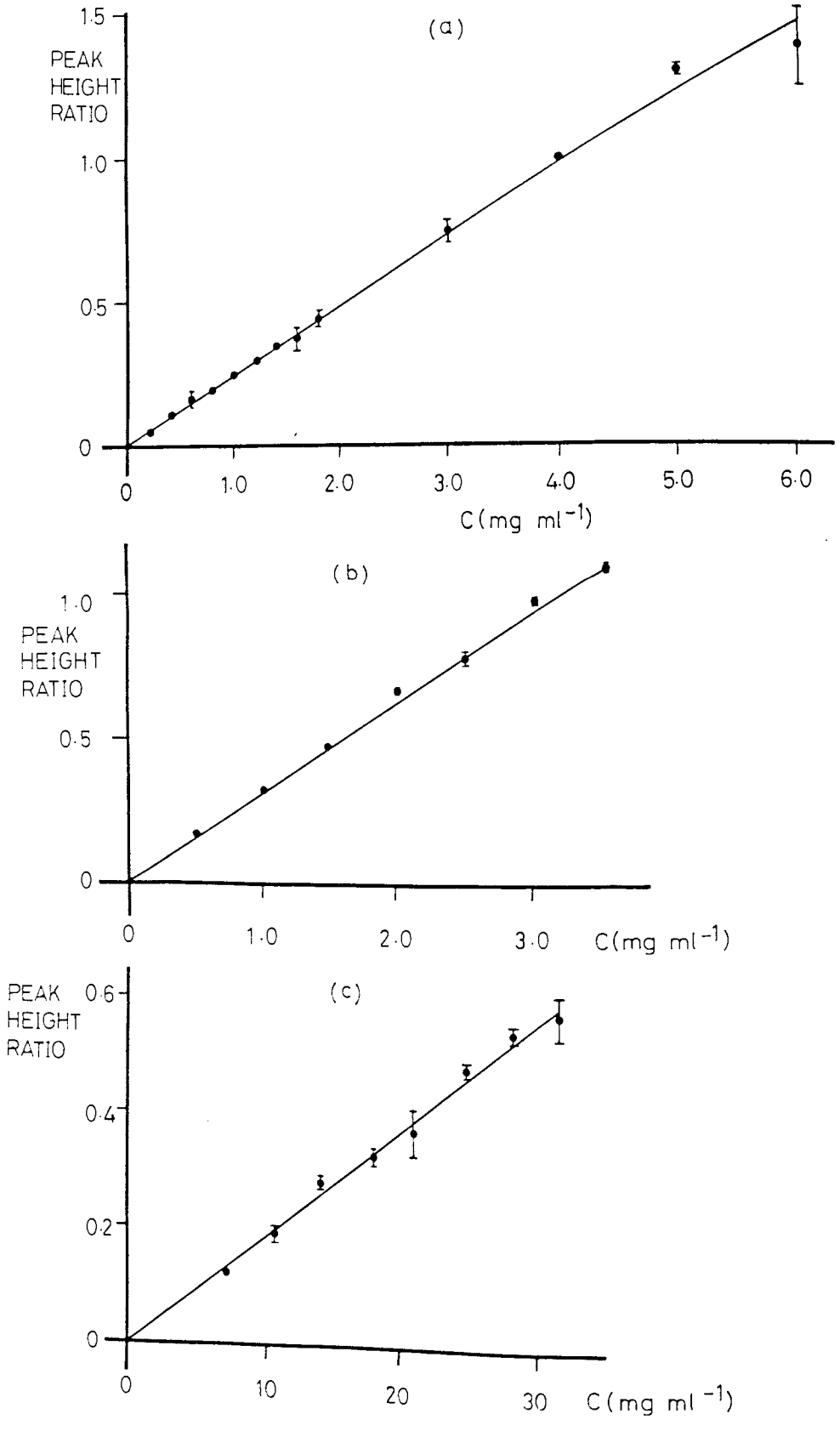

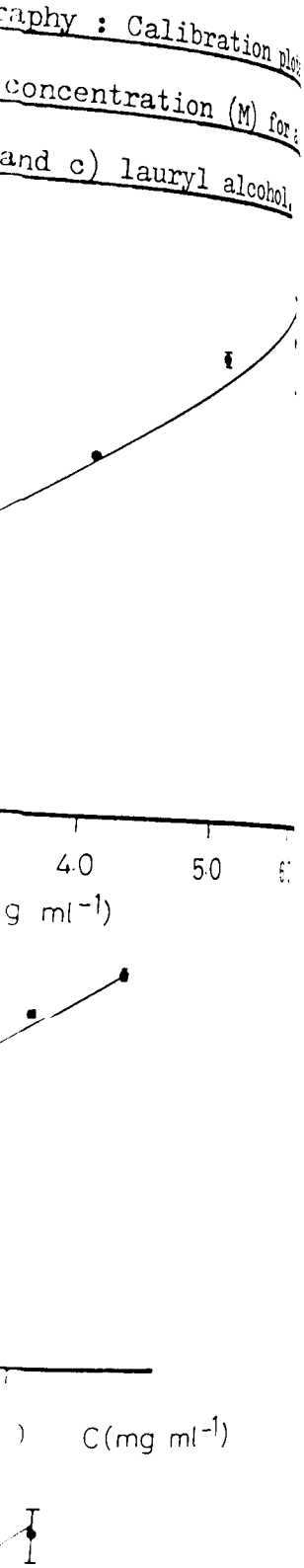

these particular surfactants in the chosen solvent. The combination of this technique and surface tension measurement and ultra - violet spectroscopy have suggested that lauric acid and lauryl alcohol may be worthy of further investigation with respect to coating disodium fluorescein powder.

It has been noted that reducing the dielectric constant of the solvent results in a reduction in the CMC of surfactants in solution (268). It may be possible, by reducing the concentrations of the surfactants below the CMC in dichloromethane and then by the addition of small quantities of a solvent with a lower dielectric constant, to optimise conditions with a view to facilitating adsorption of the surfactant at the surface of the powder.

Since gas liquid chromatography is a recognised technique for the assay of fatty acids and alcohols (260,261) this method will be pursued in preference to differential refractometry.

2.3.2.1 Gas Liquid Chromatography.

Three representative calibration curves are presented in Figure 2.10 for each of the coating compounds employed. These graphs of peak height ratio of the sample over the standard preparation against known concentrations of the surfactant in solution (mg ml^{-1}) are all linear over the range of concentrations employed.

Following the discussion to the previous section the addition of chloroform to enhance adsorption was investigated. The lauric acid adsorption isotherm shown in Figure 2.11 represents the extent of adsorption as a function of the amount of chloroform added to the mixture, none, 1.0, 2.5 and 5.0 ml respectively. Lines of best fit have been drawn through these points, after being derived by linear regression analysis

Figure 2.11 : Gas liquid chromatography : Adsorption isothems of lauric acid at the surface of disodium fluorescein from dichloromethane/chloroform solution.

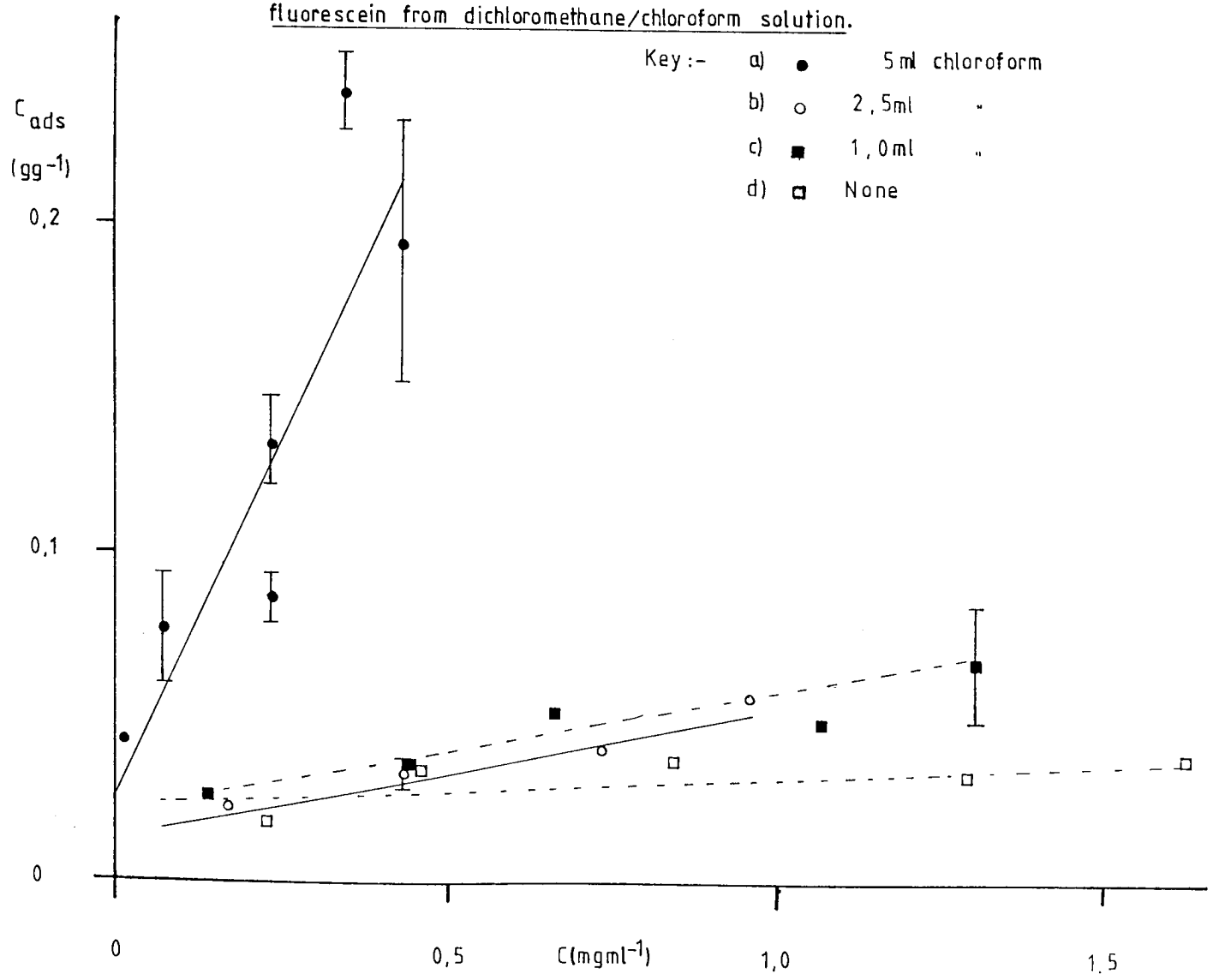

The maximum adsorbed amount, the slope, intercept and correlation coefficient for this data are shown in Table 2.10.

The addition of chloroform appears to increase the maximum amount adsorbed. A similar effect to this has been observed by altering the hydrocarbon chain length in aqueous solutions (270) and by altering the solvent properties (266). Since, from equation 2.8, the log of amount adsorbed is directly proportional to lateral and surface interaction energies, which are themselves functions of the solvent electrical properties and the structure of the surfactant molecule, these observations might be expected. The fact that the log of amount adsorbed is inversely proportional to temperature means that the observation that reduction in temperature effects an increase in the amount adsorbed (271) is hardly surprising.

An increase in the association of lecithin molecules in micelles has been observed with the reduction of the dielectric constant of the medium (267). An expression for the change in the interaction energy at the solute/solvent boundary on forming micelles has been proposed.

$$\Delta E = \gamma_{hs}(h^s - h^m) - \gamma_{ts}(t_l^s - t_l^m) \qquad 2.22$$

Where h is the area of the polar head group of the monomer, t_l is the area of the hydrocarbon tails and the superscripts s and m represent single molecules and micelles respectively, γ_{hs} and γ_{ts} being the interaction energies per unit area between the head group and the solvent and the tails and the solvent respectively.

In this context the explanation which is put forward for the increase in size of micelles with reduction in dielectric constant is a low tail group interaction, from which a small value of γ_{ts} would be expected, due to the miscible nature of these solvents with

Table 2.10 : Gas liquid chromatography : The maximum observed amount adsorbed (gg^{-1}), the slope, intercept and correlation coefficient for the data collected on the effect of the addition of different quantities of chloroform on the adsorption of lauric acid at the surface of disodium fluorescein.

Quantity of Chloroform ml ($\epsilon = 4 \cdot 806$)	Maximum observed Amount Adsorbed. gg^{-1}	Slope	Intercept	Correlation Coefficient.
None	0.047	0.01	0.022	0.82
1.0	0.066	0.03	0.024	0.923
2.5	0.055	0.039	0.015	0.972
5.0	0.238	0.328	0.041	0.942

Figure 2,12: Gas liquid cnromatography : Adsorption isotherms of lauric acid at the surface of disodium fluorescein from dichloromethane/chloroform,

a) Preliminary plot comparing supernatant with powder derived results.

b) Detailed plot derived by examining powders.

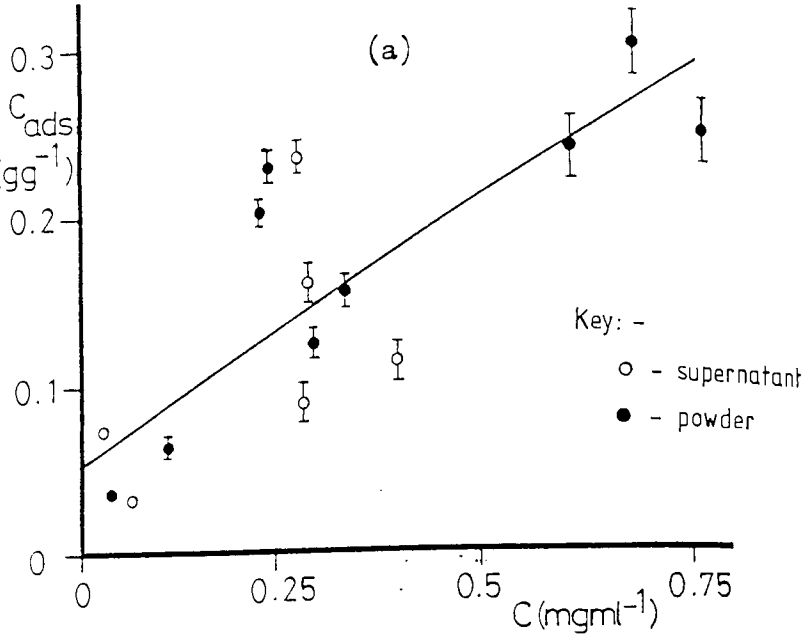

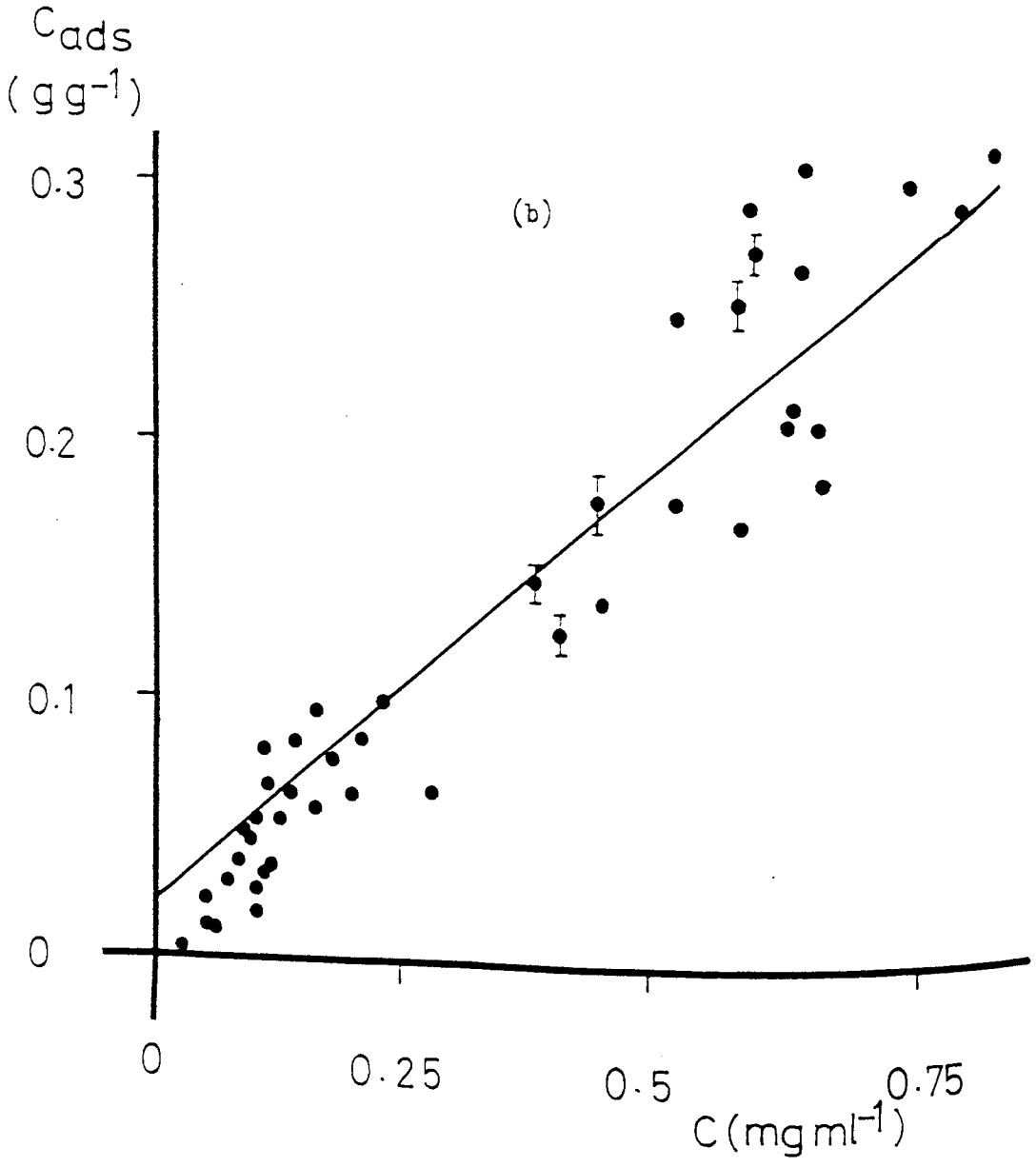

paraffin chains. It can be deduced that the term on the right of the above equation is largely responsible for the ΔE on micellisation. A high interaction energy between the head groups in the centre of the micelle. Further important factors for micellisation in non - aqueous solvents have been shown to be dipole - dipole interactions between the head groups and the possibility of hydrogen bond formation (272 - 274). It is possible that these interaction energies may be more important than solvent - tail group interactions.

The effect of the addition of chloroform on the adsorption of surfactants from dichloromethane was incorporated into the coating procedure adopted for subsequent experiments. Various surfactants were prepared in 25 ml of dichloromethane. Disodium fluorescein, 0.25 g, was added to these solutions in 50 ml stoppered conical flasks. After 6 hours 5 ml of chloroform were added to the mixture.

Seventy two hours after preparation the powders were filtered using Whatman No. 1 filter paper, a Buchner funnel and an evacuated conical flask. Finally the powders were dried at less than 40 °C.

Figure 2.12 a) was prepared from the GLC analysis of both the supernatant, from the powder coating experiments, and the dried powder. The object of this study was to establish the accuracy of the estimate of the amount of surfactant adsorbed. The supernatant sample was taken prior to filtration.

It may be observed from the figure that the supernatant and the powder results are very similar and therefore analysis of the powder indicates no association of lauric acid in excess of that observed in the supernatant. The preparation of the powder does not, therefore, result in further association of lauric acid with disodium fluorescein, through filtration and drying excesses,

The adsorption isotherm shown in Figure 2.12 a) has been fitted

Figure 2.13 : Gas liquid chromatography : Adsorption isotherms at the surface of disodium fluorescein from dichloromethane/chloroform solution of a) capric acid and b) lauryl alcohol.

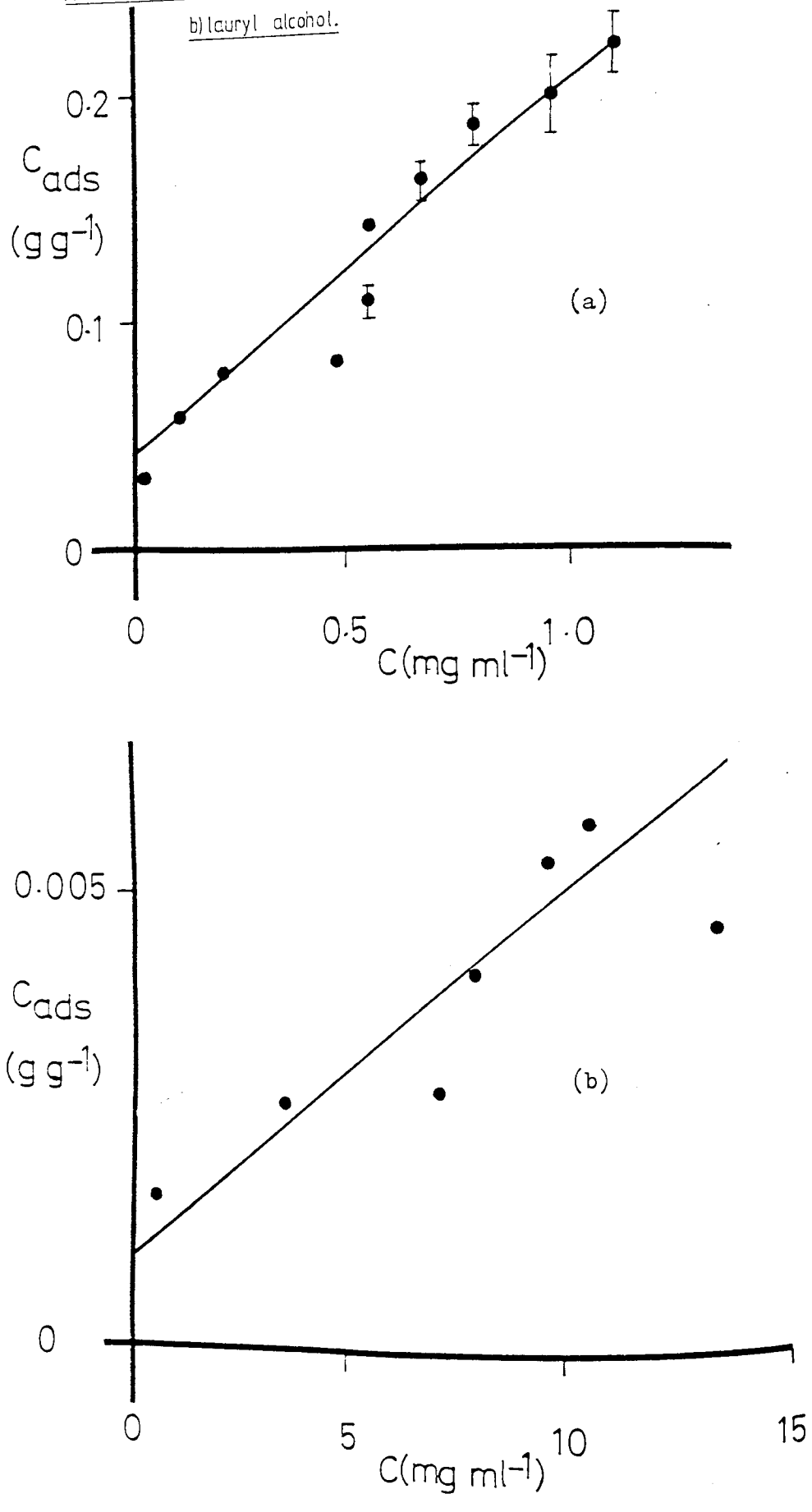

by linear regression analysis to the line described by the slope 0.275, and intercept 0.058, having a correlation coefficient of 0.74. Figure 2.12 b) shows a more detailed isotherm of lauric acid at the surface of disodium fluorescein. The analysis of the data gives a line described by the slope 0.309, and intercept 0.022, having a correlation coefficient of 0.91. An analysis of variance shows no statistically significant difference between this this more detailed plot and the initial plot at a 5% probability limit.

Figure 2.13 shows the plots of the capric acid and lauryl alcohol isotherms. The capric acid plot may be described by a line of slope 0.126, and intercept 0.045, having a correlation coefficient of 0.9. Similarly the lauryl alcohol plot may be described by the line of slope 0.0004 and intercept 0.0009, having a correlation coefficient of 0.9. The lauryl alcohol plot shows a marked reduction in adsorption over a given concentration range, in comparison with lauric and capric acid samples, having a value of 5 to 6 mg ml^{-1}. This suggests that the significant factor in the adsorption of these compounds is the nature of the polar head group since this is the most significant difference between the lauric and capric acids and lauryl alcohol.

2.3.2.2 Infra - Red Spectrophotometry.

Three applications of this technique have been employed. The first is the examination of the coated powders, their initial components and possible resultant constituents, in order to establish the nature of the association between the surfactants and the powder adsorbent. The use of areas of the spectra which can be attributed solely to individual components may give a quantitative check of the GLC data. Finally solution I.R. may give some indication of the way in which surfactant molecules associate in solution.

Table 2.11 : Summary of the qualitative findings established by infra - red spectroscopy.

Sample	CH_2/CH_3 2,900 cm^{-1}	Carboxylate 1,700 cm^{-1}	Carboxylate Anion, 1,560 cm^{-1}
Sodium Laurate	+	+*	+
Lauric Acid	+	+	-
Capric Acid	+	+	-
Disodium Fluorescein (DF)	-	-	+
DF - Lauric Acid	+	+	+
DF - Capric Acid	+	+	+
Lauric Acid Coated DF (High 0.63 gg^{-1})	+	+*	+
Lauric Acid Coated DF (Low 0.12 gg^{-1})	+	-	+
Capric Acid Coated DF (Low 0.11 gg^{-1})	+	-	+

* very weak peak.

By examining the spectra a pattern may evolve which can explain the nature of the adsorption. The molecular constituents shown in the figures, 2.14 to 2.19, are detailed below.

The two peaks which occur at approximately 2,900 cm^{-1} are attributable to methyl (CH_3,CH_2) groups of aliphatic hydrocarbons. The single strong peak at 1,700 cm^{-1} is the carboxylate peak which in this position indicates the dimer of a fatty acid. The single strong peak at 1,560 cm^{-1} is attributable to the carboxylate anion, in this case associated with a sodium atom (275). Peaks in the "fingerprint" area of the spectra (up to 1,000 cm^{-1}) are nearly all attributable to disodium fluorescein in the coated powders and one of these, at 920 cm^{-1}, has been used as the standard for the preparation of the adsorption isotherm in conjunction with the methyl peak, 2,900 cm^{-1}, for the fatty acid.

The qualitative findings established by infra - red spectroscopy are summarised in Table 2.11. The samples examined by infra - red spectroscopy can all be characterised in terms of the presence of absence of the three peaks previously mentioned.

The absence of the carboxylate peak in the case of the lower coated powders, Figure 2.16 b) and c),and its presence in the mixtures of fatty acids and disodium fluorescein, Figures 2.15 b) and c), indicates an interaction between the fatty acid and the disodium fluorescein. The appearance of a sodium carboxylate peak (carboxylate anion) in these coated powders and its absence from the mixtures suggests that a bond at one of the sodium positions has occurred between the fatty acid and the disodium fluorescein. This observation is consistent with the peaks observed for the sodium salt of lauric acid, shown in Figure 2.14 c). The absence of a carboxylate peak for these coated powders also implies that either the fatty acid is chemically bonded to the phenol

Figure 2.14 : Infra - red spectroscopy : Peaks observed for a) Lauric acid, b) Capric acid and c) sodium laurate.

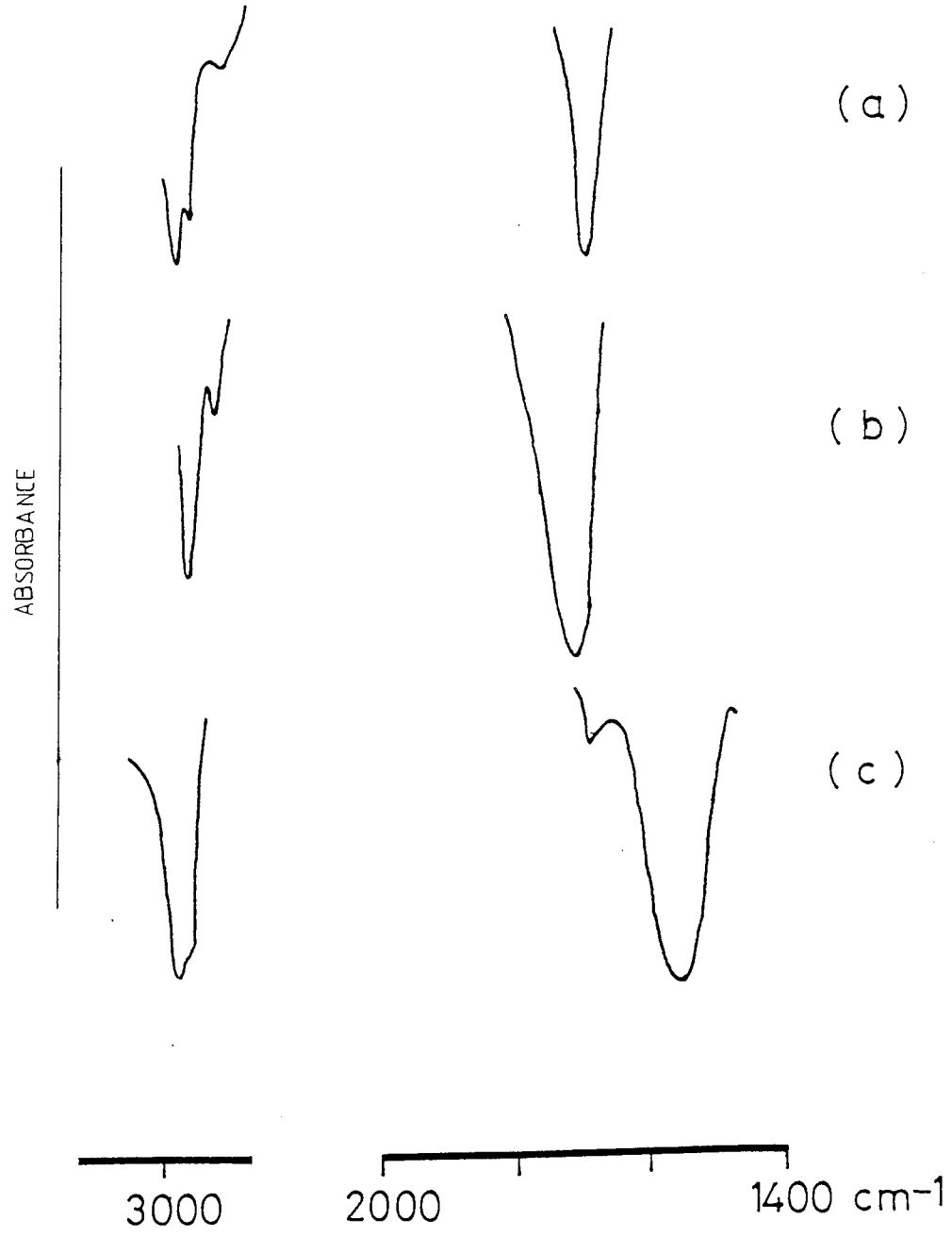

Figure 2.15 : Infra - red spectroscopy : Peaks observed for a) Disodium fluorescein, b) Disodium fluorescein mixed with lauric acid and c) Disodium fluorescein mixed with capric acid.

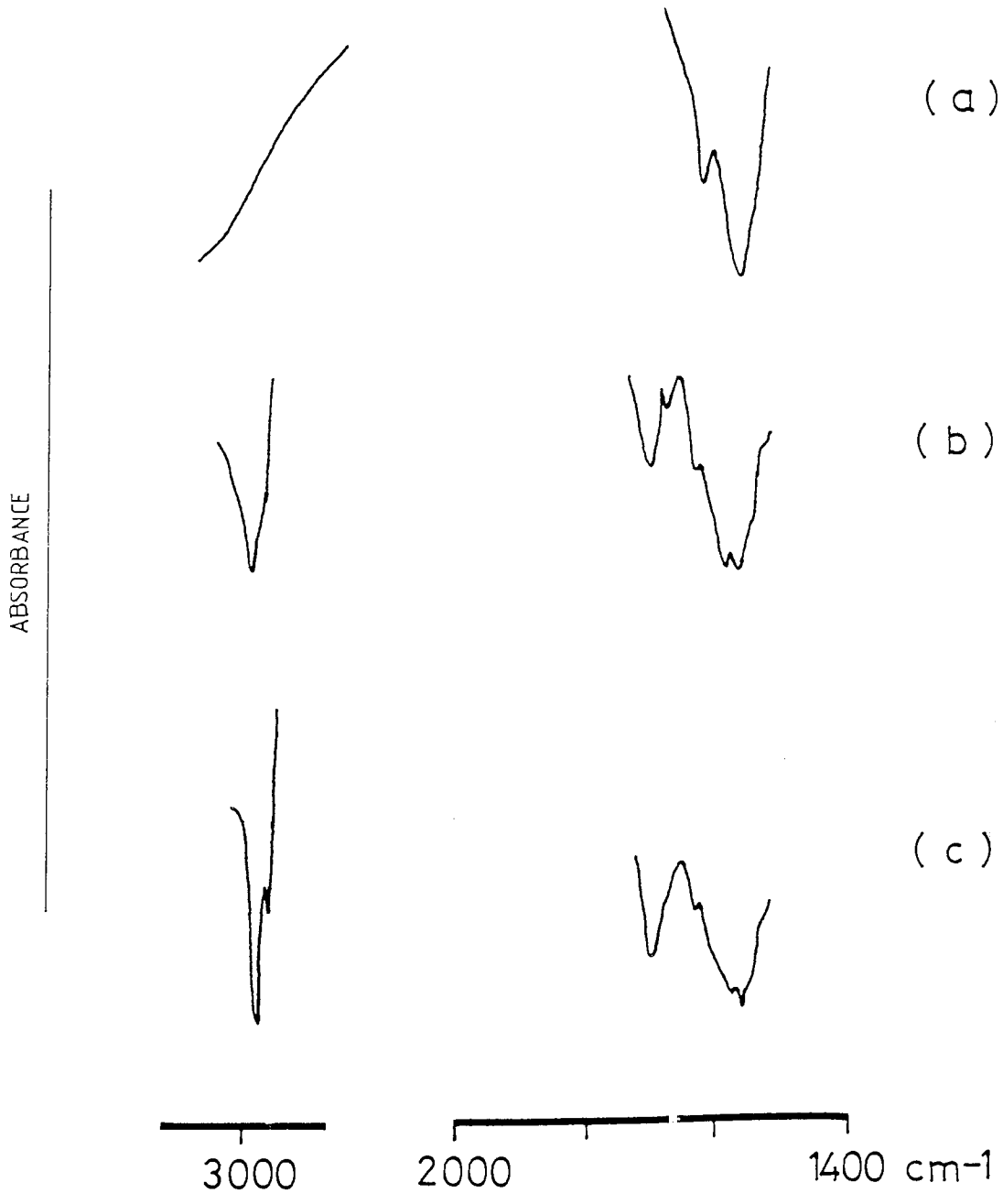

Figure 2.16 : Infra - red spectroscopy : Peaks observed for a) Disodium fluorescein nominally coated with 0.63 gg^{-1} lauric acid, b) Disodium fluorescein nominally coated with 0.12 gg^{-1} lauric acid and c) Disodium fluorescein nominally coated with 0.11 gg^{-1} capric acid.

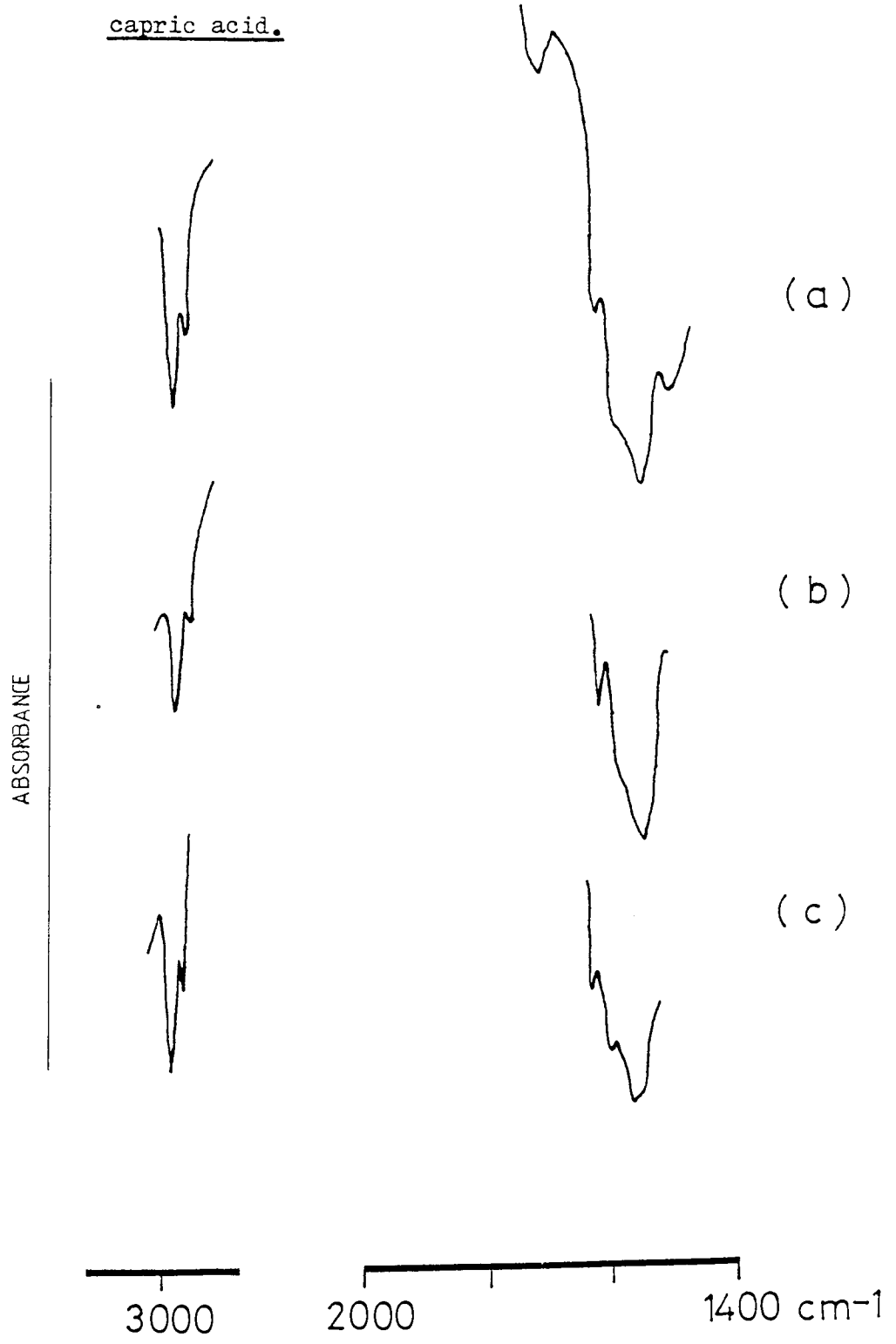

Figure 2,17: Infra-red spectroscopy: Calibration plot prepared from the ratio of the peaks at 2,900 cm-1: 920 cm-1 against the concentration of lauric acid (gg-1)

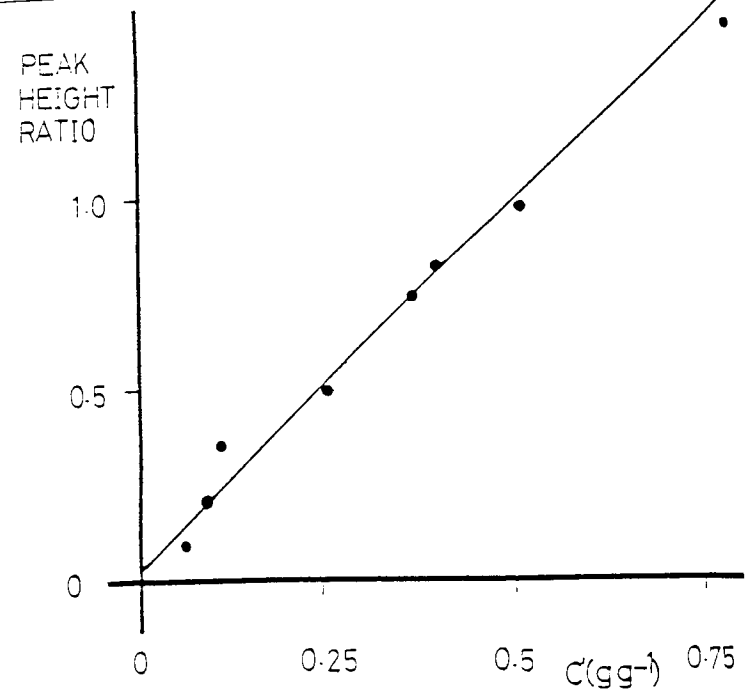

Figure 2,18 : Infra-red spectroscopy: Adsorption isotherms plotted for lauric acid at the surface of disodium fluorescein from dichloromethane/chloroform solution obtained by a) GLC and b) IR spectroscopy.

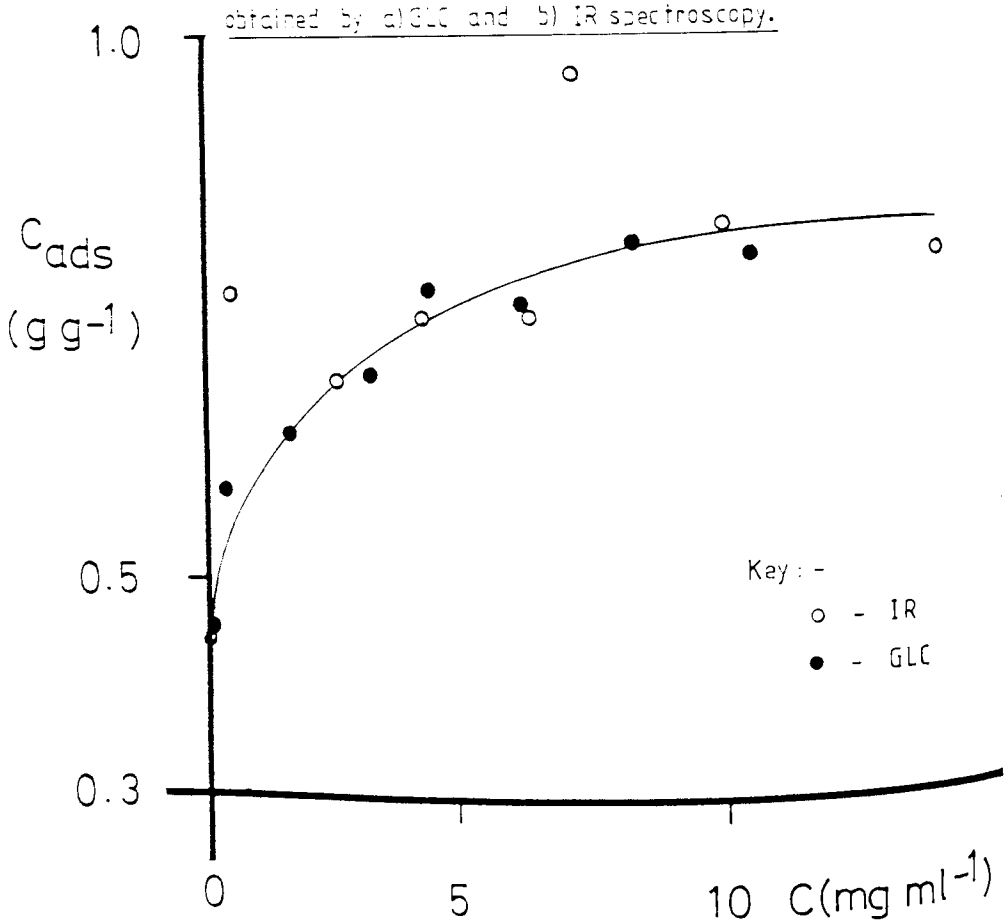

group at which the sodium atom is situated, or if the acid was bound at the carboxylate anion complete transfer of the sodium to the acid cannot have taken place otherwise the carboxylate peak would not have disappeared. The appearance of a small lauric acid peak in the more coated lauric acid sample, Figure 2.16 a), suggests that the association between the acid and the powder has passed into a second phase which might be due to the association of the free acid or to the transfer of the sodium from the acid group of the disodium fluorescein to the fatty acid.

Figures 2.17 and 2.18 b) show a calibration plot of the ratio of the methyl group peak at 2,900 cm^{-1} to the disodium fluorescein peak in the "fingerprint" area at 920 cm^{-1}, and the adsorption isotherm for lauric acid at the surface of disodium fluorescein produced using the calibration plot. Figure 2.18 a) is the GLC equivalent to the infra - red isotherm. It can be seen that in general terms the two isotherms are similar, however the maximum, indicated by the plateau, measured by IR is slightly higher than that observed by GLC. It may be assumed that this is due to the insensitivity of the technique. It would be difficult to obtain reasonable IR data in the lower range of concentrations used earlier, shown in Figure 2,12 of up to approximately 1 mg ml^{-1}, as the limit of sensitivity for this technique, approximately 0.05 gg^{-1}, would be exceeded. For more reliable data to be obtained Fourier Transform IR spectroscopy should be carried out (275). Further investigation of this approach was not carried out since it was intended to use the IR to support the GLC and not to obtain absolute quantitative information. The two data points obtained by GLC and shown in Figure 2.18 a), which are within the range of the data for lauric acid shown in Figure 2.12, seem to indicate greater surface coverage than was observed in the detailed plots.

Figure 2.19 : Infra - red spectroscopy : Solution infra - red of lauric acid in dichloromethane/chloroform showing the peak at 1,700 cm^{-1}.

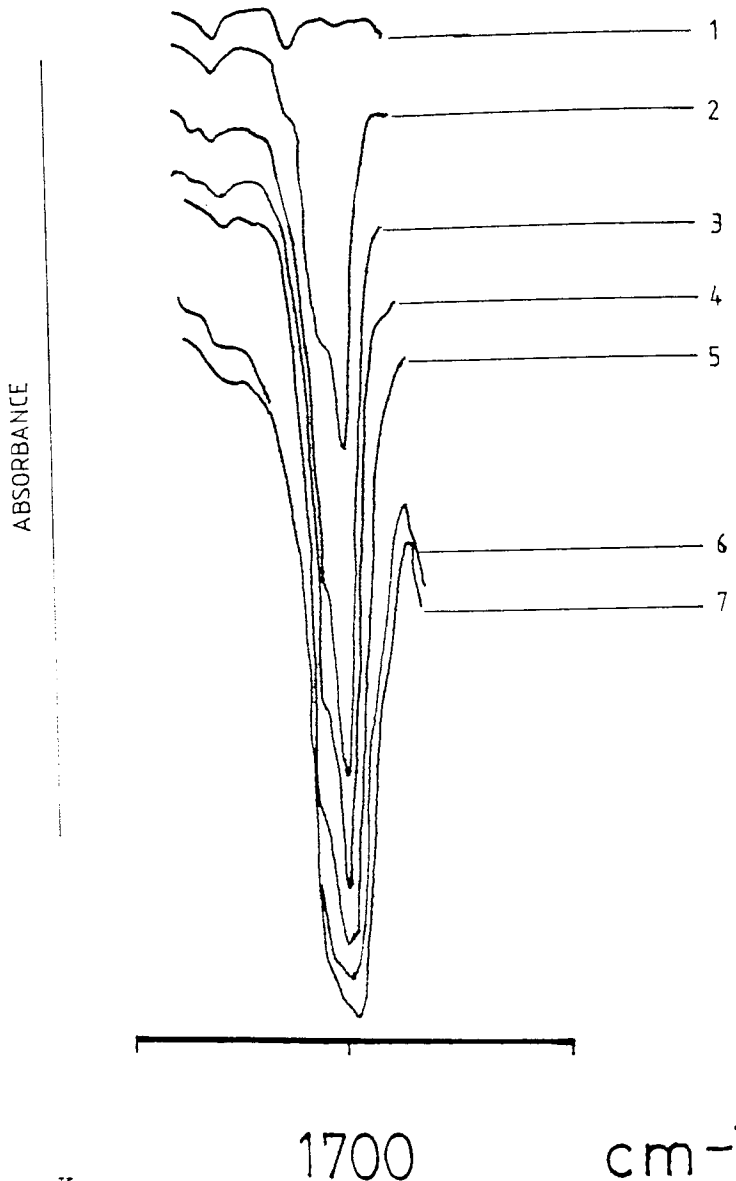

Key :-

Concentrations of lauric acid,(M),

1. 0	3. 0.05	5. 0.1	7. 0.2	
2. 0.025	4. 0.075	6. 0.15		

The formation of micelles by surfactant molecules in non - polar solvents has benn investigated by infra - red spectroscopy (264). Figure 2.19 shows the LR spectra of various concentrations of lauric acid in dichloromethane/chloroform (5:1) solution. The range shown, covering 1,700 cm^{-1}, should show any monomers or dimers present. The monomers should appear at 1,770 cm^{-1} and the dimers at 1,720 cm^{-1} (264), for lauric acid in carbon tetrachloride. The absence of a peak at 1,770 cm^{-1} except for that due to the solvent and the presence of a peak at 1,700 cm^{-1} which is within the range for dimerised carboxylic acids (275) suggests that there are few, if any, monomers present in solution at these concentrations.

It has been observed that fatty acid molecules at low concentrations in carbon tetrachloride co - exist in three forms : individual molecules; dimers and micelles (264). The CMC of fatty acid solutions was 1.0 to 1.5 orders of magnitude greater than the critical aggregation concentration corresponding to the formation of dimers. The IR spectra of stearic acid solutions in carbon tetrachloride at 298 °K indicated that increasing the concentration of the fatty acid in solution resulted in a reduction in the proportion of the total made up of monomers and an increase in the proportion consisting of dimers and micelles. Micelle formation may occur at the concentrations of surfactant employed in the experiments which have been described.

Figure 2.20 shows the surface tension data for capric acid and lauric acid in dichloromethane/chloroform. These compounds exhibit CMC's at 0.014 M or less for capric acid and 0.025 M for lauric acid. Both of these compounds have significantly reduced CMC's compared with those in pure dichloromethane, shown in Table 2.9 . This correlates with the observation that the CMC of cetylpyridinium bromide in dichloroethane was reduced significantly by the addition of benzene

Figure 2.20 : Surface tension measurement : Surface tension (mNm^{-1}) plotted against concentration (M) for a) lauric acid and b) capric acid in dichloromethane/chloroform.

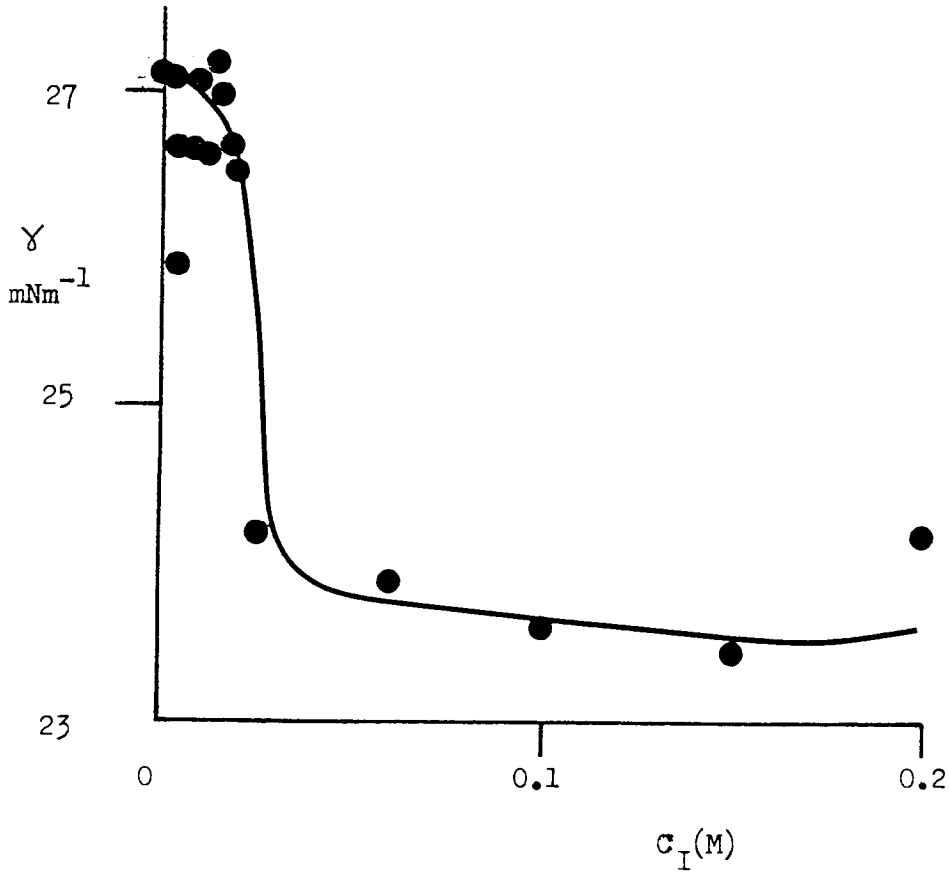

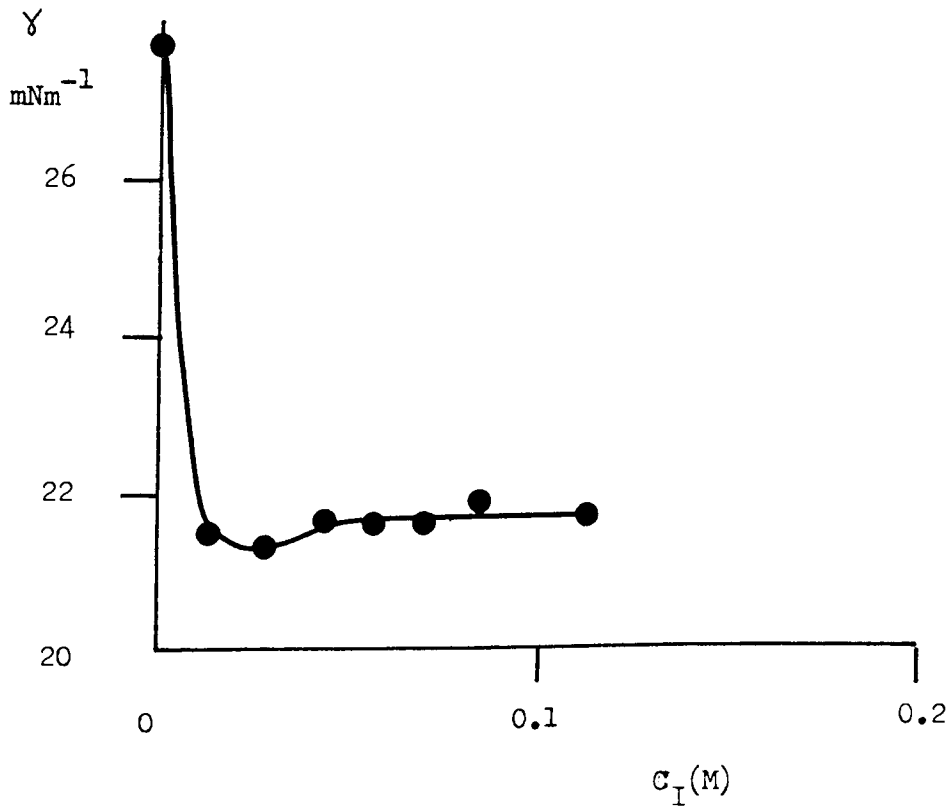

equivalent to 10% (268). The combination of the solution IR and the surface tension results suggest the coexistence of dimers and micelles of lauric acid at and above the CMC in dichloromethane/chloroform.

2.3.2.3 X - Ray Photoelectron Spectroscopy (ESCA).

Figure 2.2, page 62 , shows a schematic representation of an idealised solid surface. In addition to the valence electrons, which provide the bonding for the system, each atom present in the surface (except hydrogen) possesses core electrons not involved in bonding. The so called "binding energy" of each core electron, which is conceptually equivalent to the ionisation energy of that electron, is characteristic of the individual atom to which it is bound.The variation of core electron binding energies with atomic number is available in the literature for consultation. Thus, information on the binding energies of electrons within a sample allows qualitative elemental analysis. The electron binding energies within any one element are far from fixed, however, and small variations, of up to 10 eV, in binding energy may occur. These so - called "chemical shifts" are caused by changes inthe valence electronic structure, chemical environment, of the atoms concerned and so may be used to provide information on chemical bonding.

In the basic ESCA experiment, the sample surface is irradiated by a source of low energy X - Rays, $MgK\alpha$ = 1254 eV, under ultra - high vacuum (10^{-8} to 10^{-11} Torr) conditions. Photoionisation then takes place at the surface, the resultant photoelectrons having a kinetic energy (E_k which is related to the X - Ray energy ($h\nu$) by the Einstein relation, equation 2.16. Since the energy levels occupied by electrons are quantised the photoelectrons have a kinetic energy distribution N(E), consisting of a series of discrete bands, that

essentially reflect the shell form of the electronic structure of the sample. This experimental determination of N(E) by a kinetic energy analysis of the photoelectrons produced by exposure to X - Rays is termed X - Ray Photoelectron Spectroscopy or electron scanning chemical analysis (ESCA).

The figures, 2.21 to 2.27, show a computer interpretation of the output of the dispersive autoanalyser, which operates by dispersing the electrons in an electrostatic field according to their energies. After leaving the analyser, the energy - dispersed electrons are made to enter an electron multiplier/detector, the output of which, when operating in a pulse counting mode, where individual electrons are detected at rates up to 3×10^5 s^{-1}, is used to generate the photoelectron spectrum in the form N(E), I on the figures, versus E. This output has to be referred to a standard peak to establish the actual binding energy, thus eliminating the instrument work function, ϕ , and the energy derived from the incoming photon , $h\nu$.

The lauric acid C_{1s} spectrum, shown in 2.21 a), shows a major peak C_1 at a binding energy (BE) of 285.0 eV (by definition) and of width 1.4 eV and a minor peak C_2 at a BE of 289.5 eV. This latter BE is consistent with a carbon atom in a carbonyl group and the ratio C_1/C_2 is 11.2, which is close to the theoretical ratio of 11.0 for lauric acid, as shown in Tables 2.12 and 2.13.

The O_{1s} spectrum, shown in 2.21 b), also comprises two peaks at O_1 , with a binding energy of 532.4 eV, and O_2, with a binding energy of 533.8 eV. The ratio of the two peak areas, O_1/O_2, is 1.2, rather than the expected value of 1.0. This is indicative of slight surface oxidition.

The C_{1s} spectrum of sodium laurate, shown in Figure 2.22 a), is superficially similar to that of lauric acid, however, the major

Table 2.12: Corrected counts and binding energies for various powders.

Sample	CORRECTED COUNTS AND ( ) BINDING ENERGIES, eV							
	C_1	C_2	C_3	O_1	O_2	O_3	Na_{1s}	Na_A
Lauric acid	22728	2036	-	-	-	-	-	-
	(285.0)	(289.5)	-	-	-	-	-	-
Sodium laurate	16152	1616	-	-	-	-	1600	1593
	(285.0)	(288.2)	-	-	-	-	-	-
Disodium	14856	1056	4043	2564	627	-	1401	1661
Fluorescein	(285.0)	(288.2)	(286.0)	(531.6)	(533.3)	-	-	-
Lauric acid	-	-	-	1724	323	144	1113	1148
coated DF	-	-	-	(531.5)	(533.1)	(529.5)	-	-
Capric acid	-	-	-	2421	198	297	1543	1656
coated DF	-	-	-	(531.7)	(533.7)	(529.9)	-	-

Table 2.13:Ratios of peak intensities for various powders obtained by ESCA.

Samples	RATIOS OF PEAK INTENSITIES							
	$\frac{C_1}{C_3}$	$\frac{C_1}{C_2}$	$\frac{C_3}{C_2}$	$\frac{C_2}{O}\frac{C_3}{}$	$\frac{O_1}{O_2}$	$\frac{O}{Na_{1s}}$	$\frac{C_2 - C_3}{Na_{1s}}$	$\frac{Na_{1s}}{Na_A}$
Lauric acid	-	11.2	-	0.5	1.2	-	-	-
Theoretical	-	11.0	-	0.5	1.0	-	-	
Sodium laurate	-	10.0	-	0.6	-	1.6	1.0	1.0
Theoretical	-	11.0	-	0.5	-	2.0	1.0	
D. Fluorescein	3.7	14.1	3.8	1.6	4.1	2.3	3.6	0.84
Theoretical	3.8	15.0	4.0	1.0	4.0	2.5	2.5	
Lauric acid coated DF	-	-	-	-	5.3	-	-	0.97
Capric acid coated DF	-	-	-	-	12.2	-	-	0.93

Figure 2.21 : ESCA : Spectra a) C_{1s} lauric acid b) O_{1s} lauric acid and the curves fitted to these peaks.

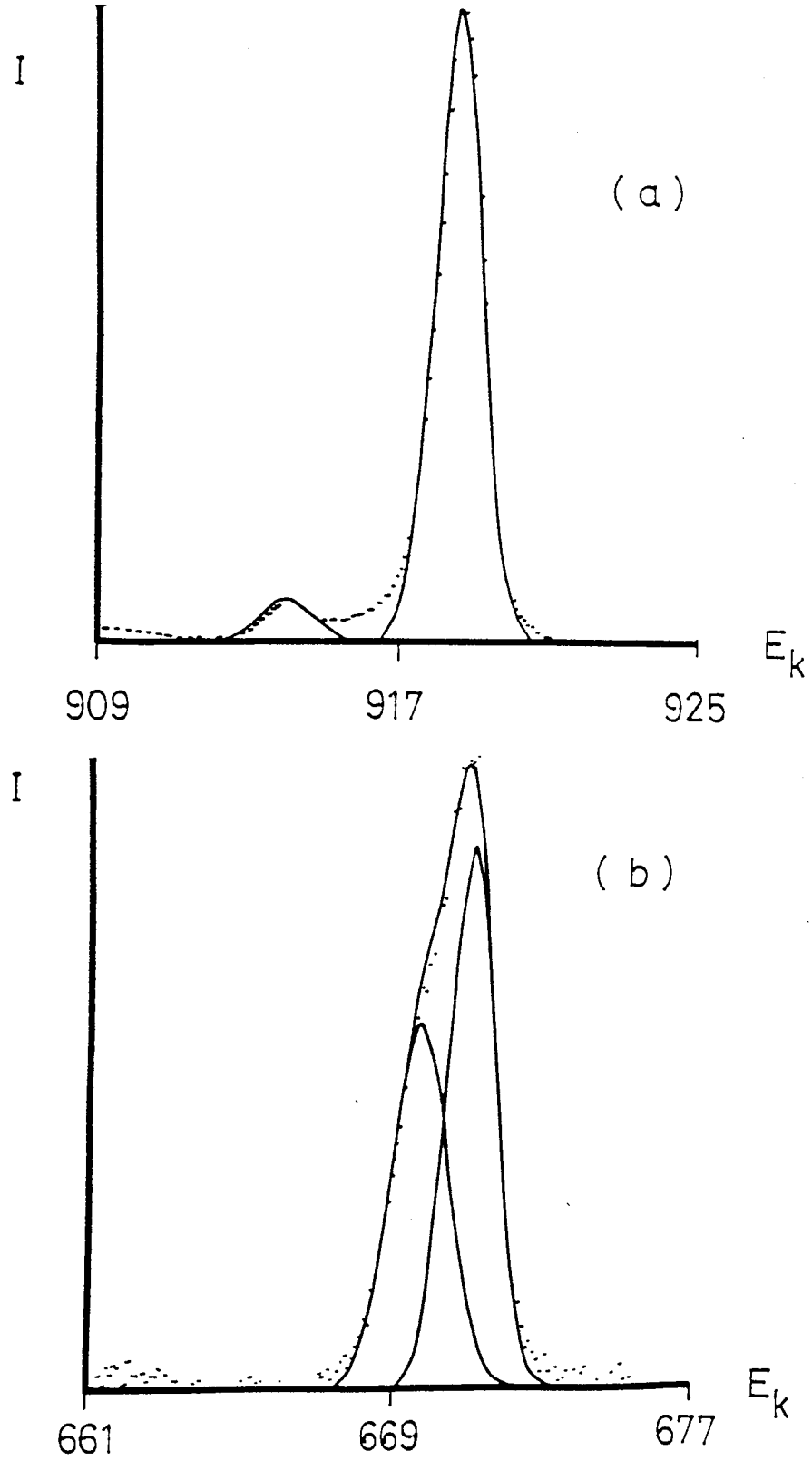

Figure 2.22 : ESCA : Spectra a) C_{1s} sodium laurate b) O_{1s} —— sodium laurate and the curves fitted to these peaks.

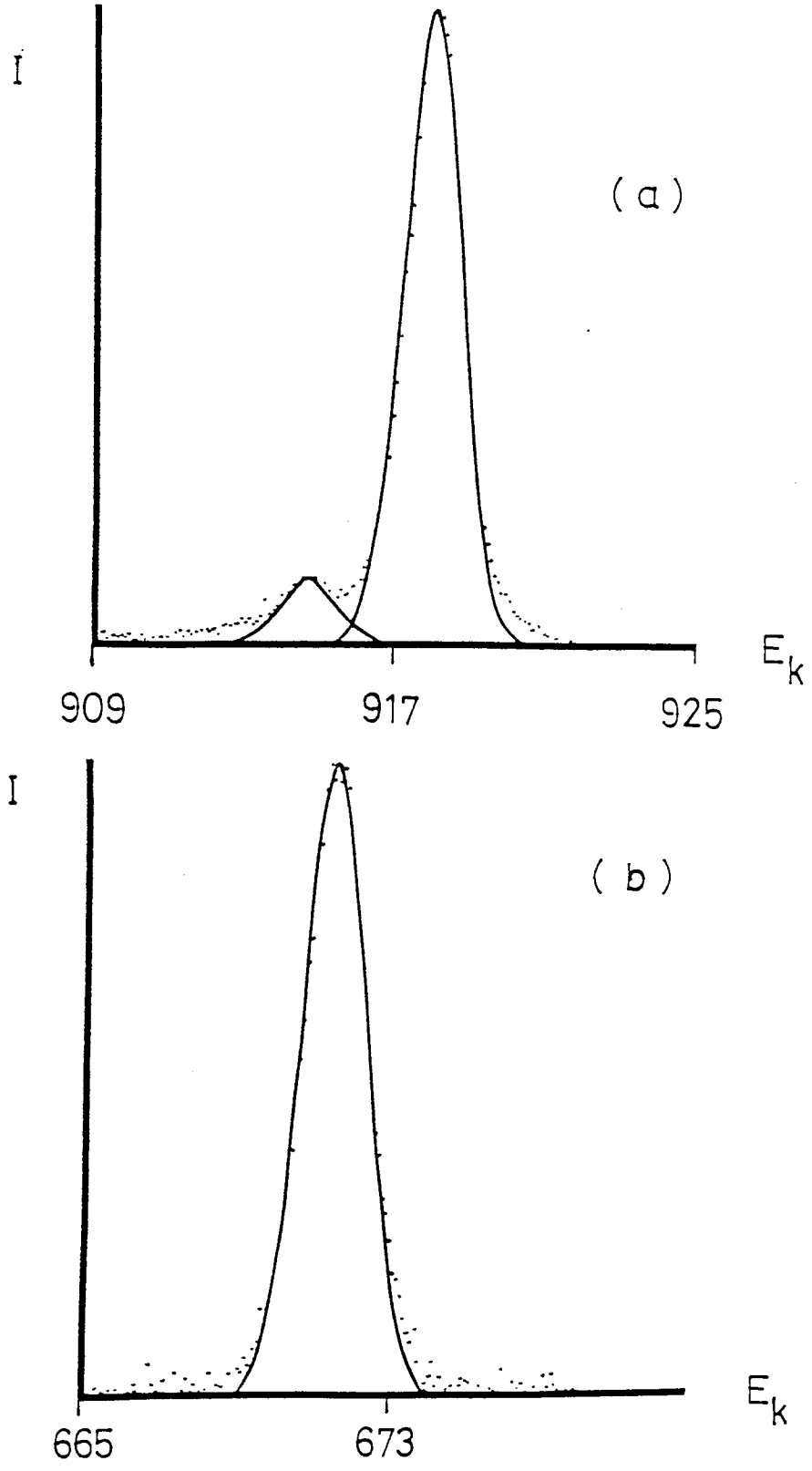

Figure 2.23 : ESCA : Spectra a) C_{1s} disodium fluorescein, b) O_{1s} - disodium fluorescein and the curves fitted to these peaks.

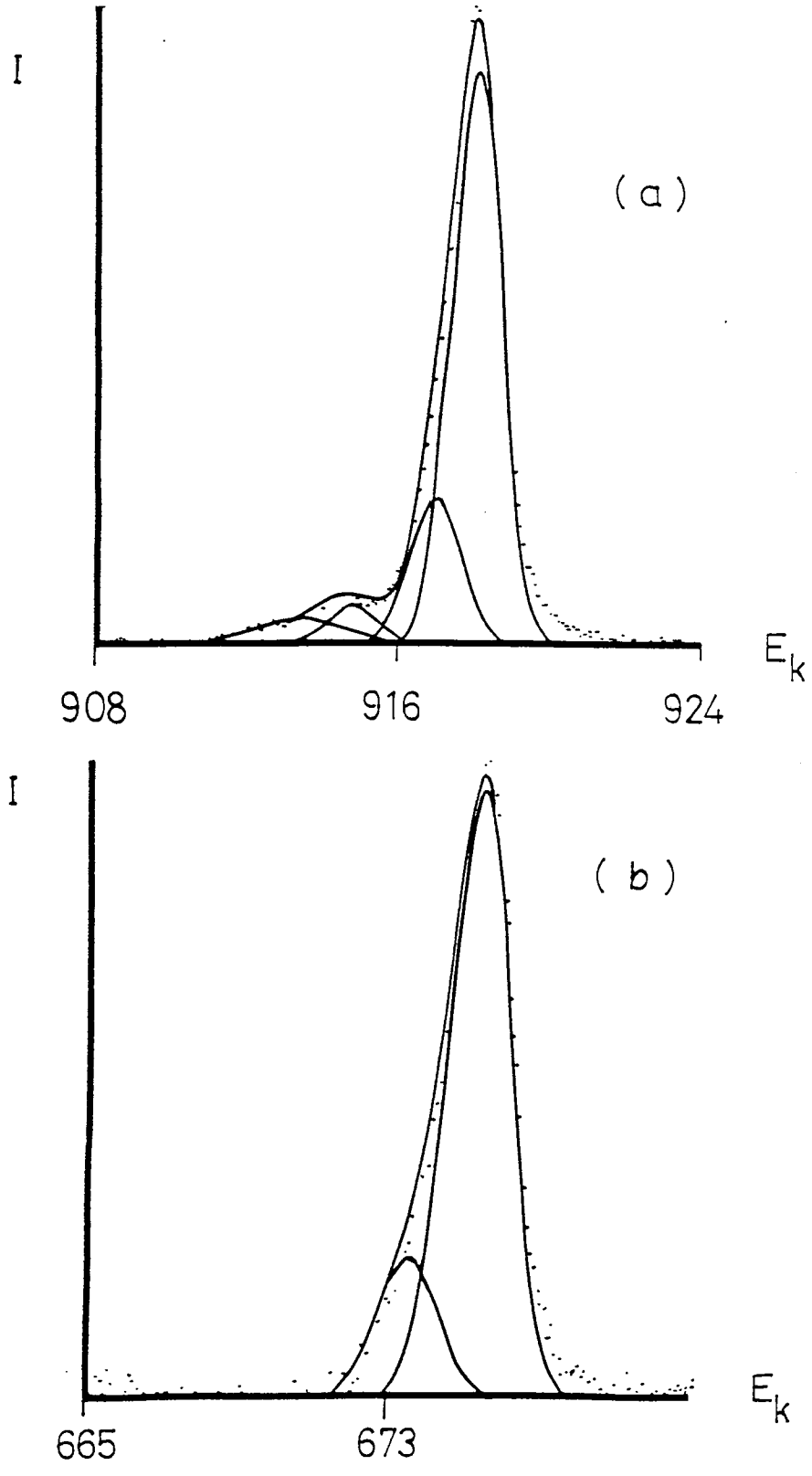

hydrocarbon peak C_1, 285 eV, is slightly broader, 1.8 eV, and the minor carboxyl peak C_2 has shifted to 288.2 eV. This shift to a lower binding energy is to be expected because the oxygen atom of the carboxyl group has acquired negative charge and thus exerts less of an electron withdrawing effect on the carbon atom. The ratio C_1/C_2 is 10, again close to the theoretical value of 11, as shown in Tables 2.12 and 2.13. The values of ratio referred to subsequently in this discussion can all be found in the aforementioned tables.

The O_{1s} spectrum of sodium laurate comprises only one peak of BE, 531.4 eV, shown in Figure 2.22 b). Presumably the electron from the sodium atom is delocalised between the two oxygen atoms of the carboxyl group and they are thus identical.

Disodium fluorescein has a very similar C_{1s} spectrum to that of sodium laurate. A difference spectrum of the two spectra, shown in Figure 2.26 a), suggests the presence of a small peak 1 eV higher in BE than the main hydrocarbon peak. The spectrum has therefore been fitted, in Figure 2.23 a), on the assumption that there is a small peak in this region which corresponds to carbon singly bonded to oxygen. On this basis C-H : C-O : C=O , are approximately in the theoretical ratio as shown in the tables. The small broad peak at a BE of 290 eV has been interpretted as a "shake up" satellite which results from a photo - electron losing some of its energy by displacing an electron as it leaves the atom.

The O_{1s} spectrum of disodium fluorescein is distinctly different from that of sodium laurate. In addition to the major peak O_1 at 531.6 eV there is a smaller peak O_2 at 533.3 eV. The ratio O_1/O_2 is 4.1. From the structure of disodium fluorescein and its canonicals :

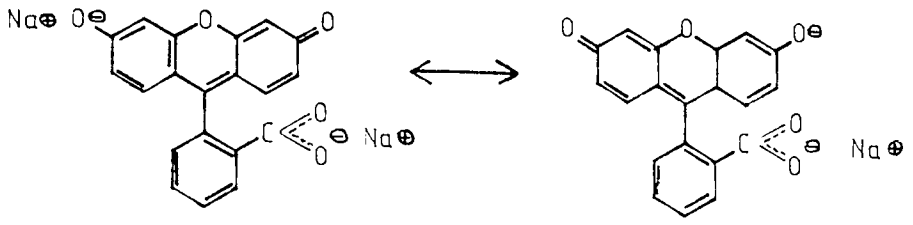

It may be deduced that the two oxygen atoms of the carboxyl group and the two phenolic oxygens have considerable $O^{\ominus}$ character while the oxygen in the centre ring does not. Indeed canonicals involving π - bonding with the oxygen would leave it with a formal positive charge.

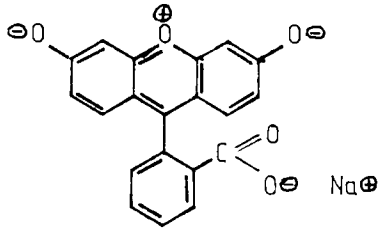

The lower binding energy peak O_1 may be interpretted as being comprised of the carboxyl oxygens and the two phenolic oxygens and the higher binding energy peak O_2 to comprise the ring oxygen and these are in the ratio 4:1 .

The details of the coated powder samples are given in Figures 2.24 and 2.25 (the C_{1s} and O_{1s} peaks) and 2,27(the O_{1s} difference spectra of the coated and uncoated powder) and tables 2.12 and 2.13.

The lauric and capric acid coated powders may be discussed concurrently. Firstly the C_{1s} spectra closely resemble the C_{1s} spectra of sodium laurate and disodium fluorescein with a major peak at 285.0 eV and a minor one at about 288 eV. These do not resemble the free acid which has a minor peak at 289.5 eV which is narrower 1.4 eV.

Figure 2.24 : ESCA : Spectra a) C_{1s} lauric acid coated disodium fluorescein b) O_{1s} lauric acid coated disodium fluorescein and the curves fitted to these peaks.

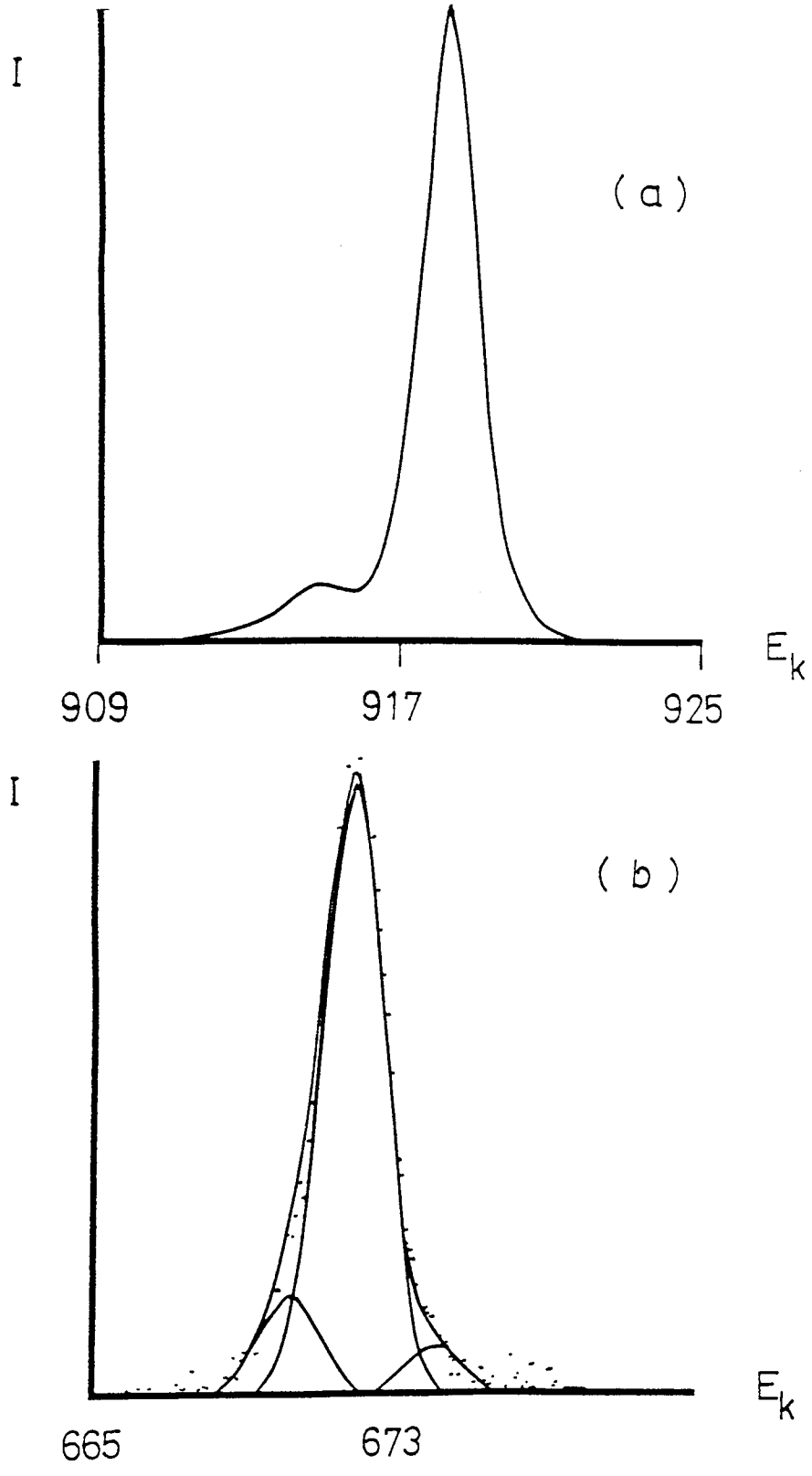

Figure 2.25 : ESCA : Spectra a) C_{1s} Capric acid coated disodium fluorescein b) O_{1s} Capric acid coated disodium fluorescein and the curves fitted to these peaks.

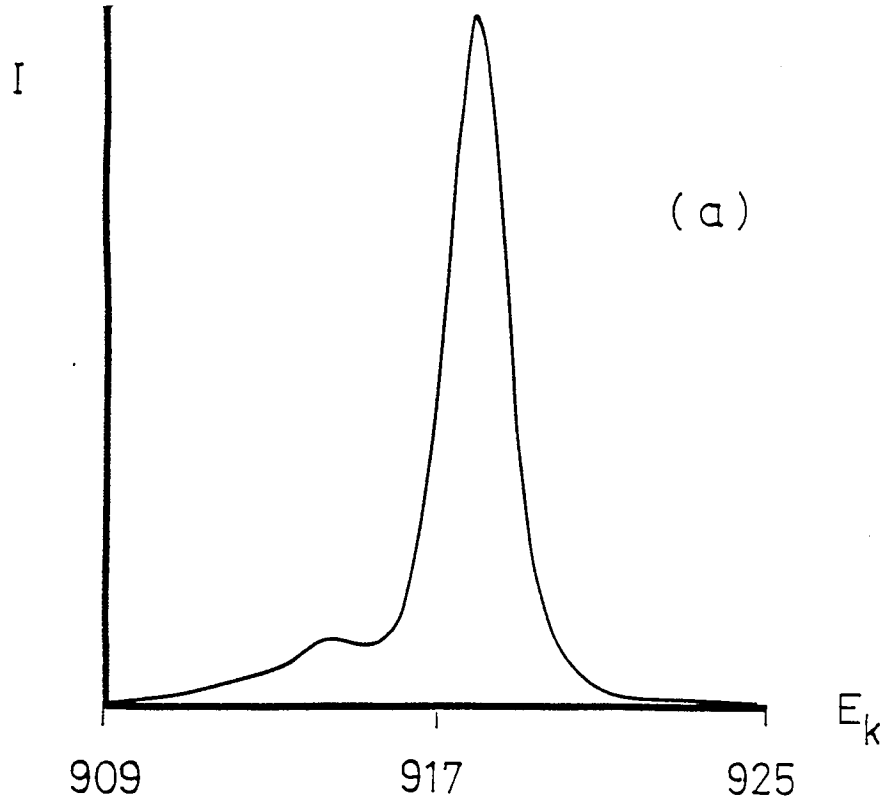

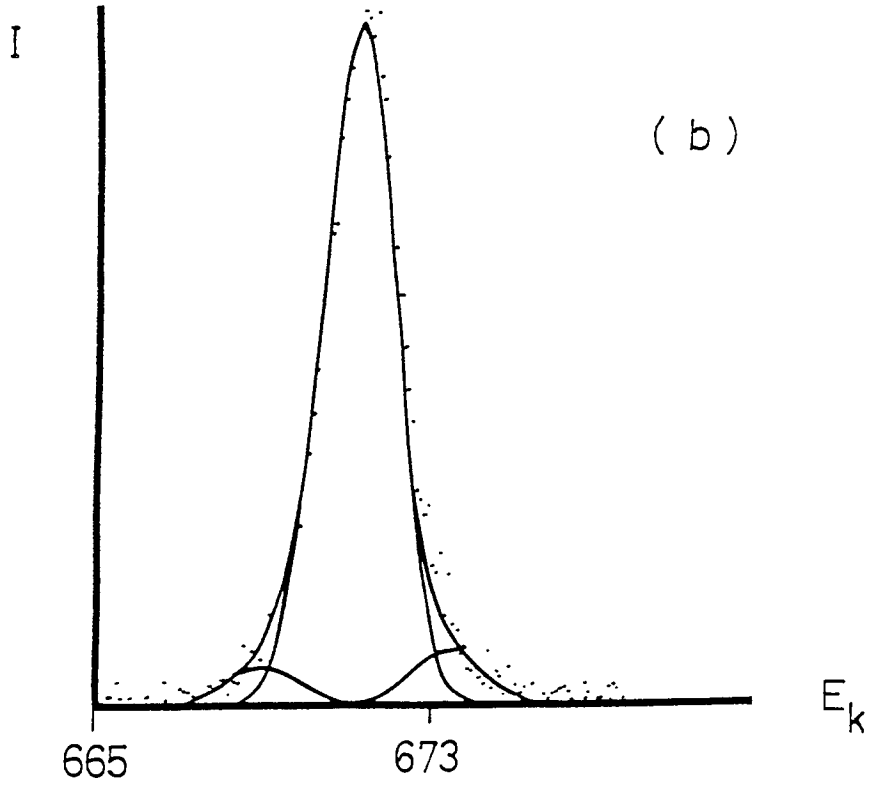

Figure 2.26 : ESCA : Spectra differences a) C_{1s} disodium fluorescein - C_{1s} sodium laurate b) O_{1s} disodium fluorescein - O_{1s} sodium laurate.

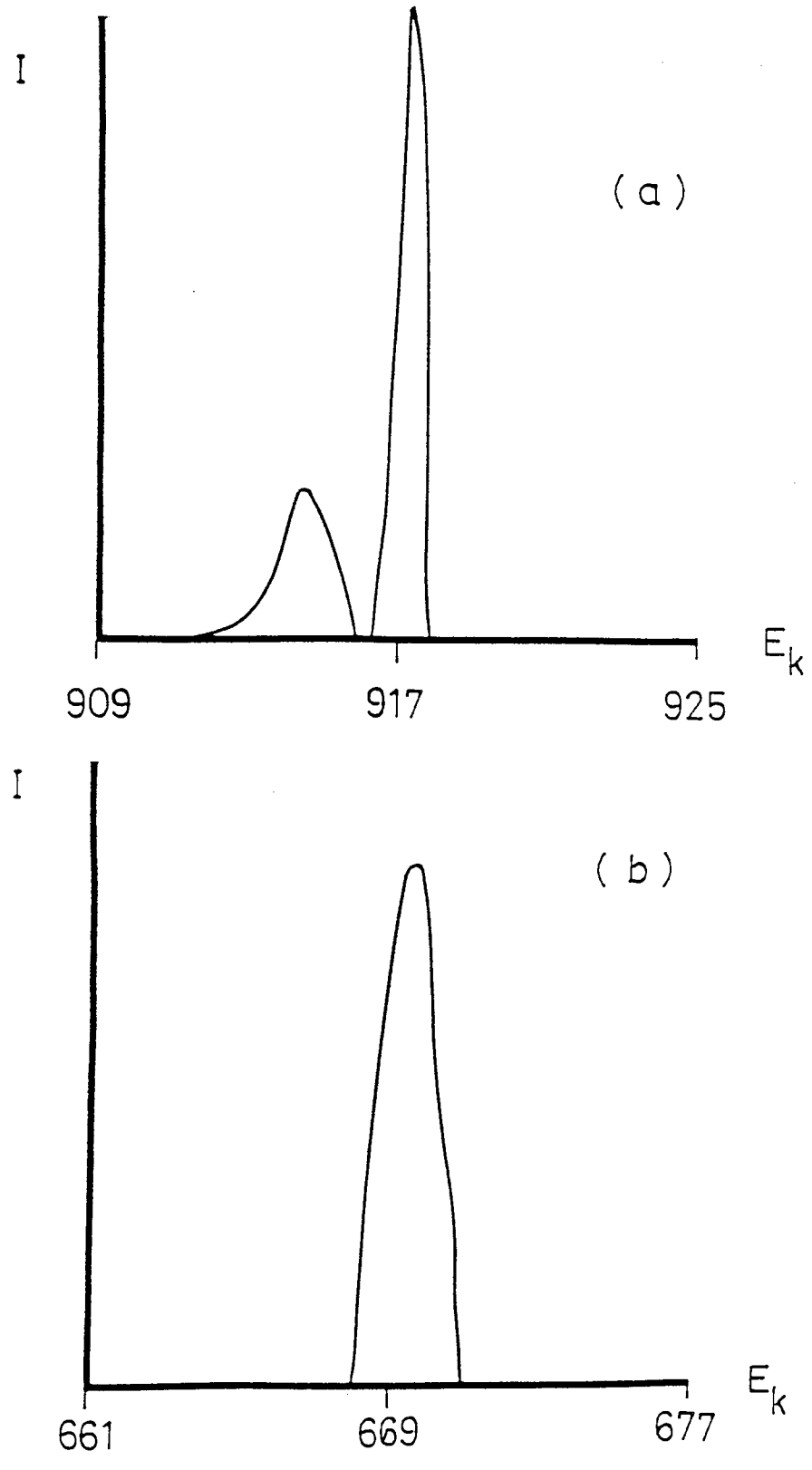

Figure 2.27 : ESCA : Spectra differences a) O_{1s} disodium fluorescein - O_{1s} lauric acid coated disodium fluorescein b) O_{1s} disodium fluorescein - O_{1s} capric acid coated disodium fluorescein.

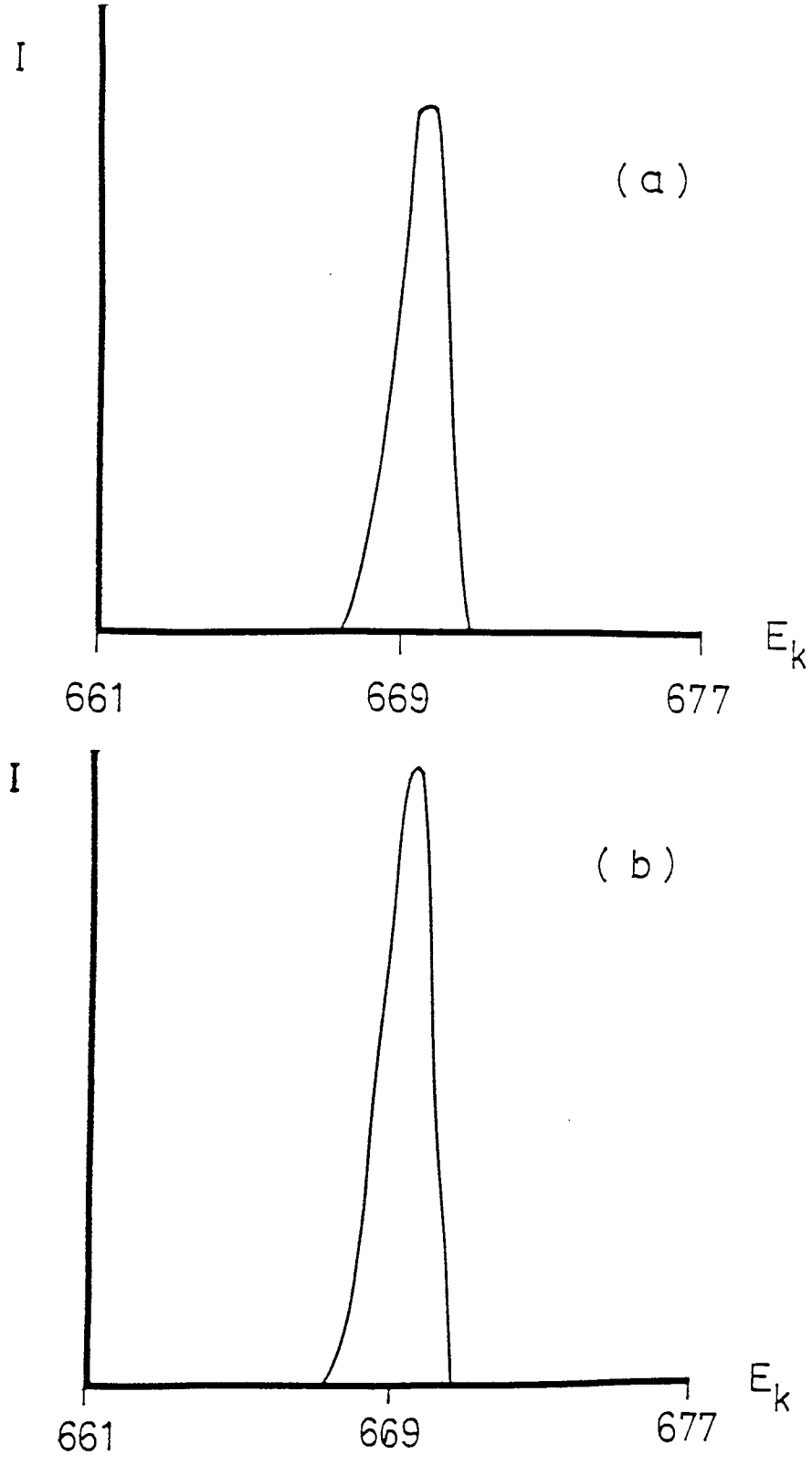

The O_{1s} peaks give considerably more information. Curve fitting of these spectra reveals two peaks, with binding energies : O_1 , 531.5 eV ; O_2 , 533.2 eV. For the lauric acid coated sample the O_1/O_2 ratio is 5.3 and for the capric acid coated sample the ratio is 12. In these case: O_1 corresponds to the major oxygen peak for both sodium laurate and disodium fluorescein, whereas O_2 derives only from the disodium fluorescein. In both coated samples the O_2 contribution to the spectrum is less than for disodium fluorescein itself and thus it must be concluded that its diminution is due to a coating around the particles.

X - Rays with an energy of 1253.6 eV were used in these experiments. Using this radiation Na_{1s} electrons have a kinetic energy of about 940 eV. Low kinetic energy (E_k) electrons are attenuated more than high E_k electrons by an overlayer of another material. Thus if disodium fluorescein has been coated with lauric acid and the ratio Na_{1s}/Na_A (Sodium 1s/Sodium Auger) for the two materials is compared the ratio should be smaller for the coated material than for the uncoated material provided that the sodium ions have remained bonded to the fluorescein during the coating process. From Table 2.13 it may be seen that for sodium laurate and the two coated samples the ratio is close to one, however, the ratio for disodium fluorescein is considerably less than one. Thus the ratio is not lower for the coated samples indicating that the sodium ions have not been covered by the coating process. This is consistent with the C_{1s} spectra which indicate that the coating is similar to the sodium salt of the acid.

The spectra of the disodium fluorescein / lauric or capric acid samples are consiste nt with the model of fluorescein particles coated with the sodium salt of the acid

Figure 2.28 : Scanning electron micrographs a) disodium fluorescein b) lauric acid coated, 0.23 gg^{-1}, disodium fluorescein and c) Capric acid coated, 0.18 gg^{-1}, disodium fluorescein.

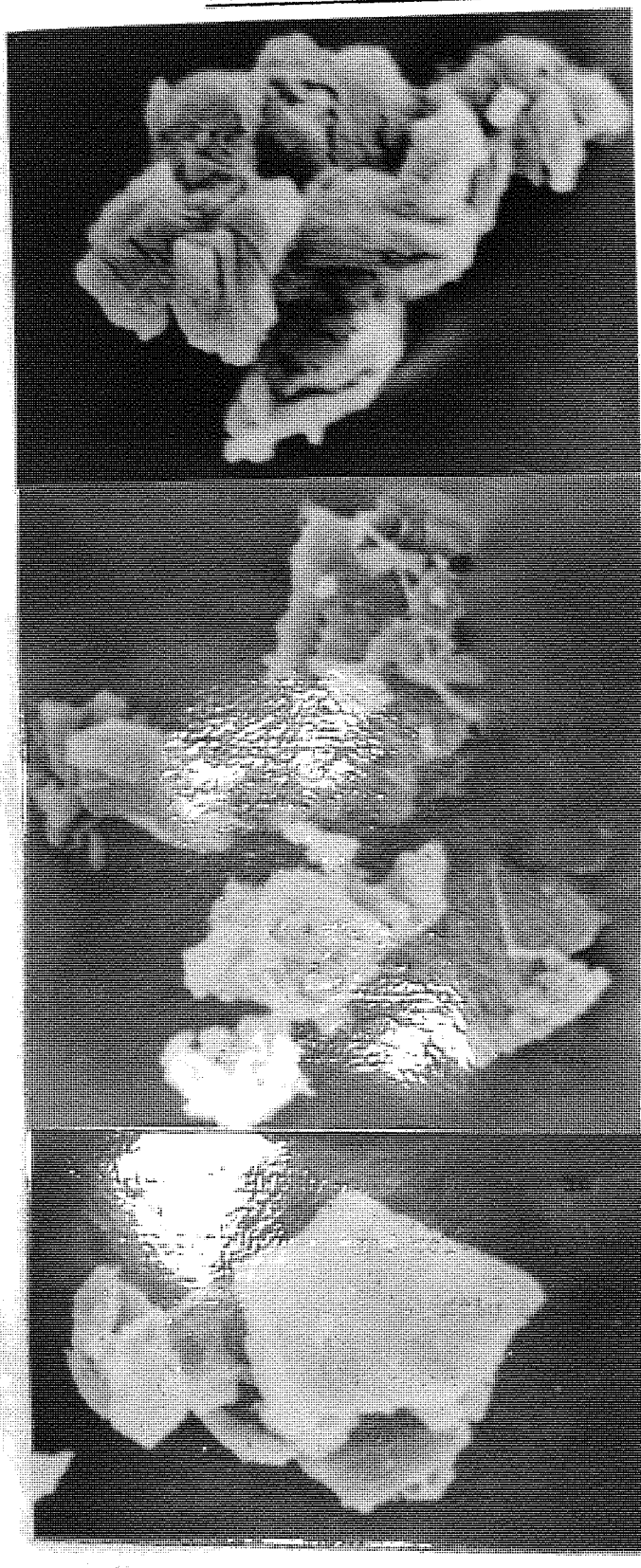

(a)

(b)

(c)

2.3.2.4 Scanning Electron Microscopy.

Figure 2.28 shows three representative electron micrographs of a disodium fluorescein particle and lauric and capric acid coated (nominally 0.23 and 0.18 gg^{-1} respectively) disodium fluorescein particles. The shape of the particles is unchanged by the addition of fatty acid. The surface morphology appears to be more irregular and fissured in the case of disodium fluorescein in comparison with the coated powders.

(a)

2.3.3 Discussion.

2.3.3.1 Summary of observations.

The GLC results for lauric and capric acids, shown in Figures 2.12, 2.13 and 2.14 may best be fitted to a straight line. The order of magnitude of the association of lauric acid with the disodium fluorescein is, up to approximately 0.3 gg^{-1}. This estimate is far in excess of monolayer coverage of 0.78 mgg^{-1}, as calculated from the specific surface area measurement, shown in Table 2.4 .

(b)

The solution infra - red data, shown in Figure 2.19, exhibit an increase in the number of dimerised molecules with increased fatty acid concentration in solution, confirming literature observations (264). The surface tension data for solutions in dichloromethane - chloroform, shown in Figure 2.20, are reduced in comparison with those observed in dichloromethane alone, shown in Table 2.9, to approximately 0.025 and 0.014 M for lauric and capric acids respectively. These observations correlate with the work of Serdyuk (268) on the effect of small quantities of non - polar solvents on the CMC in moderately polar solvent. Owing to the difficulties of examining the CMC in apolar solvent (238) there is likely to be an area prior to

(c)

the apparent CMC where the formation of micelles as a fraction of the total amount of surfactant present in solution can be examined.

The appearance of the carboxylate anion peak in both the lauric and capric acid coated specimens, as observed by infra - red spectroscopy, shown in Figures 2.16 b) and c), taken in conjunction with the observation of free acid in the higher coated powder suggests some point of saturation of the interaction with the adsorbent, to form the carboxylate anion, a feature of the carboxylate group interaction with a sodium atom. The appearance of the carboxylate anion has been confirmed by ESCA using the lower coated samples, as shown in Section 2.3.2.3 . The lowest point at which the free acid has been detected is at a nominal coverage of 0.4 gg^{-1}.

2.3.3.2 Interpretation of observations.

The distance between monomers in the crystalline state of disodium fluorescein is 3.5 to 4.0 Å (276). The surface area occupied by a vertically orientated fatty acid molecule is approximately 20 Å (259). It can be seen, therefore, that one molecule of fatty acid by adsorbing at the surface of disodium fluorescein will preclude adsorption by any further molecules to 5 disodium fluorescein molecules. The most likely sites of adsorption are the phenol groups. The pKa of the carboxylate group of disodium fluorescein in water is 4 , that of the phenol group being 6.7. The pKa of the fatty acid is 5.3. Of the two potential points of interaction between the disodium fluorescein and the fatty acid the most likely is the phenol group. The position of the carboxylate anion between two benzene rings makes it sterically an unlikely point of interaction. Since the sodium salt of the fatty acid appears to occur the phenol group with a sodium constituent takes precedence over the alternative phenol group as a point of attachment.

Figure 2.29 : C - curve adsorption isotherms described by Giles (246, 247)

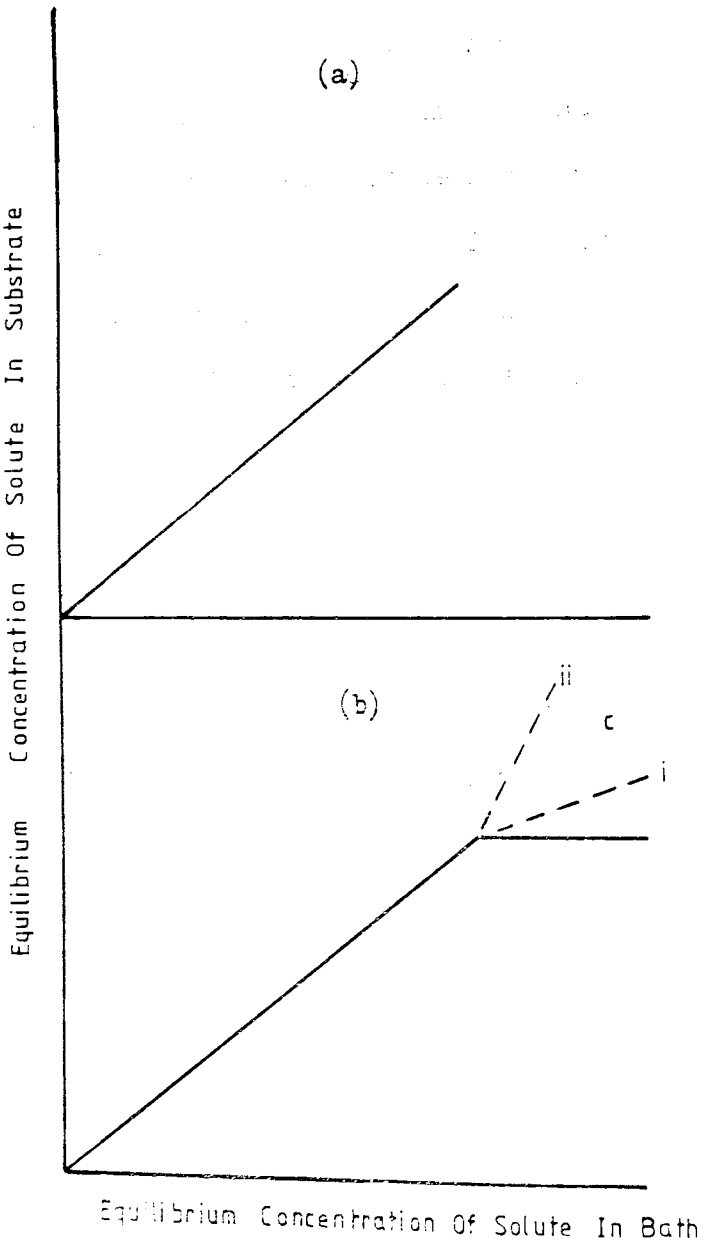

The isotherms indicate that the number of adsorption sites remain constant throughout the range of solute concentrations up to saturation of the substrate.

A horizontal plateau indicates saturation of all the internal area of substrate.

A second branch in the curve of different slope, as shown in ci and cii, indicates a change in the internal structure caused by pressure of the adsorbed solute whereby a new portion of the solid becomes accessible.

The ratio of the mass of lauric acid to that of disodium fluorescein may be considered in more detail. The molecular weights of lauric acid and disodium fluorescein are 200.3 g and 376.28 g consequently assuming a ratio by mass of 5:1 molecules, based on the argument at the beginning of this section, gives a ratio of lauric acid to disodium fluorescein of 0.11 gg^{-1}. This ratio is exceeded in the present studies. The implication of this work is that the fatty acid penetrates the particle surface to interact with the powder. The hypothetical association of lauric acid with disodium fluorescein, by penetrating the surface, implies that the surface area for adsorption is constantly increasing until the number of potential adsorption sites reaches a limit as indicated by the plateau in Figure 2.18 a).

The linear isotherm, shown in Figures 2.12, 2.13 and 2.14 are consistent with conditions in which the number of sites remains constant throughout the whole range of solute concentrations up to saturation of the substrate. This means that the surface available for adsorption expands proportionally with the amount of solute adsorbed. Linear adsorption isotherms correspond with those described as C - curves by Giles (246), shown for comparison in Figure 2.29.

The Langmuir equation, 2.7, may be expressed as,

$$bC = \theta + bC\,\theta$$

and thus,

$$\theta = bC / 1 + bC \qquad 2.23$$

Where θ is the fraction of total monolayer coverage, θ / θ_0

That is,

$$\theta = \theta_0\, bC\, (1 + bC)^{-1} \qquad 2.24$$

In the case of surface expansion,

$$\theta_0 = \theta_1 (1 + \beta C) \qquad 2.25$$

Where θ_1 is a constant, equivalent to the extent of surface available before adsorption starts, and β is a coefficient of expansion of the surface on which adsorption occurs. The general Langmuir equation can be written

$$\theta = \theta_0 bC (1 + bC)^{-1} = sC \qquad 2.26$$

Where s is a constant, thus

$$b = s/(\theta_1 + \theta_1 \beta C - sC) \qquad 2.27$$

This equation, 2.27, is valid only up to a critical value C, where $C' = \theta_1(s - \theta_1\beta)^{-1}$ because if C were greater than C' the sign of b would change from positive to negative, which is impossible because the components of b are positive. Thus $C = C'$, $b = \infty$, that is the rate of escape of adsorbed solute from the surface is zero (277). Therefore when the concentration C' is reached the value of the amount of solute adsorbed will remain fixed, provided no fresh surface is formed, and the curve will change abruptly to the horizontal.

Giles (246) has suggested that the adsorbing surface may be considered as an area which expands by an opening - up or disentangling of the structure. In this case it may be assumed that the rate of adsorption is independent of the available area of the substrate at any given time, because each molecule as it becomes adsorbed can readily generate a new vacant site. It is therefore dependent only on the

concentration C of the solute in the solution.

Expansion of the structure cannot continue indefinitely and a situation must arise where the primary expansion gives way to a secondary or even tertiary structure expansion, occurring at a slower, or at a faster rate. Thus, a change in slope will occur, the sharpness of which will depend on the degree of disparity in the relevent rates. A horizontal plateau indicates saturation of all the internal area of substrate which can be opened up by the solute.

The relationship between the amount adsorbed and the equilibrium concentration for lauric and capric acids and lauryl alcohol, as shown in Figures 2.11 to 2.13, may best be explained by a surfactant concentration dependent expanding surface area. Since the best adsorption isotherm to fit this data is linear the distribution of the data around the line of best fit , as indicated by the correlation coefficient of the linear regression analysis shown in Table 2.10 and on pages 85 and 89 , requires some consideration.

The suggestion that the present work may be explained in terms of an isotherm of the general Langmuir type as described by Giles does not take into account the lateral interaction energies, the importance of which has been emphasised in the introduction, page 41 . The aggregation of surfactant molecules in non - aqueous solution has also been considered in the introduction, page 37 . The observation of the aggregation of surfactant molecules in solution as indicated by surface tension measurement, Figures 2.7 and 2.20, and differential refractometry, Figures 2.3 to 2.5, within the range of initial concentrations employed in the GLC experiments, comparing Tables 2.1, 2.3 and 2.6, implies that lateral interaction energies might be expected to contribute significantly to the adsorption process.

The exact point at which the interaction of the surfactant molecules reaches a critical point will be influenced by the presence

of water molecules (238) which were present in the disodium fluorescein, section 2.2.1.2. Under ideal circumstances an investigation of the surfactant - surfactant association should be carried out in the absence of impurities, such as water. Since the purpose of these studies was to coat a hygroscopic powder the presence of water was unavoidable. The extent of the association of the water with the powder might have been minimised by adopting some drying procedure, such as vacuum drying and storage over phosphorus pentoxide, however the necessity to handle the powder under atmospheric conditions, during the adsorption experiments, would negate this procedure and make interpretation of the results obtained more difficult.

If an inflection in the linear isotherm occurs as illustrated by the dotted lines in the Figure 2.29 which may be explained by a reduction, ci, or increase, cii, in the rate of expansion of the particle surface area as a function of surfactant concentration, this may be influenced by the presence of water. This would result in a displacement of the data from the line of best fit

It has been observed that the aggregate states which are in equilibrium in solution, as set out on page 38, for certain fatty acids in carbon tetrachloride (264) are monomers, dimers and micelles. Similar conclusions have been drawn for lauric and capric acids in dichloromethane/chloroform, based on the solution infra - red, Figure 2.19, and the suface tension measurements, Figure 2.20. The apparent absence of the monomer from the solution at the concentrations used in these studies suggests for practical purposes that the dimer and micelle structures are in equilibrium. The greatest error in the quantitative results obtained by GLC was observed at high equilibrium concentrations, as indicated by the error bars

in Figures 2.12 and 2.13. At these concentrations the equilibrium has presumably moved towards the micelle formation at the expense of the dimer. The influence of the addition of the chloroform may well contribute to the error in this region. It has been noted that the formation of micelles is influenced by the dielectric constant of the medium (267) and that small changes in the dielectric constant brought about by the addition of a small quatities of cosolvents may be enough to significantly alter the CMC (268). It was concluded from the surface tension experiments that the addition of chloroform reduced the CMC for lauric acid in dichloromethane and that this enhanced the association of the fatty acid with disodium fluorescein, as shown in Figure 2.11. The error resulting from the presence of an impurity such as water will, therefore be magnified by the addition of chloroform.

To summarize the observations, the fatty acids appear to interact with the disodium fluorescein by penetrating the particle surface through a concentration dependent expanding surface area. There is some deviation from linearity which may be explained in terms of fatty acid molecule interactions, micelle formation, the presence of certain impurities, notably water, and finally there may be a change in the internal structure of the particle brought about by the pressure of the adsorbed solute. In the latter case an inflection in the isotherm would be expected, as in Figure 2.29b). It is possible that a phase transition in the adsorbed fatty acid might cause this to occur (278). Since this will depend on the amount of fatty acid adsorbed this would also be subject to all the inconsistensies listed above.

C H A P T E R T H R E E

Generation and characterisation of surfactant coated aerosol powders.

3. Generation and characterisation of surfactant coated aerosol powders.

3.1 Introduction.

Interest in condensation growth has arisen largely as a result of environmental aerosols such as those of car exhaust (279), cooling towers (280), gas turbines (281) and household devices (282). The problem of smoke as an atmospheeric pollutant has been recognised for some time (283). The constituents of combustion products may be broken down into water insoluble and soluble deposits (284). The insoluble components are hydrocarbons (279,282,285,286). The main soluble components are ammonia (287), nitrous oxide (281), nitrates (288), sulphates (288), sulphur and sulphur dioxide (289,290). Condensation growth and the major factors involved in total and regional deposition of aerosols in the respiratory tract were considered in the general introduction in Chapter 1.

The significance of particle size in inertial deposition, sedimentation, diffusion and electrostatic precipitation have been emphasised. Any effect on particle size will by inference effect deposition. One such factor is the growth of aerosols by condensation in regions of high relative humidity. Such conditions exist in most parts of the respiratory tract (112,206,217,291).It is,therfore, of some importance to consider the effects of relative humidity on particle growth and deposition (183,292). This is of some relevance to the deposition of pharmaceutical aerosols (105,108,109). The increase in particle size as a result of hygroscopic growth can be considerable (205,214).

An aerosol particle in the human airways is in equilibrium with the air in the lung when both the temperature of the air and of the particle surface and their water vapour concentrations, calculated

from the water vapour pressure are equal to each other. The temperature in the human airways is about 37 °C, while the water vapour concentration corresponds with a relative humidity of 99.5%. This value can be derived from the osmotic pressure or from the lowering of the freezing point of blood (293).

The relationship between particle size and relative humidity needs to be defined before it can be examined practically.

At equilibrium, the relative humidity H, expressed as a fraction is equal to the water activity a_w, from Raoult's law :

$$H = P/P_0 = a_w \qquad 3.1$$

Where a_w is the water activity expressed as mole fraction and P_0 is the saturation vapour pressure.

The concentration in a droplet which has equilibrated with the environment is not the same as the iso - osmotic solute concentration at which the test solution and isotonic saline have the same water activity at 37 °C. The reason for this is that the droplet vapour pressure P' is greater than P in the previous equation due to the Kelvin effect, which raises the vapour pressure due to the curvature of the surface. Rearranging equation 1.14 :

$$\ln P' = \ln P + 4 M_w \gamma / KT \rho_l D_i N_A \qquad 3.2$$

Where M_w is the molecular weight of water, γ is the surface tension of the solution, K is the Boltzman constant, T is the absolute temperature, ρ_l is the density of the liquid, D_i is the equilibrium droplet diameter and N_A is Avogadro's number.

The ratio of the equivalent volume diameters of the equilibrium

droplet (D_i) and the dry particle from which it originated (D_e) can be defined as :

$$R' = D_i/D_e \qquad 3.3$$

Rearranging the Kelvin equation, 1.14 :

$$R = P'/P = \exp(4M_w\gamma/KT\rho_l D_l N_A) = \exp(K/\rho_l D_l) \qquad 3.4$$

Where K has a value for pure water of $1.08 \times 10^{-7} g\ cm^{-2}$.

The water vapour concentration at the surface of a particle is in equilibrium with the water vapour concentrations in the human airways when,

$$0.995 = N\,R \qquad 3.5$$

Where N is the ratio of the water vapour concentration at the surface of the solution and of pure water.

$$N = (n_w + jn_s)/(n_w + (i + j)n_s) = (1 + j(M_w m_s/M_s m_w))/(1 + (i + j)(M_w m_s/M_s m_w)) \qquad 3.6$$

Where n_w, n_s are numbers of water and solid molecules in solution respectively ; M_w, M_s are the molecular weights of the water and the solid and ; m_w, m_s are the mass of water and the solid in the particle respectively.

Combining equations 3.5 and 3.6 :

$$n_s/n_{w,l} = (R - 0.995)/(0.995(i + j) - jR) \qquad 3.7$$

Where the index 1 indicates the lung. The solid weight particle g_s is, from equation 1.17,

$$\begin{aligned} g_s &= m_s/(m_{w,l} + m_s) \qquad 3.8 \\ &= (1 + (M_w/M_s)((0.995(i + j) - jR)/(R - 0.995)))^{-1} \end{aligned}$$

The increase in the mass of a dry solid particle in the human lung is the reciprocal of g_s. The mass of water in a particle is now,

$$m_{w,l} = m_s(M_w/M_s)((0.995(i + j) - jR)/(R - 0.995)) \qquad 3.9$$

The increase in the equivalent diameter is, from equation 3.3,

$$\begin{aligned} R' &= (\rho_s/\rho_l g_s)^{1/3} = D_e/D \\ &= ((\rho_s/\rho_l)(1 + (M_w/M_s)((0.995(i + j) - jR)/.... \\ &\qquad ....(R - 0.995))^{1/3} \qquad 3.10 \end{aligned}$$

Where D_e and D are the equivalent diameter of the particle in the lung and the dry particle respectively and ρ_l and ρ_s are the respective densities. The increase in the aerodynamic diameter is calculated from

$$\rho_0 D_{ae}^2 C(D_{ae}) = \rho/K\, D_e^2 C(D_e) \qquad 3.11$$

Where K is the shape factor. This may be expressed as,

$$R_a = D_{ae,l}/D_{ae,s}$$

$$= \left[\frac{C(D_{e,l})\ C(D_{ae,s})}{C(D_{e,s})\ C(D_{ae,l})}\right]^{1/2}(1/g_s)^{1/3}(\rho_l/\rho_s)^{1/6} \qquad 3.12$$

This equation may be simplified under conditions where the slip factors may be neglected, that is for particles greater than 1 μm, to the form showm in equation 1.16 in the general introduction.

The Kelvin equation can play an important role in equations 3.10 and 3.12. This is illustrated by an example in which a particle with an aerodynamic diameter of 0.1 μm with unit density, 1 g cm^{-3}, is considered. The R is approximately 1.01 and the denominator in equation 3.10 has the value of 0.015 instead of 0.005 for a large particle size. So the mass equilibrium of a particle of 0.1 μm in the lung is decreased by a factor of about 3.

It has been noted in the general introduction that Ferron (205) has used these equations to calculate growth of various compounds. It is evident that relative humidity can be a significant factor in particle size and deposition. Martonen (208) has noted that the effect of hygroscopic growth is to increase the total deposition in the lung but reducing the fraction deposited in the lower regions of the respiratory tract.

In order to study the particle size distribution and the growth of an aerosol some form of measurement is required. It follows that in order to measure particle size the parameter which is to be used needs to be defined. In studies which are intended to parallel respiratory tract deposition it would not seem appropriate to use parameters based on optical measurement of particle size and shape (294,295) since this gives no indication of the behaviour of such particles dynamically in the respiratory tract.

Those parameters most commonly mentioned are the equivalent volume diameter, Stokes' diameter and the aerodynamic diameter (110, 168). The equivalent volume diameter may be defined as the diameter of a sphere of the same volume as the particle. The Stokes' diameter may be defined as the diameter of a sphere of the same density as the particles and having the same falling velocity. The aerodynamic diameter may be defined as the diameter of a sphere of unit density and having the same falling velocity as the particle. The aerodynamic diameter is the most useful of these parameters since the complicating factors of shape and density need not be considered. The devices most commonly used for measuring these parameters are inertial samplers (296 -298) which can be divided into those which sample using centrifugal forces (299,300) and those whichsample by inertial impaction (301 - 303). The inertial, cascade impactor permits a direct determination of the particle size distribution, within discrete intervals, as a function of aerodynamic size. The accuracy with which such distributions can be estimated from cascade impactor data depends on the degree to which the size distribution of particles passing a given stage overlap the size distribution of particles retained on the stage. Thus, it is important that the collection efficiency for each impaction stage increase from zero to unity over a relatively small interval of particle sizes. Similarly an inertial impactor is only as accurate as the device which is used to calibrate it, namely a monodisperse aerosol generator (304,305).

In order to study aerosols in conditions approaching those in the lung,in vitro,an apparatus which maintains the atmosphere at constant temperature and relative humidity is required.

The principles involved in the design of cabinets for controlled environments have been considered in the literature (306). The

design or selection of a conditioned cabinet should only be made after thorough consideration of the requirements. Failure to recognise all the basic elements of the problem may often lead to unreasonable requirements in respect to some factors, while ignoring others which may equally influence the final performance.

The contributions to the overall temperature will be influenced not only by the air temperature but also by radient energy exchange with the cabinet walls and furnishings. The design should,therefore, ensure minimum radient transfer and high convective heat transfer to the air when control is desired. Close control of humidity, especially where relative humidity sensing is used, also requires close control of temperature because of the dependence of relative humidity on temperature. Precision in control can only be obtained by careful attention to the response characteristics of the conditioning equipment and the cabinet itself, as well as to those of the control devices. Though the performance is influenced by each component it is the interaction of one with the other and with the product being conditioned that determines the ultimate performance.

At high relative humidities the dependence of this parameter on temperature is critical and consequently close control of temperature is required before similar control of relative humidity can be considered. This observation may be emphasised by an example. To determine the growth ratio with an accuracy of 5% directly at a relative humidity of 0.995, the temperature would have to be controlled to within $\pm$ 0.015 °C (214).

3.1.1 Particle Size Distribution.

In order that inertial impactors can be used to characterise unknown aerosols in terms of particle size they must be calibrated to give

an accurate estimate of the particle size range which is being collected at each stage and the efficiency of the stages in collecting particles by impaction. The device which is used for such calibration procedure is a monodisperse aerosol generator.

The degree of dispersity of an aerosol can be conveniently characterised by the value of the relative standard deviation, α ; this is the ratio of the standard deviation of the particle radii, σ, to the mean radius $\bar{r}$, (111)

$$\alpha = \sigma/\bar{r} = ((\sum_i^N (r_i - \bar{r})^2/N)^{1/2})/\bar{r} \qquad 3.13$$

Since the particle size distribution in aerosols usually differs appreciably from the normal, Gaussian, distribution and approaches a log - normal, it is reasonable at not very small values of α to express the degree of dispersity by the value of the standard deviation of the logarithms of the radii, as in equation 1.3 and 1.4

For small values of α, where $\bar{r} \simeq \bar{r}_g$, $\ln(r_i/\bar{r}_g) \simeq (r_i - \bar{r}_g)/\bar{r}_g$ and

$$\ln \sigma_g = (\sum_i^N ((r_i - \bar{r}_g)/\bar{r}_g)^2)^{1/2} \qquad 3.14$$

The choice of criterion for practical monodispersity is of course arbitrary. Fuchs and Sutugin (111) have suggested taking a geometric standard deviation of 1.22 as the limit of monodispersity.

By combining an expression for the dispersity of an aerosol with its median diameter a complete description of the particle size distribution is obtained. It is possible to calculate the median diameter ($\bar{r}_g v$) from the geometric mean ($\bar{r}_g$) and the geometric standard deviation (σ_g) using the Hatch - Choate equation (171).

$$\ln \bar{r}_g v = \ln \bar{r}_g + 3 \ln^2 \sigma_g \qquad 3.15$$

Throughout these studies the basis for these expressions will be mass from which can be derived the term mass median diameter and where dynamic aerosol measurements are carried out, mass median aerodynamic diameter.

3.2 Materials and methods.

3.2.1 Materials.

3.2.1.1 Apparatus.

i) Delron DCI - 6 Cascade Impactor. Delron Research Products Company, P.O. Box 95, Powell,Ohio 43065.

ii) Speedivac 2, vacuum pump. Edwards High Vacuum, Crawley.

iii) Pulsatron 125, ultrasonic bath. Kerry Ultrasonics Limited, Hunting Gate, Wibury Way, Hitchin, Herts. SG4 0TQ

iv) Aminco - Bowman Spectrofluorimeter Type 4 - 8202.

v) Knauer Elect4onic Temperature Monitoring Instrument/Vapour Pressure Osmometer. KG Dr. Ing. Herbert Knauer, 1 Berlin 37 West, Holstweg 18.

vi) Water pumps Model No. C25P and Air pumps Model No. M361. Charles Austin Pumps Limited, 100 Royston Road, Byfleet, Surrey.

vii) Proportional Temperature Controllers Model No. 72 and water temperature probe (jacketed thermistor) Model No. 400. Yellow Springs Instrument Company Inc., Yellow Springs, Ohio.

viii) Air flow meters Model No.s A6 and B6. G.A.Platon Limited, Wella Road, Basingstoke, Hants.

Table 3.1 : Nominal amount of fatty acids associated with disodium fluorescein (gg^{-1}) based on mean values taken from the adsorption isotherms, Figures 2.12 a) and 2.13 a).

Sample Number	Capric Acid gg^{-1}	Lauric Acid gg^{-1}
1	0.08	0.07
2	0.08	0.12
3	0.11	0.15
4	0.14	0.2
5	0.16	0.24
6	0.18	0.23

ix) Stiebel Eltron Water Heater. Stiebel Eltron, Accrington Works, Strathmore Road, Croydon. CR9 2NA.

x) Dew Point Hygrometer. EG and G

xi) Glass fibre filters, Type A - E 76 mm, Part No. 61663, Gelman Sciences Inc., Ann Arbor, Michigan 48106. Gelman Hawksley Limited, 12 Peter Road, Lancing. BN15 8TH

xii) Swinny adapter/Millipore filters GS WP01300 - 0.22 um. Millipore (U.K.) Limited, Millipore House, Abbey Road, London. NW10 75P.

3.2.1.2 Chemicals.

i) A.R. Grade glycine. Fisons Scientific Apparatus, Lough borough, Leics.

ii) Analar sodium hydroxide, sodium chloride and potassium dichromate. BDH Chemicals Limited, Poole, England.

iii) Dow - Corning silicone fluid 200/60,000 cs. Hopkins and Williams, Chadwell Heath, Essex.

v) Coated Powders. Lauric and capric acid coated powders were selected for generation in these studies from the range of concentrations shown in the isotherms, Figures 2.12a) and 2.13a). Although some experimental variation has been noted in the amount of these surfactants associated with the disodium fluorescein nominal values have been allocated to different powders based on the means of data obtained by GLC.

3.2.2 Methods.

3.2.2.1 Aerosol Generation Procedure.

The method of aerosol generation employed in these experiments may be described as a vertical spinning disc technique.

i) Apparatus

The Nebulet® portable spinning disc device (92) has been assessed in two prototype forms. Both of these devices consist of a small motor which drives a spinning disc in a vertical plane at between 16,000 and 19,000 r.p.m. . This motor is housed such that the shaft driving the disc is sealed into a cylindrical housing for the disc. A tube leaves this housing tangentially and is the generation port for the sample aerosol. This tube may be connected to a mouthpiece for clinical use.

The housing for the disc, which may be considered as the sample reservoir, in the original model is a one piece design which allows no access to the disc for cleaning and maintenance. The second model has the improved feature of a housing which may be split into two and relocated by means of bayonet locks situated on its outer edge. The two halves are sealed by an O - ring . Similarly the disc on the original device is permanently attached to the end of the drive shaft. The improved version allows for the detachment of the disc by means of a captive O - ring between the drive shaft and the hub of the disc.

ii) Operation.

The aerosol was loaded as a powder into the device via the tangential tube. A maximum load of approximately 200mg was used. The generator was weighed prior to the addition of the powder. The generator was then discharged into the equilibrium chamber of the controlled

temperature and relative humidity apparatus, for a period of two minutes. At the end of the generation period the generator was reweighed and reloaded in preparation for any subsequent experiments. In this way the total output of the generator could be assessed.

iii) Experiments.

Several experiments were carried out with disodium fluoresceim powder aerosols to investigate the effects of using the device with : Air flow through the reservoir chamber and without the disc in motion and; Air flow through the reservoir chamber and with the disc in motion. By loading the device with various amounts of powder from approximately 10 to 190 mg an estimate of the constancy of output in that range can be obtained.

The observations on the particle size distributions, which are reported in detail will reflect the degree of success attained by optimising operating conditions,

3.2.2.2 Particle size measurement.

i) Apparatus

The Delron DCI - 6 cascade impactor is a vertically orientated, stacked, six stage instrument. The presence of a filter at the outlet effectively gives the impactor seven levels of measurement of particle size. The nominal cut off points for each stage based on a 50% collection efficiency are 11.2,5.5,3.3,2.0,1.18,0.5,and 0.22 µm aerodynamic diameter for each of the respective stages, using silicone fluid coated collection surfaces.

ii) Operation.

Air is drawn through the apparatus by a vacuum pump operating at less

than half an atmosphere and the flow rate is governed by a critical orifice placed between the pump and the chamber of the impactor. The flow rate has been calibrated, by the manufacturer, to a constant 12.45 L min^{-1}.

Larger particles have a larger moment of inertia and impact on the first stages encountered on their passage through the impactor. The small particles deposit on subsequent stages. The velocity of passage of particles from one stage to the next is increased by reducing the jet size at each stage, however the overall flow rate remains constant.

The manufacturers calibration of the deposition on each stage of the instrument may be inadequate for the experiments which will be carried out. The manufacturers calibration is based on the use of the apparatus with glass slides alone. The slides used throughout these studies are coated in accordance with observations which have been made suggesting the improved accuracy and precision of this technique (301,307).

iii) Coating glass slides.

The glass slides, 38 mm in diameter, were coated with silicone fluid by dropping 0.2 ml of a 10% silicone fluid in benzene solution on the slide and rotating the slide to effect an even surface coverage.

iv) Extraction procedure.

The coated slides underwent an extraction procedure to remove the coating material and the disodium fluorescein. 5 ml of benzene were added to the slides and they were placed in an ultrasonic bath for 5 minutes. 5 ml of Sorensen's glycine buffer pH $\geqslant$ 12.0 were added to these extracts and to the fibre glass filter from the last stage

and these samples were ultrasonicated for five to ten minutes. The aqueous solution of disodium fluorescein was then filtered and diluted and examined by spectrofluorimetry.

v) Spectrofluorimetry.

The samples were measured against 40 - 50 ng of disodium fluorescein standard, at the emission wavelength of 516 nm and an excitation wavelength of 486 nm.

Once the results have been obtained for all the slides and the filter, a total amount can be estimated by summing these values, consequently each stage may be expressed as a fraction/percentage of the total amount deposited. Using the deposition data, which can be plotted graphically an analysis of the particle size distribution can be carried out.

vi) Data inversion computer analysis of deposition data based upon the calibrated cascade impactor.

The percentage deposition data obtained by assaying each stage of the cascade impactor was fitted to a computer generated theoretical particle size distribution which uses an iterative technique. The distribution is described by the mass median aerodynamic diameter (MMAD) and the geometric standard deviation (σ_g). A least mean square analysis was used to fit the data. This data treatment has been described fully in the literature (308,309).

3.2.2.3 Controlled temperature and relative humidity apparatus.

A variety of arrangements of the apparatus to control temperature and relative humidity were investigated. For the purpose of this report it is important only to stress the significant points in the

Figure 3.1 : Photograph of the final arrangement of the controlled temperature and relative humidity apparatus.

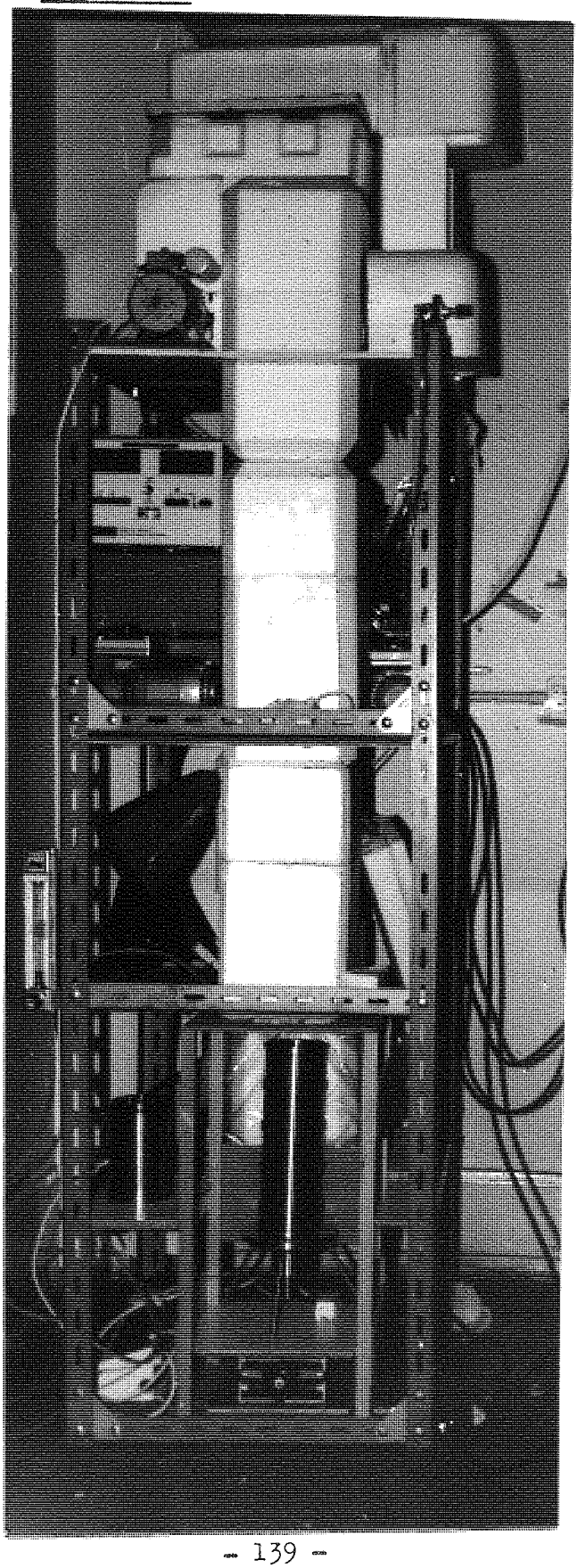

development. The first design was produced solely to investigate the problems involved and the accuracy which could be achieved. The second design was the first practical arrangement of the apparatus for use in studies of hygroscopic growth. This model has some similarities with an apparatus described by Groom (252). The third arrangement of the apparatus is the most successful and most practicable arrangement achieved and this model was used in subsequent experiments. The development stages of this apparatus are considered in the results and discussion section, 3.3.2 . Figure 3.1 shows a photograph of the final arrangement of the apparatus, from which it can be seen that a modular system of insulation was adopted.

i) Operation.

Air was pumped into this system at approximately 14.5 L min^{-1}. Two litres per minute were drawn off for analysis from the equilibrium chamber. The remaining 12.5 L min^{-1} were drawn through the cascade impactor. By placing a water manometer at the aerosol inlet port the balance of the inflow and outflow can be established. The equilibrium chamber is constructed of pyrex and is water jacketed it has a volume of approximately 7.85 L and at the flow rate above provides a residence time of approximately 40 s .

The salt solution employed throughout these studies to provide an atmosphere of high relative humidity was potassium dichromate. This theoretically gives a saturated vapour at 98% relative humidity and 37 °C.

The aerosol generation port is situated at right angles to the equilibrium chamber of the controlled temperature and relative humidity apparatus. The inlet port is designed to reduce the distance travelled by the aerosol by shaping the tube to the inlet to form the tangential

tube which is normally part of the aerosol generator. This tube is water jacketed.

The aerosol generation and collection may be carried out once the system has equilibrated. This may be established by monitoring the temperature and relative humidity within the equilibrium chamber. Equilibrium was usually achieved within three to five hours, from a cold start.

Prior to the generation of the aerosol and following the equilibration of the impactor the vacuum pump was set in operation. This allows final equilibration of the impactor and reduces the likelihood of surface condensation within the impactor. Immediately upon the operation of the pump the rubber seal between the impactor and its water jacket should be positioned. Up to this point the air was vented through the gap between the impactor and its housing.

The generation of the aerosol was then carried out after which the air flow through the impactor was continued for a further forty seconds which was approximately the retention time in the equilibrium chamber for the aerosol. The impactor was removed ensuring that the vacuum pump was left on until the instrument had been totally removed from the humidified air source. Failure to do this leaves humidified air motionless within a rapidly cooling impactor thus producing condensation. Droplets of condensation form pools on the slides at each stage which may overflow, thus ruining the particle size determination. After dismantling the impactor and removing the slides and the filter, it may be replaced in the apparatus with new slides and a filter in preparation for the next experiment. A reduced period of equilibration of the entire apparatus of approximately 30 to 60 minutes may be all that is required. It was important that while the impactor was out of the apparatus a blanking pad, of

cork, was placed over the opening to the impactor water jacket, not entirely blocking the orifice as the air was still being pumped through the system. This precaution reduces the likelihood of the incursion of cooling, destabilising air from the atmosphere into the equilibrium chamber.

3.2.2.4 Vapour pressure osmometry.

In the context of these studies vapour pressure osmometry may be used to derive theoretical growth ratios for aerosol particles of different composition based on the water activity of solution droplets containing the components of the aerosol particles.

i) Principle of operation.

By introducing the solution droplet to one thermistor and a solvent droplet to the second thermistor in an atmosphere saturated with solvent vapour, a temperature difference will occur between the thermistors as a result of the equilibration of the system.

ii) Operating procedure.

The vessel in which the experiments were carried out was moistened on the inner walls and was equipped with two wicks which ensured that the atmosphere was saturated with solvent, 20 ml of which were present.

The probe from which the two thermistors extend was adjusted so that the needles through which the solution and solvent droplets were introduced approach the thermistors, facilitating the transfer of the droplets. Five needles meet in one point and the sixth 7 mm from this point. For these experiments the vessel was maintained at 37 °C.

iii) Calibration.

A calibration curve was prepared using solutions of sodium chloride for which water activities were known (310). The galvanometer

sensitivity setting employed on the Knauer Instrument was 8. The calibration plot consists of the instrumental response, % full scale deflection plotted against minus the natural logarithm of the water activity ($-\ln a_w$).

iv) Experimental procedure.

The purpose of these experiments was to investigate the equilibrium droplet size of some specific lauric acid coated powders.

In order to examine the effect of certain concentrations of lauric acid on the growth of disodium fluorescein, knowing the growth ratio of the powder alone both from this and other work (252), it was necessary to calculate the equilibrium droplet concentration.

The dynamic growth ratio, R_a, by combining equation 1.17 and 3.3, may be expressed as

$$R_a = R'(\rho_l/\rho_s)^{1/2} \qquad 3.16$$

Where R' is as in equation 3.3. Combining equations 3.8 and 3.10 the following expression may be derived,

$$R_a = ((\rho_s/\rho_l)(1 + (1{,}000/M_s m_i)))^{1/3}(\rho_l/\rho_s)^{1/2} \qquad 3.17$$

Thus, $$(R_a)^3 = (\rho_l/\rho_s)^{1/2}(1 + (1{,}000/M_s m_i) \qquad 3.18$$

and $$m_i = ((Ra)^3(\rho_s/\rho_l)^{1/2} - 1)\ M_s/\ 1{,}000 \qquad 3.19$$

Where m_i is the molal concentration of the solid in the solvent, in this case water.

Substituting the following values in this equation : R_a is 1.45;

ρ_s is 1.49 g cm^{-3} ; ρ_l is 1.0 g cm^{-3} and M_s is 376.28 g gives a value for m_i of 1.0232 moles Kg^{-1}. This is the concentration of disodium fluorescein which was used in subsequent experiments within the limits of experimental error.

Six concentrations of disodium fluorescein were used to check the previously obtained data (252) and thus verifying the validity of using these data. The concentrations employed were 0.07, 0.14, 0.7, 1.0 and 1.02 moles Kg^{-1}.

3.2.2.5 Dissolution experiments.

i) Apparatus.

Two vessels, one for dissolution experiments and the second as a reservoir, were maintained at 37 °C. The dissolution vessel was covered with a lid in which were situated three holes. The central hole was for the drive shaft for the basket containing the sample being examined Two peripheral holes were for the positioning of the glass electrode for measuring the pH, and a sample port. Samples were taken using a microsyringe. The sample basket was rotated at 50 r.p.m., this was checked intermittently.

ii) Procedure.

The powder for examination was compressed in a die using a pressure of 10 K Tonnes cm^{-2}. The disc or compact, thus prepared was used in subsequent experiments . Discs, of approximately 0.3 g, were prepared of the following nominal associations of lauric acid in coated powders 0.07, 0.12, 0.15, 0.2, and 0.23 gg^{-1}. Disodium fluorescein alone and capric acid coated powders, 0.06, 0.08 and 0.16 gg^{-1} were also prepared. The sample was placed in a basket attached to a rod

Table 3.2 : Percentage deposition by mass on each stage of the cascade impactor, taken from the output of the generator a) with motor running, b) without motor running and c) correcting a) for b).

Stage	Cut Off Point µm	% Collected By Mass a)	b)	Correcting a)for b) c)
1	11.2	51.43	89.71	10.23
2	5.0	6.5	2.73	12.22
3	3.3	33.17	5.76	60.44
4	1.8	4.94	0.74	9.47
5	1.1	0.78	0.64	1.49
6	0.5	0.16	0.1	0.03
7	0.2	3.03	0.31	5.84

Method of calculating c) :-

For each stage, $$c = \left[\frac{(a - (a \times b/100))}{\sum_{1}^{7}(a - (a \times b/100))} \right] \times 100$$

which was rotated by an electric motor. Two 200 ml volumes of citrate phosphate buffer, pH 7.45 (311), were placed in each of the vessels The reservoir vessel was covered with a lid and a hole in the lid was used subsequently to remove small volumes of buffer.

The experiment was begun by the lowering of the basket in to the buffer to a position approximately 2 cm below the surface of the liquid, the rotation of the sample was then started. The lid was secured and the pH probe positioned. Samples were taken at 30 seconds and at one minute intervals until 9.5 minutes, then at 12 minutes, 15 minutes and subsequently every 5 minutes until solution equilibrium was achieved. One milliltre samples were taken and replaced with buffer from the reservoir. The samples were examined by ultra - violet spectroscopy at a wavelength of 420 nm, selected because of the high concentrations achieved in solution.

3.3 Results and discussion.

3.3.1 Aerosol Generation.

In the preliminary experiments using the prototype aerosol generator some experiments were carried out to optimise the operating procedure. Initially air was drawn through the generator and across the delivery port by the vacuum flow governed by the critical orifice in the base of the impactor. The amount of powder generated in two minutes with the disc spinning was 2.2 ± 0.6 mg, n = 3. The amount of powder generated in two minutes without the disc spinning was 0.3 ± 0.1 mg, n = 3 . The difference in these out puts may be readily explained by the action of the disc on the fluidity and density of the powder bed. By particle sizing these aerosol powders, some indication of the effect of the air flow and spinning disc may be derived.

Figure 3.2 : Ratio of the output of the vertical spinning disc nebuliser plotted against the loading amount (mg).

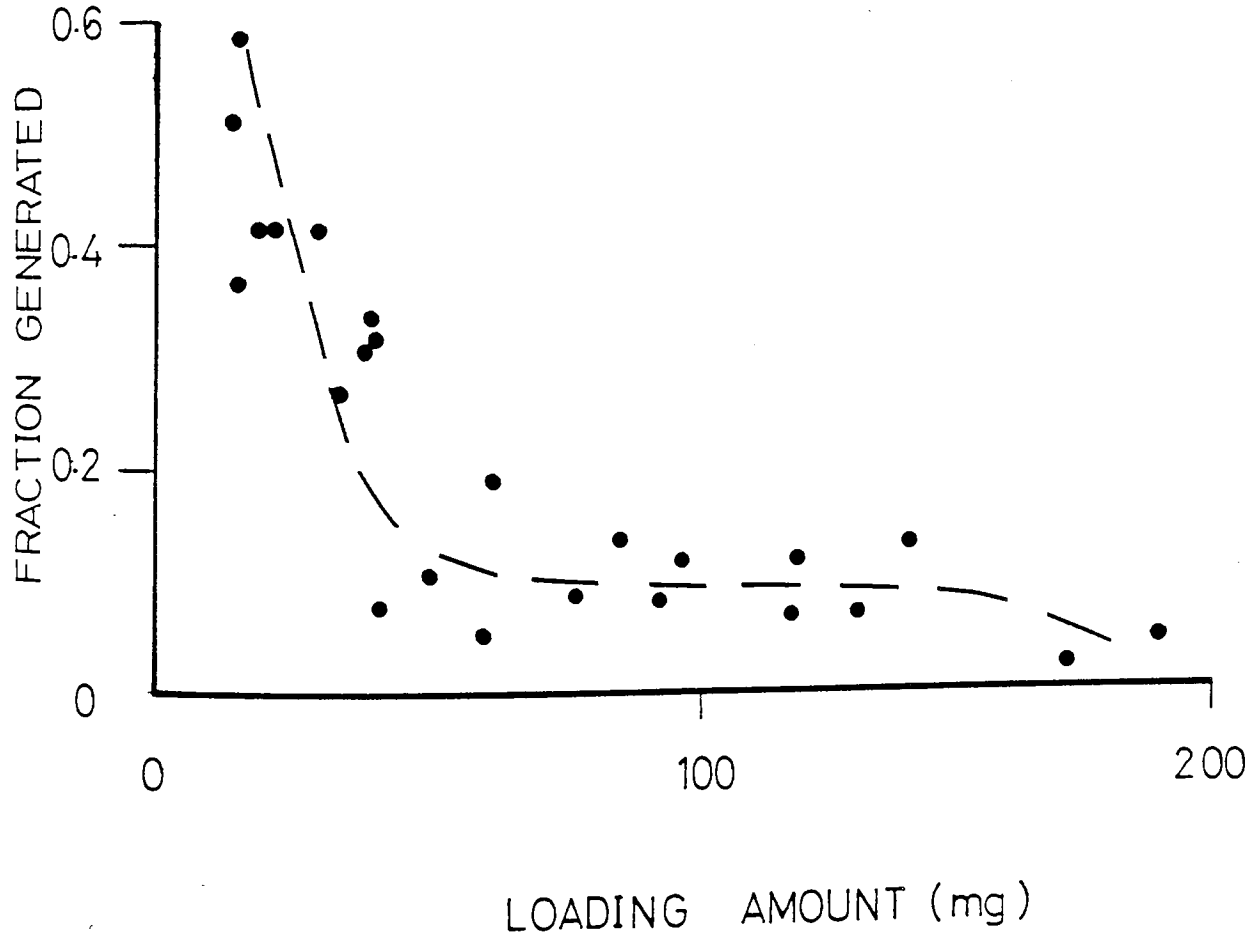

Passing air through the generator alone generates a large percentage of particles with an aerodynamic diameter greater than 11.2 μm. With the motor running and the disc rotating a second significant particle size occurs in the distribution at approximately 3.5 to 5.0 μm. The most likely explanation for this is that drawing air through the generator results in aerosols with a high proportion of aggregate particles, whereas the action of the disc breaks up these aggregates to a certain extent. In subsequent experiments no air was passed through the generator. The aerosol was therefore generated mechanically by the action of the spinning disc. Some preliminary indication of the particle size distribution of the aerosol generated in this way can be derived from the results shown in Table 3.2. By assuming that the fraction b) of a) on each stage is due to the air flow and by subtracting this value and summing the total corrected deposition, a new distribution can be derived c) in the table. This procedure indicates a smaller particle size, 3.5 to 5.0 μm, and a narrower distribution.

Figure 3.2 shows a graph of the ratio of the output of the aerosol generator to its loading value plotted against the equivalent loading value. It may be assumed that at a loading value of less than 10 mg the fraction of the load generated, the output, will fall to zero, at zero loading. It can be seen that by multiplying the loading value by the fraction of the load which was generated that the amount generated from the initial loads, of between 10 and 150 mg, based on the theoretical, dotted, line drawn between the experimental points, of powder follows a trend corresponding to 8.5 - 1.5 mg/2 minutes. The tailing off of the output from 150 mg to approximately 200mg is a consequence of overloading the device. The effect of overloading is that the powder bed absorbs the energy imparted by the disc,

as friction, both with the disc and by particle - particle interaction

There are many powder generating devices available such as spinning disc/top (312) and fluidized bed (313) aerosol generators. In these experiments the disadvantages of these devices are twofold. Firstly in order that constant output may be achieved these apparatus' need to be in operation for a considerable time, which requires a large reservoir of the aerosol powder. Secondly the generation of the aerosol relies on an air supply. The second factor becomes a complication when the control of the temperature and relative humidity is being considered. Air which is used to generate an aerosol may not be humidified because of its effects on the powder flow (314), although it may be pretreated to control temperature. Assuming that the control of temperature is accurate the effects of this incoming air on the controlled environment may be calculated. The practical complications of this technique together with the disadvantage of the amount of aerosol powder required to achieve constant output with these devices makes the aerosol generator used in these studies an appropriate choice in terms of the amount of aerosol powder available, the conditions under which it is considered practical to control the environment, into which the powder is generated, and finally the size and ease with which this device can be used.

3.3.2 Controlled temperature and relative humidity apparatus.

3.3.2.1 Development.

i) Apparatus.1.

This design was devised to investigate the problems involved and degree of accuracy which can be achieved in controlling the temperature

Figure 3.3 : Arrangement of the controlled temperature and relative humidity apparatus, first design.

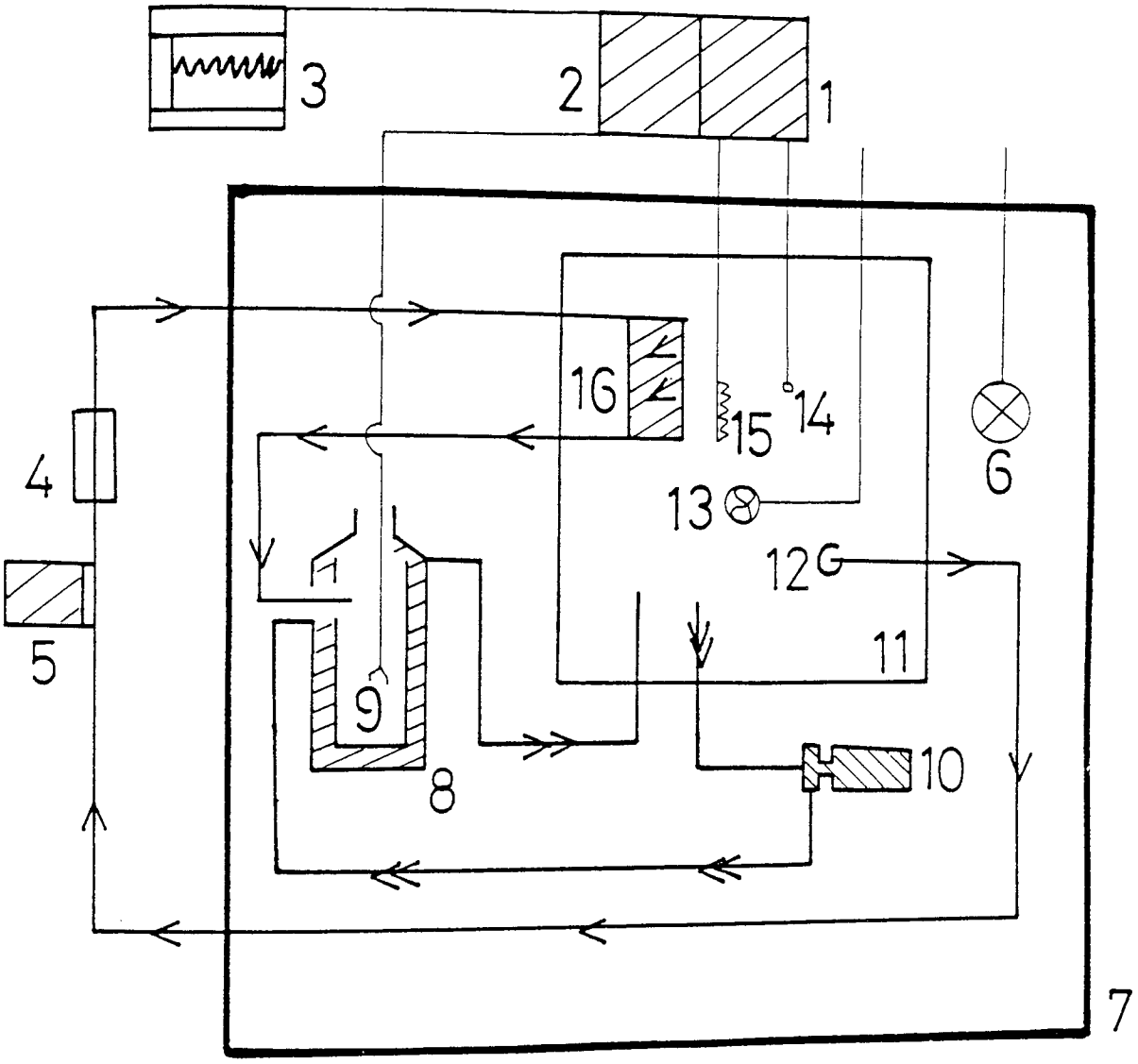

Key :-

1. Proportional temperature controller
2. Temperature measuring instrument
3. Pen recorder
4. Air flow meter
5. Air pump
6. Fan/air circulator
7. Insulated cabinet
8. Water jacketed flask
9, 14 Thermistor
10 Water pump
11. Water bath
13 Stirrer
15. Heating coil
16. Glass coil

→→ Direction of flow, water

→ Direction of flow, air

within the system.

The water system was responsible for the overall control of the temperature. Water was taken from a water bath which was maintained at a constant temperature by a proportional temperature controller. This device monitors the water temperature through a remote thermistor and was attached to a 2KW heating coil which was operated according to preset temperature requirements. The water was then pumped to a jacketed flask and from there back to the water bath. The jacketed flask simulates the controlled environment into which aerosols were eventually to be introduced.

The air was preheated by pumping it from a test tube in the water bath . The air was passed through a flow meter and through a glass coil in the water bath where it was heated again. Finally the air passed into the jacketed flask and was eventually vented into the atmosphere. A thermistor in the flask was connected to a galvanometer which in turn was connected to a pen recorder. The temperature was controlled and monitored readily in this system.

The temperature fluctuations observed , for example over a period of 45 minutes, after a 5 hour equilibrium period, with this system, were 37 ± 0.034 °C.

Some features of this arrangement which require some modification are the jacketed flask which was a much smaller vessel than the equilibrium chamber which was subsequently used and consequently had a much smaller surface area for loss of heat by conduction and radiation. A larger vessel would require a larger volume of water to control temperature consequently temperature fluctuations within the water system might be expected to be more frequent if not greater. None of the apparatus was insulated other than being confined in an insulated cabinet.

ii) Apparatus 2.

The previous system was modified to include the equilibrium chamber which would be used in the aerosol generation experiments as well as additional insulation and water heating features. Each item of the apparatus was insulated with fibre glass wool and foam rubber. The water baths were insulated with 1/4" thickness polystyrene foam.

Two independent water systems were used in this arrangement. The first water bath was used to heat the air flow. This water bath was heated by the proportional temperature controller which monitored the water temperature and maintained it as previously described.

The second system was in principle the same as the first, however water from this water bath was circulated around a jacketed equilibrium chamber , 1 metre in height with a 10 cm internal diameter.

Air was pumped through an air flow meter and through a glass coil submerged in the water bath and passed finally into the equilibrium chamber. The temperature in this vessel was monitored as described in the previous section.

With the system arranged as described, the temperature fluctuations observed, for example over a period of 61 minutes, after a 5 hour equilibrium period, were 37 ± 0.038°C.

Air was circulated within the climatic cabinet.

The slightly increased fluctuation in temperature may be explained by the increased surface area of the vessel in which the temperature was being controlled.

iii) Apparatus 3, Final Design.

Both of the previous systems were designed to observe and control the temperature within the respective environments. The final design must also control the relative humidity and allow access for analysis

Figure 3.4 : Arrangement of the controlled temperature and relative humidity apparatus, second design.

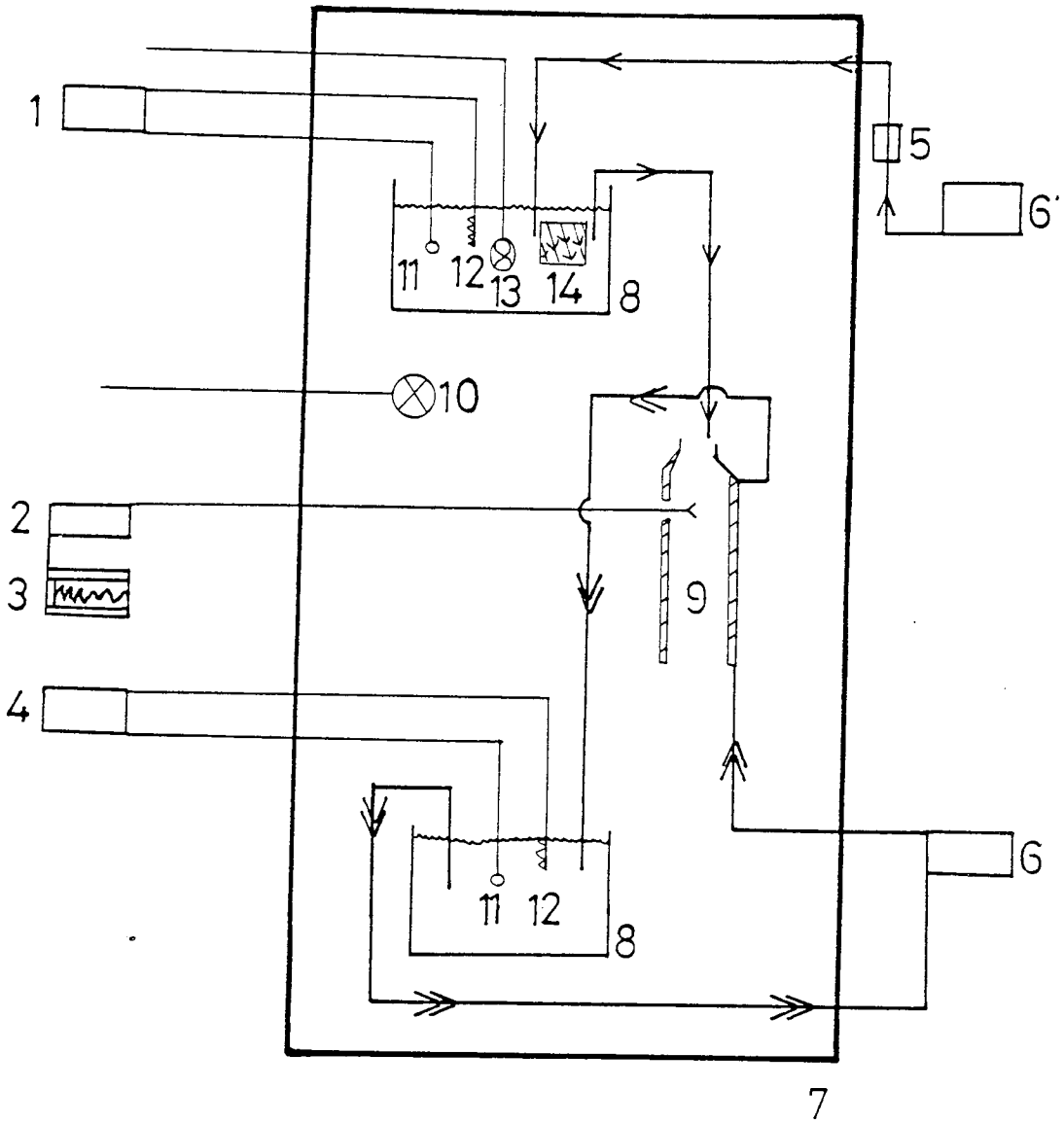

Key :-

1, 14 Proportional temperature controller
2. Temperature monitoring instrument
3. Pen recorder
5. Air flow meter
6. Air pump
7. Insulated cabinet
8. Water baths
9. Equilibrium chamber
10. Fan/air circulator
11. Thermistor
12. Heating coil
13. Stirrer
14. Glass coil

⟶⟶ Direction of flow, water

⟶ Direction of flow, air

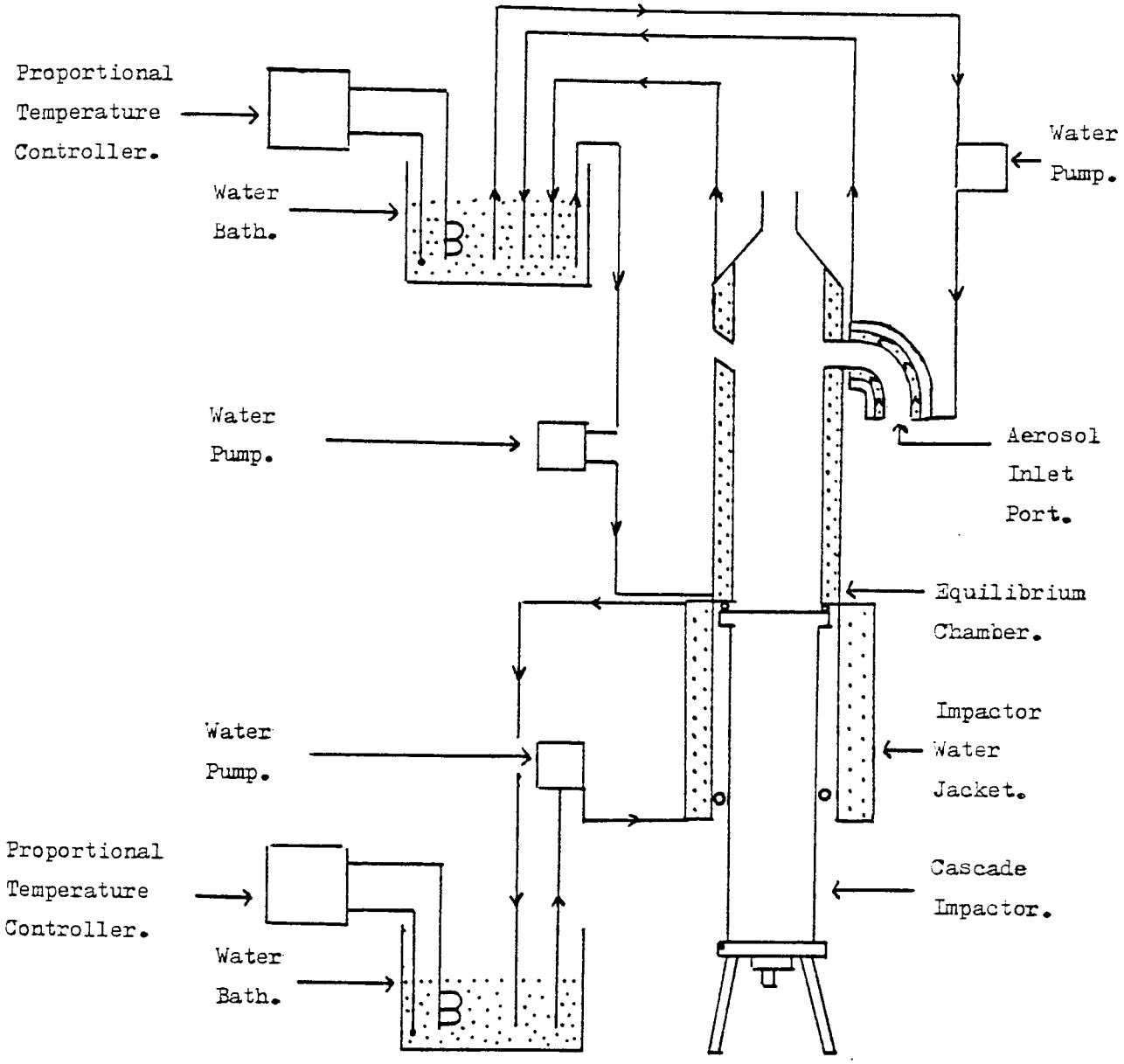

Figure 3.5: The Water System Of The Controlled Temperature And Relative Humidity Apparatus.

→ Direction of flow of water.

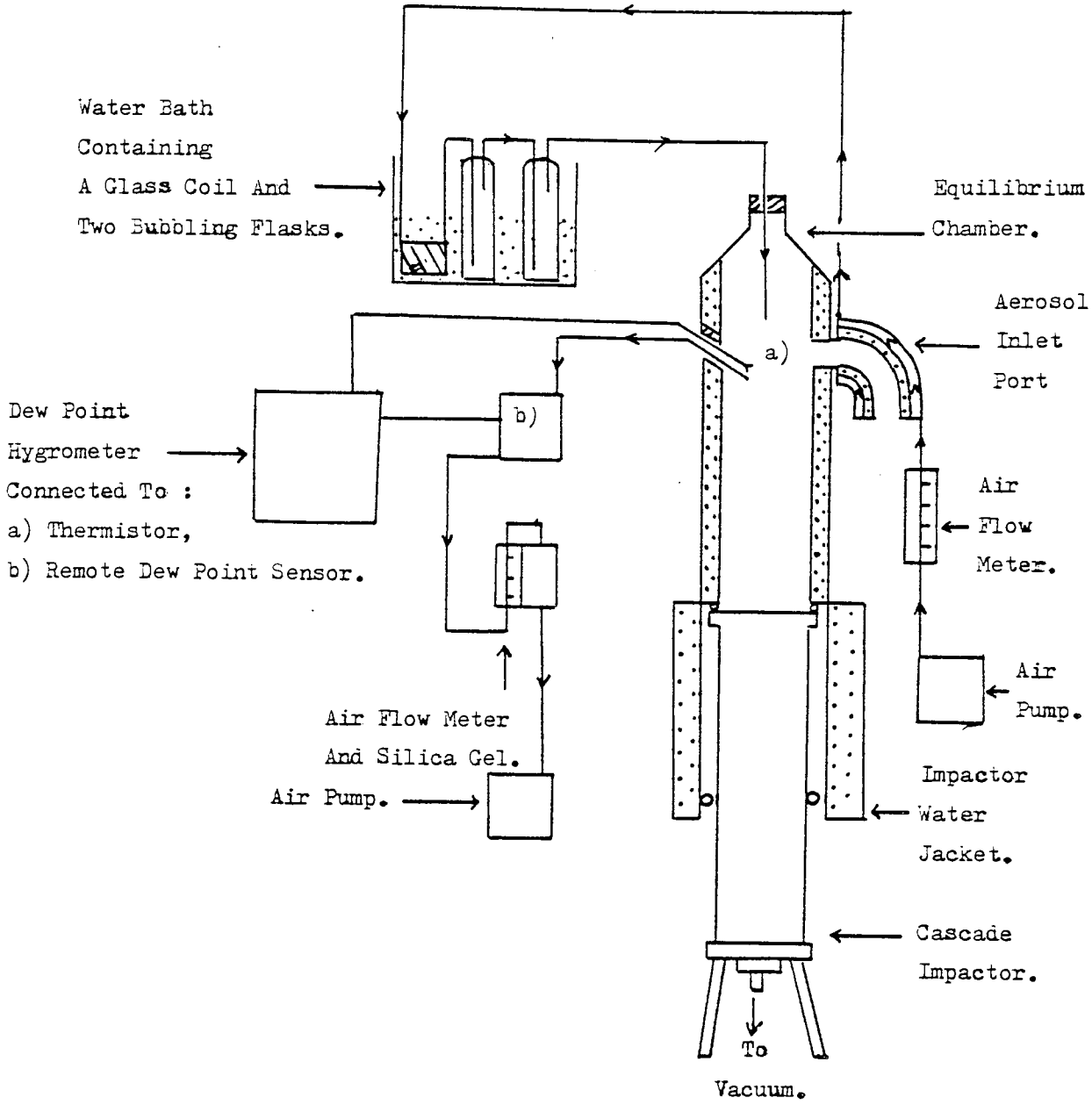

Figure 3.6: The Air System Of The Controlled Temperature And Relative Humidity Apparatus.

→ Direction of flow of air.

of the particle size during the aerosol genera tion experiments, by collection using a cascade impactor. The use of the cabinet for enclosing the apparatus as described in the previous cases precludes access to the apparatus for aerosol sampling without disturbing the control of the temperature. To avoid this hazard the entire apparatus was encased, in a modular fashion, in an expanded polystyrene housing with an average thickness of 1/4 ". In this way disturbing one section of the apparatus should not influence the equilibrium in the whole system. Figure 3.1 shows a photograph of the final arrangement of the apparatus.

Figure 3.5 shows the two water systems employed in these and subsequent experiments. The first water bath was used to heat and humidify the air and water to 37 °C and was pumped from this bath to the jacketed aerosol inlet port. Water from this bath was also pumped to the jacketed equilibrium chamber.

The second water bath supplied water for the cascade impactor jacket situated beneath the equilibrium chamber, also maintained at 37 °C.

Both of these systems were maintained under controlled conditions by means of proportional temperature controllers.

The air was preheated by passing it through a jacket around the aerosol inlet port. It was then pumped through an air flow meter and into the preheating and humidification system. The air was preheated by passing through a glass coil submerged in a water bath, maintained at constant temperature, and into bubbling flasks containing salt solutions. Finally the air passed into the equilibrium chamber. A fraction of this air was removed for analysis by a remote sensor which measures the Dew Point of the air. By placing a thermistor in the air stream, in the equilibrium chamber, and connecting this, via an electronic device,

to the remote Dew Point sensor, a digital visual display of the relative humidity was obtained. The operation of the controlled temperature and relative humidity of the apparatus which was brought about by the water system, shown in Figure 3.5 , is described in the methods, section 3.2.2.3, and refers to the air system shown in Figure 3.6 .

3.3.2.2.Discussion

i) Accuracy of control in the controlled temperature and relative humidity apparatus.

It has been demonstrated that little or no growth occurs for disodium fluorescein at 37°C up to 50 % relative humidididity (252). At high relative humidity the control of this factor and temperature is very important in the study of hygroscopic growth. In disodium fluorescein, for example , significant differences in growth, and thus in particle size, may be observed over a small interval at high relative humidity. In these studies the system was maintained at 37 ± 0.1°C. The relative humidity was controlled at 96.6 ± 1.2 % and at 20 ± 5 %, which constitute high and ambient conditions respectively.

Assuming negligible Kelvin effect and that the equilibrium droplet is below the solubility limit for disodium fluorescein equation 3.4 gives a value for R of 1. Equation 3.10 for the increase in the equivalent volume diameter then becomes,

$$R' = (\rho_s/\rho_l\,(1 + (M_w/M_s)(H(i + j) - j)/(1 - H)))^{1/3} \qquad 3.20$$

From this equation (214) it may be derived that at high relative humidity, the error in R depends on errors in H as,

$$\delta R'/R' = 1/3\ \delta H/(1 - H) = 1/3\ (\delta H/H)/((1/H) - 1) \quad 3.21$$

This will also apply to the aerodynamic growth ratio, R_a, equation 3.12 , since both the numerator and denominator of equation 3.21 are multiplied by the same factor.

The water activity of dilute electrolyte solutions is relatively insensitive to temperature changes (310). Similarly the partial vapour pressure P in equation 3.1 is not subject to large errors when temperature fluctuates, a temperature change of 1°C causes only a 0.2 % change in P at around 37 °C. However the saturation vapour pressure of pure water rises by about 5% per °C between 36.8 °C and 37.2°C (214).

Equation 3.21 above can be written as,

$$\begin{aligned} \delta R'/R' &= 1/3\ ((1/H)(\delta H/\delta T)\ T/((1/H) - 1)) \\ &= 0.017\ \delta T/(1/H) - 1 \end{aligned} \quad 3.22$$

The limit of the recorded sensitivity of the thermistor used to measure the temperature in these studies was 0.1°C. The extremes of temperature giving a recorded range of 37 ± 0.1°C might, therefore, be 37 ± 0.15 °C. From this observation and the mean and standard deviation of the relative humidity, the limit of accuracy in the measurement of the growth ratio may be calculated. This limit is based on the combination of temperature and relative humidity which gives the greatest error. Thus inserting values for H of 0.978 ((96.6 + 1.2)/100) and for T of 0.15 gives a value for R' of 11.4 %.

All of the mass median aerodynamic diameter data obtained in these experiments fell within the limit of error dividing the standard deviation by the mean. The worst example being 10.2 % for the ambient

lauric acid coated disodium fluorescein, nominally 0.24 gg^{-1}, data. Three of the samples gave errors outside this limit for their respective geometric standard deviations. These were ambient lauric acid, nominally 0.07 gg^{-1} and 0.2 gg^{-1} at high relative humidity both of which were marginally outside having errors of 13.6 % and 12.5 % respectively. Capric acid coated disodium fluorescein at a nominal concentration of 0.08 gg^{-1} and under conditions of high relative humidity exhibited an error of 16.1 % in the particle size measurements. These observations may be explained by microenviron - mental temperature fluctuations brought about by convection currents within the equilibrium chamber. Such fluctuations would go undetected by the thermistor. A temperature gradient within the equilibrium chamber was avoided by a countercurrent system passing the air through the chamber in the opposite direction to the direction of flow of the heating water. The fact that so few results are outside the range of acceptable error and those only to a slight extent suggests that the control of temperature and relative humidity within this system is very good. The sort of errors observed may well prove to be statistically insignificant if further experiments were carried out.

ii) Comparison of this controlled temperature and relative humidity apparatus with those described in the literature.

Several in vitro controlled temperature and relative humidity devices have been described in the literature. Hiller (212,213), Halbert (215) and Bell (211) employ climatic cabinets which are heated directly and are humidified either using salt solutions or by passing known volumes of air , at a constant temperature, through water. Tang (292) has used a device which is similar to that described in the present study. Tang's apparatus consists of a 850 ml pyrex jacketed growth

chamber, in which the residence time for aerosol particles is 20 seconds. A boiler condenser unit was used to humidify the air, with the cooling water thermostat regulated at 25 °C in this particular account. The efficiency of this piece of apparatus cannot be contrasted with the one used in these experiments as the temperatures at which each was undertaken are significantly different.

Bell (211) humidified the air and passed it through a water bath at constant temperature and finally into a heated cabinet. The system was maintained at 37 °C and 98 % relative humidity. Assumptions concerning the relative humidity in different parts of the apparatus were made in order to estimate the experimental conditions and it must be concluded that no error margins could, therefore, be given.

Hiller (212,213) used a 200 litre insulated plexiglass chamber with heat strips and digital thermometer to control environmental conditions. A variable speed fan inside the chamber provided thermal and aerosol mixing. The chamber was humidified by bubbling air through a heated water bath at a flow rate necessary to attain the desired humidity. For studies at ambient humidity , the temperature was maintained at 36.8 ± 0.4 °C and the relative humidity at 23.6 ± 1.4 %. For studies at airway humidity, the temperature was 37.1 ± 0.4 °C and the relative humidity at 96.4 ± 0.2 %.

A climatic cabinet has been used in our laboratories (252) consisting of an insulated box containing two water baths, one to humidify the atmosphere and heat the equilibrium chamber and a second to humidify the air into which the aerosol was introduced. A third heater directly heated the air in the cabinet and a fan circulated this air. Temperature control in this system proved difficult since the various heat control systems interacted resulting in a cycling effect in the temperature which was beyond that of the control of the thermostat.

Figure 3,7 : Example of a plot of the logarithm of the particle size(um) against cumulative % undersize for capric acid (0,08gg^{-1}) coated disodium fluorescein generated under ambient conditions of relative humidity.

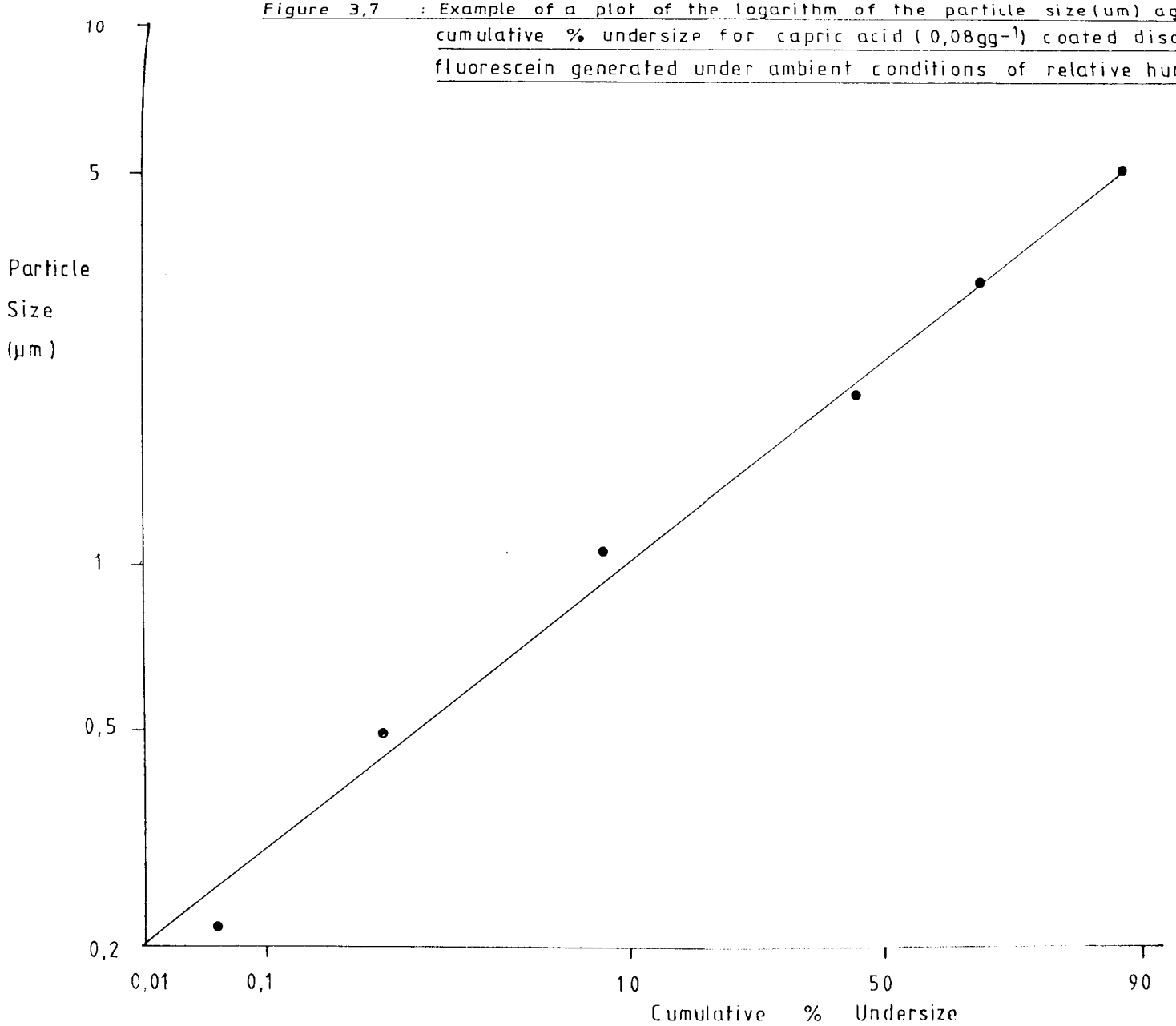

In order to overcome these problems the apparatus designed and developed for these studies was arranged such that the two heat sources could undergo minimal interaction. The volume to be maintained at constant temperature was reduced by modular insulation thus minimising the influence of convection currents. All electrical devices capable of generating heat, for example pumps, were situated outside the insulation and with maximum possible exposure to the atmosphere for the dissipation of any heat generated by their action. The use of an aerosol generator which requires no throughput of air overcomes the problem of preheating and humidifying the air used to generate aerosols in other systems, where conventional spinning disc or fluidized bed apparatus are used for example. Consequently the added variable of unequilibrated air entering the system has been avoided altogether.

The control of temperature using this device was 37 ± 0.1°C and at high relative humidity was 96.6 ± 1.2 %. This compares favourably with Hiller's values. The control of relative humidity under ambient conditions is a function of the environmental relative humidity, that observed in these studies was 20 ± 5 %.

3.3.3 Generation experiments.

3.3.3.1 Particle size distribution.

Figure 3.7 shows an example of the plot of the particle size on a logarithmic scale against the cumulative percentage undersize, for a capric acid coated disodium fluorescein aerosol powder, based on impactor data. A linear plot on this scale is indicative of a single particle size distribution. This is a useful preliminary technique to establish the nature of the distribution prior to using the computer programme to fit the data, using data on the calibration of the cascade impactor

and to establish a description of the distribution in terms of the mass median aerodynamic diameter and the geometric standard deviation.

3.3.3.2 Hygroscopic growth data.

The data describing the curves of best fit, the mass median aerodynamic diameter and the geometric standard deviation, from equations 3.15 and 1.3, to the particle size distribution obtained experimentally for disodium fluorescein, lauric and capric acid coated disodium fluorescein are presented in Tables 3.3 to 3.7.

The growth ratio of disodium fluorescein at 97 % relative humidity was 1.45. Marked reductions in hygroscopic growth of disodium fluorescein occur with both the addition of lauric acid and capric acid. The lowest surface coverage at which the reduction in hygroscopic growth occured was 0.11 gg^{-1} for capric acid and 0.2 gg^{-1} for lauric acid, having growth ratios of 1.07 and 1.0 respectively.

A more detailed examination of the lauric acid growth data shows that these samples exhibit a range of effects on hygroscopic growth. The 0.07 gg^{-1} sample of lauric acid coated powder gives a growth ratio of 1.5 which is similar to that observed for disodium fluorescein alone. The 0.12 gg^{-1} sample gives a growth ratio of 1.68 suggesting that growth above that of disodium fluorescein has occurred. This may be due to penetration of the water molecules into the particle and the subsequent effects of the surfactant on its hygroscopic growth. The 0.15 gg^{-1} sample gives a growth ratio of 1.33 which suggests a reduction in the growth ratio of the disodium fluorescein. Finally the 0.22 gg^{-1}, 0.24 gg^{-1} and 0.23 gg^{-1} samples have eliminated growth over the period that the aerosol was allowed to equilibrate, having growth ratios of 1.0, 1.05 and 1.05 respectively. The

explanation for this range of effects may be that too little surfactant coating is present at a nominal concentration of 0.07 gg^{-1} to influence the growth ratio of the disodium fluorescein, and that there is too little surfactant present at the nominal concentration of 0.12 gg^{-1} to prevent the entry of water into the particle but that the presence of this surfactant effects an increase in the growth of disodium fluorescein. From the IR and ESCA studies in section 2.3.2.2 and 2.3.2.3 the nature of this interaction probably results in the formation of the sodium salt of the fatty acid. The 0.15 gg^{-1} sample reflects a reduction in the hygroscopic growth as a critical value for the surface coverage, with respect to the prevention of the entry of water, is passed. The 0.2 gg^{-1}, 0.24 gg^{-1} and 0.23 gg^{-1} samples exhibit a further reduction, seemingly elimination, of hygroscopic growth with increasing amounts of lauric acid.

The capric acid samples only exhibit the property of reduced hygroscopic growth. The 0.08 gg^{-1} samples show a growth ratio of 1.27 and 1.33 respectively. The 0.11 gg^{-1}, 0.14 gg^{-1}, 0.16 gg^{-1} and 0.18 gg^{-1} samples exhibit eliminated growth over the period that the aerosol was allowed to equilibrate, having growth ratios of 1.07 1.1, 1.12 and 1.02 respectively. The critical surface coverage for the prevention of entry of the water, and thus reduction in growth, assuming that similar observations to lauric acid would be expected, would seem to occur at a concentration below those used in these experiments for capric acid. The critical nature of the surface coverage may be explained by the degree of penetration of the surfactant into the particle. That is to say that the expanding surface area discussed in chapter 2,which is a function of the surfactant concentration reaches a critical level with respect to its maximum expanded value.

Table 3,3 : Calculated deposition data for disodium fluorescein alone, mass median aerodynamic diameter and geometric standard deviation under both ambient (20%) and high (97%) relative humidity conditions.

Relative Humidity	Individual MMAD		Mean MMAD	Standard Deviation	Individual σ_g		Mean σ_g	Standard Deviation	Growth Ratio
ambient	3,6	4,1	3,8	0,24	1,4	1,5	1,5	0,13	
	4,0	3,7			1,7	1,6			
high	5,2	5,2	5,5	0,6	1,3	1,3	1,4	0,12	1,45
	5,2	6,4			1,5	1,5			

Table 3,4 : Calculated deposition data for nominal concentrations of a) 0,07 gg^{-1} b) 0,12 gg^{-1} and c) 0,15 gg^{-1} lauric acid coated disodium fluorescein, mass median aerodynamic diameter and geometric standard deviation under both ambient (20 %) and high (97%) relative humidity conditions.

Sample gg^{-1}	Relative Humidity	Individual MMAD		Mean MMAD	Standard Deviation	Individual σ_g		Mean σ_g	Standard Deviation	Growth Ratio
a) 0,07	ambient	4,2	4,3	4,2	0,08	1,1	1,3	1,3	0,14	
		4,2	4,1			1,4	1,4			
	high	6,3	6,7	6,3	0,25	1,7	1,8	1,8	0,05	1,5
		6,1	6,3			1,8	1,8			
b) 0,12	ambient	4,3	4,2	4,1	0,18	1,1	1,2	1,3	0,17	
		3,9	4,0			1,5	1,5			
	high	6,8	7,1	6,9	0,15	1,7	1,5	1,6	0,1	1,68
		6,8	6,8			1,7	1,7			
c) 0,15	ambient	4,5	4,3	4,4	0,26	1,3	1,3	1,3	0,05	
		4,8	4,2			1,3	1,4			
	high	5,7	6,2	5,9	0,46	1,4	1,7	1,6	0,17	1,33
		6,4	5,4			1,8	1,6			

Table 3,5 : Calculated deposition data for nominal concentrations of a)0,2 gg-1 b)0,24gg-1 and c)0,23gg-1 lauric acid coated disodium fluorescein, mass median aerodynamic diameter and geometric standard deviation under both ambient (20%) and high (97%) relative humidity conditions.

Sample gg-1	Relative Humidity	Individual MMAD		Mean MMAD	Standard Deviation	Individual σ_g		Mean σ_g	Standard Deviation	Growth Ratio
a)0,2	ambient	4,2	4,3	4,0	0,33	1,4	1,4	1,4	0,05	
		3,8	3,6			1,5	1,4			
	high	4,2	4,0	4,0	0,26	1,5	1,3	1,2	0,15	1,0
		3,5	3,7			1,2	1,3			
		4,1	4,2			1,1	1,1			
		4,0	4,2			1,1	1,1			
b)0,24	ambient	4,5	4,3	4,1	0,42	1,4	1,3	1,4	0,05	
		3,7	3,8			1,4	1,4			
	high	4,5	4,6	4,3	0,32	1,7	1,7	1,6	0,15	1,05
		4,0	4,0			1,5	1,4			
c)0,23	ambient	4,1	3,8	4,1	0,25	1,6	1,5	1,5	0,08	
		4,4	4,0			1,5	1,4			
	high	4,4	4,4	4,3	0,15	1,5	1,5	1,5	0,08	1,05
		4,1	4,2			1,6	1,4			

Table 3,6 : Calculated deposition data for nominal concentrations of a) 0,08 gg^{-1} b) 0,08 gg^{-1} and c) 0,11 gg^{-1} capric acid coated disodium fluorescein, mass median aerodynamic diameter and geometric standard deviation under both ambient (20%) and high (97%) relative humidity conditions.

Sample gg^{-1}	Relative Humidity	Individual MMAD		Mean MMAD	Standard Deviation	Individual σ_g		Mean σ_g	Standard Deviation	Growth Ratio
a)0,08	ambient	4,0	4,6	4,4	0,32	1,6	1,6	1,5	0,1	
		4,3	4,7			1,4	1,5			
	high	5,7	5,2	5,6	0,35	1,9	1,4	1,8	0,29	1,27
		6,0	5,4			2,0	2,0			
b)0,08	ambient	4,6	4,2	4,4	0,36	1,2	1,3	1,3	0,14	
		4,8	4,0			1,2	1,5			
	high	6,0	5,6	6,0	0,53	1,6	1,5	1,6	0,08	1,36
		5,8	6,8			1,6	1,7			
c)0,11	ambient	4,0	4,3	4,1	0,15	1,4	1,5	1,4	0,06	
		4,0	4,2			1,5	1,4			
	high	4,5	4,4	4,4	0,13	1,2	1,2	1,2	0,06	1,07
		4,4	4,2			1,3	1,3			

Table 3,7 : Calculated deposition data for nominal concentrations of a) 0,14 gg^{-1} b) 0,16 gg^{-1} and c) 0,18 gg^{-1} capric acid coated disodium fluorescein, mass median aerodynamic diameter and geometric standard deviation under both ambient (20%) and high (97%) relative humidity conditions.

Sample gg^{-1}	Relative Humidity	Individual MMAD		Mean MMAD	Standard Deviation	Individual σ_g		Mean σ_g	Standard Deviation	Growth Ratio
a)0,14	ambient	4,0	4,0	4,0	0,06	1,3	1,3	1,3	0,06	
		3,9	3,9			1,4	1,4			
	high	4,4	4,6	4,4	0,16	1,5	1,2	1,4	0,15	1,1
		4,2	4,4			1,5	1,3			
b)0,16	ambient	4,2	4,0	4,2	0,17	1,3	1,3	1,3	0,08	
		4,4	4,1			1,4	1,2			
	high	5,1	4,8	4,7	0,38	1,0	1,1	1,2	0,13	1,12
		4,8	4,2			1,2	1,3			
c)0,18	ambient	4,3	4,6	4,3	0,36	1,6	1,3	1,4	0,13	
		4,5	3,8			1,5	1,4			
	high	4,4	4,6	4,4	0,1	1,3	1,2	1,3	0,05	1,02
		4,4	4,4			1,3	1,3			

Figure 3.8 : Plot of the growth ratio against the nominal adsorbed amount (gg^{-1}) for lauric and capric acids.

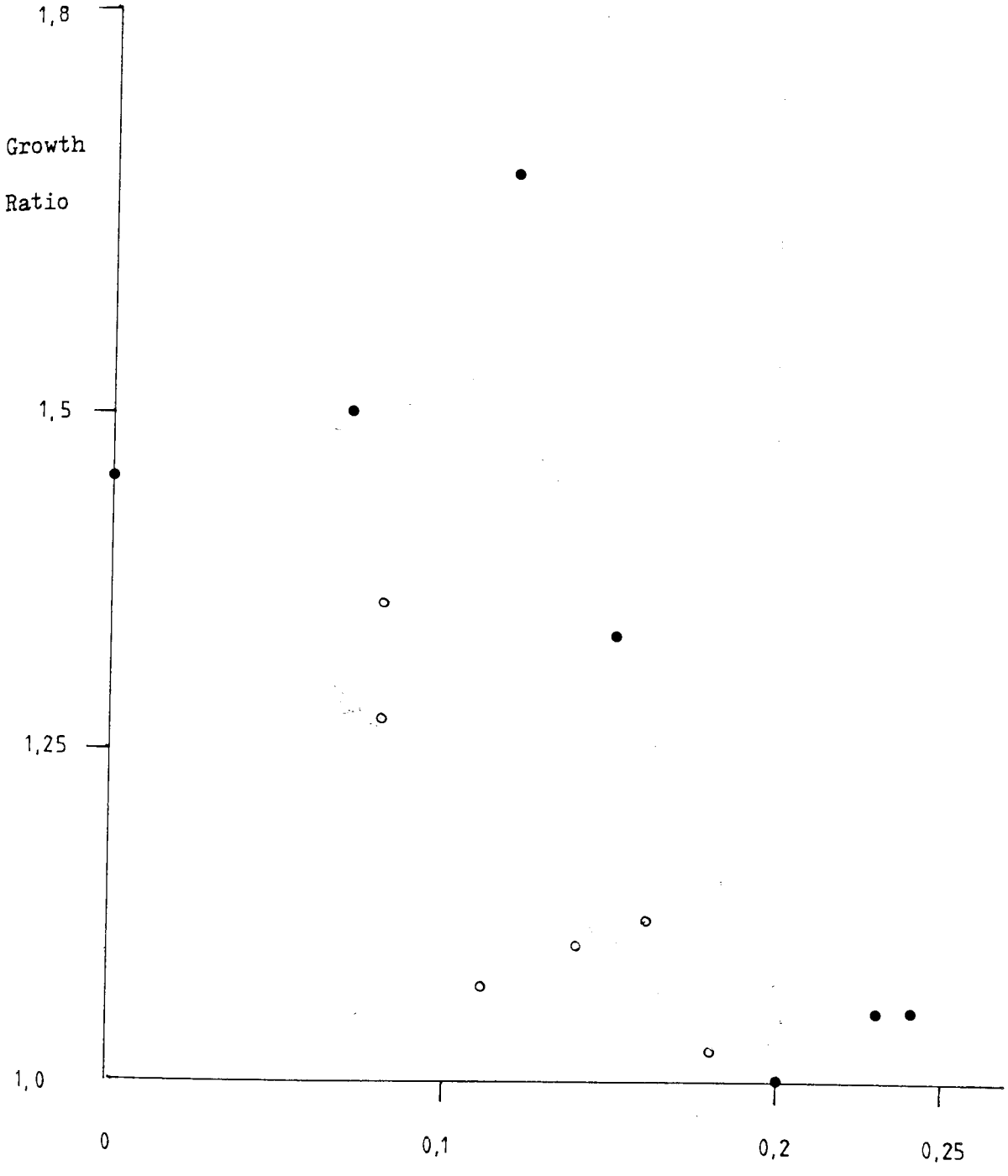

Key :-

---●---Lauric acid , —o— Capric acid.

The growth ratios and their respective nominal coatings are plotted graphically in Figure 3.8. It would seem that the effect of the lauric acid is to influence growth at higher concentrations than capric acid.

The enhanced growth at 0.12 gg^{-1} appears to be the most anomalous observation and was investigated using the predictive technique of vapour pressure osmometry.

3.3.4 Vapour pressure osmometry.

The use of vapour pressure osmometry as a tool in the prediction of the hygroscopic growth of aerosol powders has been described in the literature (214,252). It was intended to use this technique to investigate the observation that the 0.12 gg^{-1} lauric acid coated disodium fluorescein powder exhibited a growth ratio of 1.68 at 37°C and 97 % RH.

A calibration curve using sodium chloride solutions of known water activity (310) at a given temperature was prepared. The data from which the calibration plot of instrumental response against minus the natural logarithm of water activity may be plotted is shown in Table 3.8.

Using this calibration curve the instrumental response obtained for several solutions of disodium fluorescein may be converted to water activities, as shown in Table 3.9.

A chi - squared comparison between these data and the literature values (252, Figure 3.9) proves meaningless since the logarithmic relationship between water activity and instrumental response minimises any errors. A direct comparison of instrumental responses cannot be carried out as no calibration data is available for comparison since the data was collected at 37°C and sensitivity setting 8.

Table 3.8 : Data required for a calibration plot of Instrumental Response, % full scale deflection, against - ln a_w for concentrations of NaCl of known water activity, a_w.

Concentration NaCl, moles Kg^{-1}	Instrumental Response, %, n=3	a_w at 37°C	- ln a_w
0	0.0	1.0	0.0034
0.1	2.0	0.9966	0.0034
0.2	6.0	0.9933	0.0067
0.3	11.5	0.99	0.0101
0.4	18.5	0.9868	0.0133
0.5	24.0	0.9838	0.0166
0.6	31.0	0.9802	0.02
0.7	37.0	0.976	0.0243
0.8	42.5	0.9735	0.0269
0.9	49.5	0.97	0.0305
1.0	56.0	0.9667	0.0339
2.0	118.0	0.9312	0.0713

Linear regression parameters :

Correlation coefficient	0.999
Slope	1709.4
Intercept	-3.61

Table 3.9 : Concentrations, moles Kg^{-1}, of disodium fluorescein solutions and the respective water activities obtained from the calibration curve where n = 3

Concentration, disodium fluorescein, moles Kg^{-1}	Water Activity
0.07	0.9995
0.14	0.9988
0.4	0.9938
0.7	0.9829
1.0	0.9673
1.02	0.9658

Table 3.10 : Instrumental responses for solutions of disodium fluorescein, with and without lauric acid.

Amount of disodium fluorescein, moles Kg^{-1}	Amount of lauric acid, moles Kg^{-1}	Instrumental Response n = 5
1.023	-	56.0
1.023	0.1923	24.0
1.023	0.3845	14.0

Figure 3.9 : Water activity, a_w, of aqueous disodium fluorescein solution versus concentration, moles Kg^{-1}

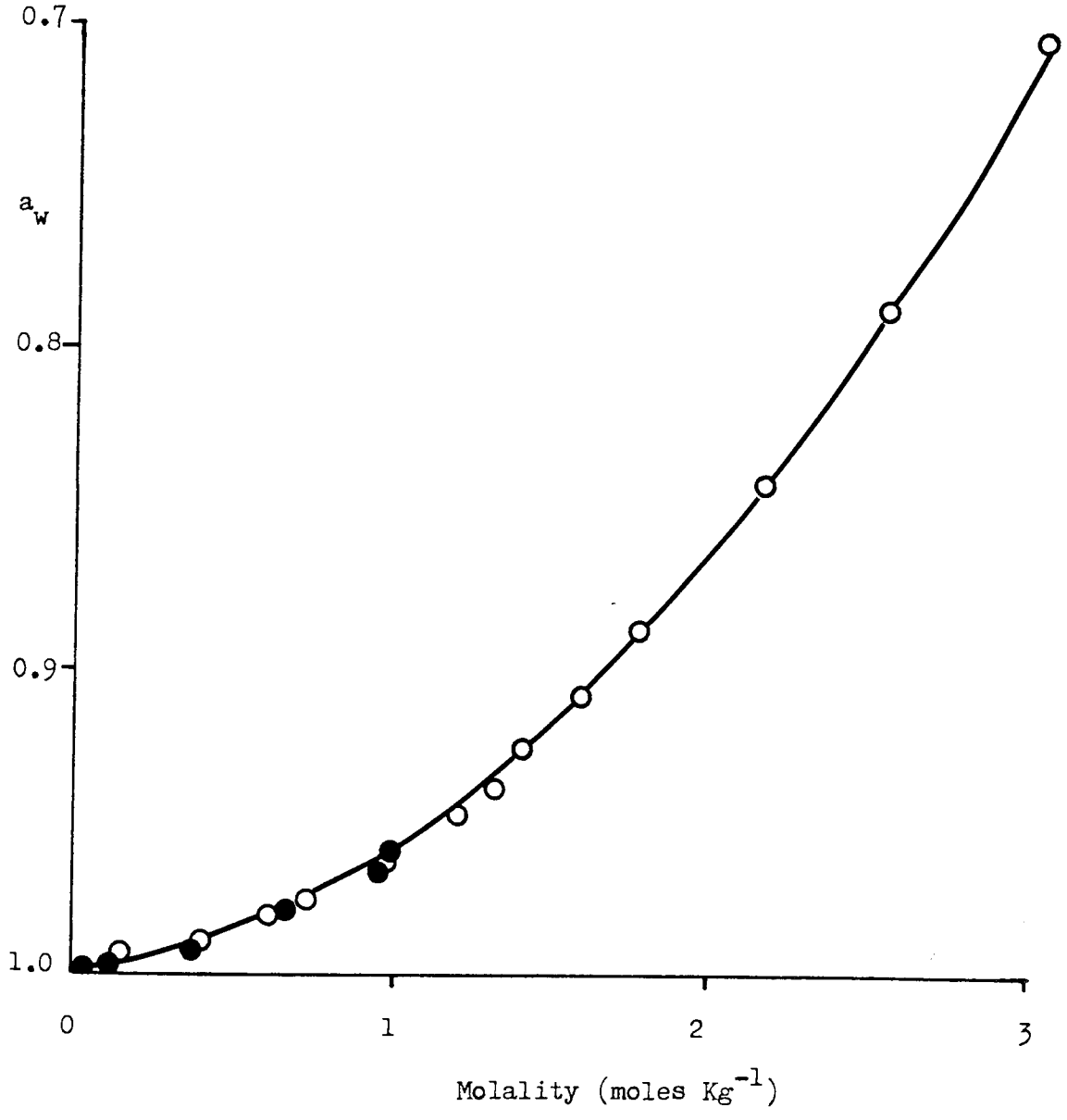

Key :-

- ● Experimental data
- ○ Literature values.

The calibration curve has been compared with gravimetric estimates of solution concentrations.

Table 3.9 shows the instrumental responses for a variety of disodium fluorescein solutions.

The equation for the calibration curve is

$$\text{Instrumental Response} = 1709.4 \; (- \ln a_w) - 3.61$$

The equation of the line describing the water activity against concentration plot is :

$$100 \; (1 - a_w) = 3 \; (\text{Mol}^2) + 0.4 \; \text{Mol}$$

Where Mol is molality in moles Kg^{-1}.

Thus for the disodium fluorescein sample of gravimetric molality 1.023 and instrumental response 56, Table 3.10, the following is true

$$- \ln a_w = \frac{56 + 3.61}{1709.4} = 3.487 \times 10^{-2}$$

Therefore $a_w = 0.9657$

and $1 - a_w = 0.0343$

It follows that,

$$100 \; (3.43 \times 10^{-2}) = 3 \; (\text{Mol}^2) + 0.4 \; \text{Mol}$$

and,

$$3 \; (\text{Mol}^2) + 0.4\text{Mol} - 3.423 = 0$$

consequently,

$$\text{Mol} = (-0.4 \pm (0.16 + (12 \times 3.43))^{1/2})/6 = 1.004 \text{ moles } Kg^{-1}$$

Table 3.11 : Steps in the calculation of the apparent molality of disodium fluorescein solutions containing lauric acid.

Amount of lauric acid, moles Kg^{-1}	Instrumental Response	$-\ln a_w \times 10^{-2}$	a_w	$1 - a_w \times 10^{-2}$	Apparent Molality
0.1923	24.0	1.6151	0.984	1.603	0.667
0.3845	14.0	1.0301	0.99	1.025	0.522

Table 3.12 : Calculation of the aerodynamic growth ratio based on the apparent molality of the solutions.

Amount of lauric acid, moles Kg^{-1}	De/D	$D_{ae,l}/D_{ae,s}$	Solution ρ n = 3
0.1923	1.91	1.61	1.065
0.3845	2.05	1.73	1.06

The error incurred in the preparation of the samples has a value of 1.86 % ((1.- (1.004/1.023)) x 100).

A similar procedure to that followed above may be adopted to investigate the effects of lauric acid on the predicted growth ratio. By following the approach above using the instrumental data in Table 3.10 the apparent molality of the solutions containing the fatty acid can be calculated these are shown in Table 3.11.

These values may be used in conjunction with particle densities and solution densities to calculate a dynamic growth ratio assuming ideal solution behaviour.

Using equation 3.18, which is derived from equation 3.12, the following example of growth ratio calculation may be carried out,

$$D_e/D = ((1.49/1.08)(1 + (1{,}000/(376{,}28 \times 1.004))))^{1/3}$$

$$= 1.714$$

and,

$$D_{ae,l}/D_{ae,s} = (1.08/1.49)^{1/2}. 1.714 = 1.46$$

The equivalent values for the samples containing lauric acid are shown in Table 3.12.

It would seem from these experiments that a growth ratio of 1.61 might be predicted for a disodium fluorescein sample containing 0.1 gg^{-1} lauric acid. The observation of a growth ratio of 1.68 for the growth of a 0.12 gg^{-1} coated sample, measured dynamically is consistent with these preliminary results obtained by vapour pressure osmometry.

3.3.5 Dissolution experiments.

The purpose of this series of experiments was to investigate the possibility that the reduced growth ratio, shown in Tables 3.3 to 3.7, might be one aspect of the effect of the surface coating on the behaviour of the particles. The overall object of these studies has been to coat and investigate the in vitro deposition of a model aerosol powder under conditions approaching those in the lung. This may have some implications for the deposition of pharmaceutical aerosols (208). It is important that once an aerosol deposits in the respiratory tract it is available for absorption, or directly to the sites of action in order that it may achieve its therapeutic effect. In vitro dissolution of aerosol particles has been correlated with in vivo dissolution in the lower respiratory tract after inhalation (315). It would be difficult to examine the dissolution of the coated disodium fluorescein particles since their density precludes their direct addition to an aqueous medium. By preparing compacts of the powders the dissolution becomes a function of the surface area and mass of the compact as well as those factors attributable to the original powder. However by comparing the dissolution of disodium fluorescein alone with the coated powders this technique might indicate differences attributable to the coating.

The trend in the lauric acid samples shown in Figure 3.10 is towards a slower dissolution with increased surface coverage. The most marked reduction occuring between consecutive samples taken from the lauric acid isotherm at 0.12 gg^{-1} and 0.15 gg^{-1} which is the same position at which reduction in growth begins in the dynamic growth experiments. Capric acid shows similar reductions in the rate of dissolution, shown in Figure 3.11.

Figure 3.10 : Dissolution of lauric acid coated disodium fluorescein powders prepared as compacts.

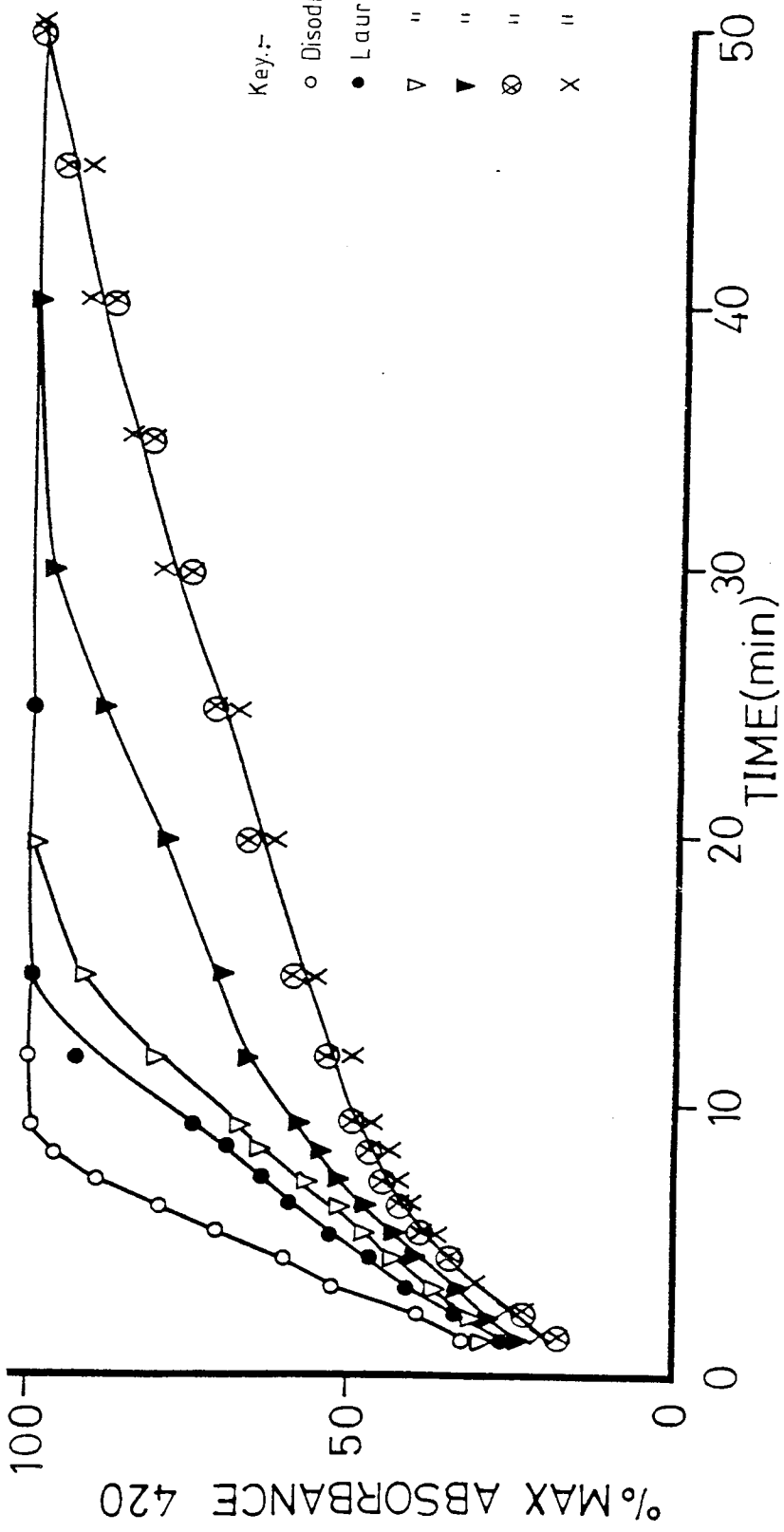

Figure 3.11 : Dissolution of capric acid coated disodium fluorescein powders prepared as compacts.

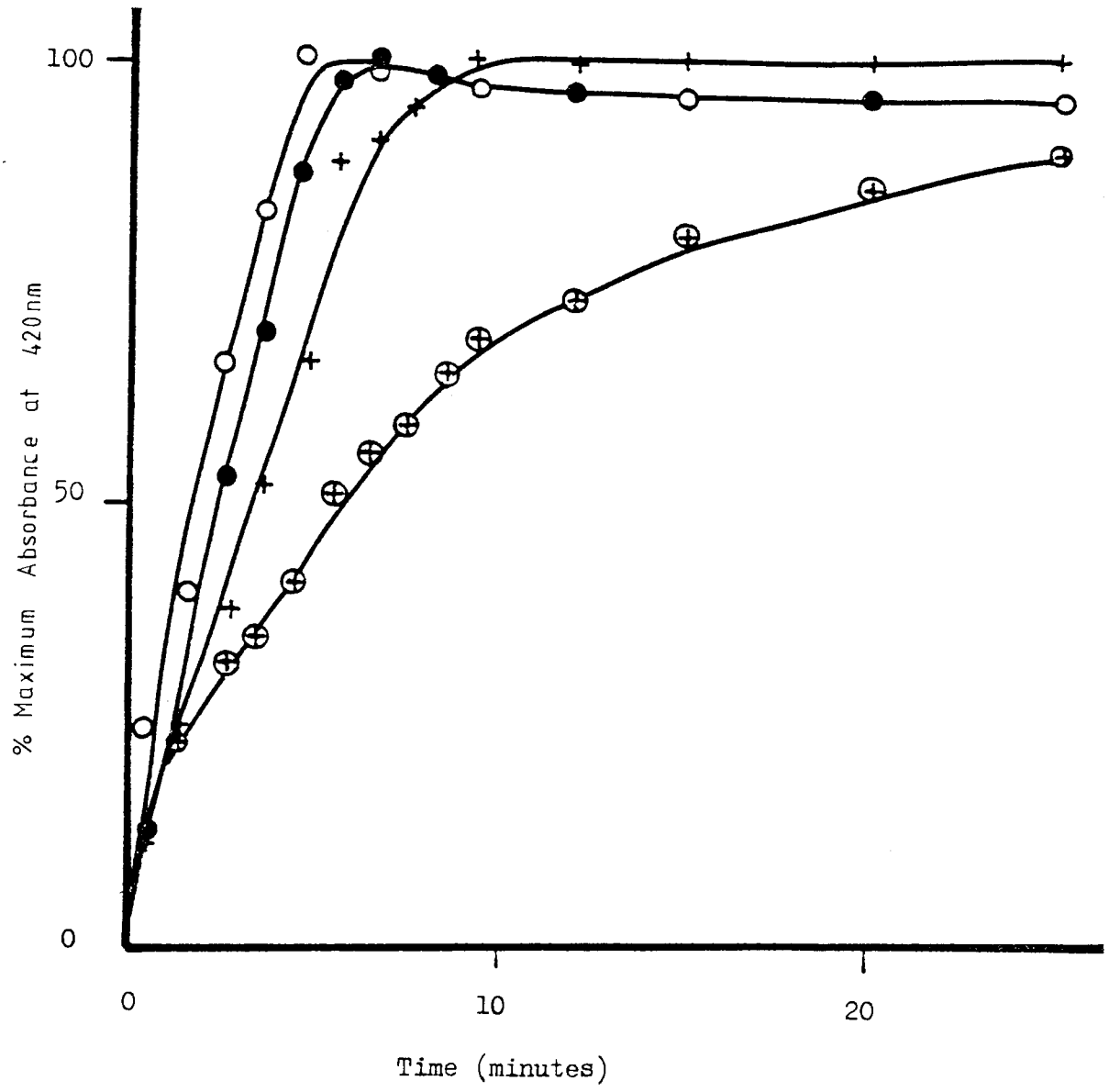

Key :-

- ○ Disodium fluorescein
- ● Capric acid, 0.06 gg^{-1}
- + Capric acid, 0.08 gg^{-1}
- ⊕ Capric acid, 0.16 gg^{-1}

3.4 Discussion.

Otanyi and Wang (221) have carried out aerosol growth studies using saline droplets with surfactants. The surfactants used were not stated. Nearly monodisperse aerosols were coated with a monolayer and generated into a horizontal elutriator 28.5 cm long by 7cm wide. The top and bottom of the elutriator were 0.5 cm apart and were made of sponge which was soaked in saline solution to maintain the relative humidity. No specific temperature or relative humidity were stated. The observations made were that the deposition of the saline droplets in the elutriator was not uniform and that the non - uniformity in deposition was more striking when the surfactant was present. Assuming that the conditions were well controlled and that non - uniformity means polydispersity the conclusion which can be drawn is that either monolayer coverage results in a nonspecific change in the deposition characteristics of the aerosol or the other more tenable explanation would be that various surface coverages exist and that the droplets have been incorrectly characterised. The non - uniformity of deposition of the saline droplets alone, which were described as nearly monodisperse, strongly suggests fluctuations in the conditions of temperature and relative humidity. The difference in growth rate between particles of different sizes should not influence the deposition of a monodisperse aerosol.

Chikazawa (222) measured the amounts of adsorbed water and the isosteric heats for water vapour adsorption on fine crystals of potassium bromide treated with various amounts of potassium oleate. A small amount of pre - adsorbed potassium oleate was recognised to prevent the water vapour adsorption on potassium bromide, and conversely, this effect dis appeared with increasing potassium oleate content while the hygroscopicity of the sample increased markedly.

The increase in hygroscopicity was explained assuming penetration of the adsorbed water molecules into potassium oleate films on the surface of the potassium bromide. Other authors (316) suggest that this may occur.

This report is of some significance in the interpretation of the aerosol hygroscopic growth studies and in the interpretation of the analytical data on the powders generated. The ESCA and infra - red evidence that sodium laurate may be formed at the surface of the disodium fluorescein coated with lauric acid makes this system similar to Chikazawa's. The observation reported in the present studies of reduction in hygroscopic growth with increasing surface coverage of disodium fluorescein with fatty acids although contradicting Chikazawa's observations are not entirely inconsistent with them. The time scale of the generation of the aerosol powder and their subsequent equilibration period may not be long enough in the case of the highest coated powders for them to completely equilibrate with the environment consequently the extent of their growth appears to be reduced. If all the powders were allowed adequate time to equilibrate then the observations made might be similar to Chikazawa's. There is some evidence for this conclusion in the growth beyond that of disodium fluorescein alone in the case of the lauric acid coated disodium fluorescein with a nominal concentration of 0.12 gg^{-1}.

On a practical level the controlled temperature and relative humidity apparatus designed and constructed for use in these experiments appears to maintain conditions with a degree of accuracy and precision comparable with the most effective device described in the literateure (211 - 213).

CHAPTER FOUR

General discussion and conclusion.

4. General Discussion and Conclusion.

4.1 General Discussion.

It has been observed that the delivery of certain pharmaceutical preparations to the lower regions of the respiratory tract is therapeutically advantageous (107). Beta - adrenergic agonists might be expected to increase in their activity as they enter the lower regions of the respiratory tract, as the density of the receptor sites for these compounds increases from the trachea to their greatest density in the lower bronchioles (34,35). A further explanation of the importance of the deposition of pharmaceutical aerosols in the lower respiratory tract, is the benefit which accrues with deposition in the most highly vascularised region of the lung, the pulmonary region. Vasoconstriction has a similar effect in terms of oxygen uptake as bronchoconstriction. Effecting vasodilation, as well as bronchodilation, alleviates the symptoms of asthma (5). Inflammatory mediators may cause vasoconstriction (317) consequently an agent which reduces their release, such as cromolyn sodium, Figure 1.3, will be beneficial. Thus in the case of allergic asthma deposition of such agents in the lower respiratory tract confers the advantage of increased therapeutic effect. It is drugs such as beta - adrenergic agonists (62) and cromolyn sodium (67,68) which may be considered suitable subjects for any applications which may be derived from the present model hygroscopic aerosol studies.

From the results and discussions, in Chapters 2 and 3, it has been established that there is an effect, most notably, a reduction in the hygroscopic growth of disodium fluorescein aerosol particles at 97 % relative humidity and 37 °C. This reduction has been achieved by an association between the powder and lauric and capric acids.

Figure 4.1: Histogram showing the fraction of the total deposited in each of the intratracheal regions for a) 3µm and 5µm non-hygroscopic particles and a 3µm NaCl, hygroscopic aerosol and b) 30, 60 and 100 L min^{-1} flow rates using a 3µm non-hygroscopic particle.

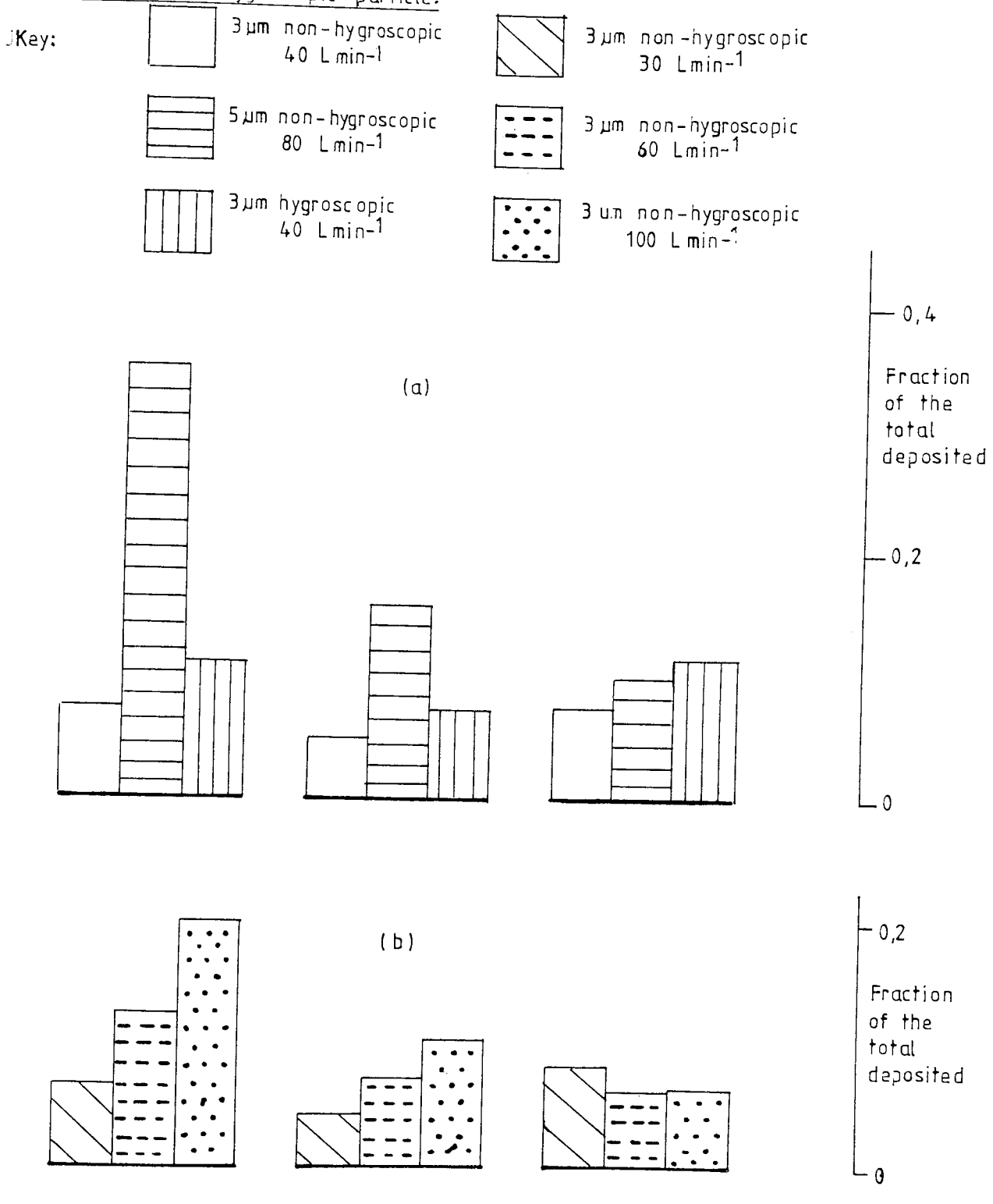

It has been suggested that the relative humidity in the respiratory tract reaches 98 % in the nasopharyngeal region (205,206). Thus the conditions employed in these studies closely resemble those in the respiratory tract. The mechanisms of deposition in the lung (318) have been shown to change in relative importance as a result of hygroscopic growth (208). Therefore the experimental results obtained in these studies have some bearing on deposition in the respiratory tract.

The growth ratio obtained experimentally for disodium fluorescein is of the same order as that described for sodium chloride by Martonen (208). These sodium chloride aerosols have been used analytically to produce parameters of deposited fraction in the tracheobronchial region and to further subdivide the deposition into the fraction deposited in three areas of the tracheobronchial region. If the parameters of deposited fraction and mass deposited in the lower tracheobronchial regions are examined for a 3 μm and a 5 μm non - hygroscopic particle and for a 3 μm hygroscopic particle, assuming an experimental growth ratio to give an equilibrium diameter of 4.2 μm, several observations can be made.

Figure 4.1 shows a histogram of the deposition data presented by Martonen (208). Figure 4.1 b) illustrates the effects of flow rates, 30, 60 and 100 L min^{-1}, on the deposition, showing that increased flow rates increase total deposition but have little effect on deposition in the lower tracheobronchial area for a 3 μm particle. Figure 4.1 a) shows the deposition of various particles, 3 μm non - hygroscopic and hygroscopic particles deposited at 40 Lmin^{-1} and 5 μm non - hygroscopic particles at 80 L min^{-1}.

There is an increase in the amount deposited between a 5 μm particle as compared with a 3 μm particle in the ratio 3.14 : 1

(0.6 : 0.191) however this considerable difference is not reflected in the deposition in the lower airways which is in the ratio 1.37 : 1 (0.097 : 0.071) .

Hygroscopic growth also results in greater total deposition, that is a hygroscopic 3 μm particle (4.2 μm) has a total tracheo - bronchial deposition in comparison with a 3 μm non - hygroscopic particle of 1.52 : 1 (0.291 : 0.191) and the fraction deposited in the lower airways is 1.56 : 1 (0.112 : 0.071). Therefore hygroscopic growth improves overall deposition in the lower airways and furthermore has better deposition properties than non - hygroscopic particles with an equivalent final diameter.

These observations may be explained in terms of the change in particle size with increasing gradient of relative humidity enabling a hygroscopic particle to overcome barriers to its penetration into the lung and then to deposit as its size increases. This explains the advantage of using a small particle and allowing it to grow prior to deposition rather than using a particle of the size of the equilibrium diameter of the hygroscopic particle. The difference in the deposition of the hygroscopic particle and a non - hygroscopic particle of the same initial diameter, 3 μm , may be explained in terms of reduced deposition due to the inefficiency of the deposition mechanisms at this particle size, for a non - hygroscopic particle. It would seem, therfore, that to optimise deposition in the lower airways the manipulation of hygroscopic growth may be used to some advantage.

Improved deposition may be expected if the particles grew more slowly, that is take longer to equilibrate. In this case the percentage of the particles penetrating due to small diameter and then depositing as a result of hygroscopic growth will increase. The observations of

hygroscopic growth made in these studies were carried out over a fixed transit time through the equilibrium chamber. The increased growth observed in the case of lauric acid coated disodium fluorescein at a nominal concentration of 0.12 gg^{-1} suggests that the initial effect of the addition of the fatty acid on growth is to increase it which has been suggested in the literature (222). Without studying the particle size distribution over a range of transit times it is impossible to say whether the particles are in equilibrium with the the surrounding atmosphere or whether their growth rate has been reduced. If the growth rate has been reduced to an extent detectable over the transit time, of approximately 40 seconds in this particular equilibrium chamber, then it should be possible to examine this phenomenon using the cascade impactor . Under normal circumstances particle or droplet growth, in the size range less than 10 μm takes place over fractions of a second and consequently more sophisticated apparatus, such as light scattering devices, are required to perform these investigations (176). Reduction in growth has been observed for 0.08 gg^{-1} capric acid coated samples , Table 3.6, and 0.15 gg^{-1} lauric acid coated samples, Table 3.4, having growth ratios of 1.27, 1.33 and 1.33 respectively, as compared to 1.45 for disodium fluorescein alone. If the increased growth of the 0.12 gg^{-1} lauric acid coated powder and the reduced growth of the concentrations beyond that are facets of the same growth pattern that is of initially reduced growth followed by increased growth then the potential for delivering an increased percentage of the total deposited amount to the lower respiratory tract, by modifying the surface characteristics of the model hygroscopic powder is great.

The time scale for the growth of aerosol particles in the lung

is much shorter in the respiratory tract, less than half a second according to Landahl (113,138), Table 1.1, than in these experiments. Conditions in the lung are somewhat different in terms of flow rates than the experimental set up, the Reynolds numbers being very much higher, making the time scales incomparable.

After presenting the respiratory tract with an increased amount of the aerosol powder it is important that this should be readily available for absorption or to the sites of action consequently the dissolution rate is of some interest. The in vitro dissolution of aerosol powder has been correlated with in vivo dissolution for certain hazardous aerosols (315). The dissolution of the compacts prepared in these studies cannot be parallelled directly with in vivo dissolution because of the contribution to the dissolution rate of the way in which the compound is presented to the solvent, The observation of reduced dissolution rate with increased surface coverage of disodium fluorescein with fatty acids, as shown in Figures 3.10 and 3.11, should be taken to imply the possible disadvantage of this coating in terms of bioavailability. Further work on the dissolution of the powder alone should be carried out to confirm this observation, however the experimental design requires some thought as the density of the powder and the fact that it is associated with fatty acid presents some problems in terms of the method of presentation to the solvent in which the experiment is to be carried out.

The methods of analysis of the surface coverage of the model aerosol powder have not been entirely successful. The major difficulty has arisen from the use of organic materials in apolar solvents. The effects of the presence of fatty acids and alcohols on the refractive index and surface tension are very small and consequently are not

very easily measured. The susceptibility of these systems to influence by small quantities of impurities has been noted (224,238). The experiments performed to investigate the behaviour of the surfactants in apolar media may have been improved by employing a battery of analytical methods which should include those mentioned and also light scattering (319), and by taking steps to purify the solvent and fatty acids employed.

The major difficulty with respect to the presence of impurities arises from the nature of the adsorbent which in order to serve as a model in these studies has to be extremely hygroscopic and consequently will always contain water as an impurity. The qualitative studies carried out have been marginally more successful in establishing the nature of the adsorption. The use of infra - red spectroscopy in the study of adsorption has recently become popular (320 - 323). This technique has the advantage of enabling physical adsorption to be studied in terms of the subtle stretching of certain bonds, which occurs during the process. There are certain problems with the examination of solid substances by infra - red, with a view to studying adsorption, concerning the possible interaction between the adsorbate and adsorbent which might occur as a result of the preparation. This has been obviated in these studies by the use of a control of mixtures of fatty acids and the disodium fluorescein in which interactions of the type observed in the coated powders might be expected to occur if the preparation had a significant effect on the results obtained. The ESCA experiments have been carried out at the limit of its sensitivity. The absence of a high molecular weight atom in the disodium fluorescein or fatty acid molecules makes the ESCA examination more complicated

Figure 4.2 : The structure of phosphotidylcholine and its precursor phosphorylcholine. (326)

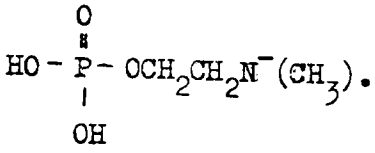

Phosphorylcholine

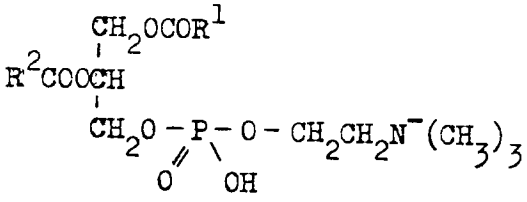

Phosphotidylcholine

since all the data on the detectable atoms must be combined to put together a coherent explanation of what is being observed. An easier approach would be to include a high molecular weight atom, as a label, in the fatty acid molecule for example. A halogen, such as bromine would be ideal. This would however mean completely reanalysing the adsorption system which would undoubtedly be influenced by the presence of such an atom.

It has already been suggested that the choice of pharmaceutical aerosol for this type of coating preparation would be either a beta - adrenergic agonist or cromolyn sodium, a mast cell membrane stabiliser. The coating material of choice would not however be a fatty acid as these have been implicated in pulmonary oedema (324). It would not be advisable to adopt a compound which is likely to bind strongly or even completely chemically react with the adsorbent since this may have both therapeutic and toxicologic implications for the action of the compound involved. Phospholipids have been administered to infants suffering with respiratory distress syndrome with the result that the symptoms of this disease were alleviated (325). Phospholipids may therefore be used in any formulation for delivery to the respiratory tract. The formation of liposomes (226) by these compounds in apolar solvents may however preclude a coating procedure such as that described in these studies. The nature of the phospholipid molecule , figure 4.2, being composed of three chains with a glycerol moiety linking them makes their interaction, to form liposomes in an apolar medium very likely. A phospholipid precursor such as phosphorylcholine may however carry the benefits of not being as interactive in apolar solvent, not being a hazard by inhalation and readily adapted to the coating procedure adopted in these studies.

4.2 Conclusion.

The aim of this project was to coat a model hygroscopic aerosol powder with a substance thought capable of influencing the hygroscopic nature of the powder and to generate this as an aerosol, under ambient conditions and 97 % relative humidity at 37 °C, to establish the effects of the coating on deposition.

Some difficulty was encountered in designing experimental coating procedures and in employing techniques for the characterisation of powders bearing in mind the purpose for which they were being coated and the nature of the model aerosol powder. The model hygroscopic aerosol powder selected was disodium fluorescein. The solvent from which the coating was to take place had to be capable of dissolving the coating material whilst having no similar effect on the model powder. Preliminary experiments indicated that aliphatic alcohols might be appropriate coating materials, however their liquid state would lead to the aggregation of aerosol particles in the reservoir of the aerosol generator. The nature and extent of the coating with two fatty acids was examined by quantitative and qualitative techniques. It would be difficult to envisage extrapolation of these experiments to a range of fatty acids however since longer chain fatty acids might be expected to bring about significant aggregation of the particles in the powder and thus influence their generation as aerosols.

The advantages of deposition in the lower respiratory airways of certain pharmaceutical compounds has been emphasised. Observations concerning the improved deposition in these airways due to hygroscopic growth, have been discussed. The reduction in growth observed in these experiments, it has been suggested, might result in further improvements in deposition in the lower respiratory tract, a possibility which has significant implications in terms of optimising the

therapeutic effect. Finally the subjects which might benefit from this formulation procedure have been indicated. Further work to improve the data base on the behaviour of the model aerosol powder has been suggested. Ultimately an in vivo investigation of the potential of this work should be considered. The work carried out in these studies may be linked to in vivo experiments by the performance of appropriate dissolution experiments as a preliminary measure of the effect of this parameter on bioavailability. The two approaches to the in vivo experiment are the systemic bioavailability, pharmacokinetic, studies or pharmacologic investigations. In the latter case an agent exhibiting pharmacologic activity in the lung, rather than the model aerosol powder used in these studies, would have to be formulated prior to the investigations.

C H A P T E R F I V E

Pulmonary ventilation studies using a simple radioaerosol generator and delivery system.

5. Pulmonary ventilation studies using a simple radioaerosol generator and delivery system.

5.1 Introduction.

The purpose of the lung is the gaseous exchange between atmospheric air and the circulatory system, resulting in the uptake of oxygen and elimination of carbon dioxide and water vapour. In studies of lung function there are two general causes for the reduction in efficiency of gaseous exchange, as symptoms of disease states. Firstly there may be a cardiovascular problem resulting in the reduction of blood flow, as for example in the case of a pulmonary embolism. The reduction of blood flow results in reduced gaseous exchange. Secondly a change in the airway calibre may occur which reduces the efficiency of gaseous exchange. Chronic obstructive lung disease is an example of the reduction of airway calibre. In order to differentiate between the two causes of reduced or inefficient gaseous exchange the technique of lung perfusion with a radiolabelled compound may be complemented with lung ventilation studies using either radioactive gas or radiolabelled aerosol. The lung may be imaged using a detector device appropriate to the type of radiation emitted by the source substance. Perfusion studies with MAA - ^{99m}Tc (Macro - Aggregated Albumin, $t_{1/2}$ 6 h., E 140 KeV) have been complemented by the use of different gases, for example ^{133}Xe (5.28 d 81 KeV), ^{127}Xe (36.4 d, 172 and 203 KeV), ^{81m}Kr (13 s, 191 KeV). There are several reasons for investigating the use of radiolabelled aerosols in lung ventilation studies, as an alternative to the use of gases. Firstly there is no ideal gas for radioisotope ventilation studies. ^{81m}Kr has a short parent half life and is expensive, whereas ^{133}Xe has a long half life and low energy emission. Secondly radioactive gases are not easily obtained for diagnostic purposes. Finally since ^{99m}Tc

is readily available and valid direct comparisons between an aerosol containing this radioisotope and that used in the perfusion studies may be carried out, attempts have been made to use this isotope with a carrier, for example diethylene triamine pentacetic acid (DTPA), as an aerosol for lung ventilation studies.

Deposition of aerosol particles in different regions of the lung is dependent on the particle size and distribution of the aerosol being considered (112,156 - 161). Radioaerosol particles of about 1um diameter are reported to produce a similar distribution compared with the radioactive gases (327). As a result of this observation much work (328 - 335) has been carried out into the production of aerosol particles suitable for ventilation studies.

As part of a project, carried out in conjunction with the Nuclear Physics Department of Dudley Road Hospital, Birmingham, to investigate the optimum conditions for use of a novel simple reusable radioaerosol generator, a comparison of the particle size distribution of aerosols produced by this device with the results of the clinical use of these diagnostic aerosols was carried out.

5.2 Materials and Methods.

5.2.1 Construction of the radioaerosol generator and delivery system.

The details of the aerosol generator and delivery system are shown in Figure 5.1 a and b respectively. The generator was constructed from a perspex rod. The solution was contained at the bottom of a centrally drilled blind hole of such dimensions that approximately 2.5 ml of solution brought its meniscus to the central axis of a disc through which compressed air was introduced. The disc, which is replaceable,

has a divergent outlet in order to spread the air stream. This ensures direct impinging of the air on to the surface of the solution even when the volume falls below 2.5 ml. Several discs were constructed with different internal diameters to vary the velocity of the air stream. The multi - stage separator, also constructed from perspex, was connected to the outlet side of the generator. This device separates larger diameter droplets from the airstream. Droplets deposited on the various stages fall back to the reservoir under gravity. The generator was housed inside a lead container (6 mm wall thickness) to minimise radiation from high activity solution.

The delivery system is illustrated in Figure 5.1 b . The patient breathed aerosol through a mouthpiece connected to a non - returnable two - way Ambu valve (1). The expiratory side of this valve was connected to a paper filter to trap the exhaled particles. Operation of valve (2) connected the patient either to the aerosol supply or room air and allowed familiarisation with breathing technique before the test. Valve (3) opened only when the patient tidal breathing exceeded the total capacity of the system. A collapsible rubber bag was used as a small reservoir to supplement the constant supply of the aerosol particles and was filled shortly before the test. Apart from valves (1) and (2) the whole system was housed inside a lead shielded (3 mm thickness) box with a lead glass window at the top to allow inspection of the bag functioning. The whole system was mounted on a trolley for ease of mobility.

5.2.2 Particle size determination.

The aerosol particle size distribution was determined using a calibrated cascade impactor, Delron Model DCI - 6. ^{99m}Tc - DTPA solution of approximate concentration 17 M Bq/ml was used in the

generator during these experiments. A compressed air cylinder was used to supply air at a flow rate of 8 $Lmin^{-1}$ and the particle stream was drawn through the impactor by means of a vacuum pump at a constant flow rate of 12.5 $Lmin^{-1}$ for a period of 1.5 minutes. Several jet sizes were obtained using different discs in the generator. The particles were collected on silicone fluid coated glass slides (307) at the six stages of the impactor and finally on a glass fibre filter. The calibrated cut off values, representing 50 % collection efficiency, for the aerodynamic diameter at each stage range from 11.2 µm at stage one to 0.2 µm at the filter (214,252,308). The distribution of the aerosol was expressed in terms of the percentage of the total radioactivity measured on each of the glass slides and the filter. This radioactivity was measured with a precalibrated 100 mm NaI(TI) detector system. The activity median aerodynamic diameter (AMAD) and the geometric standard deviation (σg) which describe the distribution of the aerosols were estimated using a data inversion method for particle sizing (308,309).

5.2.3 Patient Study.

During these studies the generator was loaded with 2.5 ml ^{99m}Tc - DTPA solution at a concentration of approximately 370 M Bq/ml and the aerosol was produced using an air flow rate of approximatley 8 $Lmin^{-1}$. After the initial familiarisation, the patient breathed aerosol through a mouthpiece, Figure 5.1 b, continuously from the system. A large field of view camera (IGE 535) fitted with a LEGP collimator was used to record the build up of the activity in the lungs and the breathing in process was continued until a count rate of approximately 2.5 Ks^{-1} was obtained. A count rate of this magnitude was found satisfactory to take four ventilation images, each of 200 K counts, within 20 minutes. from the end of the breathing in period and did not adversely effect

the perfusion images taken shortly afterwards. ^{81m}Kr ventilation and ^{99m}Tc - MAA perfusion images were then taken and compared with those of aerosol ventilation.

5.3 Results and Discussion.

The particle size distribution of ^{99m}Tc - DTPA aerosol with different jet sizes is shown in Figure 5.2. It can be seen that the distribution is skewed to the right with increasing jet size. From this distribution it can be calculated that with 0.38 mm jet size about 96 % of particles have an activity median diameter of less than 2 μm compared with only 70 % produced by the 0.68 mm diameter jet. The AMAD values and the geometric standard deviation for different jet sizes are also quoted in this diagram. It can be seen that the AMAD values increase with jet size. The geometric standard deviation in these distributions was approximately 1.5 .

As a result of these observations the 0.38 mm diameter jet was used for the production of aerosols for delivery to 16 patients over a period of 2 months. It was found that 2,5 ml ^{99m}Tc - DTPA solution in the generator was sufficient for up to four patient studies. The patient compliance was very good and all patients could breathe through the apparatus. The aerosol breathing in period to achieve a count rate of about 2.5 Ks^{-1} varied between 1.5 minutes and 3 minutes with an average value of 1.8 - 0.38 minutes. This is a two to four fold improvement compared with previous reports using different types of aerosols (336 - 338) in which the breathing period varied from five to ten minutes. Images obtained from a patient are shown in Figure 5.3 a, b and c. The quality of the aerosol images was excellent and comparable to that obtained with ^{81}Kr gas. Furthermore, there was no adverse effect of the deposition of radioaerosol on the perfusion images.

Figure 5,1: a, Details of construction of the aerosol generator and, b, that of the delivery system.

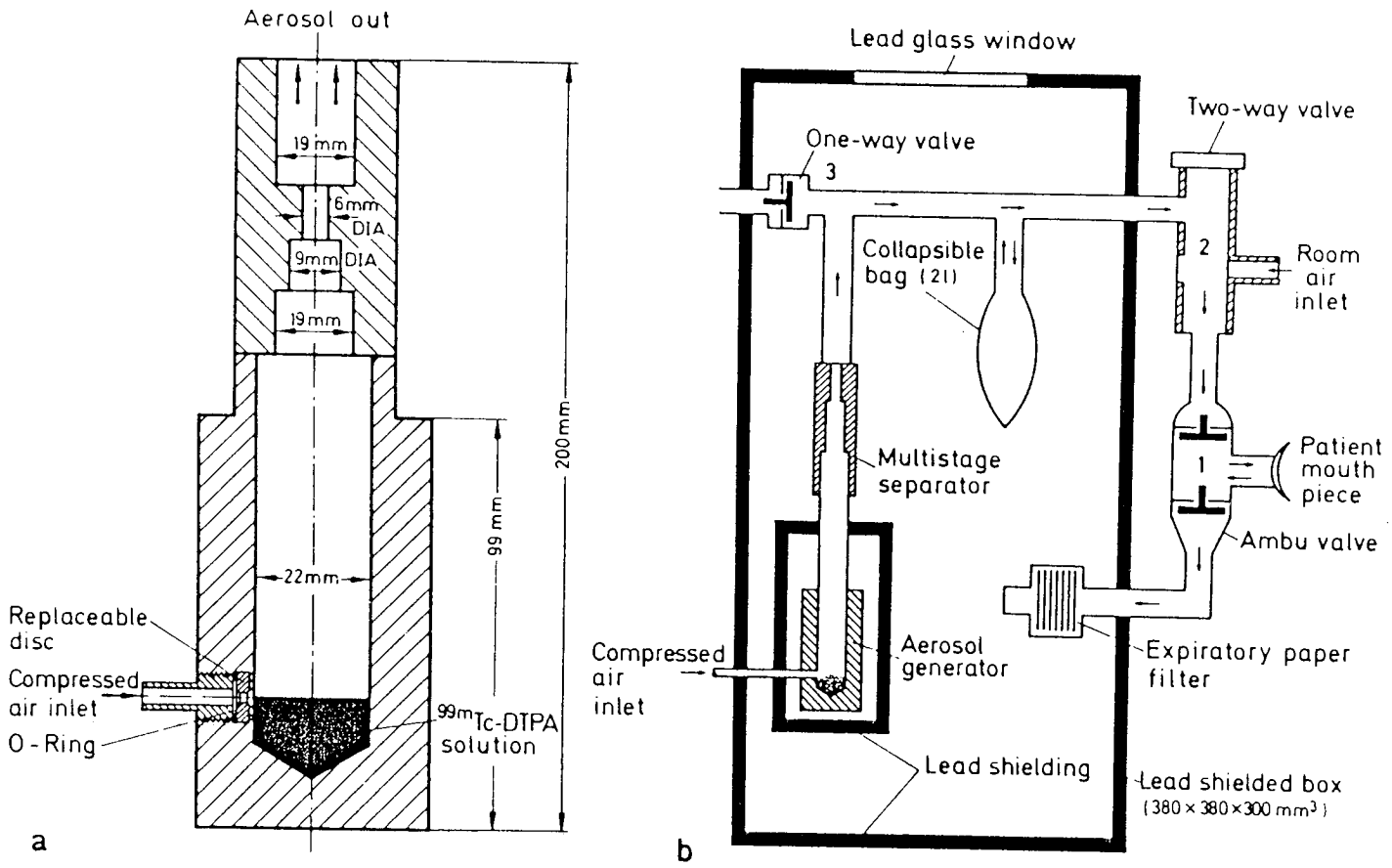

Figure 5,2 : Particle size distribution for different jet sizes. The activity median diameter (AMAD) and the geometric standard deviation (σg) are given for each distribution.

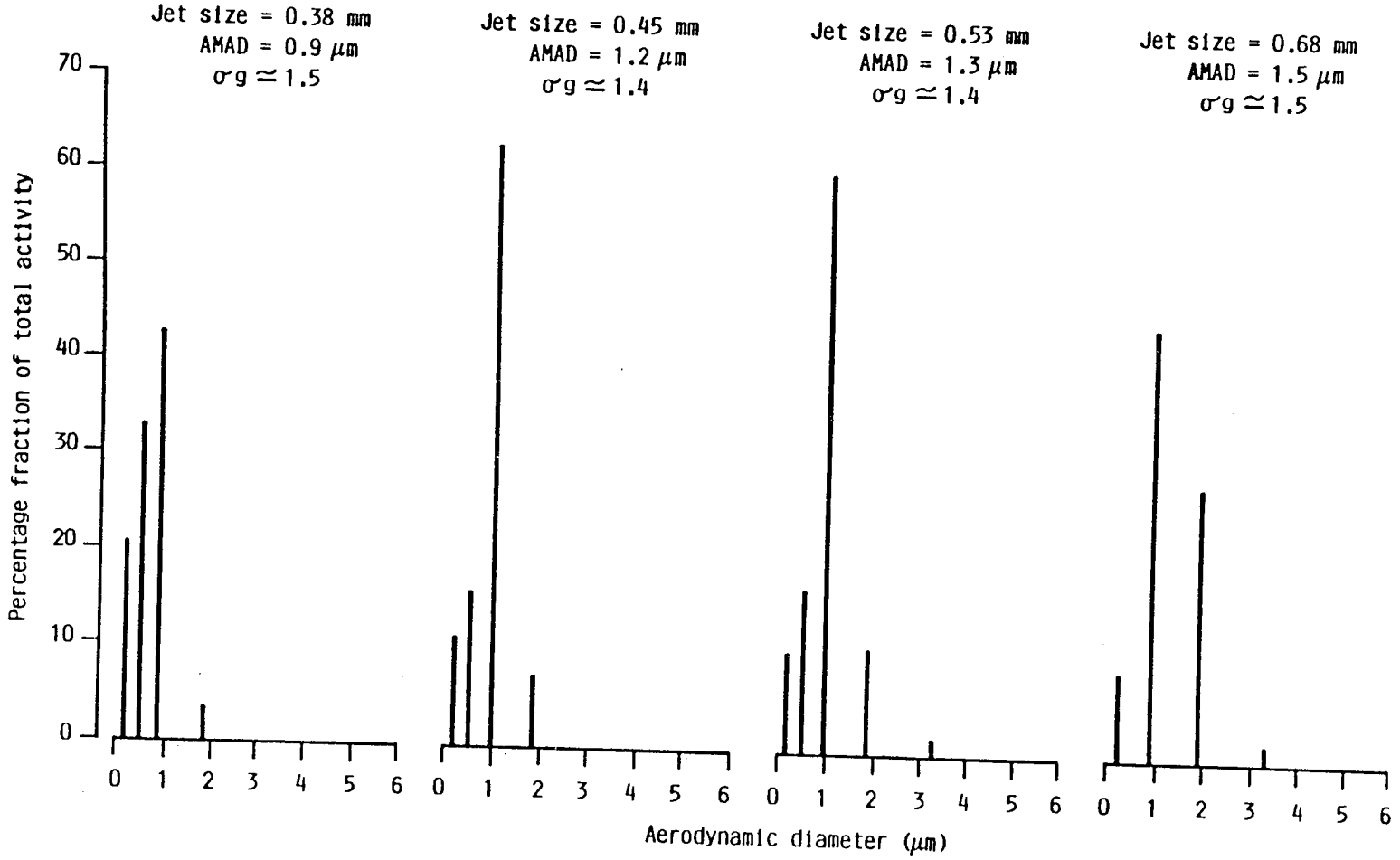

Figure 5,3 : a, A typical posterior lung ventilation image (200 K counts) obtained with ^{99m}Tc - DTPA aerosol, b, that with ^{81m}Kr gas (400K counts) and c, ^{99m}Tc - MAA perfusion image (400K counts)

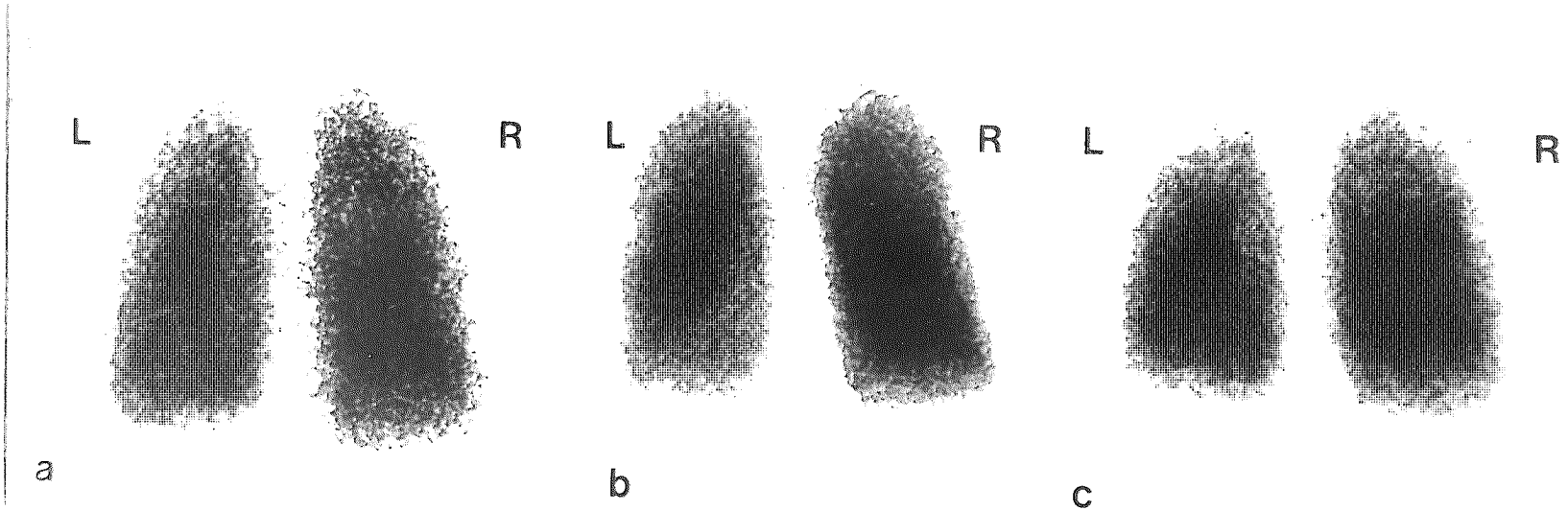

Experiments in which particle size determinations have been used to assess the output of diagnostic aerosol generators, of which those reported here are examples, have shown that this is an aid to the design of these devices with respect to optimising their clinical efficiency. It must be emphasised however that the method of particle sizing employed in these investigations may only be used as a guide to the best design since particles in the size range observed are near the limit of accuracy of the apparatus.

LIST OF SYMBOLS

Symbol	Expression
a	Lateral interaction energy.
A	Area meter coefficient.
a_m	Amount of powder derivitised for GLC.
a_s	Amount of surfactant detected by GLC.
a_w	Water activity.
b'	Adsorption variable, function of interaction energy.
b	Adsorption variable, function of energy of adsorption site.
B	Area meter coefficient.
$C(\ )$	Cunningham's slip factor.
C	Equilibrium concentration.
C_{ads}	Adsorbed amount.
C_I	Initial concentration.
$C(y)$	Concentration of element at depth y.
C_{1s}	Carbon electron from 1s orbital.
d'	Airway diameter
d	Diameter of the particle
D_{ae}	Aerodynamic equivalent diameter.
D_e	Equivalent volume diameter.
Δd	Slit image displacement.
d_1 , d_2	Differential refractometric measurement of slit image.

Symbol	Expression
d''	Depth of overlayer.
Δd_{eq}	Equilibrium concentration slit image displacement.
Δd_{In}	Initial concentration slit image displacement
D_l	Equilibrium droplet diameter.
E_k	Kinetic energy.
E_b	Binding energy.
ΔE	Interaction energy at solute/solvent boundary.
e^-	Electron.
F	Force, Nm^{-1}.
F_l	X - ray flux.
g	Acceleration due to gravity.
g_s	Mass fraction of particle in equilibrium droplet.
Δh	Pressure difference on the manometer.
h	Area of polar head group.
H	Relative humidity
h	Photon energy
I	Intensity of photoelectron peak.
K	Boltzmann's constant.
K_l	Calibration constant for a selected wavelength

Symbol	Expression
m_p	Mass of dry particle.
$m_{w,l}$	Mass of water in the aerosol particle in the lung.
m	Sample weight.
M_w	Molecular weight.
M_s	Molecular weight of solid in droplet.
N	number in sample population.
Δn	Refractive index difference.
N_A	Avogadro's number.
Na_{ls}	Sodium electron from ls orbital.
Na_{Aug}	Sodium Auger electron.
n_w, n_s	Number of water and solid molecules in solution.
O_{ls}	Oxygen electron from ls orbital.
P	Partial vapour pressure.
P_0	Saturation vapour pressure.
P'	Droplet vapour pressure.
Q	Energy of adsorption site.
$\bar{r}$	Arithmetic mean radius of particle.
r	Radius of sphere.
r_i	Individual particle radius.

Symbol	Expression
$\bar{r}_g$	Geometric mean radius of particle.
$\bar{r}_g v$	Median radius.
R'	Growth ratio.
R_a	Dynamic growth ratio.
R	Relative humidity at the droplet surface.
S_d	Stopping distance.
S	Number of adsorption sites.
S_g	Specific surface area.
s_m	Surface area occupied by one molecule.
S'	Factor of transmission of the analyser.
s	Analysed area.
T	Absolute temperature.
t	Time
t_l	Area of hydrocarbon tails.
X	Cross section of the photoelectron.
z	Number of neighbouring molecules.

Greek Symbols.

α	Ratio of standard deviation to arithmetic mean radius.

Symbol	Expression
γ_{hs}, γ_{ts}	Interaction energies per unit area between head groups and solvent and tails and the solvent
η	Viscosity at 20 C and one atmosphere.
γ	Surface free energy.
λ	Mean free path.
κ	Shape factor.
ϕ	Spectrometer work function
ρ_p	Particle density.
ρ_g	Density of air.
ρ_l	Density of particle in the lung.
ρ	Powder density.
σ	Arithmetic standard deviation.
σ	Geometric standard deviation.
θ	Monolayer coverage of the surface.
θ_l	Angle of scatter.
ν	Constant velocity of movement when g is balanced by F.
ν_{TS}	Terminal settling velocity.

REFERENCES

1. Shaw, D.J., 1980 ,
in Introduction to Colloid and Surface Chemistry, Third Edition, Butterworths, London and Boston

2. Hatch, T.F., and Gross, P., 1964 ,
in Pulmonary Deposition and Retention of Inhaled Aerosols, Academic Press, New York and London

3. Lourenco, R.V., 1982 ,
Clinical Aerosols II. Therapeutic aerosols.
Arch. Intern. Med.,142, 2299 -2306.

4. Clarke, S.W., and Newman, S.P., 1984 ,
Therapeutic aerosols 2 - Drugs available by the inhaled route.
Thorax, 39, 1, 1 - 7.

5. Rau, J.L., 1984 ,
in Respiratory Therapy Pharmacology, Second Edition, Year Book Medical Publishers Inc., Chicago

6. Barnes, P.J., 1984 ,
The third nervous system in the lung : physiology and clinical perspectives. Thorax, 39, 8, 561 - 7.

7. Nadel, J.A. and Barnes, P.J., 1984 ,
Autonomic regulation of the airways.
Ann. Rev. Med., 35, 451 - 467.

8. Davis, C., Kannan, M.S., Jones, T.R., and Daniel, E.E., 1982 , Control of human airway smooth muscle : in vitro studies. J. Appl. Physiol., 53, 1080 - 87.

9. Zaagsma, J., van der Heijden, P.J.C.M., van der Schaar, M.W.G., and Bank, C.M.C., 1983 , Comparison of functional beta - adrenoceptor heterogeneity in central and peripheral airway smooth-muscle of guinea pig and man. J. Recept. Res.,3, 89 - 106.

10. Persson, C.G.A., Ejefalt, I., Grega, G.J. and Svensjo, E., 1982 , The role of beta receptor agonists in the inhibition of pulmonary edema. Ann. N.Y. Acad. Sci., 384, 544 - 556.

11. Nadel, J.A., Widdicombe, J.H., Peatfield, A.C., 1983 , Regulation of airway secretions in Handbook of Physiology

12 Phipps, R.J., Williams, I.P., Richardson, P.S., Pell, J., Pack, R.J., and Wright, N., 1982 , Sympathomimetic drugs stimulate the output of secretory glycoproteins from human bronchii in vitro. Clin. Sci., 63, 23 - 28.

13. Morganroth, M.L., Reeves, J.T., Murphy, R.C., and Voelkel, N.F., 1984, Leukotriene synthesis and receptor blockers block hypoxic pulmonary vasoconstriction. J. Appl. Physiol., 56, 5, 1340 - 1346

14. Barnes, N.C., Piper, P.J. and Costello, J.F., 1984 , Comparative effects of inhaled leukotriene C_4, leukotriene D_4

and histamine in normal human subjects. Thorax, 39, 7, 500 - 504.

15. Davidson, A.B., McFadden, E.R., Drazen, J.M., Lee, T.H., Austen, K.F., and Corey, E.J., 1984 , Bronchoconstrictor effects of leukotriene E in normal adults. Am. Rev. Resp. Dis., Annual Meeting Supplement, A1.

16. Lamm, W.J.E., Lai, Y - L, and Hildebrandt, J., 1984 , Histamine and leukotrienes mediate pulmonary hypersensitivity to antigen in guinea pigs. J. Appl. Physiol., 56, 4, 1032 - 1038.

17. Fish, J.E., Jameson, L.S., Albright, A., and Norman, P.S., 1984 , Modulation of bronchomotor effects of chemical mediators by PGF$_{\alpha}$. Am. Rev. Resp. Dis., Annual Meeting Supplement, A2.

18. Godard, P., Damon, M., Chavis, C., Bognie, M., Crates de Paulet, A., and Michel, F.B., 1984, Arachidonic acid metabolism in alveolar macrophages: comparison of cells from healthy subjects, patients with chronic bronchitis and allergic asthma patients. Am. Rev. Resp. Dis., Annual Meeting Supplement, A1.

19. Barnes, P.J., Ind, P.W., and Dollery, C.T., 1983 , Beta adrenoceptors in asthma and their response to agonists. In Asthma III ed K.F. Austen, L.M. Lichtenstein and A.B. Kay, Academic Press, New York

20 Hoffman, B,B., and Lefkowitz, R.J., 1980 , Alpha - adrenergic receptor subtypes. N. Engl. J. Med., 302, 1390 - 96.

21. Richardson, J., and Beland, J., 1976 ,
Nonadrenergic inhibitory nervous system in human airways.
J. Appl. Physiol., 41, 764 - 771.

22. Partanen, M., Laitinen, A., Hervonen, A., Toivanen, M., and Laitinen, L.A., 1982 , Catecholamine - and acetylcholinesterase - containing nerves in human lower respiratory tract.
Histochemistry, 76, 175 - 188.

23. Sheppard, M.N., Kurian, S.S., Kenzen Logmans, S.C., Michetti, F., and Cocchia, D., 1983 , Neuron specific enolase and S - 100. New markers for delineating the innervation of the respiratory tract in man and other animals. Thorax, 38, 333 - 340.

24. Ind, P.W., Scriven, A.J.I., and Dollery, C.T., 1983 ,
Use of tyramine to probe pulmonary noradrenaline release in asthma.
Clin. Sci., 64, 9P.

25. Baker, D.J., 1982 ,
Cholinergic neurotransmission in airway ganglia : inhibition by norepinephrine. Physiologist, 25, 225.

26. Barnes, P.J., 1983 ,
Endogenous plasma adrenaline in asthma.
Eur. J. Resp. Dis., 64, 8, 559 - 563.

27. Silverberg, A.B., Shah, S.D., Haymond, M.W., and Cryer, P.E., 1978,
Norepinephrine : hormone and neurotransmitter in man.
Am. J. Physiol., 234, 252 - 256.

28. Fitzgerald, G.A. Barnes, P., Hamilton, C.A., and Dollery, C.T., 1980, Circulating adrenaline and blood pressure : the metabolic effects and kinetics of infused adrenaline in man. Eur. J. Clin. Invest., 10 , 401 - 406.

29. Warren, J.B., and Dalton, N., 1983 , A comparison of the bronchodilator and vasopressor effects of exercise levels of adrenaline in man. Clin. Sci., 64, 475 - 479.

30. Tattersfield, A.E., Leaver, D.G., and Pride, N.B., 1973 , Effects of beta - adrenergic blockade and stimulation on normal human airways. J. Appl. Physiol., 35, 613 - 619.

31. Townley, R.G., McGeady, S., and Bewtra, A., 1976 , The effect of beta - adrenergic blockade on bronchial sensitivity to acetyl - beta - methacholine in normal and allergic rhinitis subjects. J. Allergy Clin. Immunol., 57, 358 - 366.

32. McNeill, R.S., and Ingram, C.G., 1966 , Effect of propranolol on ventilatory function. Am. J. Cardiol., 18, 473 - 475.

33. Zaid, G., and Beall, G.N., 1966 , Bronchial response to beta - adrenergic blockade. N. Engl. J. Med., 275, 580 - 584.

34. Barnes, P.J., Basbaum, C.B., Nadel, J.A., and Roberts, J.M., 1982, Localization of beta - adrenoceptors in mammalian lung by

microscopic autoradiography. Nature , 299 , 444 - 447.

35. Barnes, P.J., Basbaum, C.B. and Nadel, J.A., 1983 , Autoradiographic localization of autonomic receptors in airway smooth muscle : marked differences between large and small airways. Am. Rev. Resp. Dis., 127, 758 - 762.

36. Lofdahl, C - G, Svedmyr, N., 1982 , Effects of prenalterol in asthmatic patients. Eur. J. Clin. Pharmacol., 23, 297 - 303.

37. Assem, E.S.K., and Schild, H.O., 1969 , Beta - adrenergic receptors concerned with anaphylactic mechanism. Arch. Allergy, 45, 62 - 69.

38. Orange, R.P., Kaliner, M.A., Laraia, P.J., and Austen, K.F., 1971, Immunological release of histamine and slow reacting substance of anaphylaxis from human lung. II Influence of cellular levels of cyclic AMP. Fed. Proc., 30, 1725 - 1729.

39. Butchers, P.R., Skidmore, I.F., Vardey, C.J., and Wheeldon, A., 1980, Characterisation of the receptor mediating antianaphylactic effects of beta adrenoceptor agonists in human lung tissues in vitro. Br. J. Pharmacol., 71, 663 - 667.

40. Peters, S.P., Schulman, E.S., Schleimer, R.P., MacGlashan, D.W., Newball, H.H., and Lichtenstein, L.M., 1982 , Dispersed human lung mast cells. Pharmacologic aspects and comparison with human lung tissue fragments. Am. Rev. Resp. Dis., 126, 1034 - 1039.

41. Vermeire, P.A., Vanhoutte, P.M., 1979 ,
Inhibitory effects of catecholamines in isolated canine bronchial smooth muscle. J. Appl. Physiol., 46, 787 - 791.

42. Simonsson, B.G., Svedmyr, N., Skoogh, B.E., Andersson, R., and Bergh, W.D., 1972 , In vivo and in vitro studies on alpha receptors in human airways. Potentiation with bacterial endotoxin. Scand. J. Resp. Dis., 53, 227 - 236.

43. Kneussl, M.P., and Richardson, J.B., 1978 ,
Alpha adrenergic receptors in human and canine tracheal and bronchial smooth muscle. J. Appl. Physiol., 45, 307 - 311.

44. Hoffman, B.B., and Lefkowitz, R.J., 1980 ,
Alpha - adrenergic receptor subtypes.
N. Engl. J. Med., 302, 1390 - 1396.

45. Leff, A., and Munoz, N.M., 1981 ,
Evidence for two distinct subtypes of alpha - adrenergic receptors in canine airways. J. Pharmacol. Exp. Ther., 270, 530 - 535.

46. Black, J., Turner, A., and Shaw, J., 1981 ,
Alpha - adrenoceptors in human peripheral lung.
Eur. J. Pharmacol., 72, 83 - 86.

47. Barnes, P.J., Skoogh, B.E., Nadel, J.A., and Roberts, J.M., 1983 ,
Postsynaptic alpha - adrenoceptors in canine tracheal smooth muscle and mediate neuronal and hormonal alpha - adrenergic

contraction. Mol. Pharmacol., 23, 570 - 575.

48. Kaliner, M., Orange, R.P., and Austen, K.F., 1972 ,
Immunological release of histamine and slow reacting substance of anaphylaxis from human lung. IV Enhancement by cholinergic and alpha - adrenergic stimulation. J. Exp. Med., 136, 556 - 567.

49. Richardson, J.B., 1979 ,
State of the art. Nerve supply to the lungs.
Am. Rev. Resp. Dis., 119, 785 - 802.

50. Nadel, J.A., 1980 ,
Autonomic regulation of airway smooth muscle. In Physiology and Pharmacology of the Airways, ed. J.A. Nadel, Dekker, New York, 215 - 257.

51. Marlas, C., Nadel, J.A., and Roberts, J.M., 1982 ,
The muscarinic receptors of airway smooth muscle : their characterization in vitro. J. Appl. Physiol., 52, 1084 - 1091.

52. Cheng, J.B., Townley, R.G., 1982 ,
Comparison of muscarinic and beta - adrenergic receptors between bovine peripheral lung and tracheal smooth muscles. A striking difference. Life Sci., 30, 2079 - 2086.

53. Barnes, P.J., Nadel, J.A., Roberts, J.M., and Basbaum, C.B., 1983,
Muscarinic receptors in lung and trachea : autoradiographic localization using ^{3}quinuclidinyl benzilate.
Eur. J. Pharmacol., 86, 103 - 106.

54. Basbaum, C.B., Barnes, P.J., Grillo, M.A., Widdicombe, J.H., and Nadel, J.A., 1983 , Adrenergic and cholinergic receptors in submucosal glands of the ferret trachea : autoradiographic localization. Eur. J. Resp. Dis., Suppl., 128, 433 - 435.

55. Frigo, G.M., del Tacca, M., Lechlini, S., and Crema, A., 1973 , Some observations on the intrinsic nervous system in Hirschsprung's disease. Gut, 14, 35 - 40

56. Richardson, J.B., 1981 , Nonadrenergic inhibitory innervation of the lung. Lung, 159, 315 - 322.

57. Richardson, J.B., and Bouchard, T., 1975 , Demonstration of a non - adrenergic inhibitory nervous system in the trachea of the guinea pig. J. Allergy Clin. Immunol., 56, 473 - 476.

58. Hoyes, A.D., and Barber, P., 1981 , Morphology and response to vagus nerve section of the intraepithelial axons of the rat trachea. A quantitative ultrastructural study. J. Anat., 132, 331 - 339.

59. Ghatei, M.A., Sheppard, N., O'Shaughnessy, D.J., Adrian, T.E. and McGregor, G.P., 1982 , Regulatory peptides in the mammalian respiratory tract. Endocrinology,111, 1248 - 1254.

60. Kitamura, S., Ishihara, Y., and Said, S.I., 1980 ,

Effect of VIP,phenoxybenzamine and prednisolone on cyclic nucleotide content of isolated guinea pig lung and trachea. Eur. J. Pharmacol., 67, 219 - 223.

61. Said, S.I., 1982 ,
Vasoactive peptide in the lung, with special reference to vasoactive intestinal peptide. Exp. Lung Res., 3 , 343 - 348.

62. Stainforth, J.N., Lewis, R.A., and Tattersfield, A.E., 1983 ,
Dosage and delivery of nebulised beta - agonists in hospital. Thorax, 38, 751 - 754.

63. Bierman, C.W., Shapiro, G.G., Pierson, W.E.,and Dorsett, C.S., 1977 , Acute and chronic theophylline therapy in exercise - induced bronchospasm.
Pediatrics, 60, 845 - 849.

64. Pavia, D., Bateman, J.R.H, Sheahan, N.F., 1980 ,
Clearance of lung secretions in patients with chronic bronchitis: Effect of terbutaline and ipratropium bromide aerosols.
Eur. J. Resp. Dis., 61, 245 - 253.

65. Burnstock, G., 1981 ,
Neurotransmitters and trophic factors in the autonomic nervous system. J. Physiol., 313, 1 - 35.

66. Irvin, C.G., Bodeau, R., Tremblay, J., Martin, R.P., and Macklem, P.T., 1980 , Bronchodilation : noncholinergic, nonadrenergic mediation demonstrated in vivo in the cat. Science, 207, 791 - 792.

67. Sheard, P., Killingback, P.G., and Blair, A.M., 1967 ,
Antigen induced release of histamine and SRS - A from human lung passively sensitised with reaginic serum.
Nature, 216, 283 - 284.

68. Cox, G.S., 1967 ,
Disodium cromoglycate (FPL 670)(Intal): A specific inhibitor of reaginic antibody - antigen mechanisms.
Nature, 216, 1328 - 1329.

69. Sullivan, T.Y., and Yu, P - L, 1983 ,
Airway anaesthesic effects on hypercapnic breathing patterns in humans. J. Appl. Physiol., 55, 2, 368 - 376.

70. Gal, T.J., 1980 ,
Airway response in normal subjects following topical anaesthesia with ultrasonic aerosols of 4% lidocaine.
Anaesth. Analg. Cleveland, 59, 123 - 129.

71. Jain, S.K., 1975 ,
The effect of inhalation surface anaesthesia of the lungs on respiratory reflexes : Astudy in different species. Ph. D. Thesis, University of London, London.

72. Weiss, E.B., Anderson, W.H., and O'Brien, K.P., 1975 ,
The effect of a local anaesthetic, lidocaine, guinea pig trachealis muscle in vitro. Am. Rev. Resp. Dis., 112, 393 - 400.

73. Weiss, E.B., and Patwardhan, A.V., 1977 ,
The response to lidocaine in bronchial asthma.
Chest, 72, 429 - 438.

74. Williams, M.H. Jr. , 1974 ,
Steroid and antibiotic aerosols.
Am. Rev. Resp. Dis., 110, 6, 122 - 128.

75. Eisenberg, R.S., and Oatway, W.H., 1971 ,
Nebulization of amphoteracin B.
Am. Rev. Resp. Dis., 103, 289 - 292

76. Oehling, A., Giron, M., and Subira, M., 1975 ,
Aerosol chemotherapy in bronchopulmonary candidiasis.
Respiration, 32, 179 - 184

77. Foster, W.M., Bergofsky, E.H., Bohning, D.E., Lippman, M.,
and Albert, R.E., 1976 , Effect of adrenergic agents and their
mode of action on mucociliary clearance in man.
J. Appl. Physiol., 41, 2, 146 - 152.

78. Lieberman, J., 1968 ,
Measurement of sputum viscosity in a cone - plate viscometer :
II an evaluation of mucolytic agents in vitro.
Am. Rev. Resp. Dis., 97,662 - 672.

79. Hirsch, S.R., Zastrow, J.E., and Kory, R.C., 1969 ,

Sputum liquefying agents : A comparative in vitro evaluation. J. Lab. Clin. Med., 74, 346 - 353.

80. Pavia, D., Thomson, M.L., and Clarke, S.W., 1978 , Enhanced clearance of secretions from the human lung after the administration of hypertonic saline aerosols. Am. Rev. Resp. Dis. 117, 199 - 203.

81. Wolfsdorf, J., Swift, D.L., and Avery, M.E., 1969 , Mist therapy reconsidered : An evaluation of the respiratory deposition of labelled water aerosols produced by jet and ultrasonic nebulizers. Pediatrics, 43, 799 - 808.

82. Asmundssen, T., Lohnson, R.F., and Kilburn, K.H., 1973 , Efficiency of nebulizers for depositing saline in human lung. Am. Rev. Resp. Dis., 108, 506 - 512.

83. Chang, N., Levison, H., and Cunningham, K., 1973 , An evaluation of nightly mist tent therapy for patients with cystic fibrosis. Am. Rev. Resp. Dis., 107, 672 - 675.

84. Barker, R., and Levison, H., 1972 , Effects of ultrasonically nebulised distilled water on airway dynamics in children with cystic fibrosis and asthma. J. Pediatr., 80, 396 - 400.

85. Bureau, M.A., McDougall, D.M., Beaudry, P.H., 1978 , Late effect of nocturnal mist tent therapy related to the severity of airway obstruction in children with cystic fibrosis.

Pediatrics, 61, 842 - 846.

86. Garner, F.B., Meyer, C.A., White, D.S., 1975 ,
Aerosol BCG treatment of carcinoma metastatic to the lung: A phase 1 study.
Cancer, 35, 1088 - 1094.

87. Cusumano, C.L., Jernigan, J.A., and Waldman, R.H., 1975 ,
Aerosolized BCG treatment of bronchogenic carcinoma : Phase 1 study.
JNCI, 55, 275 - 279.

88. Hegardt, B., Lowhagen, O., Svedmyr, N., and Granerus, G., 1982 ,
The protective proprrty of equipotent bronchodilating doses of inhaled KWD 2131 and terbutaline against allergen - induced bronchospasm. Allergy, 37, 407 - 416.

89. Schultze - Werninghaus, G., 1980 ,
Comparison of standardized skin and provocation tests with RAST and histamine release from leukocytes in bronchial asthma.
Allergy, 35, 259 - 261.

90. Oberdorster, G., Utell, M.J., Weber, D.A., Hyde, R.W., and Morrow, P.E., 1983 , Differential bronchial and alveolar deposition and absorption of ^{99M}Tc - DTPA (Diethylenetriamine pentacetic acid) aerosols. Am. Rev. Resp. Dis., 127, 4, 167.

91. Royston, D., and Minty, B.D., 1983 ,

A cheap simple particle generator system for use with in vivo measurement of alveolar - capillary barrier permeability Am. Rev. Resp. Dis., 127, 4, 319.

92. Malem, H., Ward, M., Henry, D., Smith, W.H.R., and Gonda, I., 1981, Early experience with a vertical spinning disc nebuliser. The Lancet, 664 - 666.

93. Ishfaq, M.M., Ghosh, S.K., Mostafa, A.B., Hesslewood, S.R., Williams, N.R., and Hickey, A.J., 1984 ,
A simple radioaerosol generator and delivery system for pulmonary ventilation studies. Eur. J. Nucl. Med., 9, 141 - 143.

94. Williams, N.R., Ghosh, S.K., Ishfaq, M.M., Mostafa, A.B., Hickey, A., and Hesslewood, S.R., 1984 ,
A simple re - usable radioaerosol system. Eur. J. Nucl. Med.

95. Clay, M.M., Pavia, D., Newman, S.P., and Clarke, S.W., 1983 ,
Factors influencing the size distribution of aerosols from jet nebulisers. Thorax, 38, 755 - 759.

96. Davies, P.J., Amin, K.K., and Mott, G.A., 1980 ,
Particle size of inhalation aerosol systems 1 : Production of homogeneous dispersions. Drug Dev. Ind. Pharm., 6, 6, 645 - 651.

97. Davies, P.J., Amin, K.K., and Mott, G.A., 1980 ,
Particle size of inhalation aerosol systems 2 : Uniformity of delivery of some commercial inhalation aerosol systems.
Drug Dev. Ind. Pharm., 6, 6, 653 - 658.

98. Ellul - Micallef, R., Moren, F., Wetterlin, K., and Hidinger, K.C., 1980, Use of a special inhaler attachment in asthmatic children. Thorax, 35, 620 - 623.

99. Harper, T.B., and Strunk, R.C., 1981 , Techniques of administration of metered aerosolized drugs in asthmatic children. Am. J. Dis. Child., 135, 3, 218 - 221.

100. Hodges, I.G.C., Milner, R.P., and Stokes, G.M., 1981 , Assessment of a new device for delivering aerosol drugs to asthmatic children. Arch. Dis. In. Child., 56, 10, 787 - 788.

101. Orehek, J., Gayrard, P., Grimaud, C.H., and Charpin, J., 1976 , Patient error in use of bronchodilator metered aerosols. B.M.J., i, 76.

102. Paterson, I.C., and Cromton, G.K.,1976 , Use of pressurized aerosols by asthmatic patients. B.M.J., i, 76 - 77.

103. Ruffin, R.E., Kenworthy, M.C., and Newhouse, M.T., 1978 , Response of asthmatic patients to fenoterol inhalation : a method of quantifying the airway bronchodilator dose. Clin. Pharmacol. Ther., 23, 338 - 345.

104. Saunders, K.B., 1965 , Misuse of inhaled bronchodilator agents. B.M.J., i, 1037 - 1038.

105. Newman, S.P., and Clarke, S.W., 1983 ,
Therapeutic aerosols I. Physical and practical considerations.
Thorax, 38, 881 - 886.

106. Newman, S.P., Moren, F., Pavia, D., Corrado, O., and Clarke, S.W., 1982 , The effects of changes in metered volume and propellent vapour pressure on the deposition of pressurised inhalation aerosols. Int. J. Pharmaceutics, 11, 337 - 344.

107. Miller, W.F., 1973 ,
Aerosol therapy in acute and chronic respiratory disease.
Arch. Intern. Med., 131, 148 - 155.

108. Byron, P.R., Davis, S.S. , Bubb, M.D., and Cooper, P., 1977 ,
Pharmaceutical implications of particle growth at high relative humidities. Pestic. Sci., 8, 521 - 526.

109. Gonda, I., and Byron, P.R., 1978 ,
Perspectives on the biopharmacy of inhalation aerosols.
Drug Dev. Ind. Pharm., 4,3, 243 - 259.

110. Raabe, O.G., 1976 ,
Aerosol aerodynamic size conventions for inertial sampler calibration. J. Air Pollut. Control Assoc., 26, 9, 856 - 860.

111. Fuchs, N.A., and Sutugin, A.G., 1966 ,
Generation and use of monodisperse aerosols., in Aerosol Science ed. C.N. Davies, Academic Press, London, 1 - 30.

112. Task Group on Lung Dynamics, 1966 ,
Deposition and retention models for internal dosimetry of the human respiratory tract.
Health Physics, 12, 173 - 207.

113. Landahl, H.D., 1950 ,
On the removal of airborne droplets by the human respiratory tract. I : The lung.
Bull. Math. Biophysics, 12, 43 - 56.

114. Chan, T.L., and Lippmann, M., 1980 ,
Regional deposition of inhaled particles.
Am. Ind. Hyg. Assoc. J., 399.

115. Chan, T.L., Schrenck, R.M., and Lippmann, M., 1980 ,
Effect of the laryngeal jet on particle deposition in the human trachea and upper bronchial airways. Aerosol Sci., II, 447 - 459.

116. Ferron, G.A., 1977 ,
The size of soluble aerosol particles as a function of the humidity of air. Application to the human respiratory tract.
J. Aerosol Sci., 8, 251 - 267.

117. Schlesinger, R.B., Bohning, D.E., Chan, T.L., and Lippmann, M., 1977 , Particle deposition in a hollow cast of the human tracheobronchial tree. J. Aerosol Sci., 8, 429 - 495.

118. Martonen, T.B., 1983 ,

Measurement of particle dose distribution in a model of a human larynx and tracheobronchial tree.
J. Aerosol Sci., 14, 1, 11 - 24.

119. Ferron, G.A., 1977 ,
Deposition of polydisperse aerosols in two glass models representing the upper human airways.
J. Aerosol Sci., 8, 409 - 427.

120. Davies, C.N., 1980 ,
An algebraic model for the deposition of aerosols in the human respiratory tract during steady state breathing. Addendum.
J. Aerosol Sci., 11, 213 - 224.

121. Gerrity, T.R., Lee, P.S., Hass, F.J., Marinelli, A., Werner, P., and Lourenco, R.V., 1979 , Calculated deposition of inhaled particles in the airway generations of normal subjects.
J. Appl. Physiol., 47, 4, 867 - 873.

122. Horsfield, K., 1976 ,
Some mathematical properties of branching trees with application to the respiratory system. Bull. Math. Biol., 38, 305 - 315.

123. Lee, W - C, and Wang, C - S, 1976 ,
Particle deposition in systems of repeatedly bifurcating tubes.
In Inhaled Particles, ed. W.H. Walton, Pergamon Press Inc., Oxford, iv, 1, 49 - 60.

124. Yeh, H.C., and Schum, G.M., 1980 ,

Models of human lung airways and their application to inhaled particle deposition. Bull. Math. Biol., 42, 461 - 480.

125. Yeh, H.C., Schum, G.M., and Duggan, M.T., 1979 ,
Anatomic models of the tracheobronchial and pulmonary regions of the rat. The Anatomical Record, 195, 3, 483 - 492.

126. Yu, C.P., and Diu, C.K., 1983 ,
Total and regional deposition of inhaled aerosols in humans. J. Aerosol Sci., 14, 5, 599 - 610.

127. Rudolf, G., 1984 ,
A mathematical model for the deposition of aerosol particles in the human respiratory tract.
J. Aerosol Sci., 15, 3, 195 - 199.

128. Dubois, A.B., Botelho, S.Y., and Comroe, J.H., 1956 ,
A new method for measuring airway resistance in man using a body plethysmograph : values in normal subjects and in patients with respiratory disease. J. Clin. Invest., 35, 327 - 335.

129. Emmett, P.C., Aitken, R.J., and Muir, D.C.F., 1979 ,
A new apparatus for use in studies of the total and regional deposition of aerosol particles in the human respiratory tract during steady breathing. J. Aerosol Sci., 10, 123 - 131.

130. Williams, T.J., 1982 ,
The importance of aerosol technique : Does speed of inhalation matter ? Br. J. Dis. Chest, 76, 223 - 228.

131. Lawford, P., and McKenzie, D., 1982 ,
Pressurized bronchodilator aerosol technique : Influence of breath holding time and relationship of inhaler to the mouth. Br. J. Dis. Chest, 76, 229 - 233.

132. Palmes, E.D., Wang, C - S, Goldring, R.M., and Altshuler, B., 1973 , Effect of depth of inhalation on aerosol persistence during breath holding. J. Appl. Physiol., 34, 3, 356 - 360.

133. Yu, C - P, and Thiagarajen, C., 1979 ,
Decay of aerosols in the lung during breath holding. J. Aerosol Sci., 10, 11 - 19.

134. Taylor, S.M., Paré, P.D., and Schellenberg, R.R., 1984 ,
Cholinergic and nonadrenergic mechanisms in human and guinea pig airways. J. Appl. Physiol., 56, 4, 958 - 965.

135. Brain, J.D., Sweeney, T.D., Tryka, A.F., Skornik, W.A., and Godleski, J.J. , 1984 , Effects of pulmonary fibrosis on aerosol deposition in hamsters. J. Aerosol Sci., 15, 3, 217 - 218.

136. Stahlhofen, W., Gebhart, J., Heyder,J., Scheuch, G., and Juraske, P., 1984 , Particle deposition in extrathoracic airways of healthy subjects and of patients with early stages of laryngeal carcinoma. J. Aerosol Sci., 15, 3, 215 - 217.

137. Findeisen, W., 1935 ,
Uber das absetzen kleiner, in der luft suspendierten teilchen in

der menschlichen lunge bei der atmung.
Arch. Ges. Physiol., 236, 367 - 379.

138. Landahl, H.D., 1950 ,
On the removal of airborne droplets by the human respiratory tract II : The nasal passages.
Bull. Math. Biophysics, 12, 161 - 175.

139. Weibel, E.R., 1963 ,
Morphometry of the human lung. Springer Verlag, Berlin.

140. Rohrer, F., 1915 ,
Flow resistence in the human air passages and the effect of irregular branching of the bronchial system on the respiratory process in various regions of the lungs. Pfluger's Archiv. für die gesamte Physiologie des Menschen und der Tiere, 162 , 225 - 299. In Translations in Respiratory Physiology. Ed. J.B. West, Dowden, Hutchinson and Ross Inc., Stroudsberg, Pennsylvania,1975, 3 - 66.

141. Beeckmans, J.M., 1965 ,
The deposition of aerosols in the respiratory tract I. Mathematical analysis and comparison with experimental data.
Can. J. Physiol. Pharmacol., 43, 157 - 172.

142. Lippmann, M., 1970 ,
In Assessment of Airborne Particles, Rochester Third International Conference on Environmental Toxicity, eds. T.T. Mercer, P.E. Morrow and W. Stober, C.C. Thomas Publisher, Springfield

Illinois, 23, 449 - 464

143. Lippmann, M., and Albert, R.E., 1969 ,
The effect of particle size on the regional deposition of inhaled aerosols in the human respiratory tract.
Am. Ind. Hyg. Assoc. J., 30, 257 - 275.

144. Lippmann, M., Albert, R.E., and Peterson, H.T., 1971 ,
The regional deposition of inhaled aerosols in man. In Inhaled Particles, ed. W.H. Walton, Pergamon Press Inc., Oxford, III, 1, 105 - 115.

145. Altshuler, B., Palmes, E.D., Yarmus, L., and Nelson, N., 1959 ,
Intrapulmonary mixing of gases studied with aerosols.
J. Appl. Physiol., 14, 321 - 327.

146. Davies, C.N., 1970 ,
Deposition and recovery of 0.5 um diameter aerosol particles from the human lungs. In Assessment of Airborne Particles, Rochester Third International Conference on Environmental Toxicity, eds. T.T. Mercer, P.E. Morrow and W. Stober, C.C.Thomas Publisher, Springfield, Illinois, 18, 371 - 381.

147. Davies, C.N., Heyder, J., and Subba - Ramu, M.C., 1972 ,
Breathing of half micron aerosols I Experimental.
J. Appl. Physiol., 32, 5, 591 - 600.

148. Hounam, R.F., Black, A., and Walsh, M., 1971 ,
The deposition of aerosol particles in the nasopharyngeal region

of the human respiratory tract. In Inhaled Particles, ed. W.H. Walton, Pergamon Press Inc., Oxford, III, 1, 71 - 80.

149. George, A.C. and Breslin, A.J., 1967 ,
Deposition of natural radon daughters in human subjects. Health Physics, 13, 375 - 378.

150. Heyder, J., and Rudolf, G., 1977 ,
Deposition of aerosol particles in the human nose. In Inhaled Particles, ed. W.H. Walton, Pergamon Press Inc., Oxford, IV, 1, 107 - 125.

151. Gormley, P.G., and Kennedy, M., 1949 ,
Diffusion from a stream flowing through a cylindrical tube. Proc. Royal Irish Acad., 52A, 163 - 169.

152. Gonda, I., 1981 ,
The effect of polydispersiveness on deposition of therapeutic aerosols during mouth inhalation. In the International Symposium on Deposition and Clearance of Aerosols in the Human Respiratory Tract, May 22/23, Bad Gleichenberg, Austria, GAF and IGA and M.

153. Morrow, P.E., 1981 ,
An evaluation of the physical properties of monodisperse aerosols used in the assessment of bronchial function. Chest, 80, 6, 809 - 813.

154. Mercer, T.T., Goddard, R.F. and Flores, R.L., 1968 ,

Output characteristics of three ultrasonic nebulisers.
Ann. Allergy, 26, 18 - 27.

155. Gonda, I., 1981 ,
A semi - empirical model of aerosol deposition in the human respiratory tract for mouth inhalation.
J. Pharm. Pharmacol., 33, 692 - 696.

156. Davies, C.N., 1964 ,
Deposition and retention of dust in the human re piratory tract.
Ann. Occup. Hyg., 7, 169 - 183.

157. Lippmann, M., and Altshuler, B., 1976 ,
Regional deposition of aerosols. In Air Pollution and the Lung, eds. E.F. Aharonson, A. Ben - David and M.A. Klingberg, John Wiley and Sons, New York, 25 - 48.

158. Lippmann, M., Yeates, D.B., and Albert R.E., 1980 ,
Deposition, retention and clearance of inhaled particles.
Br. J. Ind. Med., 37, 337 - 362.

159. Mercer, T.T., 1975 ,
The deposition model of the Task Group on Lung Dynamics. A comparison with recent experimental data.
Health Physics, 29, 673 - 680.

160. Morrow, P.E., 1974 ,
Aerosol characterisation and deposition.
Am. Rev. Resp. Dis., 110, 88 - 89.

161. NRC Subcommittee on Airborne Particles, 1979 ,
Effects of inhaled particles on humans and animals : Deposition, retention and clearance. In Airborne Particles, International Symposium on Deposition and Clearance of Aerosols, ed. H.H. Ruck, Baltimore University Press, 6, 107 - 145, 1981.

162. Busugin, A., van der Vooren, A., and Phillips, C.R., 1981 ,
Measurement of the total and radioactive size distribution in a Canadian uranium mine. Am. Ind. Hyg. Assoc. J., 42, 4, 310 - 314.

163. Foord, N., Black, A., and Walsh, W., 19?? ,
Pulmonary deposition of inhaled particles with diameters in the range 2.5 to 7.5 um. In Inhaled Particles, ed. W.H. Walton, Pergamon Press Inc., Oxford, IV, 1, 137 - 149.

164. Fuchs, N.A., 1964 ,
Size and shape of aerosol particles. In Mechanisms of Aerosols, ed. C.N. Davies, Pergamon Press Inc., Revised Edition, London, 1 - 20.

165. Sudlow, M.F., Olson, D.E., and Schroter, R.C., 1971 ,
Fluid mechanics of bronchial flow. In Inhaled Particles, ed. W.H. Walton, Pergamon Press Inc., Oxford, III, 1, 19 - 31.

166. Davies, C.N., 1979 ,
Particle fluid interaction.
J. Aerosol Sci., 10, 477 - 513.

167. Harris, R.L., and Timbrell, V., 1977 ,

The influence of fibre shape in lung deposition. Mathematical estimates. In Inhaled Particles, ed. W.H. Walton, Pergamon Press Inc., Oxford, IV, 1, 75 - 89.

168. Kottrappa, P., 1970 ,

Shape factors for aerosols of coal, UO_2 and ThO_2 in respirable size range. In Assessment of Airborne Particles, Rochester Third International Conference on Environmental Toxicity, eds. T.T. Mercer, P.E. Morrow and W. Stober, C.C. Thomas Publisher, Springfield, Illinois, 16, 331 - 358.

169. Stober, W., 1970 ,

Dynamic shape factors of non - spherical aerosol particles. In Assessment of Airborne Particles, Rochester Third International Conference on Environmental Toxicity, eds. T.T. Mercer, P.E. Morrow and W. Stober, C.C. Thomas Publisher, Springfield, Illinois,14, 249 - 289.

170. Reif, A.E., 1958 ,

Aerosols : Physical properties, instrumentation and techniques. In Aviation Medicine Selected Reviews, eds. C.S. White, W.R. Lovelace II and F.G. Hirsch, Pergamon Press, New York, 168 - 244.

171. Hinds, W.C., 1982 ,

In Aerosol Technology. Properties, behaviour and measurement of airborne particles. John Wiley and Sons, New York,

172. Cunningham, E., 1910 ,

On the velocity of steady fall of particlesthrough fluid medium.

Proc. Roy. Soc. (London) Ser. A., 83, 357 - 365

173. Mercer, T.T., 1973 ,

In Aerosol Technology and Hazard Evaluation, Academic Press Inc.,

New York and London, 38 -39 and 3.

174. Yu, C.P., and Chandra, K., 1978 ,

Deposition of charged particles from laminar flows in rectangular

and cylindrical channels by image force.

J. Aerosol Sci., 9, 175 - 180.

175. Tang, I.N., 1980 ,

Deliquescence properties and particle size change of hygroscopic

aerosols. In Generation of Aerosols and Facilities for Exposure

Experiments, ed K. Willeke, Ann Arbor Science, Michigan, 153 - 167.

176. Cocks, A.T., and Fernado, R.P., 1982 ,

The growth of sulphate aerosols in the human airways.

J. Aerosol Sci., 13, 1, 9 - 19.

177. Smolik, J., and Vitovec, J., 1983 ,

Condensation of supersaturated vapours in the downward and upward

thermal diffusion cloud chamber : Homogeneous nucleation of

stearic acid. J. Aerosol Sci., 14, 6, 697 - 702.

178. Strey, P., and Wagner, P.E., 1983 ,

Measurements of homogeneous nucleation rates for the homologous series of alcohols and comparison with the classical nucleation theory. J. Aerosol Sci., 14, 1, 162 - 163.

179. Mason, B.J., 1971 ,
Homogeneous nucleation. In The Physics of Clouds, Monographs on Meteorology, ed. P.A. Sheppard, Clarendon Press, Oxford,

180. Michalsky, J.J., and Stokes, G.M., 1983 ,
Mt. St. Helens' Aerosols : Some troposheric and stratosheric effects. J. Appl. Meteor., 22, 4, 640 - 648.

181. Willeke, K., and Whitby, K.T., 1975 ,
Atmospheric aerosols: size distribution interpretation. J. Air Pollut. Control Assoc., 25, 5, 529 - 535.

182. Green, H.L., and Lane, W.R., 1964 ,
Particulate Clouds : Dusts , Smokes and Mists, E. and F.N. Spon Ltd., London.

183. Haenel, G., 1976 ,
The properties of atmospheric aerosol particles as functions of the relative humidity at thermodynamic equilibrium with the surrounding moist air. Advances in Geophysics, 19, 73 - 187.

184. Haenel, G., and Zankl, B., 1979 ,

Aerosol size and relative humidity : water uptake by mixtures of salts. Tellus, 31, 6, 478 - 486.

185. Haenel, G., and Lehmann, M., 1981 ,
Equilibrium size of aerosol particles and relative humidity : new experimental data from various aerosol types and their treatment for cloud physics application.
Contrib. Atmos. Phys., 54, 1, 57 - 71.

186. Sahni, D.C., 1980 ,
Evaporation and condensational growth of tiny droplets.
J. Aerosol Sci., 11, 293 - 304.

187. Steele, H.M., Hamill, P., McCormick, M.P., and Swissler, T.J.,1983,
The formation of polar stratospheric clouds
J. Atmos. Sci., 40, 8, 2055 - 2067.

188. Steele, H.M., and Hamill, P., 1981 ,
Effects of temperature and humidity on the growth and optical properties of sulphuric acid - water droplets in the stratosphere,
J. Aerosol Sci., 12, 6, 517 - 528.

189. Chang, J - S, 1983 ,
Aerosol particle growth rates in an ionized environment.
J. Aerosol Sci., 14, 3, 391 - 393.

190. Butler, C.C., 1982 ,
Early cloud chamber experiments at the Pic - du - Midi.
International Colloquium on the History of Particle Physics,

Paris, 21 - 23 July, 1982, J. Phys. Colloq. (France), 43, C-8, 177 - 184.

191. Brown, J.T., and Showengerdt, F.D., 1979 ,
Water droplet growth measurements in a continuous flow parallel plate thermal diffusion cloud chamber.
J. Aerosol Sci., 10, 515 - 526.

192. Orr, C., Hurd, F.K., and Corbett, W.J., 1958 ,
Aerosol size and relative humidity.
J. Colloid Sci., 13, 472 - 482.

193. Kasper, G., 1977 ,
On the density of sodium chloride aerosols formed by condensation.
J. Colloid Interface Sci., 62, 2, 359 - 360.

194. Fairall, C.W., and Larsen, S.E., 1984 ,
Dry deposition, surface production and dynamics of aerosols in the marine boundary layer.
Atmos. Env., 18, 1, 69 - 77.

195. Thudium, J., 1978 ,
Water uptake and equilibrium sizes of aerosol particles at high relative humidities : Their dependence on the composition of the water - soluble material.
Pure and Applied Geophysics, 116, 130 - 148.

196. Straubel, H., 1980 ,
Aerosol particles in air with a gradient of humidity.
Stud. Environ. Sci., 8 (Atmos. Pollut.), 239 - 244.

197. Stelson, A.W., and Seinfeld, J.H., 1982,
Relative humidity and pH dependence of the vapor pressure of ammonium nitrate - nitric acid solutions at 25 °C.

198. Holleman, D.F., Martz, D.E., and Schiager, K.J., 1969 ,
Total respiratory deposition of radon daughters from inhalation of uranium mine atmospheres.
Health Physics, 17, 187 - 192.

199. Bailey, M., Anderson, K.R., Whynot, J.D., Medway, D.A., and Hackney, J.D., 1981 ,
Human exposure to iron III sulphate aerosol : Effects on pulmonary function and respiratory symptoms.
Am. Ind. Hyg. Assoc. J., 42, 4, 298 - 304.

200. Martonen, T.B., and Patel, M., 1981 ,
Computation of ammonium bisulfate aerosol deposition in conducting airways. J. Toxicol. Environ. Health, 8, 1001 - 1014.

201. Martonen, T.B., and Patel, M., 1981 ,
Modeling the dose distribution of H_2SO_4 aerosols in the human tracheobronchial tree.
Am. Ind. Hyg. Assoc. J., 42, 6, 453 - 460.

202. Lundgren, D.L., Hahn, F.F., and McClellan, R.O., 1981 ,
Single and repeated inhalation exposure of mice to aerosols of plutonium - 239 dioxide.
Radiat. Res., 87, 2, 388.

203. Mewhinney, J.A., and Griffith, W.C., 1982 ,
The influence of aerosol size on retention and translocation of ^{241}Am following inhalation of $^{241}AmO_2$ by beagles.
Health Physics, 42,5, 611 - 627.

204. Wolff, R.K., Muggenburg, B.A., and Silbaugh, S.A., 1981 ,
Effect of 0.3 and 0.9 micrometer sulphuric acid aerosols on tracheal mucus clearance in beagle dogs.
Am. Rev. Resp. Dis., 123, 3, 291 - 294.

205. Ferron, G.A., 1983 ,
Aerosol particle growth in the human airways using a calculated humidity profile.
J. Aerosol Sci., 14, 3, 196 - 199.

206. Muir, D.C.F., 1972 ,
In Clinical Aspects of Inhaled Particles, William Heineman Medical Books, London, 179.

207. Sundararajan, A.R., Mitragotri, D.S., and Mukunda Rao, S.R., 1982,
Effect of relative humidity on growth of sodium oxide aerosols.
J. Nucl. Sci. Technol., 19, 2, 151 - 157.

208. Martonen, T.B., 1982 ,
Analytical model of hygroscopic particle behaviour in human airways.
Bull. Math. Biol., 44, 3, 425 - 442.

209. Martonen, T.B., and Wilson, A.F., 1983 ,
The influence of hygroscopic growth upon the deposition of bronchodilator aerosols in upper human airways.
J. Aerosol Sci., 14, 3, 208 - 211.

210. Martonen, T.B., Bell, K.A., Phalen, R.F., Wilson, A.F., and Ho, A., 1982 , Growth rate measurements and deposition modelling of hygroscopic aerosols in human tracheobronchial models.
Ann. Occup. Hyg., 26, 93 - 108.

211. Bell, K.A., and Ho, A., 1981 ,
Growth rate measurements of hygroscopic aerosols under conditions simulating the respiratory tract.
J. Aerosol Sci., 12, 3, 247 - 254.

212. Hiller, F.C., Mazumder, M.K., Wilson, J.D., and Bone, R.C., 1980 ,
Effect of low and high relative humidity on metered - dose bronchodilator solution and powder aerosols.
J. Pharm. Sci., 69, 3, 334 - 337.

213. Hiller, F.C., Mazumder, M.K., Wilson, J.D., and Bone, R.C., 1980 ,
Aerodynamic size distribution, hygroscopicity and deposition estimations of beclomethasone dipropionate aerosol.
J. Pharm. Pharmacol., 32, 605 - 609.

214. Gonda, I., Kayes, J.B., Groom, C.V., and Fildes, F.J.T., 1981 ,
Characterisation of hygroscopic inhalation aerosols. In
Particle Size Analysis, eds. N. Stanley - Wood and T. Allen,

J. Wiley and Sons Publishers, New York, 31 - 43.

215. Halbert, M.K., Mazumder, M.K., and Bond, R.L., 1982 ,
Inhalation simulation and the effects of lung environment conditions on consumer aerosol products and NaCl aerosols.
Environ, Res., 29, 263 - 271.

216. Mokler, B.V., Wong, B.A., and Snow, M.J., 1979 ,
Respirable particulates generated by pressurized consumer products II Influence of experimental conditions.
Am. Ind. Hyg. Assoc. J., 40, 4, 339 - 347.

217 Ferron, G.A., and Hornik, S., 1984 ,
Influence of different humidity profiles on the deposition probability of soluble particles in the human lung.
J. Aerosol Sci., 15, 3, 209 - 211.

218. Milburn, R.H., Crider, W.L. and Morton, S.D., 1957 ,
The retention of hygroscopic dusts in the lung.
A.M.A. Arch. Ind. Health, 15, 59 - 62.

219. Malton, C.A., Halworth, G.W., and Padfield, J.M., 1982 ,
The association and particle size distribution of drug and surfactant discharged from a metered - dose inhalation aerosol.
J. Pharm. Pharmacol., 65P.

220. Sanders, P.A., 1980 ,
in Principles of Aerosol Technology, Van Nostra and Reinhold Company, New York, 317.

221. Otanyi, Y., and Wang, C - S, 1981 ,
Growth of saline droplets with surfactants .
In the Fourth International Conference on Surface and Colloid Science, IUPAC, Jerusalem, Israel, 5 - 10. 7, 319.

222. Chikazawa, M., Yamamoto, F., Saita, E., Kahto, M., and Kanazawa, T., 1970 , Water vapour affinity of potassium bromide with potassium oleate.
Bull. Chem. Soc. Japan, 50, 2, 337 - 340.

223. Kertes, A.S., 1977 ,
Aggregation of surfactants in hydrocarbons. Incompatability of the critical micelle concentration concept with experimental data.
In Micellization, Solubilization and Microemulsions, ed. K.L. Mittal, Plenum Press, New York and London, 1, 445 - 454.

224. Eicke, H.F., 1977 ,
Micelles in apolar media. In Micellization, Solubilization and Microemulsions, ed. K.L. Mittal, Plenum Press, New York and London, 1, 429 - 443.

225. Ravey, J.C., Buzier, M., and Picot, C., 1984 ,
Micellar structures of non - ionic surfactants in apolar media.
J. Colloid Interface Sci., 97, 1, 9 - 25.

226. Tanford, C., 1980 ,
in The Hydrophobic Effect, J. Wiley and Sons Publishers, New York, Second Edition.

227. Mukerjee, P., 1974 ,
Micellar properties of drugs : Micellar and non - micellar patterns of self association of hydrophobic solutes of different molecular structures, monomer frqction, availability, and misuses of micellar hypothesis.
J. Pharm. Sci., 63, 972 - 981.

228. Hartley, G.S., 1936 ,
in Aqueous Solutions of Paraffin Chain Salts, Heman at Cie, Paris.

229. Hartley, G.S., 1955 ,
in Progress in the Chemistry of Fats and Other Lipids , Pergammon Press, London.

230. O'Connor, C.J., and Lomax, T.D., 1983 ,
Evidence for the sequential self - association model in reversed micelles. Tetrahedron Letters, 24, 28, 2917 - 2920.

231. Shinoda, K., and Hutchinson, E., 1962 ,
Pseudo - phase separation model for thermodynamic calculations on micellar solutions.
J. Phys. Chem., 66, 577 - 582.

232. Singleterry, C.R., 1955 ,
Micelle formation and solubilisation in non - aqueous solvents.
J. Amer. Oil. Chemists Soc., 32, 446 - 452.

233. Fowkes, F.M., 1962 ,
The micelle phase of calcium dinonylnaphthalene sulfonate in n - decane.
J. Phys. Chem., 66, 1843 - 1845.

234. Lo, F. Y - F, Escott, B.M., Fendler, E.J., Adams, E.T., Larson, R.D., and Smith, P.W., 1975 , Temperature - dependent self - association of dodecylammonium propionate in benzene cyclohexane. J. Phys. Chem., 79, 2609 - 2621.

235. Eicke, H.F., 1980 , 1980 ,
Aggregation in surfactant solutions : formation and properties of micelles and microemulsions.
Pure Appl. Chem., 52, 5, 1349 - 1357.

236. Muto, S., Shimazaki, Y., and Meguro, K., 1974 ,
The effect of counterion on critical micelle concentration of surfactant in non - aqueous media.
J. Colloid Interface Sci., 49, 173 - 176.

237. Fendler, J.H., and Fendler, E.J., 1975 ,
in Catalysis in Micellar and Macromolecular Systems, Academic Press, New York.

238. Kertes, A.S., and Gutmann, H., 1976 ,
Surfactants in organic solvents: The physical chemistry of aggregation and micellization. In Surface and Colloid Science, ed. E. Matijevic, J. Wiley and Sons Publishers, New York, 8, 193 - 295.

239. Philippoff, W., 1950 ,
Micelles and X - rays.
J. Colloid Sci., 5, 169 - 191.

240. Mayer, I., Gutmann, H., and Kertes, A.S., 1969 ,
in Solvent Extraction Research, eds. A.S. Kertes and Y. Marcus,
Wiley - Interscience, New York, 195

241. Yamashita, T., Yano, H., Harada, S., and Yasunaga, T., 1982 ,
Kinetic studies of the micelle system of octylammonium
alkanoates in hexane solution by the ultrasonic absorption
method. Bull. Chem. Soc. Jpn., 55, 3403 - 3406.

242. Langmuir, I., 1917 ,
The constitution and fundamental properties of solids and liquids
II Liquids.
J. Am. Chem. Soc., 39, 1848 - 1906.

243. Fowler, R., and Guggenheim, E.A., 1960 ,
in Statistical Thermodynamics, Cambridge University Press,
Cambridge,

244. Brunauer, S., Emmett, P.H., and Teller, E., 1938 ,
Adsorption of gases in multimolecular layers.
J. Am. Chem. Soc., 60, 309 - 319.

245. Brunauer, S., 1945 ,

The Adsorption of Gases and Vapors, I, Princeton University Press, Princeton, New Jersey.

246. Giles, C.H., D'Silva, A.P., and Easton, I.A., 1974 , A general treatment and classification of the solute adsorption isotherm I. Theoretical. J. Colloid Interface Sci., 47, 3, 755 - 765.

247. Giles, C.H., D'Silva, A.P., and Easton, I.A., 1974 , A general treatment and classification of the solute adsorption isotherm II. Experimental interpretation. J. Colloid Interface Sci., 47, 3, 766 - 778.

248. Rudzinski, W., and Narkiewicz - Michalek, J., 1982 , Adsorption from solutions onto solid surfaces. J. Chem. Soc. Faraday Trans. I, 78, 2361 - 2368.

249. Mabire, F., Audebert, R., and Quivoron, C., 1984 , Flocculation properties of some water soluble cationic copolymers towards silica suspensions : A semiquantitative interpretation of the role of molecular weight and cationicity through a "patchwork" model. J. Colloid Interface Sci., 97, 1, 12 - 136

250. Damaskin, B.B., Petrii, O.A., and Batrakov, V.V., 1971 , in Adsorption of Organic Compounds on Electrodes, Plenum Press, New York and London, 90.

251. Giles, C.H., 1982 ,

Forces operating in adsorption of surfactants and other solutes at solid surfaces: A survey. In Solution Behaviour of Surfactants. Theoretical and Applied Aspects, eds. K.L. Mittal and E.J. Fendler, Plenum Press, New York and London, 1, 123 - 248.

252. Groom, C.V., 1981 ,
Effects of relative humidity on inhalation aerosols. Ph. D. Thesis, University of Aston in Birmingham.

253. Leong, K.H., Wang, H - C, Stukel, J.J., and Hopke, P.K., 1982 ,
An improved constant output atomizer.
Am. Ind. Hyg. Assoc. J., 43, 2, 135 - 136.

254. Scherer, P.W., Haselton, F.R., Hanna, L.M., and Stone, D.R., 1979,
Growth of hygroscopic aerosols in a model of the bronchial airways. J. Appl. Physiol., 47, 3, 544 - 550.

255. Weast, , 1978/9
Handbook of Physics and Chemistry, CRC Press Inc., 59th Edition, Boca Raton, Florida, D232, E34 - 35.

256. Smith, A., 1975 ,
The influence of the chemical nature of dispersed phase on stability in oil - in - water emulsions. Ph. D. Thesis, University of Aston in Birmingham.

257. Padday, J.F., and Russell, D.R., 1960 ,
The measurement of the surface tension of pure liquids and solutions, J. Colloid Sci., 15, 503 - 511.

258. Sonntag, H., and Strenge, K., 1970 ,
The influence of adsorbed layers on the determination of interfacial tension using different methods.
J. Colloid Interface Sci., 32, 159 -

259. Kipling, J.J., 1965 ,
in Adsorption from Solutions of Non - Electrolytes, Academic Press, New York and London.

260. Knapp, D.R., 1979 ,
in The Handbook of Analytical Derivitization Reactions, J. Wiley and Sons, New York, 154.

261. Blau, K., and King, G., 1978 ,
in Handbook of Derivatives for Chromatography, Heydon and Son Limited, London, 62.

262. Jaurand, M - C, Baillif, B., Thomassin, J - H, Magne, L., and Touray, J.C., 1983 , X - ray photoelectron spectroscopy and chemical study of the adsorption of biological molecules on chrysotile asbestos surface.
J. Colloid Interface Sci., 95, 1, 1 - 9.

263. Hering, S.V., Friedlander, S.K., Collins, J.J., and Richards, L.W., 1979 , Design and evaluation of a new low pressure impactor. Env. Sci. Tech., 13, 2, 184 - 188.

264. Fuks, G.I., Tikhonov, V.P., and Lebedev, R.A., 1982 ,
Investigation of micelle formation by surfactants in non - polar liquids by means of IR spectroscopy 1. Solutions of fatty acids in carbon tetrachloride.
Translated from Kolloidnyi Zhurnal, 44, 1, 77 - 82.

265. Stapleton, I.W., 1983 ,
The adsorption of long - chain amines and diamines on keratin fibers.
J. Soc. Cosmet. Chem., 34, 285 - 300.

266. Koltoff, I.M., Gutmacher, R.G., and Kahn, A., 1951 ,
Sorption of GR - S type rubber by carbon black II.
J. Phys. Chem., 55, 1240 - 1246.

267. Elworthy, P.H., and McIntosh, D.S., 1964 ,
The effect of solvent dielectric constant on micellisation by lecithin. Kolloid Zeitschrift und Zeitschrift fur Polymere, 195, 1, 27 - 34.

268. Serdyuk, A.I., Fuks, G.I., Podmarkov, V.I., Chervinskii, A.Y., and Vashun, Z.M., 1983 , Influence of additions of organic compounds on the micelle formation of surface - active substances in non - polar media.
Translated from Kolloidnyi Zhurnal, 45, 2, 363 - 368.

269. Tikhonov, V.P., Lebedev, R.A., and Fuks, G.I., 1982 ,
Study of micelle formation of surfactants in non - polar liquids

by means of infra - red spectroscopy 2. Solutions of aliphatic alcohols in carbon tetrachloride.
Translated from Kolloidnyi Zhurnal, 44, 1, 57 - 61.

270. Chander, S., Fuerstenau, D.W., and Stigter, D., 1982 ,
On hemimicelle formation at oxide/water interfaces. In Symposium on Adsorption from Solution, Bristol, 8 - 10 September, Academic Press, New York and London.

271. Legenchenko, I.A., Skrylev, L.D., and Strel' tsova, E.A., 1982,
Analysis of isotherms for the adsorption of cationic surfactants by silicon dioxide, by means of mathematical modeling.
Translated from Kolloidnyi Zhurnal, 44(1), 129 - 132.

272. Copenhafer, D.T., and Kraus, C.A., 1951 ,
Properties of electrolyte solutions. LIII Molecular weight of salts in benzene by the cryoscopic method.
J. Am. Chem. Soc., 73, 4557 - 4561.

273. Pilpel, N., 1963 ,
Properties of organic solutions of heavy metal soaps.
Chem. Revs., 63, 221 - 234.

274. Nelson, S.M., and Pink, R.C., 1952 ,
Solutions of metal soapsin organic solvents. Part III. The aggregation of metal soaps in toluene, isobutyl alcohol and pyridine. J. Chem. Soc., 2, 1744 - 1750.

275. Cross, A.D. and Jones, R.A., 1969 ,

in Practical Infra - Red Spectroscopy, Third Edition, Butterworths, London, 47.

276. Arbeloa, I.L., 1981 ,
Dimeric and trimeric states of the fluorescein dianion. J. Chem. Soc., Faraday Trans. 2, 77, 1725 - 1733.

277. Gregg, S.J., 1961 ,
in The Surface Chemistry of Solids, Second Edition, Chapman and Hall, London.

278. Georgallas, A., and Pink, D.A., 1982 ,
Phase transitions in monolayers of saturated lipids. Exact results and Monte Carlo simulations. J. Colloid Interface Sci., 89, 1, 107 - 116.

279. Nelson, P.F., and Quigley, S.M., 1984 ,
The hydrocarbon composition of exhaust amitted from gasoline fuelled vehicles. Atmos. Env., 18, 1, 79 - 88.

280. Uthe, E.E., 1984 ,
Cooling tower plume rise analyses by airborne lidar. Atmos. Env., 18, 1, 107 - 120.

281. Leahey, D.M., Davies, M.J.E., and Bambrough, H.A., 1983 ,
Values of NO_2:NO_x observed in the exhaust plume from a turbine driven compressor installation. Atmos. Env., 17, 5, 991 - 998.

282. Ryan, P.B., Spengler, J.D., and Letz, R., 1983 ,
The effects of Kerosene heaters on indoor pollutant concentrations a monitoring and modeling study.
Atmos. Env., 17, 7, 1139 - 1146.

283. Marsh, A., 1947 ,
in Smoke, The Problem Of Coal And The Atmosphere, Faber and Faber Limited, London.

284. Ghandour, M.F.M. El, Abdel Salam, M.S., Hindy, K.T., Kamel, M.M., 1983 , Studies on air pollution from construction plants in Helwan industrial area - II Water soluble and insoluble deposits. Atmos. Env., 17, 3, 573 - 579.

285. Mohan Rao, A.M., Netravalkar, A.J., Arora, P.K., and Vohra, K.G., 1983, Determination of ethylene and other reactive hydrocarbons in the atmospheric air at Trombay, Bombay by gas chromatography using - chemiluminescent. Atmos. Env. 17, 6, 1093 - 1097.

286. Barkenbus, B.D., MacDougall, C.S., Griest, W.H., and Caton, J.E., 1983, Methodology for the extraction and analysis of hydrocarbons and carboxylic acids in atmospheric particulate matter.
Atmos. Env., 17, 8, 1537 - 1543.

287. Gras, J.L., 1983 ,
Ammonia and ammonium concentrations in the antarctic atmosphere. Atmos. Env., 17, 4, 815 - 818.

288. Bassett, M., and Seinfeld, J.H., 1983 ,
Atmospheric equilibrium models of sulphate and nitrate aerosols.
Atmos. Env., 17, 11, 2237 - 2252.

289. Altshuler, A.P., 1984 ,
Atmospheric particle sulfur and sulfur dioxide relationship
at urban and non - urban locations.
Atmos. Env., 18, 7, 1421 - 1432.

290. Nagamoto, C.T., Parungo, F., Reinking, R., Pueschel, R. ,
and Gerish, T., 1983 , Acid clouds and precipitation in
Eastern Colarado. Atmos. Env., 17, 6, 1073 - 1082.

291. Walker, J.E.C., Wells, R.E., and Merrill, E.W., 1961 ,
Heat and water exchange in the respiratory tract.
Am. J. Med., 30, 259 - 267.

292. Tang, I.N., Munkelwitz, M.R., and Davis, J.G., 1977 ,
Aerosol growth studies II : Preparation and growth measurements
of monodisperse salt aerosols.
J. Aerosol Sci., 8, 147 - 159.

293. Diem, K., 1968 ,
Scientific Tables, 6th Edition, Geigy Pharmaceuticals,
Ardsley.

294. Heywood, H., 1945/6 ,

A comparison of methods of measuring microscopical particles. Trans. Inst. Min. Metall., 55, 391 - 404.

295. Heywood, H., 1947 ,
The scope of particle size analysis and standardisation. Inst. Chem. Eng. Suppl., 25, 14, 14 - 24.

296. Hsu, S.I., 1983 ,
Impactor design. Atmos. Env., 17, 5, 1029.

297. Boesch, P., 1983 ,
Practical comparison of three cascade impactors. J. Aerosol Sci., 14, 3, 325 - 330.

298. Marple, V.A., and Willeke, K., 1979 ,
Inertial impactors. In Aerosol Measurement, eds D.A. Lundgren, M. Lippmann, F.S. Harris, W.E. Clark, W.H. Marlow and M.D. Durham, University Press of Florida, Gainsville, 90 - 107.

299. Stober, W., Martonen, T.B., and Osborne, S., 1978 ,
On the limitations of aerodynamic size separation of dense aerosols with the spiral duct centrifuge. In Recent Developments In Aerosol Science, ed D.T. Shaw, J. Wiley and Sons, New York, 279 - 321.

300. Stober, W., and Hederer, E., 1978 ,
On the secondary flow inthe spinning spiral duct of an aerosol centrifuge. In Recent Developments In Aerosol Science, ed D.T. Shaw

J. Wiley and Sons, New York, 239 - 262.

301. Lundgren, D.A., and Balfour, W.D., 1982 ,
Size classification of industrial aerosols using in - stack impactors. J. Aerosol Sci., 13, 3, 181 - 184.

302. Jupe, H., Richter, F.W., and Wätjen, U., 1981 ,
Deposition problems and secondary deposits in a single jet cascade impactor. J. Aerosol Sci., 12, 3, 221.

303. Boulaud, D., Diouri, M., and Madelaine, G., 1982 ,
Parameters influencing the collection efficiency of solid aerosols in cascade impactors.
J. Aerosol Sci., 13, 3, 187 - 188.

304. Berglund, R.N., and Liu, B.Y.H., 1973 ,
Generation of monodisperse aerosol standards.
Env. Sci. Tech., 7, 147 - 153.

305. Leong, K.H., Wang, H.C., Stukel, J.J., and Hopke, P.K., 1982 ,
An improved constant output atomizer.
Am. Ind. Hyg. Assoc. J., 43, 2, 135 - 136.

306. Solvason, K.R., and Hutcheon, N.B., 1963 ,
Principles in the design of cabinets for controlled environments.
In Humidity and Moisture, ed A. Wexler, Volume 2, Applications,
Reinhold Publishing Corporation, New York, 30, 241.

307. Groom, C.V., and Gonda, I., 1980 ,

Cascade impaction : The performance of different collection surfaces. J. Pharm. Pharmacol., 32 (Suppl.), 93P.

308. Gonda, I., 1981 ,
A data inversion method for particle sizing using a calibrated cascade impactor. International Symposium on Deposition and Clearance of Aerosols in the Human Respiratory Tract, May 22/23, Bad Gleichenberg, Austria, GAF and IGA and M.

309. Raabe, O.G., 1978 ,
A general method for fitting size distributions to multicomponent aerosol data using weighted least - squares.
Env. Sci. Tech., 12, 1162 - 1167.

310. Robinson, R.A., and Stokes, R.H., 1959 ,
In Electrolyte Solutions, Butterworths, London.

311. Diem, K., 1968 ,
Scientific Tables, 6th Edition, Geigy Pharmaceuticals, Ardsley.

312. Mitchell, J.P., Ramsey, C.A., and Rowe, N.A., 1983
The generation of calibration aerosols of known particle number concentrations.
J. Aerosol Sci., 14, 3, 257 - 260.

313. Marple, V.A., Liu, B.Y.H., and Rubow, K.L., 1978 ,
A dust generator for laboratory use.
Am. Ind. Hyg. Assoc. J., 39, 26 - 32.

314. Wolny, A., 1979 ,
Effect of air humidity on the hydrodynamics of a fluidized bed of particles differing in size.
Pr. Inst. Inz. Chem. Politech. Warsz., 8, 1 - 2, 21 - 35.

315. Kanapilly, G.M., Raabe, O.G., Goh, C.H.T., and Chimenti, R.A., 1973, Measurement of in vitro dissolution of aerosol particles for comparison to in vivo dissolution in the lower respiratory tract after inhalation.
Health Physics, 24, 497 - 507.

316. Lagaly, G., Witter, R., and Sander, H., 1982 ,
Water on hydrophobic surfaces. In Symposium on Adsorption from Solution, 8 - 10 September, Bristol, Academic Press, New York and London.

317. Suves, M., and Uotila, P., 1982 ,
The effect of sodium nitroprusside on the metabolism of prostaglandin E_2 in rat isolated lungs.
Res. Commun. Chem. Path. Pharmac., 36, 2, 333 - 336.

318. Heyder, J., 1981 ,
Mechanisms of aerosol particle deposition.
Chest, 80S, 820S - 823S.

319. Güveli, D.E., Davis, S.S., and Kayes, J.B., 1982 ,
Partial molal volume and light scattering studies oncertain polyoxyethylene monohexadecyl ethers, and the effect of added aromatic solutes. J. Colloid Interface Sci., 86, 1, 213 - 225.

320. Pohle, W., 1982,
Infrared study of the adsorption of aromatic molecules onto silica and chlorinated silica.
J. Chem. Soc. Faraday Trans. 1, 78, 2101 - 2109.

321. Acosta Saracual, A.R., Pulton, S.K., and Vicary, G., 1982 ,
Infrared study of the adsorption of fluoroalcohols on silica.
J. Chem. Soc. Faraday Trans. 1, 78, 2285 - 2296.

322. Acosta Saracual, A.R., and Rochester, C.H., 1982 ,
Evidence for the mode of adsorption of anisoles on silica from an infrared study of hydrogen bonds between triphenyl - silanol and anisoles in solution.
J. Chem. Soc. Faraday Trans. 1, 78, 2787 - 2791.

323. Neagle, W., and Rochester, C.H., 1982 ,
Infrared study of 1,2 dihydroxyethane and its methyl ethers adsorbed on silica immersed in carbon tetrachloride.
J. Chem. Soc. Faraday Trans. 1, 78, 3081 - 3087.

324. Morley, C,J., Bangham, A.D., Miller, N., and Davis, J.A., 1981 ,
Dry artificial lung surfactant and its effect on very premature babies . The Lancet, 64 - 68.

325. Haldén, E., Hedstrand, U., and Torsner, K., 1982 ,
Oleic acid lung damage in pigs.
Acta. Anaesth. Scand., 26, 121 - 125.

326. Conn, E.E., and Stumpf, P.K., 1972
Outlines of Biochemistry, Third Edition, J. Wiley and Sons,
New York and London, 299.

327. Newman, S.P., Agnew, J.E., Pavia, D.,and Clarke, S.W., 1982 ,
Inhaled aerosols : Lung deposition and clinical applications.
Clin. Phys. Physiol. Meas., 3, 1 - 20.

328. Pircher, F.J., Lerner, S.R., Cooper, P.H., and Eastland, D.K.,
1971 , Aerosol scans with particles in the submicronic range.
J. Nucl. Med., 12, 385 - 386.

329. Mullins, J. and Hayes, M., 1972 ,
Improved technique for aerosol inhalation scanning (abstr.).
J. Nucl. Med., 13, 872.

330. Salk, R. and Mullins, J., 1976 ,
A simple effective method for aerosol inhalation scanning.
J. Nucl. Med. Technol., 4, 94 - 95.

331. Hayes, M., Taplin, G.V., Chopra, S.W., Knox, D.E. and Elam, D.,
1979 , Improved radioaerosol administration system for routine
inhalation lung imaging. Radiology, 131, 256 - 258.

332. Francis, R.A., Agnew, J.E., Sutton, P.P., Pavia, D. and Clarke, S.W., 1981 , Ventilation imaging with easily prepared ^{99m}Tc aerosols. Nucl. Med. Commun., 2, 203 - 208.

333. Arborelius Jr, M., 1982 , Generation of microaerosol suitable for deposition in the peripheral airways. Eur. J. Respir. Dis. (Suppl. 119), 63, 19 - 27.

334. Suzuki, T., Swift, D.L., Wagner, H.N., and Proctor, D.F., 1982 , A new apparatus for generating hygroscopic radioactive aerosols for inhalation studies. Eur. J. Nucl. Med., 7, 474 - 479.

335. Royston, D., and Minty, B.D., 1983 , A cheap simple particle generator system for use with in vivo measurement of alveolar - capillary barrier permeability. Am. Rev. Resp. Dis., 127, 4, 319.

336. Short, M.D., Dowsett, D.J., Heaf, P.J.D., Pavia, D. and Thompson, M.L., 1979 , A comparison between monodisperse Tc - 99m labelled aerosol particles and Kr - 81m for the assessment of lung function. J. Nucl. Med., 20, 194 - 200.

337. Santolicandro, A. and Giuntini, C., 1979 , Patterns of deposition of labelled monodisperse aerosol in obstructive lung disease. J. Nucl. Med. All. Sci., 23, 3, 115 - 127.

338. Greening, A.P., Miniati, M., and Fazio, F., 1980 , Regional deposition of aerosols in health and in airways obstruction : A comparison with krypton - 81m ventilation

scanning. Bull. Eur. Physiopathol. Respir., 16, 287 - 298.

BNMS ANNUAL MEETING 1984 ABSTRACT SHEET

LONDON 16th-18th APRIL 1984

versity

en removed for copyright reasons

Aston University

Content has been removed for copyright reasons

Eur J Nucl Med 9:141–143

European Journal of Nuclear Medicine

Short communication

A simple radioaerosol generator and delivery system for pulmonary ventilation studies

M.M. Ishfaq, S.K. Ghosh, A.B. Mostafa, S.R. Hesslewood, N.R. Williams, and A.J. Hickey[1]
Department of Physics and Nuclear Medicine, Dudley Road Hospital, Dudley Road, Birmingham B18 7QH, UK, and
[1] Department of Pharmacy, The University of Aston in Birmingham, UK

Eur J Nucl Med (1984) 9:144–146

European Journal of Nuclear Medicine

Case report

Reversible diminished renal ^{99m}Tc-DMSA uptake during converting-enzyme inhibition in a patient with renal artery stenosis

T.K. Kremer Hovinga [1], J.R. Beukhof [1], W.H.J. van Luyk [2], D.A. Piers [3], and A.J.M. Donker [1]

[1] Department of Internal Medicine, Division of Nephrology,
[3] Department of Pediatrics [2] and [3] Department of Nuclear Medicine, University Hospital, Groningen, The Netherlands